INVESTIGATION OF THE AMORPHOUS AND CRYSTALLINE PROPERTIES OF LACTOSE AND RAFFINOSE

A thesis submitted in partial fulfilment of the requirements for the degree of Doctor of Philosophy

Sarah Eve Hogan

Department of Pharmaceutics
The School of Pharmacy
University of London
2002

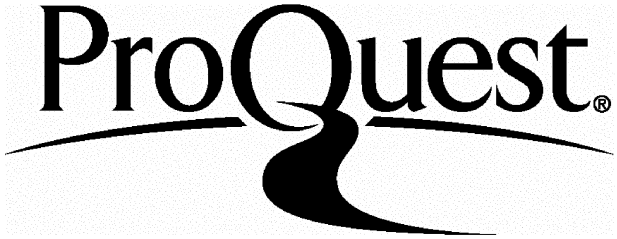

ABSTRACT

Amorphous material is often induced accidentally during the processing of crystals and can have a detrimental effect on product performance. This thesis aimed to develop techniques for the quantification of such amorphous material occurring at less than 10% w/w in the bulk, using lactose as a model. An investigation of the amorphous and crystalline behaviour of raffinose at various relative humidities was also undertaken.

It has previously been shown that changes in physical form are reflected in enthalpy of solution. Solution Calorimetry was found capable of quantifying amorphous content to ± 1% w/w. Similarly, enthalpy of crystallisation values from Isothermal Microcalorimetry, calculated via both a sealed ampoule and RH perfusion technique, were also used to successfully quantify amorphous content.

Dynamic Vapour Sorption and Near Infrared Spectroscopy (DVS/NIRS) were employed in a technique combining two independent quantification methods simultaneously. With the gravimetric approach it was found possible to correlate water sorption and expulsion during crystallisation with amorphous content. NIRS correlated amorphous content with absorbance at several wavelengths, achieving quantification to ± 1% w/w.

The above-mentioned techniques were used to characterise the hydration and dehydration behaviour of amorphous and crystalline raffinose. Through a combination of DVS/NIRS and calorimetric data it was found that, unlike other common carbohydrates, raffinose does not expel plasticising water upon crystallisation. Data from these techniques also showed that crystallisation of amorphous raffinose leads to the formation of different hydrates or hydrate mixes, depending on the amount of water available to the sample. These were characterised by their enthalpies of crystallisation, fusion and solution.

The applicability of the above techniques to study the physical properties of carbohydrates has been demonstrated. In addition to the quantification of disorder in crystalline lactose, they have been used to improve our understanding of the complex amorphous and crystalline behaviour of raffinose.

ACKNOWLEDGMENTS

I would like to express my sincere gratitude to Prof. Graham Buckton for his supervision, guidance, enthusiasm and support throughout my PhD. The financial support of the Royal Pharmaceutical Society of Great Britain is gratefully acknowledged.

Thanks are due to Simon Gaisford and Roy Lane for taking the time to reveal the joys of calorimetry to me, and to Mark Phipps of Thermometric Ltd for lending much needed technical assistance. The efforts of the technical staff of the Pharmaceutics Dept, especially Keith Barnes and Brian Bissenden, are also appreciated.

All the Pharmaceutics postgrads and postdocs helped make the three years really enjoyable, and I would especially like to thank Abi, Angela, Dima, Helen, Juliette, Kevin, Leticia, Magda and Nadeen.

And finally, I would like to thank my parents for their support, and Clive for providing the weekend retreats in the sun.

TABLE OF CONTENTS

LIST OF FIGURES

LIST OF TABLES

ABBREVIATIONS

TAM	Thermal Activity Monitor
IMC	Isothermal Microcalorimetry
DVS	Dynamic Vapour Sorption
NIRS	Near Infrared Spectroscopy
XRPD	X-Ray Powder Diffraction
DSC	Differential Scanning Calorimetry
T_g	Glass Transition Temperature
T_k	Kaufmann Temperature
T_c	Collapse Temperature
T_m	Melting Temperature
J	Joule
Pa	Pascal
s	Second
H	Enthalpy
U	Internal Energy
P	Pressure
V	Volume
T	Temperature
S	Entropy
G	Gibb's Energy
ΔH	Enthalpy
Q	Power
W	Work done
°C	Degree celcius
K	Kelvin
C_p	Heat Capacity
WLF	William-Landel-Ferry
K	Rate constant
ΔE^*	activation energy
R	universal gas constant
w	Weight fraction
k	constant
ρ	density
w/w	weight per weight
w/v	weight per volume
dQ/dt	heat flow
DCT	Differential Control Temperature
SNV	Standard Normal Variate
sd	Standard Deviation

CHAPTER ONE

INTRODUCTION

1.1. THE CRYSTALLINE STATE

1.1.1. DEFINITION AND DESCRIPTION

The crystalline state involves a three-dimensional ordered array of molecules in which there is periodicity and symmetry, with atoms and molecules in a regular and repeating arrangement. All molecules are equivalent with respect to their binding energy, which results in the breakdown of the crystal occurring at a fixed, unique energy level (*i.e.* temperature).

The nature of crystalline structure is that molecules occur in definite, repeating units with defined stoiciometric composition, and may be characterised by their specific chemical, thermal, optical and mechanical properties. Drugs substances are usually purified by crystallisation or precipitation, and the formation of crystals occurs from melted solids or solution, by either nucleation or seeding (see Sections 1.8.2. and 1.8.3.).

1.1.2. POLYMORPHISM AND PSEUDOPOLYMORPHISM

Polymorphism is the existence of two or more different crystal forms (polymorphs) of the same species, due to different molecular packing arrangements within the material.

Many different crystal systems exist, including the cube system, orthorhombic and monoclinic systems. In general, inorganic molecules will crystallise into a specific system, *e.g.* sodium chloride into the cubic system. However, organic molecules frequently crystallise to form different systems, depending on the crystallisation or precipitation conditions to which they are exposed. This leads to the phenomenon of polymorphism, whereby the same compound can exist in two or more crystal forms. Polymorphism is of significance since it impacts upon the physical properties of the material in question, as the same molecules have a different packing arrangement.

Different melting points occur due to different lattice energies resulting from the different crystal arrangements. The impact of polymorphism extends to solubility, dissolution rate, bioavailability and compression properties. The most stable polymorph (*i.e.* that with the lower lattice energy) will have the highest melting point and slowest dissolution, and vice versa.

Polymorphs may exist in either an enantropic state (transitions between two equally stable forms) or a monotropic form (transition from the metastable to the stable form).

Pseudopolymorphism is the incorporation of solvent molecules into the lattice arrangement of a crystal, leading to change in the physical properties of the material in a manner similar to that of actual polymorphism.

Pseudopolymorphism is sometimes termed solvation, and may be stoichiometric or non-stoichiometric. The incorporation of a solvate into the crystal structure may either strengthen or weaken the lattice. Frequently, water is the solvating molecule, and the solvate in this case is termed a hydrate. The conversion of solvates, *e.g.* from mono- to dihydrate, can alter processing ability. The solubility of solvated and unsolvated crystals will differ. For example, if a hydrate is formed, then the interaction between the substance and water that occurs in the crystal phase reduces the amount of energy liberated upon dissolution of the solid hydrate in water. Consequently, hydrated crystals tend to display lower aqueous solubility than their anhydrous counterparts.

It is possible to differentiate between polymorphs and pseudopolymorphs by observing their melting behaviour, since pseudopolymorphs will evolve a gas whereas true polymorphs simply melt.

1.1.3. CRYSTAL HABIT AND GROWTH

Crystal habit, or the actual shape of the crystal, is altered by the crystal growth rate at the different faces of the crystal. This will often depend on the crystal arrangement, as in many cases one face of the crystal may be hydrophilic, whilst another is hydrophobic. Therefore, the hydrophilicity of the environment in which the crystal is grown will affect the growth rate, and the direction in which the crystal grows. Cubic crystals will form if crystal growth is at the same rate in all directions, whilst if growth is inhibited in one direction, a plate may form. If growth has been inhibited in two directions, the resulting crystal may have a needle-like shape. Crystal habit will affect properties including mixing and flow, dissolution rate (due to changes in the surface area to volume ratio) and suspension stability.

1.2. THE AMORPHOUS STATE

1.2.1. DEFINITION AND DESCRIPTION

The three-dimensional long range order that is associated with the crystalline state does not exist in the amorphous state, the positions of the molecules relative to each other being as random as is the case of the liquid state (Hancock and Zografi, 1997). Amorphous solids exhibit short range order over a few molecular dimensions and their physical properties differ from those of the crystalline state. Therefore, the ideal amorphous state can be described as randomly positioned molecules without any repetition in structure.

Amorphous materials consist of a disordered structure which is often compared with the liquid state. A typical liquid, if cooled rapidly, will remain in the liquid phase well below its freezing point, forming what is known as a supercooled liquid (Carstensen, 1993). It will only reach this state if the rate of cooling is greater than the rate of crystallisation. As cooling continues, there is a rise in the rate of increase in viscosity of the supercooled liquid per unit drop in temperature. This causes the initially mobile fluid to form a viscoelastic rubber and finally a brittle glass. Usually

a glass will form when the material is cooled to a point approximately 100 °C (for many pure liquids) below its equilibrium crystalline melting point (T_m), at a cooling rate sufficiently high to avoid crystallisation (Ferry, 1980). This solidification process is known as vitrification (Luyet, 1960) and results in the immobilisation of the disordered structure of the liquid state (Wunderlich, 1981) such that the resulting glass is spatially homogeneous without any long range lattice order and incapable of exhibiting any long range co-operative relaxation behaviour on a practical time scale (Ferry, 1980). The degree of local order depends on the geometry of the molecules and the formation of hydrogen or valence bonds as the liquid is cooled. Therefore, glass formation is associated with the freezing out of the long range thermal motion of individual molecules where glasses are made up of relatively small molecules. A glass may be described as a supercooled liquid of such high viscosity (10^{10} - 10^{14} Pa.s) (Ferry, 1980) that it exists in a metastable, mechanically solid state in which it is capable of supporting its own weight against flow due to the force of gravity (Haward, 1973). Mechanically, if not structurally, a glass may be regarded as a solid.

Amorphous character in a solid can be induced by the following methods:

- condensation from the vapour state
- supercooling of the melt
- mechanical activation of a crystalline material (*e.g.* milling, grinding, micronising)
- rapid precipitation from solution (*e.g.* spray and freeze drying).

1.3. THERMODYNAMIC CONCEPTS RELATING TO THE AMORPHOUS AND CRYSTALLINE STATES

Thermodynamics is used to study the transformation of energy, and to investigate the release of energy stored by molecules, due to the production of heat. Thermodynamic properties include temperature (T), pressure (P), volume (V),

internal energy (U), enthalpy (H), Gibbs' free energy (G) and entropy (S). These properties are related in the following equations:

$$H = U + PV \qquad \text{..... Equation 1.1}$$

$$G = H - TS \qquad \text{..... Equation 1.2}$$

The First Law of Thermodynamics states that energy can neither be created nor destroyed, but may be changed from one form to another. The energy change for a system can be described as:

$$\Delta U = Q - W \qquad \text{..... Equation 1.3}$$

where:

Q = absorption of heat

W = work done by the system.

Since the internal energy (U) of a system is related to the enthalpy (H), the enthalpy change (ΔH) is the heat that is absorbed or evolved when a system changes its thermodynamic state under constant pressure.

When heat flows into a substance, the motion of the atoms and molecules in the system increases. As a result of their increased motion, the atoms or molecules occupy more space and the substance expands. This motion gives every object its internal energy, while heat on the other hand is the passage of energy from one object to another. As heat raises the internal energy of an object, that object's atoms and molecules gain motion and become increasingly disordered. The term entropy is used to describe the amount of disorder in an object.

The entropy of a substance increases whenever the energy it possesses to do work decreases. A system that has a high degree of unpredictability has high entropy.

Heat, therefore, flowing into an object, will always increase the internal energy and disorder of that object and increase its temperature. Consequently, heat disrupts the orderly arrangement of the atoms and molecules of an object.

The Second Law of Thermodynamics, which describes the degree of disorder of a system, states that a spontaneous change in an isolated system proceeds in the direction of increased entropy. This law deals with heat efficiency and is also related to the definition of energy as the stored ability to do work. The internal energy of a system is stored in the movement of the molecules, but this law states that a temperature difference is necessary before work can be done. Therefore, according to this law, a consequence of a spontaneous process is that there is an increase in the disorder or decrease in ΔG. It involves the entropy change ΔS, which is related to the enthalpy and free energy according to Equation 1.2. A decrease is not the preferred direction for entropy changes, consequently there must be a favourable change in the enthalpy which more than compensates for the loss of entropy.

In the context of powdered materials, processing may involve the use of high energy procedures such as comminution, which consume a great deal of energy although only a very small proportion of that energy is used to fracture the material. Energy is also released as heat, vibration and sound. Similarly, the efficiency with which the applied force is used is very low in grinding processes since many particles are deformed by the applied force, but are not broken, resulting in the energy expended on squeezing and releasing them being turned into heat. Laws governing the energy requirements for grinding processes predict that the energy requirement must increase as the particle size decreases.

1.4. THE GLASS TRANSITION TEMPERATURE

1.4.1. DEFINITION AND DESCRIPTION

The glass transition temperature may be defined as a temperature, time and component dependent material-specific change in physical state from a glassy mechanical solid to a rubbery liquid which is capable of flow in real time (Ferry, 1980).

Upon cooling, the rapid molecular motions of the rubbery phase are slowed down, until eventually a temperature is reached at which the system viscosity is said to have become too high for volume relaxation to follow temperature lowering, and non-equilibrium conditions are established (Hancock et al., 1995). That temperature is the glass transition temperature (T_g). However, below T_g, translational molecular motions in the amorphous material still occur, but are relatively slower and occur over much longer periods of time (Hancock et al., 1995). Amorphous solids therefore undergo increasing translational and rotational motion as temperature increases, with the most significant changes occurring above T_g in the rubbery state. Above T_g both the internal energy and entropy adjust to changing temperatures, so that volume is at a minimum and the system is at equilibrium (Figure 1.1). The molecular movements (rotational, translational and vibrational) are such that they overlap and thus free volume exists throughout the system. Free volume is the volume unoccupied by the 'solid matter' of the molecules and represents the volume available for free movement of the molecules (Flink, 1983). Cooling above T_g causes liquids to contract, and kinetic energy decreases are accompanied by decreases in free volume. As long as free volume extends throughout the system, formation of the crystalline form is possible. However, at the point when free volume no longer exists, the glassy state has been reached.

Re-heating causes molecules to absorb some thermal energy and movements again increase. When the range of movements begin to overlap and extend throughout the

system, it then adopts the properties of a liquid, and T_g has been passed. The glass transition temperature is therefore the change between the solid, glassy phase and rubbery, liquid-like phase.

The glass transition temperature is very poorly understood, and whilst many theories exist which attempt to explain it, none is capable of successfully predicting the T_g of a given material, or of explaining the dependence of T_g on such variables as pressure, solute concentration and the molecular weight, chain architecture and stiffness of polymers. Differential Scanning Calorimetry (DSC) is the most commonly used technique to identify the position of a T_g (Ford and Timmons, 1989). It is characterised as a change in the heat capacity of a sample, and seen as an area of discontinuity between the specific heat of the sample and its temperature, usually as an endothermic baseline shift. It is typically associated with an increase in the viscosity of a material, and the temperature at which it occurs will vary with the composition of the amorphous phase, particularly the water content of the material (see Section 1.6.).

1.5. Molecular Mobility and Associated Energy in Amorphous and Crystalline Systems

At very low temperatures, a small increase in the enthalpy (H) and volume (V) of a crystalline material with respect to temperature occurs, indicative of a certain heat capacity (C_p) and thermal expansion coefficient (α) (Hancock and Zografi, 1997) (Figure 1.1). At the melting point, T_m, there is then a discontinuity in both H and V, representing the first-order phase transition to the liquid state. Rapid cooling of the melt may cause H and V to follow the equilibrium line for the liquid beyond T_m, becoming an equilibrium supercooled liquid. This amorphous state is also known as the 'rubbery' state due to the macroscopic properties of amorphous materials in this region. The rubbery state is characterised by the highly temperature-dependent rate and extent of its molecular motions. Further cooling of the supercooled liquid leads

to a change in slope which will be observed at the characteristic glass transition temperature for that material.

Following further cooling beyond T_g, the properties of the material deviate from those of an equilibrium supercooled liquid, reducing the molecular mobility of the material to a point at which it is kinetically unable to attain equilibrium. This non-equilibrium state has higher H and V than it would have had, were it not for its deviation from equilibrium at T_g. This higher internal energy gives rise to an amorphous state with enhanced thermodynamic properties and greater molecular motion relative to the crystalline state. This can lead to enhanced dissolution and bioavailability, but also creates the possibility of spontaneous reversion from the amorphous to the crystalline state (see Section 1.8.). The glass transition may be considered a thermodynamic requirement of a supercooled liquid, since without such

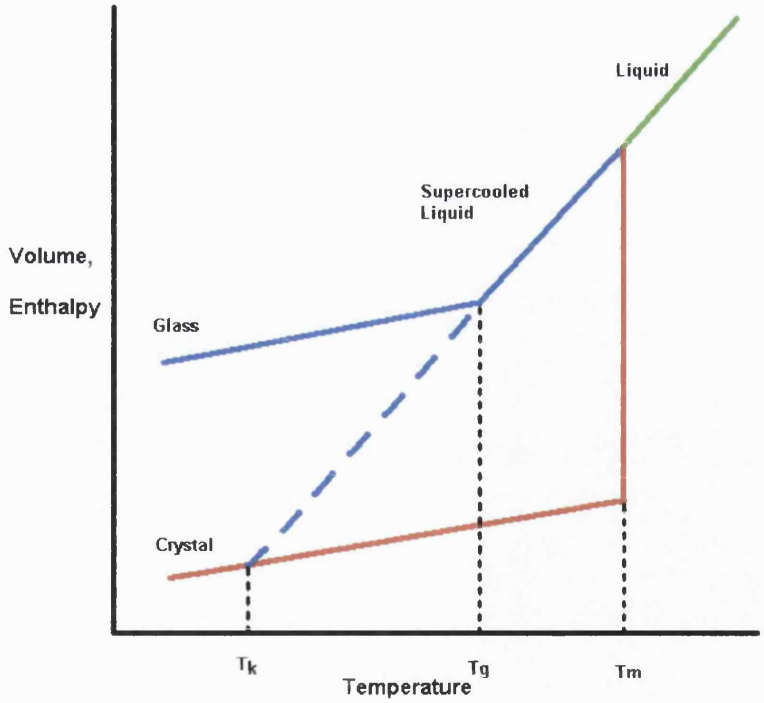

Figure 1.1 *Schematic representation of the enthalpy (H) or volume (V) and temperature relationship for a typical amorphous solid. (Adapted from Hancock and Zografi, 1997.)*

a transition the amorphous material would attain a lower enthalpy than the crystalline state at some critical temperature, and would at some point achieve a negative enthalpy. That critical temperature is known as the Kauzmann temperature (T_k) (Figure 1.1) and is thought to represent the lower limit of the experimental T_g (Hancock and Zografi, 1997).

The determining factor as to whether or not a crystal-forming material achieves the amorphous or crystalline state is the extent to which molecules will attain equilibrium configuration. Low molecular mobility due to high viscosity will prevent equilibrium configurations being attained, rendering the material amorphous (Flink, 1983).

An amorphous system is one which is metastable and has a higher free energy (G) than the corresponding crystalline state. The internal energy (U) and the entropy (S) are also larger than the corresponding values for a pure crystal (York and Grant, 1995). Salvetti et al. (1996) used enthalpy of solution measurements in order to indicate the excess energy of the amorphous/glassy forms of sucrose and glucose compared with their crystalline forms. They stated that the difference in energy is due to differences in Van der Waals interaction energy, the extent of the total energy associated with H-bonding in the two solids and their vibrational frequencies. They also suggested that the enthalpies of solution of a glass will vary depending on the thermal history of that glass, since one of the characteristics of a glass is that its enthalpy decreases upon spontaneous structural relaxation during its physical ageing.

The irregular arrangement of molecules in the amorphous state usually results in their being positioned further apart than they would be in the crystalline state. This leads to a greater specific volume and lower density than in the amorphous state, and a greater free volume (Hancock and Zografi, 1997).

Flink (1983) has suggested that the existence of a metastable amorphous form indicates that free energy barriers exist which hinder the attainment of the stable

crystalline state (Figure 1.2). The amorphous state existing as a supercooled liquid can be said to exist in a non-equilibrium state as if it were at equilibrium. The barrier that prevents a system achieving its equilibrium state is termed an activation step. Figure 1.2 illustrates that a system may need to undergo an energetically unfavourable transition in order to achieve an equilibrium state. It may therefore be necessary to supply sufficient energy to a system in order for it to overcome this activation energy barrier and reach equilibrium.

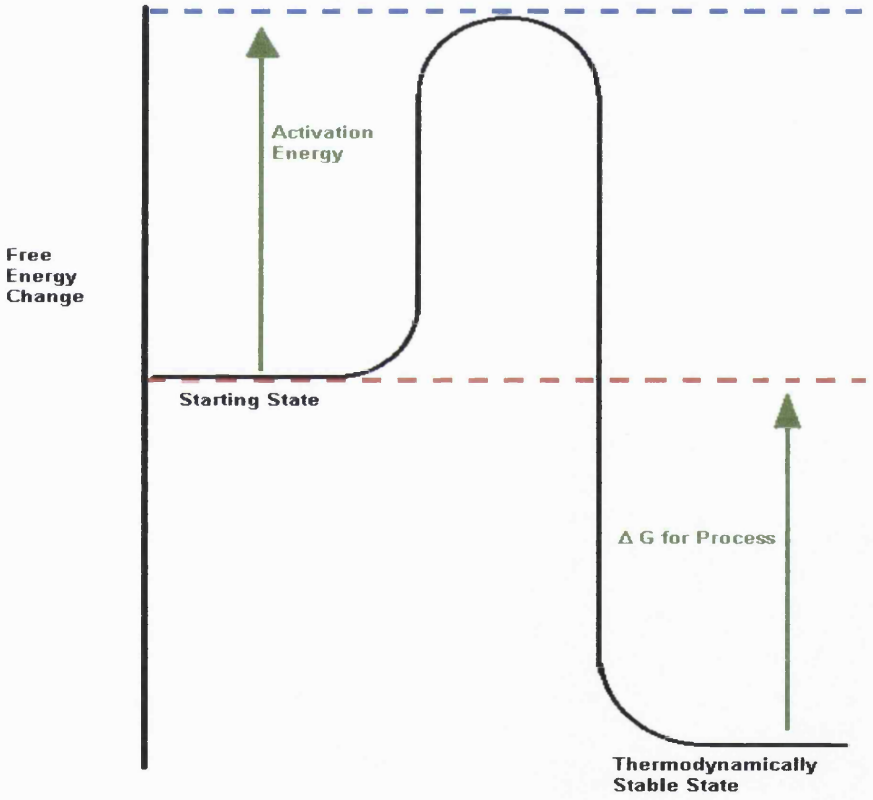

Figure 1.2 *Energy diagram showing an activation barrier that must be overcome before a process can move to the thermodynamically stable state. (Adapted from Buckton, 1995.)*

1.5.1. THE KINETICS OF THE AMORPHOUS STATE

When an amorphous material is in the low viscosity liquid state above T_m, Arrhenius kinetics (Equation 1.4), which are linear, may be applied in order to predict its

behaviour. The glassy solid of very low mobility and very slow dissolution can be considered quite unreactive. However, through a temperature range from T_m to T_g, *i.e.* when an amorphous material is in the rubbery state, completely different non-linear kinetics will be obeyed, following the Williams-Landel-Ferry (WLF) equation (Williams et al., 1955) (Equation 1.5). Williams et al. (1955) found that mathematical analyses used for glass transition phenomena in polymers could also be applied to low molecular weight organic glasses, *e.g.* sucrose. They demonstrated a relationship between the various properties of a material near T_g and the difference in temperature from T_g ($T-T_g$). In this case, a very large temperature dependence will be observed (Franks and Grigera, 1990), and the material will show accelerated mobility and diffusion and can be considered much more reactive.

$$\frac{d \ln k}{dT} = \frac{\Delta E^*}{RT^2} \qquad \text{..... Equation 1.4}$$

$$\ln k = \frac{-C_1(T - T_g)}{C_2 + (T - T_g)} \qquad \text{..... Equation 1.5}$$

where:

C_1 and C_2 = universal constants

T_g = the glass transition temperature (K)

T = temperature (K)

K = a rate constant describing viscous flow or mechanical deformation

ΔE^* = the characteristic activation energy

R = the universal gas constant

The WLF equation defines the kinetics of molecular level relaxation processes, which will occur in practical time frames only in the rubbery state above T_g. It describes the range of kinetics between T_m and T_g, with corresponding implications for process control, product quality, safety and shelf life (Levine and Slade, 1989). Zografi and Hancock (1993) showed that the viscosity of an amorphous solid

changes from about 10^{13} Pa.s at T_g (*i.e.* $T-T_g = 0$) to 10^8 Pa.s when going just 20 K above T_g (*i.e.* $T-T_g = 20$). This indicates that the behaviour of all glasses is based on the principle that, as T_g is approached (by cooling), the relative free volume of the material decreases sharply, resulting in an increase in viscosity. Therefore, $T-T_g$ has a large impact on the solid state molecular mobility of drugs and excipients, which in turn affects their chemical degradation, solid state phase transformations and mechanical strength (Ahlneck and Zografi, 1990).

Hancock et al. (1995) investigated the molecular mobility of amorphous pharmaceutical solids below their glass transition temperatures, and their findings agreed with those of earlier publications in classifying amorphous materials as either 'strong' or 'fragile' glass formers. Strong glass formers typically exhibit relatively small changes in heat capacity at their T_g, whilst the opposite applies to fragile glass formers. They suggested that the reason for these two groups is the manner in which molecular structures of different systems respond to changes in temperature. The important factor in investigating the molecular mobility of a system is the molecular relaxation time, which represents the average time taken for a single molecular motion of a particular type to occur, and is calculated from enthalpy relaxation data. According to Hancock et al. (1995), such is the dependence of molecular mobility on T_g for a system, that the experimental temperature must be lowered to at least 50 K below the experimental T_g before the molecular motions detected by DSC can be considered negligible over the lifetime of a typical pharmaceutical product.

1.6. THE INTERACTION OF WATER WITH AMORPHOUS SOLIDS

1.6.1. ADSORPTION AND ABSORPTION

Generally, amorphous materials take up considerably more water than their crystalline counterparts (Nakai et al., 1977, Pikal et al., 1978). This is due to the fact that it is possible for water to dissolve within the disorganised amorphous structure, whereas this does not usually occur in crystalline materials. Water uptake by crystalline materials is generally termed 'adsorption', and is limited by the available

surface area of the material. Generally, the first layer is hydrogen bonded to the solid, and then a maximum of 2-3 additional layers can form at higher relative humidities. Such adsorption is usually easily reversed, either by a small increase in temperature or a small decrease in relative humidity (Thiel and Madey, 1987). Generally, these adsorbed layers of water have little effect on the properties of that material (Kontny et al., 1987). They can be ad- and desorbed reproducibly, depending on the temperature and relative humidity to which the material is exposed. It is also possible for water to exist in other states or locations in crystalline materials. Capillary condensation can occur in solids with microvoid spaces, leading to occluded water (Carstensen et al., 1980). Deliquescence occurs with water-soluble materials when the relative humidity of the atmosphere exceeds the relative humidity of a saturated solution of that solid, *e.g.* sodium chloride. Both these processes can lead to condensed water in a solid which is capable of dissolving water-soluble compounds. Crystalline substances are also capable of interacting with water to form hydrates, the hydrate water penetrating the crystal lattice (Byrn, 1982).

For an amorphous material, however, water uptake is predominantly determined by the total mass of solid, with significant uptake into the solid structure. This large water uptake is termed 'absorption', whilst 'sorption' is used as a general term to refer to both ad- and absorption. Absorption by amorphous materials generally exhibits significant hysteresis compared with desorption. Water is taken up by dissolution into the solid or by a simultaneous filling up of 'micropores' within the solid.

1.6.2. DEFINITION OF A PLASTICISER

When a substance lowers the glass transition temperature of an amorphous material, it is referred to as a plasticiser (Hancock and Zografi, 1994).

1.6.3. THE PLASTICISING EFFECT OF WATER

When water molecules dissolve into a solid, they increase the free volume of the material by rupturing hydrogen bonds between solid molecules (Franks, 1982, Slade and Levine, 1988). It is known that the addition of an amorphous material to an amorphous solid can alter the glass transition temperature of that solid due to its effect on the overall free volume, which in turn affects $T-T_g$ for the system (at constant T) and alters molecular mobility.

Water has a very low T_g (135 K) (Sugisaki et al., 1968) and small molecular size, which, when coupled with its hydrogen bonding ability, renders it capable of reducing the T_g of a solid system as its own concentration in the solid increases (Hancock and Zografi, 1994). Therefore, in addition to the effect of temperature on T_g, a material may change from its glassy form to the rubbery form due to an increase in its water content depressing T_g to below the storage temperature of that material.

Using a mixing rule, an equation has been developed whereby an estimate of the effect of adding a given amount of one substance to another may be made, based on free volume theories. It is known as the Gordon Taylor Equation (Gordon and Taylor, 1952) (Equation 1.6), and for a two component mixture is as follows:

$$T_{gmix} = \frac{w_1 T_{g1} + k w_2 T_{g2}}{w_1 + k w_2} \qquad \text{..... Equation 1.6}$$

where:

$T_{g\,mix}$ = T_g of a mixture containing components 1 and 2

T_{g1} = T_g of component 1

T_{g2} = T_g of component 2

w_1 = weight fraction of component 1

w_2 = weight fraction of component 2

k = a constant, and a measure of the free volume contributed to the mixture by each of its components at any temperature. Defined as:

$$k = \frac{\rho_1 T_{g1}}{\rho_2 T_{g2}} \qquad \text{..... Equation 1.7}$$

where:

ρ_1 = density of component 1

ρ_2 = density of component 2

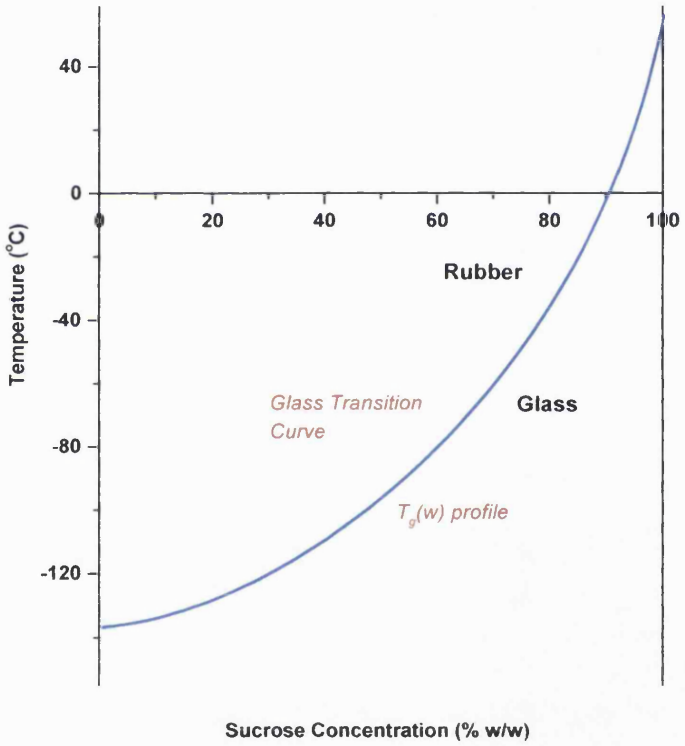

Figure 1.3 *The glass transition curve for a sucrose-water system. (Adapted from Franks et al., 1991).*

A glass transition curve can be a helpful tool in predicting the behaviour of a system (Figure 1.3). Examining the curve reveals that for a sucrose concentration of 100% (*i.e.* no water present) the corresponding temperature is 56 °C, which is the T_g of

sucrose. A 0% w/w sucrose mixture (*i.e.* 100% water) has a T_g of –138 °C (Sugisaki et al., 1968). If kept below the glass transition line, the sucrose-water mixture will remain a glass, and therefore be immobilised in a viscous glassy solution. However, if the temperature of the system is allowed exceed the glass transition curve, the mixture will transform to the less viscous, rubbery state, with enhanced molecular mobility of both the sucrose and water.

Oksanen and Zografi (1990) observed that a critical water content exists at which a glassy molecular material is sufficiently plasticised by a low molecular weight material (*e.g.* water) that it transforms to a rubbery amorphous solid under ambient conditions. Furthermore, they concluded that rubbery materials are capable of sorbing greater quantities of vapour than their respective glasses due to changes in morphology. They found that a sample of PVP, an amorphous polymer, stored at 25 °C and 80% RH would have a T_g of approximately 10 °C. However, storage at 40 °C required only 65% RH in order to exceed the glass transition. Use of the Gordon-Taylor equation facilitates the calculation of the quantity of water required to lower T_g to T, and from the $T_{g\ mix}$ value, provides an indication of the stability of the system under particular storage conditions.

1.7. THE COLLAPSE PHENOMENON

1.7.1. DEFINITION AND DESCRIPTION

The collapse temperature (T_c) may be described as that temperature at which a rubbery amorphous material ceases to be capable of supporting its own weight under gravity.

The collapse temperature is a characteristic of amorphous materials, which, if present in particulate form and above their glass transition temperature, may be susceptible to this phenomenon. It is known that above the glass transition temperature, molecular mobility and viscosity change, resulting in a loss of

structure. Levine and Slade (1986) stated that the structural relaxation which occurs at T_g represents the underlying molecular transformation from the kinetically metastable amorphous solid to the unstable amorphous liquid. White and Cakebread (1966) linked the causes of collapse with plasticisation by water, stating low solute concentration, high residual moisture and high storage temperature as potential factors, all of which induce collapse by decreasing viscosity.

Collapse may be said to encompass the macroscopic effects of a glass transition, whereby viscous flow is capable of occurring over a short space of time. The formerly porous solid now resembles a highly viscous glassy material, and a dramatic reduction in sample volume is observed as a result of this loss of porosity. However, the important difference between the glass transition and collapse is that while the former is a reversible process, the latter is not (Flink, 1983).

1.7.2. THE MECHANISM OF COLLAPSE

Levine and Slade (1986) proposed a mechanism for collapse based upon the structural relaxation which occurs at the glass transition temperature, and viscous flow of the rubbery state. From the WLF theory (see Section 1.5.1.), it is known that upon transition from the glassy to rubbery state, a decreased viscosity occurs and free volume increases. In this rubbery state, translational diffusion is possible, and diffusion-controlled relaxations can occur. Therefore, collapse is as dependent on water content and temperature as is T_g. Franks (1982) stated that if the glass transition and collapse share a common time frame, the minimum onset temperature should be attributed to T_g. Collapse is not a true transition in the thermodynamic sense, and it has also been shown to be dependent on sample weight, morphology, degree of dispersion, *etc* (Shalaev, 1991). Although collapse has the appearance of a T_g as observed by DSC, it is not associated with a change in heat capacity.

It has been shown (Darcy and Buckton, 1996) that longer exposure to elevated humidities may increase the degree of collapse which a sample will undergo. Prior to collapse, water may be relatively easily absorbed or desorbed from a sample.

However, there is a point at which the material's molecular motion increases sufficiently as to prevent it from being able to support its own structure under the force of gravity, and it collapses, thus entrapping water within the particle. At this point, removal of water from the sample is governed primarily by diffusion within that sample, and not by the external relative humidity. Therefore, collapsed materials are associated with large quantities of water, which may have a detrimental effect on the behaviour of that material.

1.8. THE AMORPHOUS TO CRYSTALLINE TRANSITION

1.8.1. INTRODUCTION

From previous discussions on the glass transition and collapse phenomena (Sections 1.4. to 1.7.) it is clear that maintaining a sample below its glass transition temperature, either by storage at $T < T_g$, or preventing the incorporation of plasticising agents into the material, restricts the molecular motions and viscosity of that material. However, if those conditions are not maintained, increased molecular mobility can result in crystallisation. As already mentioned, Hancock et al. (1995) showed that a material must be maintained at ca. 50 K below its glass transition temperature in order to avoid crystallisation. However, although a dried material should ideally be stored at temperatures below T_g in order to inhibit diffusion-controlled chemical deterioration, Ediger et al. (1996) have stated that chemical processes in so-called 'strong' liquids can be inhibited for long periods even at temperatures substantially above T_g.

It has been observed (Makower and Dye, 1956) that upon crystallisation, water which was present in the amorphous material is expelled from that material. This water loss has also been found to occur at a specific relative humidity, supporting the theory that a critical water content is required to induce crystallisation (see Section 1.6.2.). The expulsion of water is associated with the fact that the plasticising water is no longer required in the crystalline material, although some of that water may be retained if a hydrate is formed. Since crystallisation results in the

transformation of a material from its metastable amorphous form to the stable crystalline form, it is considered a deactivation process.

The crystallisation process has been studied in detail in order to provide an understanding of how it may be potentiated or inhibited. It may occur via two mechanisms, nucleation and seeding.

1.8.2. NUCLEATION

Nucleation is the process by which individual molecules come together to form solid state nuclei from which individual crystals can grow. There are two types of primary nucleation. Homogeneous nucleation involves molecules coming together to form a cluster, whilst heterogeneous nucleation results from molecules clustering around a foreign body within the system. Secondary nucleation occurs when new nuclei form from existing crystals which are present in a saturated solution, and differs from primary nucleation in that the nuclei are small pieces of solute which have been displaced from existing crystals *e.g.* by stirring.

Saleki-Gerhardt and Zografi (1994) described the important balance which exists within a crystallising system. They discussed the effects of two opposing factors on nucleation, namely nucleation rate and viscosity, which both increase with decreasing temperature. Hence, when the temperature of a system is reduced below its melting point, T_m, supercooling is increased and the nucleation rate increases significantly. Simultaneously, however, a significant increase in viscosity is also noted, which in turn reduces diffusion and molecular motion and impedes nucleation. There is therefore an optimum balance between supercooling below T_m to increase nucleation rate, and reduction in molecular motion, which leads to a crystallisation temperature, T_c, and maximum crystallisation rate which lie between T_m and T_g. Hancock and Zografi (1997) stated that crystallisation from the amorphous state is primarily governed by the same factors that determine crystallisation from the melt, *i.e.* nucleation and crystal growth.

Makower and Dye (1956) investigated the crystallisation of spray dried sucrose and glucose at different relative humidities, determining that crystallisation with subsequent release of moisture occurred at high humidities, yielding anhydrous crystals. They evaluated the rate of crystallisation and noted that there was an initial induction period, which they concluded was necessary in order to produce a sufficient number of nuclei in order to initiate a sufficient rate of crystallisation.

Iglesias and Chirife (1978) investigated the effects of additives (*e.g.* carboxymethylcellulose and microcrystalline cellulose) on the rate of crystallisation of sucrose, and found it was greatly reduced due to an increase in the viscosity reducing molecular mobility, as well as other interactions between the components. Van Scoik and Carstensen (1990) investigated the effect of additives, temperature and relative humidity on nucleation in freeze dried sucrose, with a view to producing a stable amorphous material. They found that although the inclusion of materials such as lactose could delay nucleation, once nucleation occurred crystallisation was rapid. They suggested that possible mechanisms of nucleation inhibition included a mass transfer step, whereby hydrophilic agents with a strong tendency to hydrogen bond with available water could impede the mobility of sucrose molecules and thus prevent the collisions required to establish nuclei. They also spoke of the potential of some materials to prevent individual molecules approaching established nuclei in the correct orientation. They discussed how insoluble additives can been used in order to promote nucleation in various crystallisation operations, suggesting that solid surfaces may act as a heterogeneity, decreasing the free energy necessary for the formation of critical nuclei.

1.8.3. SEEDING

Seeding is the process of introducing an additive to a system (*e.g.* a species of the crystal desired) in order to stimulate nucleation and crystal growth to produce crystals of a particular form. Ahlneck (1993) stated that through the addition of a material with different properties from the crystallising substance, it is possible to produce different crystal forms. Yoshioka et al. (1994) showed that the isothermal

crystallisation of two different forms of amorphous indomethacin can be dramatically altered by temperature and the type of seed crystal introduced. This would imply that the amorphous form is capable of responding to different types of surface nucleation, selecting one crystal form over another.

1.9. PROCESSING INDUCED DISORDER IN CRYSTALLINE MATERIALS

1.9.1. INTRODUCTION

Processing of powders is capable of altering the particle surface to a certain extent, be it intentional or otherwise. For example, it is often desirable to increase the dissolution rate of a drug substance and this can be achieved through comminution, which reduces particle size, thus increasing surface area and subsequently, bioavailability. Particle size reduction is also desired in order to achieve dose uniformity in inhalation formulations. However, such processes are capable of inducing undesirable amorphous material, and the effect of this disordered material can be considerable. It is possible for a particle to be only partially amorphous, but since that disordered material resides primarily on the surface of the particles, it is capable of exerting a much greater effect on the behaviour of the bulk than its proportion of the mass would indicate possible. Processes such as spray- or freeze drying may be controlled in order for the yield to be rendered partially or entirely amorphous.

1.9.2. COMMINUTION

The aim of comminution, as has already been mentioned, is a reduction of particle size, often with a view to improving bioavailability. Comminution is carried out by a process of crack propagation whereby localised stresses produce strains in the particles which are large enough to cause bond rupture and thus propagate the crack. In general, these cracks are propagated through the regions of a material which possess the most flaws or discontinuities. Only a very small amount of the total energy involved in the comminution process actually affects size reduction, the remainder being lost in many ways, including elastic deformation of particles

without fracture, deformation to initiate cracks which cause fracture, deformation of metal machine components, interparticle friction, particle-machine wall friction, heat, sound and vibration. A high degree of activation of pharmaceutical materials due to endothermic (formation and deformation) and exothermic (bonding) processes occurs. Particles are subjected to stress and are thereby strained and deformed (Ahlneck, 1993). After completion of the comminution process, cracks and defects will remain, thus creating local 'hot spots' which store energy at the surface of the particles. These changes in the crystalline material manifest themselves in product performance, and characteristics such as solubility, dissolution, chemical stability and tablet compression (see Section 1.10.).

Forni et al. (1988) found that the grinding of polymorphic forms A and B of a material resulted in the conversion of form A to form B. However, other studies have noted the induction of amorphous material by comminution. Lerk et al. (1984) found that intensive grinding caused α-lactose monohydrate to lose its hydrate water and β-lactose to become amorphous, whilst Saleki-Gerhardt et al. (1994) were able to produce sucrose of increasing amorphous content by increasing milling time. Furthermore, a study by Florence and Salole (1976) showed that milling is capable of improving the dissolution rate of digoxin by 2.6 times due to changes in particle size, agglomeration and polymorphism

1.9.3. HEAT DRYING

Hüttenrauch and Keiner (1979) found that progressive drying of α-lactose monohydrate under vacuum at 125-126 °C resulted in a continuous decrease in the degree of order of the material. This led to the conclusion that heat-drying could be used to induce crystal defects. The process is now commonly used to produce amorphous carbohydrates such as trehalose (Ding et al., 1996, Roberts and Franks, 1996) and raffinose (*e.g.* Saleki-Gerhardt et al., 1995). Heat drying is discussed further in Section 2.6.

1.9.4. SPRAY- AND FREEZE DRYING

Spray drying involves the production of small droplets from a solution or suspension, which are then exposed to temperatures sufficient to evaporate the solvent and dry the solute to the solid state, commonly in less than one second. Depending upon the nature of the feed material, the yield will be a partially amorphous or amorphous material. Spray drying is discussed in further detail in Section 2.5.

Freeze drying, or lyophilisation, also yields a dry solid whilst avoiding the application of high temperatures. Initially, a solution is frozen, with water being converted to ice for removal via sublimation. Optimisation of conditions can lead to the production of an amorphous cake, from which the residual water content may be removed by diffusion. Freeze drying is a widely employed process for the production of amorphous materials, often with a view to reconstitution of the final product.

1.9.5. MIXING

Mixing has also been shown capable of disrupting the order of a crystalline substance. Reduced pressure mixing was employed by Konno (1990) to mix an organic crystalline drug with an adsorbant to produce an amorphous system. The temperature, pressure and rotation speed all affected the degree of crystallinity of the final product.

1.9.6. A ONE-STATE VERSUS A TWO-STATE MODEL

It must be noted that the use of physical mixtures of amorphous and crystalline particles to produce powders of known overall amorphous content represents the used of a 'two-state' model, whereby each particle is either entirely amorphous, or entirely crystalline. This is in contrast with mechanically processed powders, where it would be expected that all or most particles exist in an intermediate, or partially crystalline or amorphous state. This is termed a 'one-state' model (Huttenrauch et al., 1985). Since it is not possible to process a sample to achieve an exact known

amorphous content, it is necessary to prepare 'two-state' samples in order to represent a processed, partially amorphous material. Work has been carried out (Saleki-Gerhardt et al., 1994; Taylor and Zografi, 1998) which has shown that 'two-state' models offer a good representation of a 'one-state' system.

1.10. ADVANTAGES AND DISADVANTAGES OF AMORPHOUS MATERIAL

1.10.1. ADVANTAGES

Amorphous materials have several advantages over crystalline materials. Burt and Mitchell (1981) claimed that dislocations in crystal form (including defects arising from processing) are thermodynamically unstable, which results in their higher free energy and thus a reduced activation energy for dissolution. Therefore, a crystal with a larger number of defects will have a higher thermodynamic activity, greater chemical reactivity and subsequently an increased rate of dissolution, which is advantageous in many circumstances. Such crystals will also exhibit greater chemical reactivity due to their increased mobility and also in some cases due to an increased number of chemical groups being exposed (Hüttenrauch, 1983, Hersey and Kruger, 1980, Hüttenrauch et al., 1985).

Mosharraf and Nyström (1996) reported that for hydrophilic drugs of low solubility, apparent solubility increases dramatically with increased disorder. Elamin et al. (1994) studied the effects of milling on a hydrophobic drug, griseofulvin. They found that although material bulk properties and particle size had not been affected by processing, disordering of the solid structure led to an increase in the free energy of the system, coupled with a decrease in the enthalpy of solution and an increased solubility.

Improved tablet strength is another advantage of amorphous material. Sebhatu et al. (1994a, 1997) proposed that an increase in sucrose and sodium chloride tablet strength was due to a rearrangement of solid material at the particle surface by the action of limited amounts of sorbed water, which caused the disordered material to

crystallise, forming solid bridges. They reported reduced tablet porosity and increased fracture resistance. Elamin et al. (1994) have also reported increased tablet strength with amorphous material

Freeze drying in particular is used in the production of biotechnology products. The reasons for this are two fold. Primarily, the amorphous state is thought to play an important role in the stabilisation of macromolecular drugs by carbohydrates. Although the mechanisms involved in this are poorly understood, they are thought to include an ability of amorphous sugars to hold proteins rigid in their glassy matrix, thus retaining their tertiary structure (Green and Angell, 1995). In addition, it is thought that, upon drying, sugars are capable of replacing the hydrogen bonds which are present in solution between proteins and water (Hanafusa, 1985, Clegg, 1986), again helping to preserve tertiary structure. It has also been suggested that the ability of some sugars to form hydrates upon crystallisation, simultaneously removing water form the remaining amorphous phase, may be an explanation for their ability to stabilise protein formulations during the drying process (Aldous et al., 1995).

1.10.2. DISADVANTAGES

The physical and chemical instability of the amorphous form has already been discussed in detail. The principle disadvantage pertaining to the amorphous state is its tendency to crystallise, thus altering the physical properties of the product. Accidentally induced amorphous material is of greatest interest. As has been stated, this material exists mostly on particle surfaces, and as such is capable of exerting a much greater effect on the behaviour of that material than its proportion of the bulk would indicate. It is therefore the amorphous material which controls the interaction of the material with other phases. Amorphous materials often demonstrate a higher affinity for moisture than the crystalline form of the same chemical entity (Nakai et al., 1977, Pikal et al., 1978, Kontny et al., 1987), which may induce structural collapse or crystallisation, or simply lead to a risk of microbial contamination. Ahlneck and Zografi (1990) highlighted this affinity for water uptake by the

amorphous form. They stated that a crystalline sample of sucrose would be expected to adsorb 0.1% w/w water. However, if that sample were in fact 1 % w/w amorphous, and it was assumed that all the water sorbed had been preferentially taken up into those disordered regions, the local moisture content would in fact approach 20% w/w, thus reducing the T_g of that material to 27 °C. Higher moisture contents would obviously further lower the glass transition temperature. Water absorbed into these amorphous regions can plasticise the solid and further promote the molecular mobility needed to support chemical degradation as well as solid-state changes. This effect of water is known as amplification.

In addition, it has been shown (Skrabanja et al., 1994) that absorbed water may cause discreet amorphous regions to undergo collapse. Subsequent drying will not remove that water, since it may only be removed by slow diffusion from the collapsed material.

The effect of crystallisation of discrete areas of disorder within a crystalline particle can be dramatic. Ward and Schultz (1995) and Leung and Schultz (1996) found that micronised salbutamol sulphate and terbutaline sulphate were prone to agglomeration of particles. It was discovered that if two adjacent crystalline particles had developed amorphous regions during the milling process and were subsequently exposed to elevated relative humidity or heat, the metastable regions rearranged to form a stable crystalline structure, thus forming a bridge between the particles, and thus reversing the efforts of particle size reduction. This in turn can impede the performance of such materials in dry powder inhalers. The role of energetic amorphous regions on particle surfaces or thin amorphous layers surrounding particles in acting as sites for chemical degradation of the solid, especially under conditions of increased temperature or humidity has been discussed by Ng (1975) and Hasegawa et al. (1975). Increased tablet hardness due to crystallisation of surface amorphous material has been found by Ahlneck and Alderborn (1989a,b).

Another consideration is that accidentally induced amorphous material will vary between batches, which in turn means that it is not possible to predict the behaviour of the product due to batch to batch variation. The problem of this surface disorder is that it has the potential to produce instability and unwanted changes in the physical and chemical properties of a system. Thus the need to detect and quantify disorder exists.

1.11. MODEL CARBOHYDRATES FOR THE INVESTIGATION OF AMORPHOUS/ CRYSTALLINE BEHAVIOUR

1.11.1 LACTOSE

1.11.1.1. Introduction

Lactose is a whitish, odourless, slightly sweet tasting powder, which occurs in mammals' milk at levels between 1-7% w/v. It is the disaccharide of glucose and galactose, as shown in its structural formula. It has two natural optical isomeric forms, the α and β forms (Figure 1.4), which differ in the orientation of a –H and –OH. Lactose may exist in the α–monohydrate form (O-β-D-Galactopyranosyl-(1-4)-α-D-glucopyranose monohydrate), the α-anhydrous form or the β-anhydrous form (O-β-D-Galactopyranosyl-(1-4)-α-D-glucopyranose anhydrous). In aqueous solution at equilibrium, lactose will comprise 38% α-form and 62% β-form. The empirical formula of anhydrous lactose is $C_{12}H_{22}O_{11}$, with a molecular weight of 342.3, whilst the monohydrate exists as $C_{12}H_{22}O_{11}.H_2O$ with a molecular weight of 360.3.

1.11.1.2. Production of Crystalline Lactose

Commercially, lactose is produced from the whey of cow's milk. The manufacturing process for α-lactose monohydrate involves crystallisation from a supersaturated whey solution below 93 °C, (the β-form is more saturated than the α-form in that temperature range). Hygroscopic α-anhydrate is formed, which absorbs one molecule of water per molecule of lactose. Two anhydrous α-forms exist. The hygroscopic form can be produced from α-lactose monohydrate if stored under

vacuum between 100-130 °C. The non-hygroscopic form is more difficult to produce and requires thermal treatment of the monohydrate at elevated relative humidity, above 110 °C, or desiccation over dry methanol.

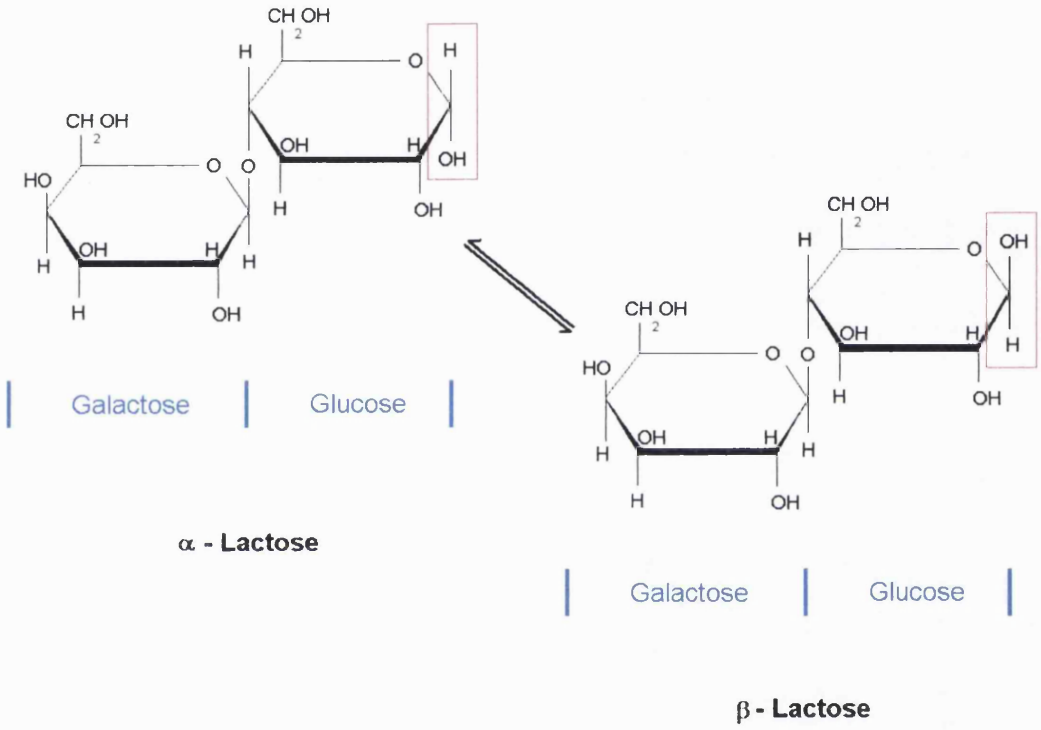

Figure 1.4 *α- and β-lactose, the two optical isomers of the molecule.*

β-lactose anhydrate is produced by precipitation from a concentrated whey solution above 93 °C, where the α-form is more soluble. No water is incorporated into the crystal lattice in this case. Berlin et al. (1973) stated that the β-lactose form has a higher density than α-lactose, so that its structure must therefore be more compact. The energy expenditure would be too large to allow the expansion of the β-form, therefore it cannot form a hydrate. The β-lactose form is non-hygroscopic and stable except at elevated relative humidities (probably up to approximately 75% RH, although there is confusion over the exact value, according to Angberg et al., 1991

(see Section 1.11.1.4.)). Commercial β-lactose generally contains up to 30% α-lactose monohydrate, and is prepared by roller drying.

1.11.1.3. Pharmaceutical Applications of Lactose

Lactose is a commonly used excipient in the pharmaceutical industry. It is frequently employed as a filler or diluent in tabletting and capsule filling. In lyophilisation, it acts to increase the plug size and aid caking. Lactose is also a major constituent of many infant feed formula products.

Many grades and forms of lactose exist and advantage is taken of the properties of certain forms for different applications. For example, spray-dried lactose (α-lactose monohydrate with a quantity of amorphous material) is favoured in direct compression for the production of tablets with higher breaking strength. This is due to its superior flow properties and the fact that it is more compressible than crystalline or powdered lactose.

Spray dried lactose has had a place in the formulation of solid dosage forms for over 50 years. Lactose has also found use in dry powder inhalers, which have been available since the early 1970's (Bell et al., 1971), where it is often the carrier diluent on which drug molecules are mounted for administration to the lung. It is this application, which requires strict control over particle size and density in order to target the correct parts of the lung, that often requires micronisation or milling and results in the generation of unwanted and often detrimental amorphous material. Lactose is also used in combination with sucrose in sugar coating.

1.11.1.4. Analysis of Lactose

Lactose has been studied extensively in each of its physical forms. The main tool for this work has been Thermal Analysis. Differential Scanning Calorimetry (DSC) has been used in order to characterise its different thermal transitions and melting points. Lerk (1983) established that the melting point of α-lactose monohydrate is 212 °C, whilst stable α-anhydrate melts at 216 °C and β-anhydrate melts at 239 °C.

In addition both Lerk (1983) and Olano et al. (1983) found that mutarotation of the α-form to the β-form is possible upon heating, which renders use of DSC to calculate α:β ratios inaccurate. DSC has also been used in order to show crystallisation of amorphous lactose and its glass transition. The glass transition temperature of dry amorphous lactose is located at 114 °C (Schmitt et al., 1998), whilst crystallisation of an amorphous sample occurs at 187 °C. α-lactose monohydrate may also be shown to lose its water of crystallisation at approximately 145-150 °C (Schmitt et al., 1998).

Isothermal Microcalorimetry (IMC) has been used extensively to characterise lactose. It is possible to detect amorphous material by providing it with the conditions required in order to induce crystallisation and to subsequently measure the heat evolved during that crystallisation event. Although DSC is capable of carrying out such determinations, it is limited to samples with high amounts of disorder (Saleki-Gerhardt et al., 1994). IMC has a higher sensitivity for such measurements, and as such the crystallisation of amorphous lactose has been studied in great detail. Further discussion of such investigations can be found in Chapter 5.

Solution Calorimetry is another thermal method with which to analyse the physical state of pharmaceutical materials through the determination of enthalpy of dissolution. Since amorphous and crystalline materials comprise molecules with different molecular packing, their bond energies differ and, thus, characteristic enthalpies result.

Gravimetric vapour sorption is a further technique that can be used to monitor the crystallisation of amorphous materials. Amorphous lactose is more hygroscopic than crystalline lactose and can be shown to sorb large quantities of moisture prior to its crystallisation. Monitoring of the crystallisation event itself is possible since amorphous lactose, like many other materials, expels its plasticising water upon rearrangement of the molecules into the crystal lattice.

X-Ray Powder Diffraction can be used in order to assess the crystallinity of lactose. However, as in the case of DSC, it has been shown capable of detecting disorder only when it occurs at greater than 5-10% w/w of the bulk (Saleki-Gerhardt et al., 1994). An alternative method with which to analyse amorphous/crystalline lactose is Near Infrared Spectroscopy. It has been shown (Buckton et al., 1998, Lane and Buckton, 2000) that it is possible to follow the crystallisation of amorphous lactose by use of this technique.

1.11.2. RAFFINOSE

1.11.2.1. Introduction

Raffinose (β-D-fructofuranosyl-o-α-D-galactopyranosyl-(1-6)-α-glucopyranoside) is a trisaccharide carbohydrate. Acid hydrolysis of raffinose yields D-galactose, D-glucose and D-fructose. In the anhydrous/amorphous form, its molecular weight is 504.4 and its empirical formula is $C_{18}H_{32}O_{16}$ (Figure 1.5). It may be obtained as a crystalline pentahydrate, which has a melting point of 80 °C (Saleki-Gerhardt et al., 1995), and it will lose its water of crystallisation on slow heating up to 100 °C. Dry amorphous raffinose has a glass transition temperature of 103 °C (Saleki-Gerhardt et al., 1995).

1.11.2.2. Pharmaceutical Applications of Raffinose

Raffinose is of interest pharmaceutically as it exists as a stable pentahydrate, the highest hydrate of any known oligosaccharide. It is also possible to render raffinose pentahydrate amorphous by dehydration (heat drying).

The use of disaccharides such as sucrose and trehalose as cryo- and lyoprotectants during the freeze drying of proteins, liposomes and related pharmaceuticals is well established. The theories which exist to explain the nature of the stabilising effect of these carbohydrates have been mentioned briefly in Section 1.10.1. Since raffinose has such a complex interaction with water and a large hydrogen bonding capacity, and also exists in the amorphous state, it is regarded as a potentially useful excipient with which to formulate labile substances. To date, little is known about the solid-

state properties of raffinose in relations to water, and it is therefore an appropriate candidate for further investigation. Although raffinose has been cited in a number of patents, it has yet to be included in the formulation of a marketed pharmaceutical product.

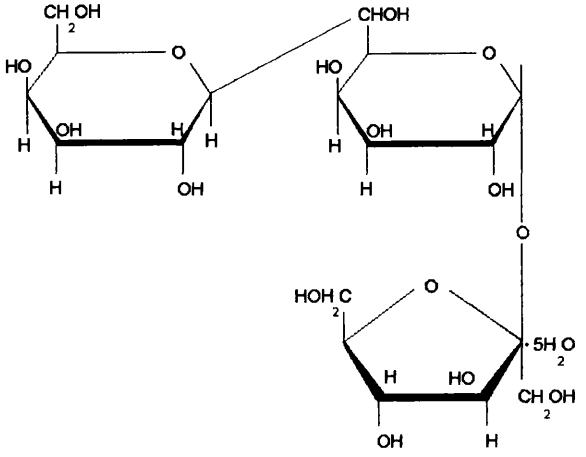

***Figure 1.5** The molecular structure of raffinose pentahydrate.*

1.11.2.3. Analysis of Raffinose

It has already been mentioned that few investigations have been carried out on raffinose to date. Work has concentrated mostly on exposing amorphous and crystalline raffinose to hydrating or dehydrating environments, and thermal analysis by DSC has been carried out (Saleki-Gerhardt et al., 1995, Kajiwara and Franks, 1998, Kajiwara et al., 1999, Iglesias et al. 2000). A further review of these studies is included in Chapter 6.

1.12. Aims of this Thesis

The aims of this thesis were to explore the capabilities and limitations of various thermal analysis techniques, gravimetry and near infra-red spectroscopy, in order to investigate the behaviour of two carbohydrates, lactose and raffinose. Primarily, the techniques were assessed in terms of their ability to quantify low levels of amorphous content (less than 10% w/w) in lactose. They were further used in order to investigate the complex behaviour of both amorphous and crystalline raffinose under dry and elevated humidity conditions.

CHAPTER TWO

METHODS AND MATERIALS

2.1. ISOTHERMAL MICROCALORIMETRY

2.1.1. INTRODUCTION

Isothermal Microcalorimetry is a technique which measures heat flow. Almost all chemical and physical processes are accompanied by heat changes, be they exothermic (heat producing) or endothermic (heat absorbing). The sample is maintained under isothermal conditions within the microcalorimeter, and when a reaction occurs, a temperature gradient is formed between the sample and its surroundings. The resulting heat flow (rate of thermal energy produced or absorbed by the sample) is measured as a function of time, and information can be gained on such variables as rate and extent of reaction, change of phase or physical form and metabolism of biological systems. It is a non-invasive technique which does not require any sample pre-treatment and is not limited by the physical state of the sample, being suitable for the study of solids, liquids and gases. Solid state isothermal microcalorimetry applications in the pharmaceutical industry generally concern stability determination (chemical and physical) and physical form characterisation. Reviews of the applications of microcalorimetry to physical pharmacy and pharmaceutics include those undertaken by Buckton and Beezer (1991), Buckton (1995), Wadso (1997) and Phipps and Mackin (2000).

2.1.2. INSTRUMENTATION

The instrument employed in these studies was a Thermal Activity Monitor (TAM) 2277, Thermometric AB, Järfälla, Sweden. The instrument set-up comprises four calorimetric channels, each of which houses a twin detector, *i.e.* it is equipped with a sample (side A) and reference (side B) measuring cup. These channels are housed within a 25 L water bath (distilled water containing 4% corrosion inhibitor (Thermometric AB, Järfälla, Sweden)), and acts as an infinite heat sink. The instrument is capable of operating between 5 – 80 °C. An external water circulator (2219 MultiTemp, Thermometric AB, Järfälla, Sweden) was employed to aid accurate temperature control, resulting in a temperature stability of $\pm$ 2 x 10^{-4} °C.

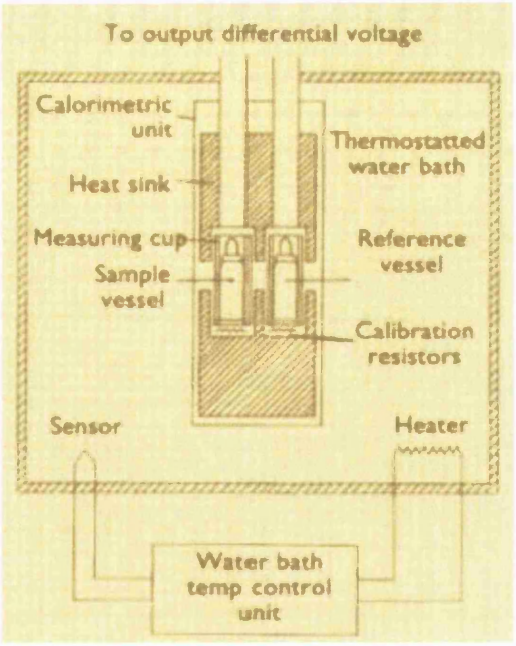

Figure 2.1 *Outline of the functional design of the TAM (reproduced with the permission of Thermometric AB, Sweden).*

This highly accurate temperature control facilitates the measurement of extremely small heat flows, making Batch Isothermal Microcalorimetry an extremely sensitive technique. In addition, the comparison of the sample and reference cells enables the elimination of certain changes in the temperature of the heat sink, such that changes in sample temperature in the order of 10^{-6} °C are detectable as an out of balance signal. An outline of the functional design of the TAM appears in Figure 2.1.

Each calorimetric channel is surrounded by highly sensitive heat-conducting thermopiles (Figure 2.2). Any thermal energy change occurring in a channel results in a slight temperature difference (relative to the heat sink). The heat produced in the thermally-defined vessel flows away in an effort to restore thermal equilibrium with its surroundings. The heat energy is channelled through the thermopile blankets before escaping into the heat sink. In the thermopiles, the heat energy is converted into a voltage signal proportional to the heat flow, and results are presented as a measure of the thermal energy produced by the sample per unit time (dQ/dt).

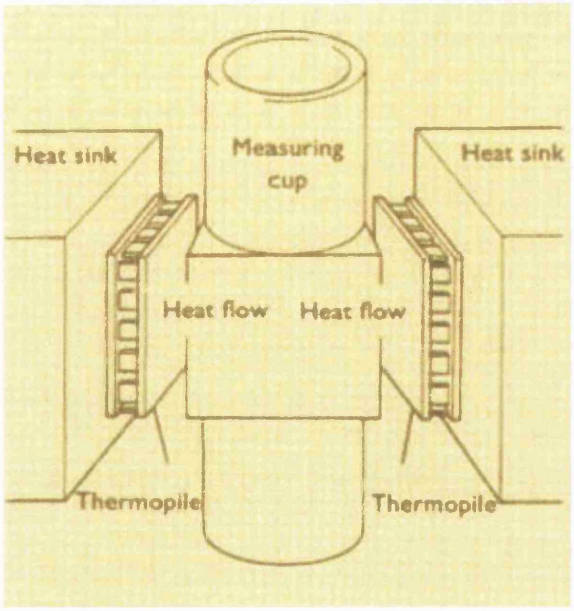

Figure 2.2 *Diagram of the TAM detection and measurement unit (reproduced with the permission of Thermometric AB, Sweden).*

An amplifier is connected to each channel, enabling a selection of full-scale measurement ranges between 3 and 3000 μW. The output signal from a thermal event in the channel is sent directly through the amplifier to a computer, where the data are collected via the dedicated 'Digitam 4.1 for Windows'® software. All data analyses (integration of peak areas *etc*) were carried out with Microcal Origin© versions 3.5 and 5.0.

A range of different reaction vessels is available to fit in the calorimetric channel, *e.g.* closed reaction vessels such as stainless steel or glass ampoules, open reaction vessels including perfusion, titration and flow cells. With these a wide range of experiments can be carried out.

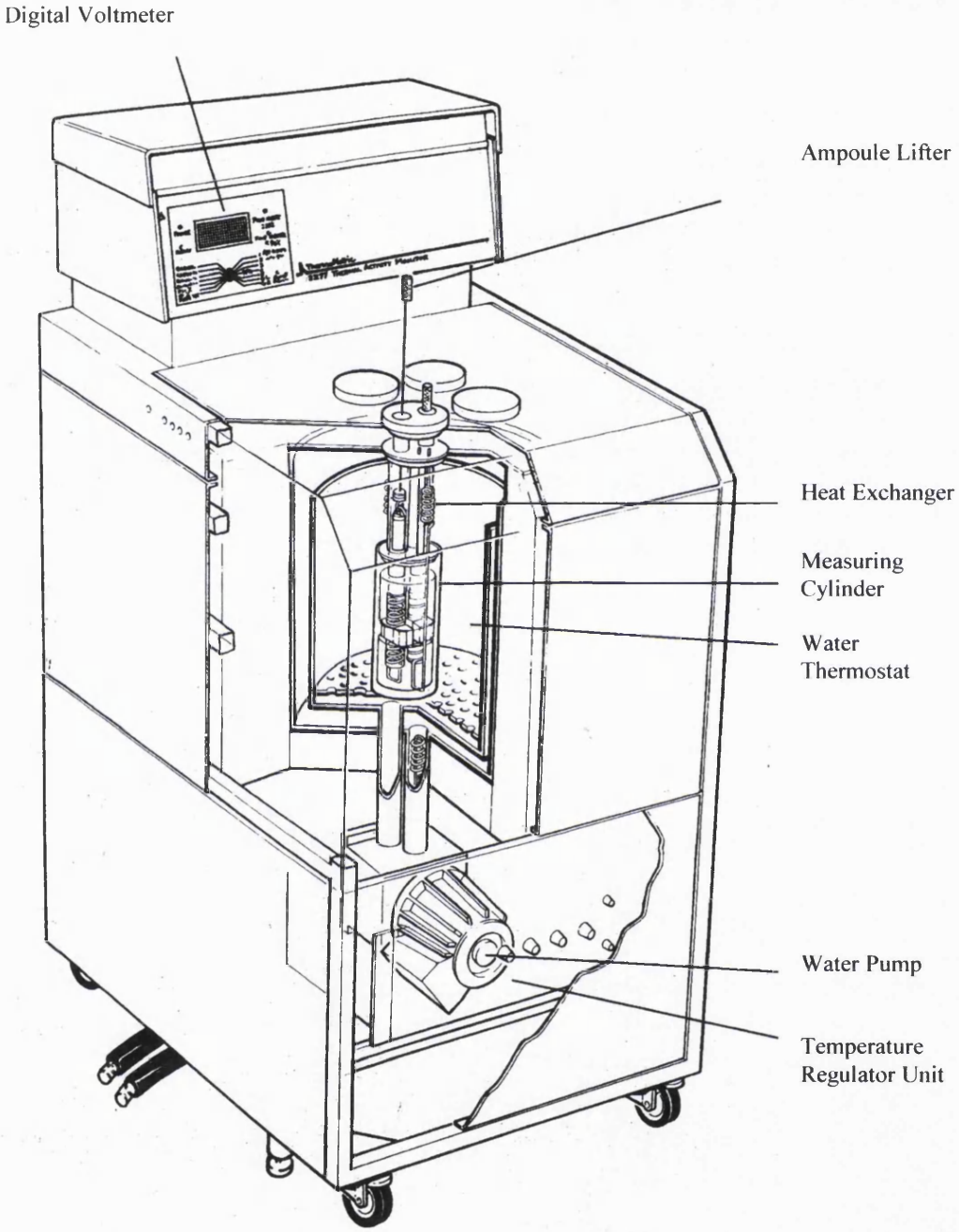

Figure 2.3 *Diagram of a Thermal Activity Monitor (reproduced with the permission of Thermometric AB, Sweden).*

2.1.3. EXPERIMENTAL

Two different experimental set-ups were employed, the first being a closed system (Batch Isothermal Microcalorimetry) and the second an open system (Isothermal RH Perfusion Microcalorimetry).

2.1.3.1. Batch Isothermal Microcalorimetry

All experiments carried out in these studies employed sealed 3 mL glass ampoules for both the sample and reference sides of the channel. In each case the reference ampoule was set up to match the sample ampoule as closely as possible. In all cases, samples were to be exposed to elevated humidities, by means of the inclusion of a mini-hygrostat filled with a saturated salt solution in the ampoule. Therefore, the reference ampoule in each case contained a mini-hygrostat containing the same quantity of the salt solution. Sample ampoules contained between approximately 20-800 mg (accurately weighed), and were sealed with a Teflon seal and aluminium cap.

The ampoules were lowered to the intermediate temperature equilibration position of the channel and data collection initiated. They were maintained in this position until such a time as the heat flow recorded from the channel was zero (usually requiring approximately 20 mins). At this time the ampoules were then lowered so as to occupy the measuring site of the channel. All experiments were carried out at 25.00 °C.

2.1.3.2. Isothermal RH Perfusion Microcalorimetry

A 2250 Micro Reaction RH Perfusion insertion vessel (Figure 2.4) (Thermometric AB, Järfälla, Sweden) was employed in all experiments. A solid sample (between approximately 10-300 mg, accurately weighed) was loaded into the 4 mL stainless steel ampoule and the unit sealed and lowered into the measuring site of the calorimetric channel. A flow of Nitrogen gas at 2-6 mL/min, created by a pulse free pump action was passed over the solid sample. The required RH value was produced by mixing dry gas (0% RH) with wet gas (100% RH) which had been

passed through two humidifier chambers within the unit. The required ratio of dry: saturated gas was achieved via a 2281 Precision Flow Switching Valve (Thermometric AB, Järfälla, Sweden) connected to the computer and the Digitam software using the Flow Switch Module installed in the 2280 TAM Accessory Interface (Thermometric AB, Järfälla, Sweden). In addition to its RH controlling function, the Flow Switch also contained a heater which was employed to heat the Flow Switch Valve in order to prevent condensation forming in the outlet tube from the RH Perfusion unit. Temperatures between room temperature and 93 °C could be set, however, for all experiments a temperature of 40 °C was selected in order to reduce the risk of condensation of water vapour within the perfusion unit itself.

Lowering of the RH perfusion unit to the measuring site of the calorimetric channel was carried out in stages, using a circular clamp to hold the unit in the three equilibration positions illustrated in Figure 2.4 for the periods of time indicated. An empty stainless steel 4 mL reference ampoule was employed for each unit throughout the studies. It was also necessary to charge the humidifier chambers with distilled water (0.5 mL in each) by means of a syringe. This was required to be carried out once every week.

2.1.4. CALIBRATION

Calibration procedures for the two techniques were as follows:

2.1.4.1. Calibration in Batch Isothermal Microcalorimetry

Calibration of each calorimetric channel was carried out once a fortnight, whenever the amplifier range was altered, or if experimental conditions were adjusted, *e.g.* use of a different salt solution in the mini-hygrostats. Two sealed glass ampoules were employed for this purpose, and inserted into each was a mini-hygrostat containing the saturated salt solution to be employed in the set of experiments to be undertaken. A range of amplifier setting (3, 10, 30, 100, 300, 1000 and 3000 μW) was available, although in these studies only the 300, 1000 or 3000 μW settings

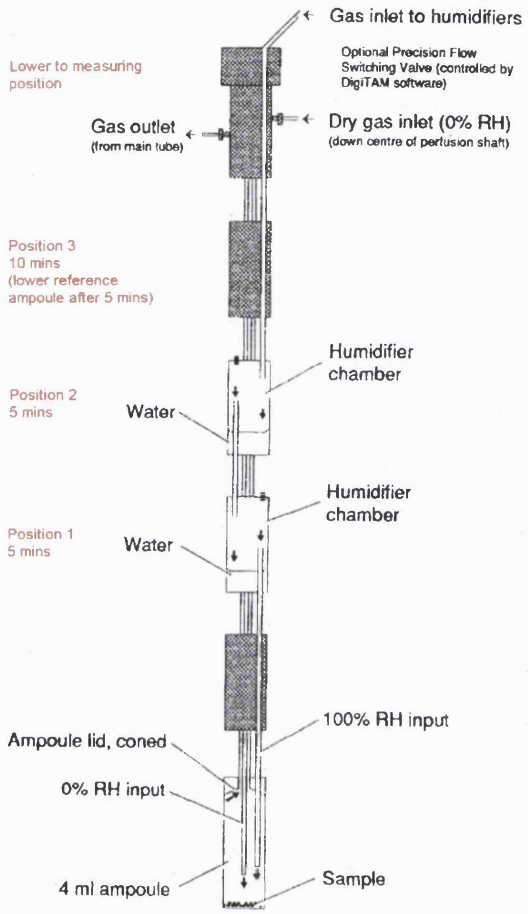

Figure 2.4 *Schematic of an Isothermal RH Perfusion Microcalorimeter (reproduced with the permission of Thermometric AB, Sweden).*

were employed. Ampoules were lowered into the measuring position of the channel as described in section 2.1.3.1., and once the ampoules had equilibrated and a steady baseline had been achieved, the signal was adjusted using the zeroing dial in order that it be 0.000 ± 0.100 μW. At this point, an accurate quantity of heat was generated by the application of a specific current to the channel heater resistor, (located in the measuring cup of the channel in order to simulate as closely as possible the position of a reaction). Because a known current was applied to the resistor, a specific thermal power was dissipated, and this was recorded as an

exothermic response by Digitam. This deflection from baseline provided a signal which could be adjusted to the correct value (± 0.100 μW) by means of a 'fine' adjusting dial. In all instances, a static calibration was carried out for batch experiments. Once the signal had been adjusted, the calibration heater was switched off, and the signal allowed to return to baseline. Once a steady baseline was achieved its 'zero' signal was checked.

2.1.4.2. Calibration in Isothermal RH Perfusion Calorimetry

Calibrations were carried out after two experiments had been carried out in each unit, or if amplifier range was to be altered. Amplifier settings of 300, 1000 or 3000 μW were employed. Empty sample and reference stainless steel ampoules were used for calibration purposes. Once the RH Perfusion unit and reference ampoule had been lowered into the measuring positions of the channel as outlined in section 2.1.3.2., the calibration procedure was carried out exactly as was stated in section in 2.1.4.1., excepting the fact that the acceptable noise level in this instance was ± 0.200 μW.

2.2. SOLUTION CALORIMETRY

2.2.1. INTRODUCTION

Solution Calorimetry is a technique which has been used pharmaceutically for many years, the principle of which is to create a system where very small enthalpy changes in a liquid system can be detected due to the dispersion or dissolution of a solute (be it solid or liquid) as a function of time. Enthalpy of solution of a solute in any one of its particular solvents may be measured enabling the detection of minor changes in the physico-chemical characteristics of a material, *e.g.* polymorphism. Other uses of the technique include the study of swelling and wetting of solids and determination of heat capacity.

2.2.2. INSTRUMENTATION

A Thermometric 2225 Precision Solution Calorimeter (Thermometric AB, Järfälla, Sweden) was employed. It consists of three main components, the calorimetric unit itself (Figure 2.5), the calorimeter cylinder in which the unit is mounted during experimental work, and the Solution Calorimeter Module (Thermometric AB, Järfälla, Sweden) through which communication between the calorimeter and computer is controlled. The calorimetric unit consists of two sections, the reaction vessel together with its holder, and the stirrer unit. In these studies the reaction vessel used was a 100 mL thin-walled Pyrex glass vessel, within which were situated a thermistor and a heater, permanently mounted in two pockets descending from the top of the vessel. There was also a sapphire breaking tip mounted on a pin at the bottom of the vessel. The reaction vessel is attached to the holder above it by a large locking nut, which contains the Wheatstone bridge, the electrical component of the calorimeter, which also serves as a thermal insulator. The stirrer system comprises an upper component containing the motor, and the gold stirrer. The

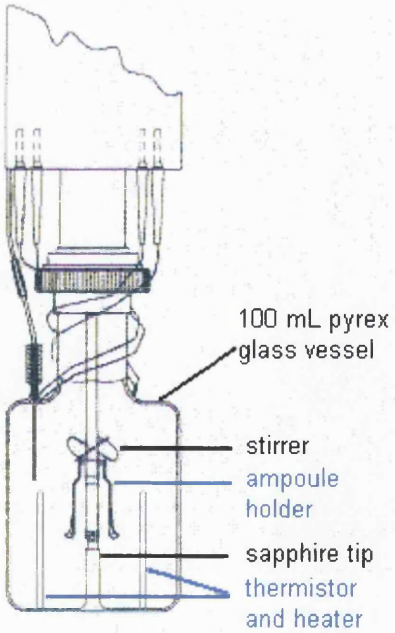

Figure 2.5. *Diagram of the Solution Calorimeter (reproduced with the permission of Thermometric AB, Sweden).*

stirrer also functions as the glass ampoule holder. The stirrer system is inserted into the reaction vessel during experiments and is mounted on a spring to function as a plunger, the entire system being pushed down at the point of the experiment where the ampoule is required to be broken in order to initiate the reaction.

The Wheatstone bridge has been designed to carry out three main functions:

- To monitor the temperature of the reaction vessel and hence measure the heat produced by a solution reaction using the thermistor, the resistance of which is related to the temperature in the reaction vessel. The resistance measured by the Wheatstone Bridge is then amplified and reported to the SolCal program.
- To stir the solution in the reaction vessel by controlling the stirrer motor, and report the stirrer speed to the SolCal program.
- To heat the solution in the reaction vessel, either for calibration or equilibration purposes.

The Solution Calorimeter used had a thermal long time drift of less than ± 100 μ°C over 24 hours and a thermal short time noise of less than ± 10 μ°C. However, it was necessary for the system to be immersed in a thermostat that could achieve suitable temperature control, and was therefore installed in the Thermometric 2277 Thermometric Activity Monitor (see Section 2.1.). With noise reduction, the temperature resolution was close to 1 μK, which gave a heat resolution of 1-4 mJ.

The Solution Calorimeter was a semi-adiabatic (isoperibolic) calorimeter, with a time constant of 2.22 h. The glass ampoules employed were hand blown and had a volume of 1.1 mL. The system was capable of operating between 0-90 °C, although practically, this was limited to between 5-80 °C, since that was the operating range of the TAM. Data were collected by the 'Software for Solution Calorimeter' version 1.2 (Thermometric AB, Järfälla, Sweden) in terms of temperature offset from a predefined zero point (actually the temperature of the air bath of the TAM).

2.2.3. EXPERIMENTAL

All experiments were carried out with the TAM water bath set to 25.0000 ± 0.0001 °C. Sample masses of between approximately 135-220 mg (accurately weighed) were employed, and filled into the ampoules following their storage at 0% RH (either in a desiccator over Phosphorous Pentoxide, or in a vacuum oven (Sanyo-Gallenkamp etc) at 50 °C and –300 mbar. The ampoules were then plugged with a silicon bung and sealed with molten bees' wax, and loaded into the stirrer unit of the calorimeter. This unit was then inserted into the glass vessel containing 100 mL of solvent (distilled water in all cases), the glass ampoule isolating the solute from the solvent. The combined unit was then lowered into the solution calorimeter channel of the TAM, initially being held in the equilibration position of the channel to maintain contact with the water bath of the TAM. Upon equilibration to approximately 25 °C, the unit was lowered into the experimental position, in contact with the air bath, and allowed to further equilibrate. Upon completion, an electrical calibration was undertaken (the parameters of which were selected in order to mimic the magnitude of the break experiment as closely as possible). Following this, the stirrer unit was lowered in order to break the ampoule on the sapphire tip at the bottom of the vessel. This action released the solute so as to be in contact with the solvent, allowing wetting, dissolution *etc.* The ensuing heat change was detected and measured by the thermistor. Following the break, a second electrical calibration was carried out, using the same parameters as the first.

2.2.4. CALIBRATION

The Solution Calorimeter was calibrated electrically as part of each experiment. The small heat exchange between the calorimeter and the environment during the reaction and the heat arising from stirring were adjusted for mathematically using the information obtained from the baseline temperatures before and after the calibrations. Most importantly, the electrical calibration supplied the system with thermal energy information upon which it could base its calculations through direct comparison of heats evolved. A known amount of energy was supplied to the system by the heater to duplicate the thermal energy accompanying a chemical or

physical process. For all data reported here a calibration before **and** after the break reaction was performed. The post-ampoule breakage calibration was expected to provide most reliable data (although very similar to the pre-break calibration), since throughout the duration of the break itself and the latter calibration, the systems were more similar, because, for example, they both contained the broken ampoule rather than 100 mL of solute with a 1.1 mL reservoir of air and sample. In addition there was the potential for a change in the heat capacity of the sample if a solution or suspension formed after the reaction has taken place. The parameters selected in setting up the break, *i.e.* the heat and power settings, were selected so as to match as closely as possible the magnitude of the break reaction with the calibrations. This ensured the most accurate calibrations were being performed in terms of measuring the heat exchanges occurring *etc.*

2.3. DYNAMIC VAPOUR SORPTION AND NEAR INFRARED SPECTROSCOPY

2.3.3. INTRODUCTION

Dynamic Vapour Sorption (DVS) and Near Infrared Spectroscopy (NIRS) form a combined technique which facilitates the combination of gravimetric and spectroscopic data in order to gain both chemical and physical data pertaining to the effects of exposure of a sample to controlled relative humidity conditions. DVS enables the accurate recording of the mass of a sample following exposure to a humidified or dry Nitrogen atmosphere.

The Near Infrared region of the electromagnetic spectrum is found between 1100-2500 nm, and provides a good signal to noise ratio. Overtones and combinations contribute to NIR spectra, which are very broad. Therefore frequency ranges are often assigned to particular bonds, as opposed to specific wavelengths. With the aid of computers, better interpretation of results may be made through the mathematic manipulation (chemometrics) to treat raw data. NIRS benefits from being a fast, non-destructive technique which requires no sample preparation, although obviously through its combination with DVS these advantages may be lost. It has

been shown capable of detecting polymorphism (Aldridge et al., 1996), crystallisation (Buckton et al., 1998) as well as yielding particle size information. The entire NIR spectrum has been characterised, so spectral information can be very valuable. Changes in the position and intensity of peaks and troughs, as well as baseline shifts, can be interpreted to aid the quantitative and qualitative assessment of samples.

2.3.4. INSTRUMENTATION

Gravimetric studies were undertaken in a humidity controlled ultra-sensitive recording microbalance system (DVS-1, Surface Measurement Systems, London, UK), which is capable of measuring changes in sample mass to $\pm$ 1 x 10^{-4} mg. This was housed in a precisely controlled constant temperature incubator (Surface Measurement Systems, London UK). Accurate control of the relative humidity was achieved by controlling the dry nitrogen flow into the incubator, through switching valves, which regulated the total amount of gas to pass to the humidification stage. Through mixing the dry and saturated gas flows in the correct proportions using mass flow controllers, both the sample and reference sides of the balance were exposed the pre-determined relative humidity. Humidity and temperature probes were situated just below the sample and reference pans to give independent verification of system performance. On both sides there was situated an identical flat-bottomed quartz-glass pan, which on the sample side contained the material to be studies, and on the reference side was empty. The mass change of a sample could be determined across an RH range of between 0-98 % RH, and between temperatures of 0-80 °C. The instrument was computer controlled (DVS-1 software, Surface Measurement Systems, London, UK), allowing for programming of experimental runs and the choice of sorption/desorption ramp or step cycles at particular RH values and time periods. Sample mass was between 25-80 mg.

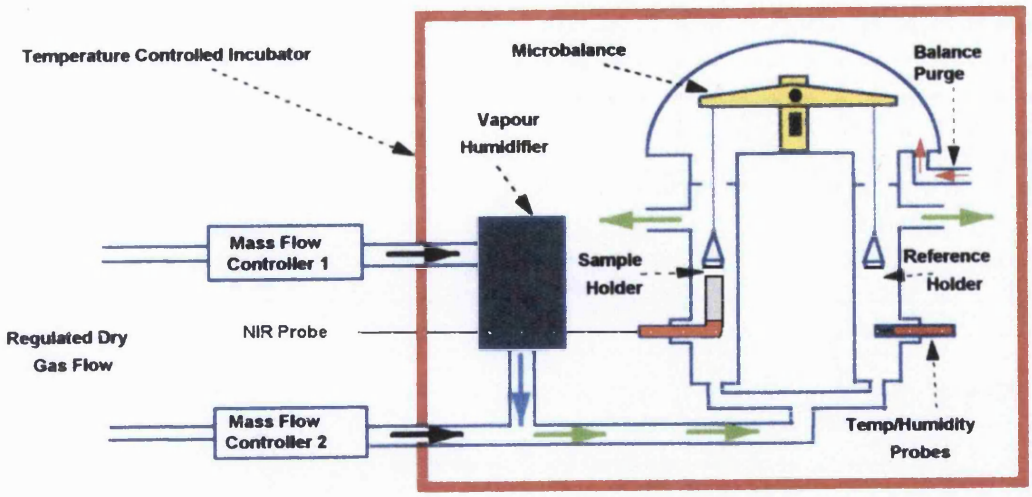

Figure 2.6. *Schematic layout of the DVS-1 system.*

Thorough cleaning of sample and reference pans was required in order to maintain accuracy of results. This was achieved by soaking and rinsing the pans in distilled water, followed by rinsing in absolute alcohol. Following this the pan(s) could be returned to the balance to dry at 0% RH. In order to remove any static build up, pans were then exposed to 90% RH. 10 mins were usually sufficient to remove any static build up. The balance was then zeroed and observed for a further 10 mins to ensure a steady baseline (± 0.001 mg) had been achieved.

The specially adapted optical reflectance Near Infrared probe (Foss NIRSystems, Maryland, USA) was situated approximately 4 mm below the DVS sample pan. Spectra could be recorded at regular intervals of up to 15 minutes throughout the DVS experiment. NIR absorbance spectra were recorded as log (1/R), where R is reflectance. The NIRS instrument recorded the mean spectrum of 32 scans (taking approximately 40 s) over the wavelength region of 1100-2500 nm. NIRS data processing and analysis was carried out using the Vision ® software (Version 2.21) (© Foss NIRSystems, Maryland, USA).

In all cases the spectra which are shown throughout this thesis are representative of trends observed in at least three samples under the same conditions.

2.3.5. CALIBRATION

Procedures for calibration and validation of DVS/NIRS were as follows:

2.3.5.1. Weight Calibration

Weight calibrations were performed on a monthly basis, if the operating temperature was changed or after the instrument had been turned off. The empty sample pan was tared and then a 100 mg calibration (class M) weight placed onto it. Any difference between the value shown and that expected was recorded by the DVS operating system and adjusted for.

2.3.5.2. Relative Humidity Validation

The vapour pressure of water above a saturated salt solution in equilibrium with its surrounding is constant at a particular temperature. By placing a particular salt on the sample pan, and setting up an experiment to ramp at 1 % RH/h over a 10% RH range around the literature value for the critical RH of each salt (Nyqvist, 1983), the critical RH of the salt could be calculated by plotting rate of change of mass with time (dm/dt) against RH. This facilitated validation of the system, however there was no facility for in-house calibration of RH. Sodium chloride (75.5% RH at 25 °C) and lithium chloride (12.0% RH at 25 °C) were employed.

2.3.5.3. NIRS Calibration

Fortnightly, or after the NIR lamp had been turned off, a ceramic reference spectrum was taken. This provided a background spectrum against which experimental data were recorded. In addition, a performance test and, if necessary following that test, wavelength linearisation, were carried out monthly in order to ensure optimum performance of the lamp.

2.4. DIFFERENTIAL SCANNING CALORIMETRY

2.4.3. INTRODUCTION

Power Compensation Differential Scanning Calorimetry (DSC) involves heating a sample and reference pan separately, with the power supply to the sample heater variable so that the temperature difference can be maintained at zero even when a thermal transition (a chemical or physical change that results in the emission or absorption of heat) occurs in the sample. The difference in power supplied to the two heaters is exactly equivalent in magnitude to the energy absorbed or evolved in the transition and therefore yields a direct calorimetric measurement (ΔH) of the transition energy. The types of transitions and reaction which can be measured using this technique include fusion, sublimation and vaporisation (exothermic heat changes), crystallisation (an endothermic heat change) and glass transitions (baseline shifts resulting from a change in the heat capacity of the sample). Generally, slow scanning rates improve peak resolution, whilst faster scanning rates improve the sensitivity of the technique. Consequently, enthalpy determinations can be made at any heating rate, but as heating rate increases, so do the observed temperatures.

2.4.4. INSTRUMENTATION

The DSC 7 Differential Scanning Calorimeter (PerkinElmer Instruments, Beaconsfield, Bucks, UK) was used. It operates with a power compensation design, employing individual sample and reference micro-furnaces, operating the 'thermal-null' system. The micro-furnace facilitates very fast heating and cooling rates, rapid temperature equilibrium and fast sample turn around time. Platinum resistance thermometers (PRTs) are used to make the temperature and energy measurements. The micro-furnaces, being made of a platinum-iridium alloy, are very inert in order to resist chemical attack. In the base of the furnace are two identical platinum resistance elements, one of which was used to provide power (heat) to the furnace, whilst the other was used to detect changes in temperature of

that furnace. The platinum windings are distributed over the full area of the furnace base and so provided truly distributed heating and temperature monitoring at all points in the furnace. Both sample and reference furnaces were mounted in cavities of a large aluminium block or 'heat-sink'. The heat sink was kept at a constant temperature well below the temperature range of the experiment to ensure that the heat could be lost from the micro-furnace to the large heat sink very quickly. The instrument was operated by Pyris Software for Windows®, version 3.81 (PerkinElmer Instruments, Beaconsfield, Bucks, UK).

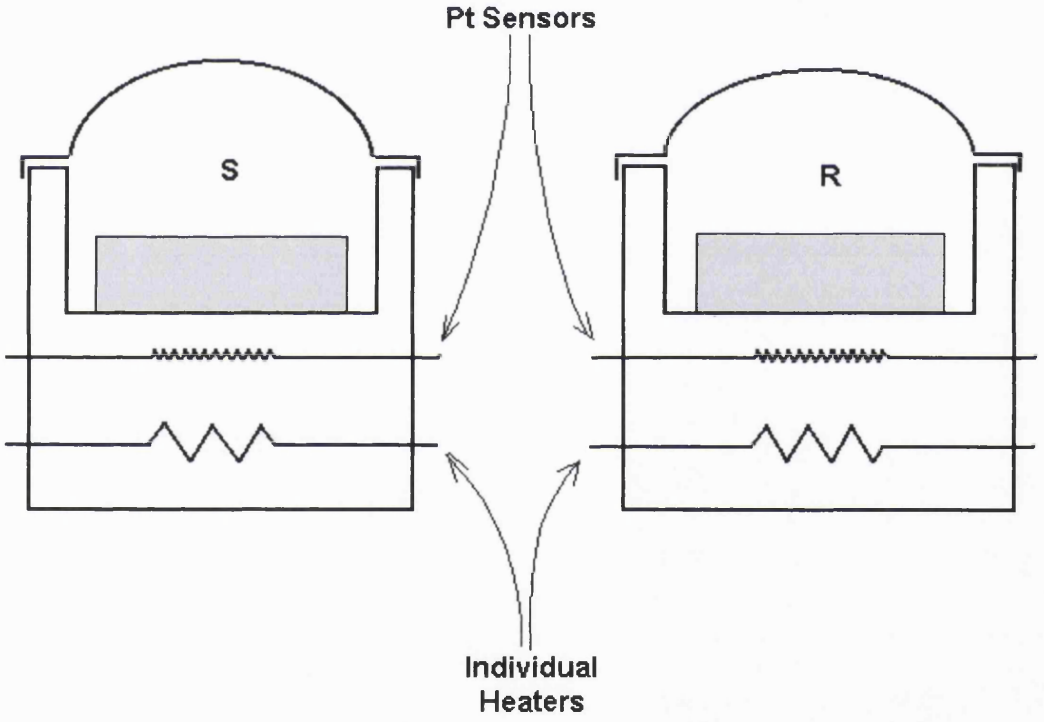

Figure 2.7. *The design of a power compensated DSC (reproduced from 7 Series/UNIX DSC 7 Differential Scanning Calorimeter Users Manual).*

2.4.4.1. The 'Null Balance' Principle

Two separate control loops are used to precisely control the temperature of the sample and reference furnaces as follows:

Average Temperature Control: This loop provides power to the sample and reference furnaces in accordance with the program temperature selected, and therefore ensures that heat is supplied at the selected rate over the chosen temperature range and that the two furnaces are always at the same temperature.

Differential Temperature Control (DCT): This loop is the actual measuring circuit that drives the instrument's output signal. The system measures precisely any differences in the temperature that occurs between the sample and reference furnaces. If the material in the sample furnace gives out or takes up energy, the temperature of the sample furnace will change slightly from that of the reference furnace. This temperature change is accurately sensed by the platinum resistance thermometer in the base of the furnace and the DCT loop will adjust the power to bring the two furnaces back to the same temperature, thus the system is always kept at a thermal null. The amount of energy that must be provided or removed from the system to maintain the thermal null by the DCT loop is directly proportional to the energy changes of the system, thus no heat flux equations are necessary. Direct measurements of energy and therefore ΔH can be made with a power compensation DSC.

2.4.3. EXPERIMENTAL

To achieve maximum peak sharpness and resolution, proper sample preparation was needed, in order to maximise the contact surface between the pan and sample, thus reducing the resistance of the sample to heat flow through the DSC temperature sensors. Powder samples were spread in a thin later on the bottom of the pan for optimum performance. Perkin Elmer non hermetically sealed volatile aluminium pans (cat. no. 0219-0062) were used. The sample was encapsulated in the pan which ensured good thermal contact between the pan and the furnace. Sample mass used in these studies was between 1.5-5 mg, depending on the density of the material to be studied. Samples were weighed using a Perkin Elmer autobalance AD-4 (PerkinElmer Instruments, Beaconsfield, Bucks, UK).

The purge gas was nitrogen and a flow rate of 20-30 psi was used. The temperature range over which the samples were scanned was normally 25-250 °C, at a scan rate of 10 °C/min. An empty sealed aluminium pan was used as a reference.

2.4.4. CALIBRATION

Calibration was achieved through the used of high purity standard materials with known temperature and energy transitions. The standard materials used to calibrate the DSC 7 were Indium and Zinc (values shown in Table 2.1). The instrument was adjusted once the calibration check had been carried out if the observed values differed from those expected by more than 10%. Calibration checks were carried out weekly, if experimental conditions (*e.g.* scanning rate) were changed, or after the instrument had been turned off.

Table 2.1 *The melting points and enthalpy of fusion for Indium and Zinc calibrants for DSC.*

MATERIAL	MELTING POINT (Temperature Onset °C)	ENTHALPY OF FUSION (J/g)
Indium	156.60	28.45
Zinc	419.47	-

2.5. SPRAY DRYING

2.5.3. INTRODUCTION

Spray drying is the process of drying a fluid feed mixture by spraying into a hot dry air stream to obtain a dried product in the form of a powder, granulate or agglomerate. The fluid mixture may be a solution, suspension, dispersion or emulsion, but may only be spray-dried if the final product behaves as a non-sticky, flowing powder. The physical properties of the final product depend to a certain extent on the physical and chemical properties of the feed material and the design and operation of the spray drier employed.

Aside from the pharmaceutical industry, spray drying is also widely used in the food industry since products retain their nutritive content and are easily reconstituted (Masters, 1976). Pharmaceutically, spray drying is favoured as a method of optimising properties such as particle shape, size and density, porosity, moisture content, stability, flowability and friability (Corrigan, 1995). Physicochemical properties affected by the spray drying process include melting point, solubility, dissolution rate and crystal habit (Grant and York, 1986).

A study of the crystallinity of β-lactam antibiotics (Pikal et al., 1978) illustrated, through the use of Solution Calorimetry, that spray- and freeze-dried products had increased enthalpy and entropy values in comparison with the unprocessed material. Spray-dried material is often in the glassy or amorphous phase, *i.e.* in a high energy state (Corrigan, 1995). Since process parameters can be manipulated in order to control the final product, spray drying was employed in this study to produce 100% amorphous carbohydrates. Florence and Salole (1976) showed that the higher thermodynamic activity of the amorphous state of a material (relative to that of the crystalline state) can be manipulated pharmaceutically in order to provide products with preferential solubility profiles, thus resulting in improved biological activity and product efficacy.

The spray drying process involves four main stages, namely, atomisation, spray-air contact, drying of liquid drops and removal of material from the hot air stream. Atomisation is the process of transforming the liquid feed material into small individual droplets. In doing so, the surface area of the material is dramatically increased, aiding the vaporisation of the droplet, which begins immediately upon contact with the hot air. Finally, the dried product is removed form the air steam to a cyclone collection vessel.

The process as a whole and the final product are influenced by many parameters. Inlet temperature alters the rate at which drying proceeds, as it controls the temperature of the drying air. If too high, this will have a detrimental impact on

thermolabile substances, although since the evaporation of water is an endothermic process, the actual temperature of the material does not reach the inlet temperature until its surface is dry. The outlet temperature is that of the air as the particulate material enters the collection vessel, although again this may not be the temperature of the product since vaporisation removes heat from the product. It is important to be aware of factors such as the impact of any residual moisture content on the glass transition temperature of the product, as it is possible for the amorphous glass to transform in to the rubbery phase, facilitating collapse and crystallisation.

Particle size is affected by such variables as the flow rate of the compressed air, which, when increased, will result in reduced particle size, as will increasing the feed rate of the initial liquid. Increasing the concentration of the feed mixture will, however, produce larger and more porous particles. The hollow nature of the spray dried particle is said to give a low bulk density, and its spherical form and relatively narrow particle size distribution often result in free flowing powders advantageous to tabletting (Newton, 1966).

The control over particle size, shape and porosity offered by spray drying is attractive to those who wish to formulate products for delivery to the lung, or for controlled release systems. Spray drying is also employed to produce encapsulated products, biodegradable microparticles and to entrap therapeutic agents such as polymers into materials (Corrigan, 1985).

2.5.4. INSTRUMENTATION

A Buchi 190 mini spray-dried (Buchi, Switzerland) was employed to produce 100% amorphous carbohydrate products.

2.5.5. EXPERIMENTAL

Spray drying was used in order to produce 100% amorphous lactose and raffinose as follows:

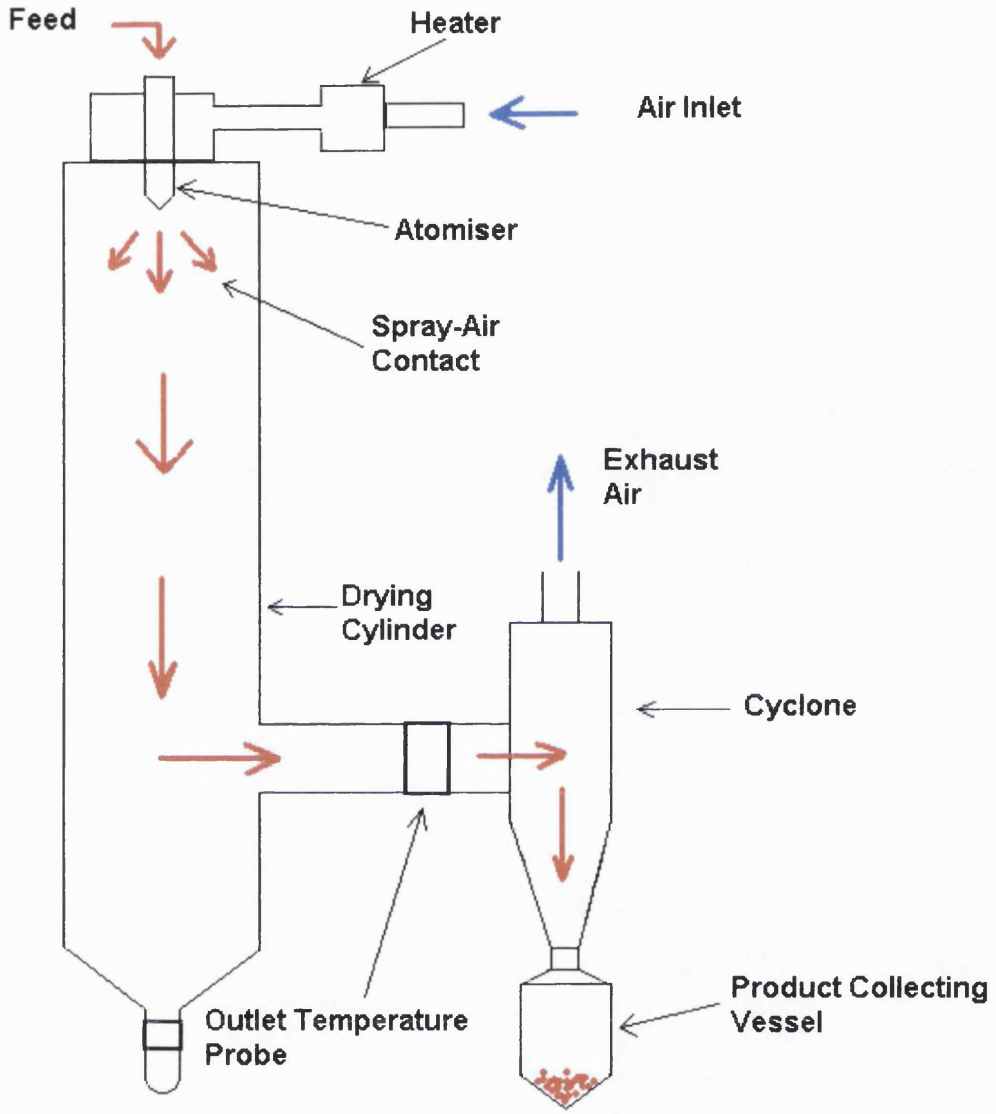

Figure 2.8. *Diagrammatic representation of the Buchi 190 mini spray dryer.*

2.5.3.1. Production of 100% Amorphous Lactose

A 10% w/v solution of amorphous lactose was prepared, and the operating parameters are outlined in Table 2.2. A sample yield of approximately 35% was usually achieved. Confirmation of the amorphous nature of the product was achieved via X-Ray Powder Diffraction (XRPD, Philips, Cambridge, UK). Sample collection was carried out as quickly as possible in order to reduce exposure to the

atmosphere. Storage of the product was either in an evacuated desiccator over Phosphorous Pentoxide, or in a vacuum oven at 50 °C and -300 mbar.

2.5.3.2. Production of 100% Amorphous Raffinose

A 10% w/v solution of amorphous raffinose was prepared, and the operating conditions are outlined in Table 2.2. A sample yield of approximately 35-50% was usually achieved. Confirmation of the amorphous nature of the product was achieved via XRPD (Philips, Cambridge, UK). Sample collection was carried out as quickly as possible so as to reduce exposure of the product to the atmosphere. Storage of the amorphous raffinose was in a vacuum oven (Sanyo-Gallenkamp, UK) at 50 °C and -300 mbar.

Table 2.2 *Operating parameters for the preparation of 100% amorphous lactose and raffinose by spray drying in a Buchi 190 mini spray drier.*

OPERATING PARAMETER		SETTING	
		Lactose	**Raffinose**
Inlet Temperature (°C)		185-190	120-130
Outlet Temperature (°C)		80-90	60-65
Feed Rate (mL/min)		2	2
Pressure (bar)		3	3
Solution Concentration (% w/v)		10	10
Atomiser Air Flow Rate (normliter/h)		400	700
Dials –	Aspirator*	12	5
	Speed*	8	3
	Heat Control*	9.5	3.5

*** signifies dial setting. Average values are shown as adjustment was required to control the other parameters.**

2.6. HEAT DRYING

2.6.3. INTRODUCTION

Heat drying is a process by which the amorphisation of a material may be carried out through the manipulation of temperature and pressure conditions. The application of heat is known to be able to induce disorder in some materials, particularly those in which water may be incorporated so that aqueous ions occupy lattice positions (Hüttenrauch and Keiner, 1979). Thus with progressive drying the corresponding loss of water results in increasing lattice defects. Such dehydration amorphisations have been reported for several materials, *e.g.* α,α-trehalose dihydrate (Ding et al., 1996), β,β-trehalose tetrahydrate (Roberts and Franks, 1996) and raffinose pentahydrate (Saleki-Gerhardt et al., 1995). A completely amorphous product may be achieved which has retained its macroscopic crystalline appearance and original particle size. This technique is not suitable for many materials. In addition it does not offer the scope for optimisation of particle characteristics available with spray drying.

2.6.4. EXPERIMENTAL

For the production of amorphous raffinose, a vacuum oven (Sanyo-Gallenkamp, UK) was employed. A small layer of raffinose pentahydrate was placed in a shallow glass dish in the oven at 100 °C for 24 h at –300 mbar. The product was confirmed amorphous by X-Ray Powder Diffraction (Philips, Cambridge, UK). .

2.7. X-RAY POWDER DIFFRACTION

2.7.1. INTRODUCTION

Processing often results in the disruption or activation of crystal structure, leading to various degrees of disorder in the form of crystal defects and/or amorphous regions. It is important to be able to assess the extent of disorder in a solid quantitatively, and X-Ray Power Diffraction (XRPD) is a widely used technique in such work. Characteristic peak intensities or integrated peak intensities can be

measured, and it is possible to establish a calibration plot with samples of known amorphous contents (Black and Lovering, 1977). Similar measurements on samples of unknown disorder are made in order to assign the corresponding percent disorder using such a calibration curve. However XRPD reflects the average degree of disorder directly detected by measurement throughout the bulk, as opposed to other techniques which may measure characteristics of the material which arise directly from the higher energy state of its amorphous portion (*e.g.* crystallisation by isothermal microcalorimetry). Therefore as the amorphous content decreases, the sensitivity of the technique is reduced, so that it becomes impossible to distinguish a 90% crystalline sample from a 100% crystalline material (Saleki-Gerhardt et al., 1994). Nonetheless, XRPD has become a widely accepted technique to conclude the crystallinity or amorphicity of materials.

2.7.2. EXPERIMENTAL

A Philips PW3710 X-Ray Powder Diffractometer (Philips, Cambridge, UK) was employed for all studies. Approximately 1 g of each sample was loaded into the sample holder, resulting in a powder bed of 2 mm thickness, and scanned at a rate of 5 ° 2Θ/min. All measurements were taken at 45 kV and 40 mA.

2.8. SCANNING ELECTRON MICROSCOPY

2.8.1. INTRODUCTION

Scanning Electron Microscopy (SEM) is a technique which is used to examine the surfaces of structures only. It has a very large depth of field, producing images which have almost a three-dimensional quality. The sizing of very small particles (from 1 μm) may be performed and as such is very useful as a tool for studying spray-dried materials. SEM is also an appropriate technique to study crystal habit.

2.8.2. EXPERIMENTAL

Samples were mounted onto adhesive carbon discs attached to SEM stubs, and coated with gold by sputtering (Emitech K550 sputter coater, Emitech, Kent, UK)

for 4 mins at 30 mA. Scanning electron micrographs were obtained using a Philips L20 SEM (Philips, Eindhoven, Netherlands) (voltages displayed on micrographs).

2.9. Preparation of Saturated Salt Solutions for Maintaining Specified Relative Humidities

2.9.1. Introduction

Air at a given temperature is capable of taking up water vapour until it is saturated (*i.e.* at 100% RH). If the temperature is raised, the air will be capable of taking up more moisture and the relative humidity falls. Relative humidity (%) may be defined as:

$$\frac{\text{Vapour pressure of water vapour in the air}}{\text{Vapour pressure of water vapour in air saturated at the same temperature}} \times 100$$

Saturated salt solutions can be used to maintain specific RHs in closed chambers (Nyqvist, 1983). Table 2.3 outlines the common salts used in this application, and the RHs they provide at various temperatures.

Table 2.3 *Saturated salt solutions and their relative humidities over a range of temperatures. Reproduced from Wade (1980) and Nyqvist (1983).*

Salt	Temperature (°C)					
	20	**25**	**30**	**35**	**45**	**50**
Potassium Sulphate, K_2SO_4	97.6	97.3	97.0	96.7	96.2	95.8
Ammonium-Dihydrogen Orthophosphate, $NH_4H_2PO_4$	93.0	93.0				
Zinc Sulphate, $ZnSO_4{,}7H_2O$	90.0					
Potassium Chloride, KCl	85.1	84.3	83.6	82.9	81.7	81.3
Ammonium Sulphate, $(NH_4)_2SO_4$	81.	80.0	80.0	80.0	79.0	79.0
Sodium Chloride, NaCl	75.5	75.3	75.1	74.8	74.7	74.7
Sodium Bromide, $NaBr{,}2H_2O$		58.0				
Magnesium Nitrate, $Mg(NO_3)_2{,}6H_2O$	54.5	52.8	51.5	50.0	47.1	45.5
Sodium Dichromate, $Na_2Cr_2O_7{,}2H_2O$	54.8	54.4	54.0	53.5	51.8	51.4
Potassium Thiocyanate, KSCN	47.0					

SALT	TEMPERATURE (°C)					
	20	**25**	**30**	**35**	**45**	**50**
Potassium Carbonate, K_2CO_3	44.0	43.0	43.0	43.0	42.0	
Magnesium Chloride, $MgCl_2,6H_2O$	33.1	32.8	32.4	32.0	31.1	30.5
Potassium Acetate, $KC_2H_3O_2$	23.0	22.0	22.0	21.0	20.0	
Lithium Chloride, LiCl	11.3	11.3	11.3	11.2	11.2	11.1

2.9.2. EXPERIMENTAL

Saturated salt solutions were prepared adding distilled water to the particular salt, whilst ensuring that an excess of salt remained at the bottom of the container. The quantity of salt and water used depended on the solubility of the salt and the final solution volume required. The solutions were heated to 20 °C higher than the temperature of their intended use, and stirred for 20 minutes. They were then slowly cooled whilst continuing to be stirred, ensuring that by the time they reached their final temperature, excess salt still remained. Storage of these solutions was at the temperature at which they were to be used.

2.10. PREPARATION OF PARTIALLY AMORPHOUS LACTOSE SAMPLES

Quantities of dried amorphous and crystalline lactose were sieved to produce a particle size of less than 425 μm and then accurately weighed and combined to produce powder mixes of 0-10% w/w amorphous lactose, increasing in increments of 1%. The samples were subsequently mixed in a Turbula mixer (Basel, Switzerland) for twenty minutes to ensure a homogeneous amorphous content. Storage of the product was either in an evacuated desiccator over Phosphorous Pentoxide, or in a vacuum oven at 50 °C and -300 mbar.

2.11. MATERIALS

Table 2.4 *Materials used and their suppliers and batch numbers.*

MATERIAL	SUPPLIER	BATCH NO.
Lactose Monohydrate	Borculo Whey Products UK Ltd., Saltney, Cheshire, UK.	SD B23416
Raffinose Pentahydrate	Pfanstiehl Laboratories Inc., Waukegan, IL., USA.	24887A
Sodium Chloride	BDH Lab Supplies, Poole, Dorset, UK.	K27808133
Lithium Chloride	Sigma, Poole, Dorset, UK.	118H0314
Magnesium Chloride	BDH Lab Supplies, Poole, Dorset, UK.	TA480433
Potassium Carbonate	Sigma, Poole, Dorset, UK.	68H3641
Sodium Bromide	Sigma, Poole, Dorset, UK.	114H0274
Phosphorous Pentoxide	Lancaster, Morecombe, Lancs, UK.	10048993
Silica Gel	BDH Lab Supplies, Poole, Dorset, UK.	K28810214
Absolute Alcohol (Ethanol 99.7 – 100% v/v)	BDH Lab Supplies, Poole, Dorset, UK.	L131610
Acetone General Purpose Reagent	BDH Lab Supplies, Poole, Dorset, UK.	K29322705

Purified water was obtained from a USF ELGA water purifier (option 4).

CHAPTER THREE

THE APPLICATION OF NEAR INFRARED SPECTROSCOPY AND DYNAMIC VAPOUR SORPTION IN COMBINATION TO QUANTIFY LOW AMORPHOUS CONTENTS IN CRYSTALLINE LACTOSE

3.1. AN INVESTIGATION OF THE CRYSTALLISATION OF AMORPHOUS LACTOSE BY DYNAMIC VAPOUR SORPTION AND NEAR INFRARED SPECTROSCOPY

3.1.1. INTRODUCTION

3.1.1.1. Pharmaceutical Applications of Gravimetric Vapour Sorption

Many of the analytical techniques available to the pharmaceutical industry to investigate the effects of processing on powder properties are unable to differentiate between materials which have been shown to behave differently. A reason for this is that the changes invoked by processing have their greatest effect on the surface of powder particles. Therefore, surface interactions of the material can be dramatically affected, despite the disrupted material occupying only a small proportion of the bulk. The majority of techniques assess bulk properties, *e.g.* X-Ray Powder Diffraction (XRPD), and are therefore incapable of detecting the presence of this material on the particle surface. Gravimetric vapour sorption, however, has been shown capable of such differentiation since it is primarily a surface technique. Kontny et al. (1987) compared the water vapour sorption of ground and unground water-soluble crystalline salts, and found that processing induces subtle changes to the surface of materials which changes their reactivity to water. They found that ground samples were capable of sorbing more water than their unground counterparts at low RHs, and that a relatively small degree of water sorption by the ground samples led to specific surface area decreases which were caused by surface dissolution and crystallisation. Buckton and Darcy (1995) were able to differentiate between the adsorption of water by totally crystalline and 0.05% w/w amorphous lactose at elevated RHs.

Water vapour sorption has been used in order to assess the physical stability of many pharmaceutical systems. Forbes et al. (1998) and Costantino et al. (1998) exposed protein-sugar systems to elevated RHs and looked for inhibition of crystallisation as evidence of protein stabilisation by the carbohydrate. Tzannis and Prestrelski (1998)

used water sorption as a probe in order to examine the hydrogen bonding between a protein and sucrose, and determined that the optimal bonding network for stabilisation of the protein occurs at low sucrose concentrations.

Water sorption has been used to study amorphous and partially amorphous materials, *e.g.* sucrose (Saleki-Gerhardt et al., 1994), raffinose (Saleki-Gerhardt et al., 1995), salbutamol sulphate (Ward and Schultz, 1995) and lactose (Buckton and Darcy, 1995, 1996, Darcy and Buckton, 1997). It is possible to follow the crystallisation event since a mass loss representing the expulsion of plasticising water is observed upon reorganisation of molecules into the crystal lattice. The potentiation or inhibition of crystallisation by additives has also been investigated. Stubberud and Forbes (1998) examined the ability of polyvinyl pyrrolidone (PVP) to delay the onset of crystallisation in lactose, determining that it acts as an 'internal desiccant', preferentially absorbing water and thus preventing plasticisation of the carbohydrate. They also found that colloidal silicon dioxide, a non-hygroscopic excipient, accelerated the crystallisation event by isolating and deaggregating the amorphous lactose. The work carried out to date using gravimetric vapour sorption illustrates the advantages of this surface technique in characterising materials and their interactions with the vapour phase.

3.1.1.2. Pharmaceutical Applications of Near Infrared Spectroscopy

The near infrared (NIR) region of the absorption spectrum was the first non-visible region to be discovered. However, since it lacks the ability of mid infrared (MIR) spectroscopy to identify samples by mere inspection of spectra, the pharmaceutical industry has been slow to adopt the NIR technique. The near infrared regions lies between the visible and MID regions of the electromagnetic spectrum, spanning the wavelength range 780 – 2526 nm. Light absorption in this region is primarily due to overtones and combinations of fundamental vibration bands occurring in the MIR region. For infrared light to be absorbed, its energy must be high enough to produce vibrational transitions in the molecules concerned, *i.e.* the light frequency should be

identical to the fundamental vibration frequency for a specific molecule and the molecule should undergo a change in its dipole moment by virtue of its fundamental vibration. The low molar absorptivity of NIR bands permits operation in reflectance mode and hence the recording of spectra of solid samples with minimal or no sample pre-treatment. NIR spectroscopy has aroused growing interest in recent years due to instrument developments (*e.g.* improved detectors, fast-scan instruments and fibre-optic probes) and advances in mathematical software for processing NIR spectra.

NIR spectra are a function of both the chemical and physical properties of the sample, rendering it a highly useful tool in physical characterisation and the determination of physical parameters. This can be a disadvantage if the aim is to identify a product in which physical appearance is not important, or to quantify a chemical component. In such cases, mathematical pre-treatment of spectra can be used to minimise physical effects (Aucott et al., 1988, Hailey et al., 1996). Such treatments include normalisation, derivatisation and multiplicative scatter correction.

NIRS has a number of advantages over other analytical techniques. These include the rapidity of analysis, with 20-40 seconds often being sufficient to collect a spectrum. Little or no sample preparation is required, and the technique is equally suited to solid or liquid samples. It is both non-invasive and non-destructive, and quartz and glass are transparent to NIR light. Pharmaceutical applications of NIR spectroscopy are diverse. They have included the differentiation between amorphous and crystalline forms of a drug (Dreassi et al., 1995), the detection of polymorphs of a drug (Aldridge et al., 1996), the monitoring of polymorphic conversion (Norris et al., 1997) and the qualitative control of a dimorphic analgesic (Gimet and Luong, 1987). The development of fibre optic probes has facilitated the monitoring of bulk materials during product manufacture and processing in order to obtain on-line information, *e.g.* achieving a suitable drying end-point.

The determination of moisture content by NIRS is facilitated by the presence of five absorption maxima in the NIR spectrum, at 760, 970, 1190, 1450 and 1940 nm respectively, although these positions can be slightly affected both by temperature changes (Lin and Brown, 1992) and hydrogen bonding between the analyte and matrix (Sinsheimer and Poswalk, 1968). The bands at 760, 970 and 1450 nm correspond to the first three overtones of O-H stretching bands, whilst the other two bands result from combinations of O-H oscillations and stretching.

Kirsch and Drennen (1996) have demonstrated the applicability of NIRS as a simple, non-destructive and cost effective means for the monitoring of polymer film thickness in the film coating process. Kreft et al. (1999) have used NIRS to differentiate between PVP type, and they have shown the method to be rapid, reliable and non-destructive, and more favourable than the conventional method of characterisation by viscosity in water.

Lactose has also been investigated by NIRS. The crystallisation of amorphous lactose has been followed, using equilibrium vapour sorption at room temperature for various periods of time at different relative humidities (RHs) (Buckton et al., 1998). Real time crystallisation has been followed by NIRS using the combined DVS/NIRS apparatus (Lane and Buckton, 2000) in order to show that the combined apparatus operates to a high performance standard, as the data generated for each technique in combination are comparable with those generated by each technique independently.

3.1.2. Aims of this Study

As already stated, the crystallisation of amorphous lactose has been followed both by DVS and NIRS (Lane and Buckton, 2000). This study aimed to couple the information provided by both techniques in order to gain a greater understanding of the crystallisation of carbohydrates, especially in terms of determining the point of onset of crystallisation, and the duration of the event.

3.1.3. EXPERIMENTAL

3.1.3.1. Preparation of 100% Amorphous Lactose

100% amorphous lactose was prepared by spray drying as outlined in Section 2.5.3.1. Confirmation of the amorphous nature of the yield was obtained from XRPD, and the characteristic crystallisation peak was observed by Isothermal Microcalorimetry at 75% RH.

3.1.3.2. Dynamic Vapour Sorption

The crystallisation of 100% amorphous lactose was carried out in a DVS apparatus (Surface Measurement Systems, UK) (Section 2.3.). Samples of approximately 30-40 mg were dried at 0% RH at 298K for six hours. Following drying, samples were exposed to an elevated RH of 75% at 298K for ten hours in order to induce plasticisation, crystallisation and mutarotation. Subsequent to this step, samples were again dried at 0% RH for six hours.

3.1.3.3. Near Infrared Spectroscopy

NIR spectra of 100% amorphous lactose samples were recorded (Foss NIRSystems, Maryland, USA) (see section 2.3.) throughout the duration of the experiment at each RH environment. Mathematical processing of the spectra was carried out in order to eliminate multiplicative interferences of scatter and particle size by performing a Standard Normal Variate (SNV) transformation. The second derivative of the spectra was then calculated, and these treated spectra were then examined in order to assess the onset of plasticisation, crystallisation and mutarotation.

3.1.4. RESULTS AND DISCUSSION

A typical DVS experiment (at 298 K) for the drying and crystallisation of amorphous lactose is shown in Figure 3.1. A sample of 100% amorphous lactose (approximately 31.5 mg) was exposed to steps of 0% RH for 360 mins, 75% RH for 600 mins and finally another 0% RH step for 360 mins. SNV second derivative NIR

absorbance spectra were recorded every 10 mins throughout the duration of the experiment. It should be pointed out that in the second derivative, only negative peaks are of interest, as they correspond directly with positively displaced peaks in the original spectrum. Any upward baseline shift is excluded.

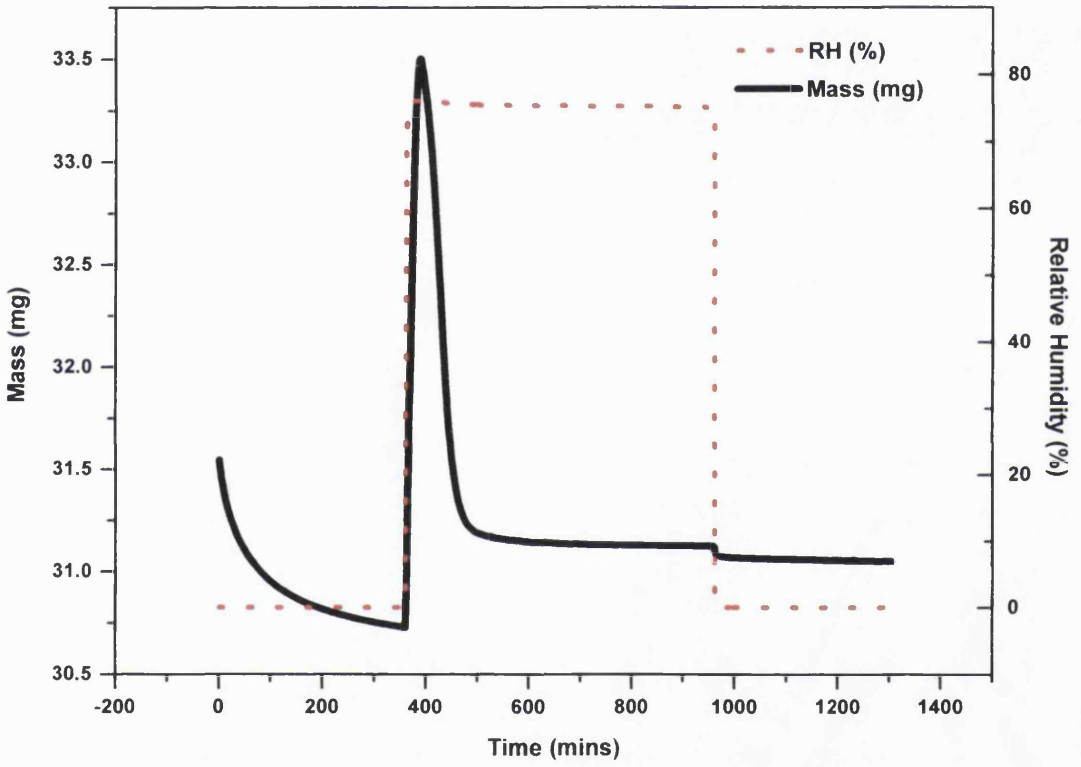

Figure 3.1 *DVS plot showing the drying and crystallisation of 100% amorphous lactose. The characteristic water uptake and expulsion is illustrated.*

3.1.4.1. Drying

The NIR spectra corresponding to the drying of amorphous lactose are illustrated in Figure 3.2. Notable changes were observed in several regions, particularly in the vicinity of 1440 and 1930 nm, which are two peaks relating to the first overtone –OH and the –OH deformation combination respectively. Peak intensity was seen to

increase at the former and decrease at the latter, as water which had been previously been absorbed into the amorphous structure during either spray drying or storage was removed.

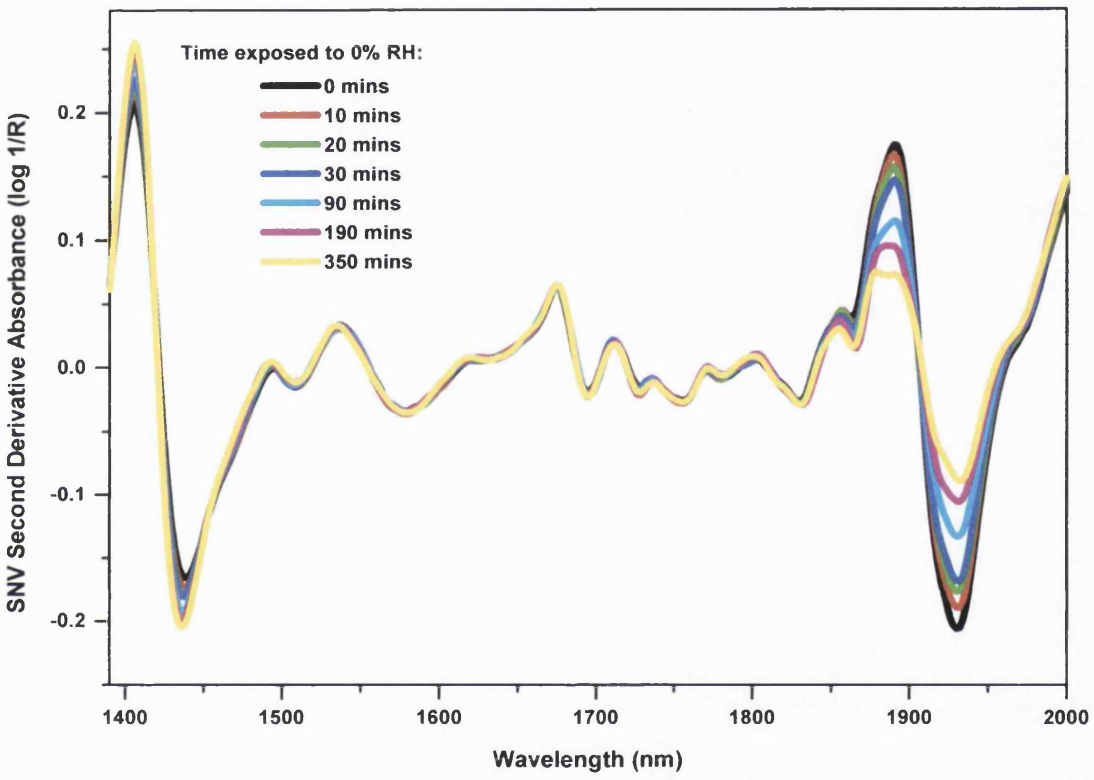

Figure 3.2 *SNV second derivative NIR absorbance spectra representing the drying of 100% amorphous lactose. The regions of interest are the (negative) peaks located at 1440 and 1930 nm, which correspond to the first overtone -OH and the –OH deformation combination respectively.*

3.1.4.2. Wetting and Plasticisation

After the drying step shown in Figure 3.1, the sample was exposed to 75% RH. Immediately, a sharp mass increase was observed as the sample absorbed significant quantities of water vapour from the atmosphere. It is known that the absorption of water induces plasticisation of the amorphous phase, lowering the glass transition

temperature of the material. From the Gordon-Taylor Equation (Gordon and Taylor, 1952) (Equation 3.1), the amount of water required to reduce the T_g of lactose to 298 K (the experimental temperature) can be calculated from the proportion of lactose to water that is present in the binary system at that temperature.

$$T_g = \frac{w_1 T_{g1} + k w_2 T_{g2}}{w_1 + k w_2} \qquad \text{.....Equation 3.1}$$

Where:

$T_{g\,mix}$ = T_g of a mixture containing components 1 and 2

T_{g1} = T_g of component 1

T_{g2} = T_g of component 2

w_1 = weight fraction of component 1

w_2 = weight fraction of component 2

k = a constant, and a measure of the free volume contributed to the mixture by each of its components at any temperature, defined as:

$$k = \frac{\rho_1 T_{g1}}{\rho_2 T_{g2}} \qquad \text{..... Equation 3.2}$$

Where:

ρ_1 = density of component 1

ρ_2 = density of component 2

An estimate of k (6.56) is available from the literature (Roos, 1993), the glass transition temperature of lactose has been found experimentally to be 114 °C (Schmitt et al., 1998), and the T_g of water is –138 °C (Sugisaki et al., 1968). From these values, the weight fractions in the binary mixture which has a T_g of 25 °C may be determined as 0.92 and 0.08 for lactose and water respectively.

From the DVS data it can be seen that the mass of the dried lactose sample was 30.73 mg. Therefore, the sample needed to achieve a mass of 33.40 mg in order for its glass transition temperature to have reached 298 K, according to the Gordon-Taylor Equation. In fact, the sample achieved a maximum mass of 33.50 mg (after 28 mins at 75% RH), which is in excellent agreement with the equation. It has previously been assumed that the onset of crystallisation may be determined as the point at which expulsion of water commences (Buckton and Darcy, 1996). These data are in agreement with this, implying that the sample in Figure 3.1 underwent only wetting and plasticisation on the up-slope of the DVS plot at 75% RH.

To date it has not been possible to determine the exact mechanism of crystallisation. Although it has been stated that the crystallisation process is spontaneous (Buckton and Darcy, 1995a) the point of onset of crystallisation during the water uptake and expulsion pattern has not been exactly determined. Examination of the NIR spectra in the regions of the peaks at 1440 nm and 1930 nm showed that the first 30 mins of exposure to elevated RH saw a reversal of the effects of drying on the spectra, as would be expected. However, the amount of water absorbed far exceeded the residual moisture content of the initial amorphous sample, and therefore the changes observed extended far beyond those seen during the drying step. This is in good agreement with the DVS findings already stated. It is interesting to note that the trend observed in this study in the region of 1440 nm differs from that noted in the study by Buckton et al. (1999), where the spectra of samples stored in several humidity environments for prolonged periods of time were examined (drying was not investigated). It was stated that with increased exposure to elevated relative humidities (between 33% and 58% RH), the peak at 1440 nm, representing absorbed water, increased in size and displaced to lower wavelengths. The increase in intensity of the peak was said to be due to increased quantities of absorbed water, whilst the change in wavelength was attributed to changes in median interaction energy. In this study, drying was seen to increase the peak's intensity, and the opposite occurred with wetting. It is possible that the spectral changes noted by

Buckton et al. (1999) were related at least in part to the prolonged exposure of amorphous samples to elevated RH without undergoing crystallisation. In this study, the onset of crystallisation occurred after approx. 30 mins exposure to 75% RH, and thus may have preventing such changes from occurring. In a study using the combined DVS/NIRS apparatus, Lane and Buckton (2000) reported the same spectral trends as have been noted in this study, supporting the suggestion that the different experimental set-up may be responsible for the different findings.

Drying was seen to displace the peak at 1440 nm to a lower wavelength, and wetting to a higher wavelength, which again is the opposite of the trends observed by Buckton et al. (1999). It is possible that this also reflects a change in the median energy of the interaction, but that since the samples in this study are not undergoing the degree of collapses seen in that study, the interaction with water is of a different nature. Here, the driest amorphous sample showed a peak at 1436 nm, whilst when wet, the peak moved to 1440 nm. The peak at 1933 nm moved to a lower wavelength as the sample absorbed water, as observed by Buckton et al. (1999).

The first spectral changes which hinted at an effect of water beyond that of wetting were seen not at the two major peaks already mentioned, but elsewhere in the spectra, and were more subtle. Following approximately 20 mins exposure to 75% RH (equivalent to a water uptake of 2.5 mg, or 7.46 % w/w), a small shoulder developed on the (negative) peak at 1436 nm, and between approximately 1500-1550 nm, the spectral pattern changed (Figure 3.3). In addition, the peak at 1576 nm shifted to 1587 nm after half an hour at the elevated RH. Between approximately 1725 – 1800 nm, shifts in the spectra were again observed. And finally, the peak at 1930 nm again began to decrease in intensity after 20 mins at 75% RH. It is possible that these changes were associated with the plasticisation of the sample, or even the onset of crystallisation in a portion of the sample.

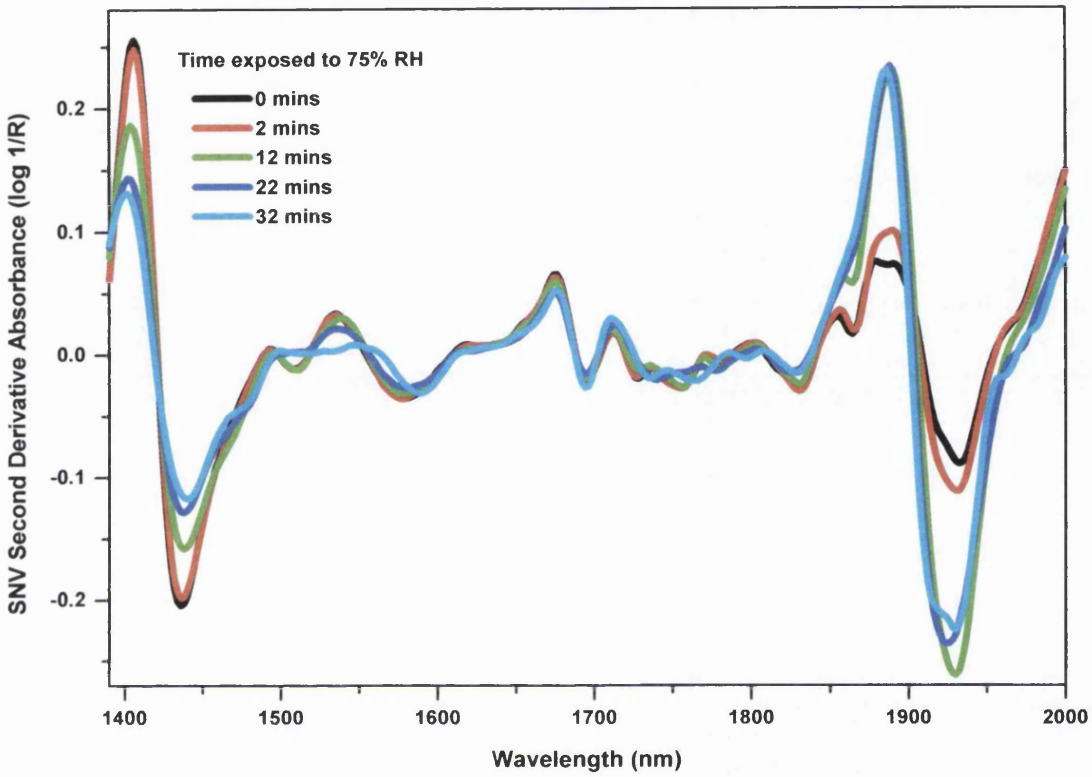

Figure 3.3 *SNV second derivative NIR absorbance spectra for 100% amorphous lactose during its first 30 mins exposed to 75% RH. Initial spectral changes indicated a wetting effect consistent with a reversal of the changes observed during drying. However, after approximately 20 mins at the elevated RH, changes in the spectral pattern emerged.*

3.1.4.3. The Crystallisation Process

It was only subsequent to the first half hour at 75% RH that considerable spectral changes were evident, consistent with the onset of crystallisation itself (Figures 3.4 and 3.5). This would indicate that water sorption sufficient to reduce the glass transition temperature to below 298 K had taken place. This is consistent with the DVS data, which showed that the sample required 28 mins at 75% RH in order to achieve its maximum mass. From this point a decrease in mass was measured,

indicating that expulsion of water was occurring as the sample underwent crystallisation.

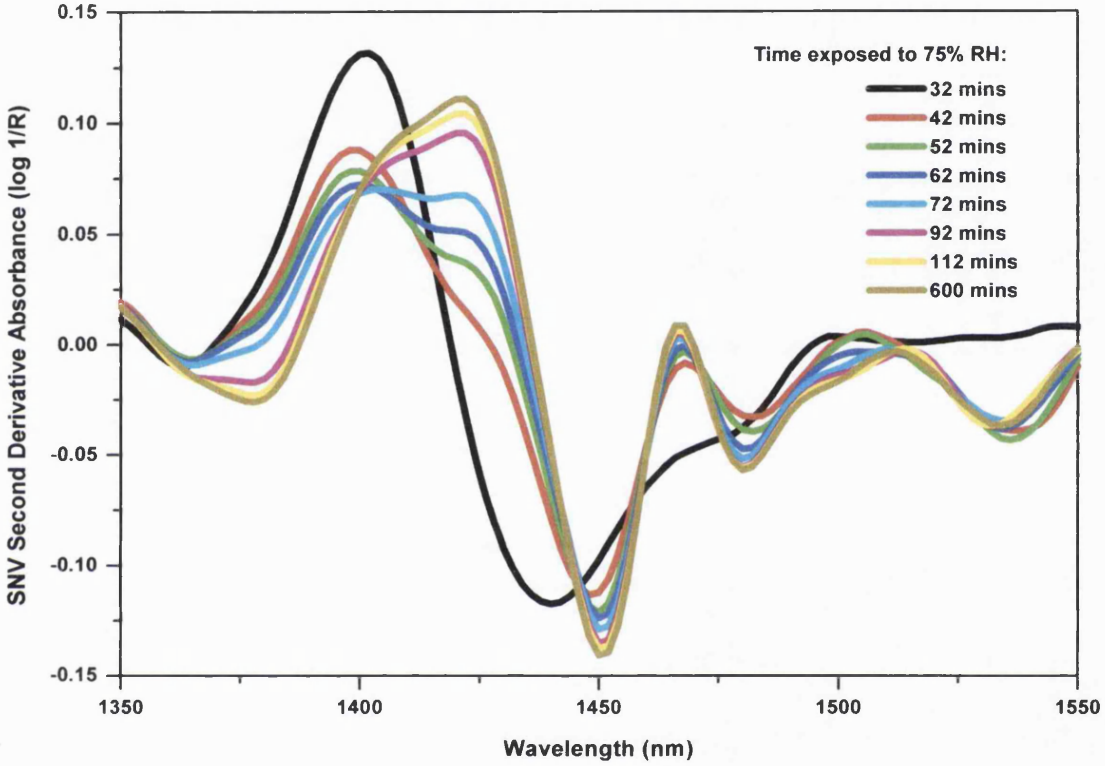

Figure 3.4 *SNV second derivative NIR absorbance spectra representing the crystallisation of amorphous lactose in the region of the first overtone –OH. A shift in the peak from 1440 to 1450 nm was clear, and this new peak may be termed a sharp monohydrate peak.*

In association with the expulsion of water, considerable spectral changes were now underway. Figures 3.4 and 3.5 show the spectra of crystallising lactose in two regions. Figure 3.4 clearly illustrates that the amorphous water peak at 1436 nm relocated to 1450 nm. The initial peak was broad, representing the spread of energies of interaction for absorbed water in the amorphous sample. The relocated

peak has been described as a sharp monohydrate water peak (Buckton et al., 1999). It represents the more uniform interaction present in the crystalline material and it clearly grew in intensity as increasing quantities of amorphous lactose underwent crystallization. Having first appeared after approximately 40 mins exposure to 75% RH it continued to intensify for a further 70 mins. From this point, despite continued exposure to elevated RH for several hours more, no further change was observed here. Two new peaks were seen to develop in this region, the first at 1480 nm, and the second, and most notable, at 1535 nm, during the same time scale as the other changes observed (*i.e.* between approximately 40 and 100 mins at 75% RH).

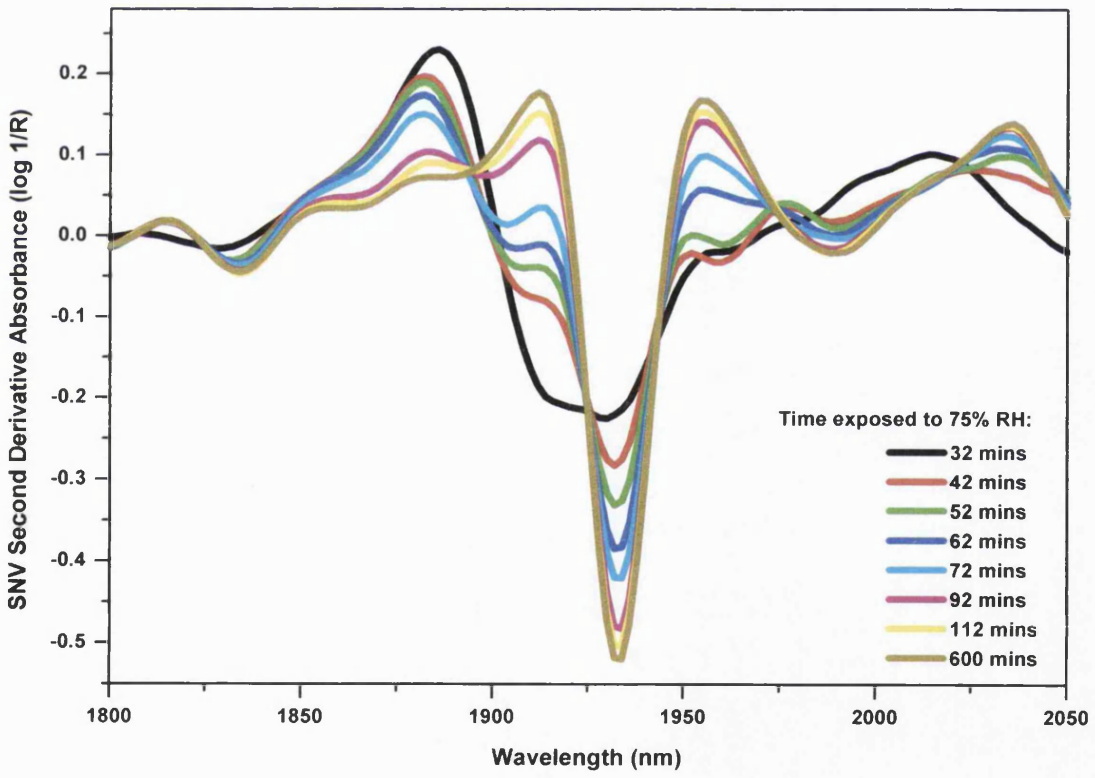

Figure 3.5 *SNV second derivative NIR absorbance spectra for the crystallisation of amorphous lactose in the region of the –OH deformation combination. The development of several distinct spectra features can be noted, most obviously the sharp peak at 1930 nm.*

The peak in the region of 1930 nm (Figure 3.5) indicates the extent of crystallisation. With the onset of crystallisation, the peak for the remaining absorbed water shifted to a higher interaction energy (at 1904 nm) indicating a clear transition. In fact, the spectrum representing the sample after 32 mins at 75% RH seemed to show evidence of both the absorbed water peak at 1930 nm, and the early formation of a new peak. This monohydrate peak at 1934 nm was then seen to develop (Figure 3.5), much in the same way as the peak at 1440 nm. It grew in intensity until the sample had been exposed to 75% RH for approximately 110 mins, and then, despite continued exposure to elevated humidity for several hours more, the peak ceased to develop further.

An area of confusion in the crystallisation process concerns the progress of water sorption and desorption. It is possible that crystallisation, and thus desorption, commenced before a mass loss was observed, but that it was disguised by the continued absorption of water by the remaining amorphous portion of the sample. In keeping with this then is the possibility that water sorption had not ceased by the time the loss in mass was observed. It could be that those parts of the sample which had undergone crystallisation expelled water which was absorbed by the remaining amorphous material in the sample, thus facilitating its crystallisation.

3.1.4.4. Mutarotation

Buckton et al. (1999) discussed the use of NIRS in determining the proportions of α- and β-lactose in a sample, and found that characteristic peaks exist in the region of approximately 2050-2150 nm which aid this determination. The dry spray-dried amorphous lactose sample in this study did not exhibit any notable peaks in this region, as shown in Figure 3.6. This is in agreement with the findings of Lane and Buckton (2000). However, after 32 mins at 75% RH, a time which would appear from both the DVS and NIRS data to correspond to that at which crystallisation commenced, peaks at 2092 and 2116 nm appeared. This corresponds to the spectrum shown by Buckton et al. (1999) for a sample which had just started to crystallise. After 42 mins at 75% RH, the peak at 2092 nm had further developed

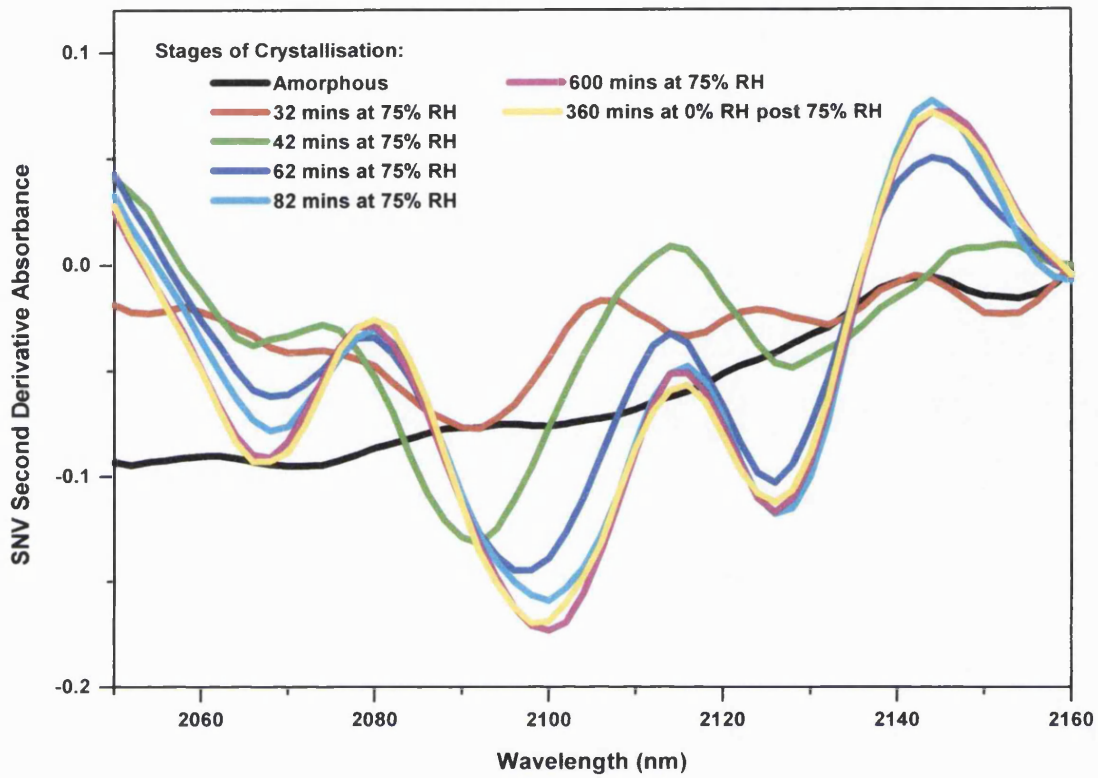

Figure 3.6 *SNV second derivative NIR absorbance spectra for the lactose sample prior to, during and after crystallisation, in the region where mutarotation could be detected.*

(Figure 3.6). This peak has been shown to correspond to the α-monohydrate form (Buckton et al., 1999). With time, these peaks were seen to move to occupy higher wavelengths until, after 82 mins at 75% RH, they had reached their final location at 2100 nm and 2126 nm respectively. This is in good agreement with a β-lactose spectrum (Buckton et al., 1999), which shows characteristic peaks in the second derivative NIR absorbance spectrum at 2104 nm and 2126 nm, due to O-H deformation and C-H stretching. Lane and Buckton (2000) also showed very similar spectral changes. This would imply that mutarotation from the α- to the β-form was occurring. It has been shown elsewhere (Briggner et al., 1994) that upon

crystallisation, lactose forms a mixture of the α- and β-forms. Angberg et al. (1991) have shown that mutarotation occurs in the direction of the β- to the α-form, and that slow incorporation of hydrate water occurs. It is therefore unlikely that in this situation the sample mutarotated from the α- to the β-form. Throughout the duration of the experiment, strong monohydrate peaks were present at both 1930 nm and 1450 nm, confirming the presence of the α-form. It is likely that what was present throughout crystallisation and subsequent drying is a mixture of the two crystalline forms. After approximately 1.5 hours at 75% RH the spectra ceased to change in this region, indicating that if further mutarotation occurred, it was not detectable by NIRS. It is possible that the NIR response for the β-from masked the response for the monohydrate in the proportions that were present in the sample.

3.1.4. CONCLUSIONS

This work has shown that the coupling of two techniques to provide simultaneous information on a process can lead to further understanding of the events taking place. The use of DVS/NIRS in combination has helped elucidate the underlying events which occur during the crystallisation of amorphous lactose, a model carbohydrate. From these data, it can be seen that despite a rapid uptake of water by the sample subsequent to exposure to 75% RH, it is only wetting and plasticisation which occurs for almost half an hour (this time will be dependent on sample size). Furthermore, despite continued exposure to elevated relative humidity for ten hours, it would appear that crystallisation was complete within approximately two hours. DVS data indicate that the expulsion of plasticising water ceased after approximately 160 mins at 75% RH, showing that crystallisation is not an instantaneous process.

3.2. QUANTIFICATION OF AMORPHOUS CONTENT BY DYNAMIC VAPOUR SORPTION AND NEAR INFRARED SPECTROSCOPY IN PREDOMINANTLY CRYSTALLINE SAMPLES

3.2.1. INTRODUCTION

3.2.1.1. Conventional Approaches to Determining Amorphous Content

It is known that some pharmaceutical processing techniques, *e.g.* milling (Hancock and Zografi, 1997), can induce changes in the crystallinity of materials, rendering them partially amorphous. As discussed in Chapter 1, it is also widely accepted that amorphous material induced in this way, although perhaps occupying only a very small proportion of the bulk, may contribute greatly to the behaviour of that material as it resides primarily on the particle surface. The relative advantages and disadvantages of amorphous material have been discussed, and relate to issues such as solubility and chemical and physical stability. The effects of imparting a crystalline material with even very small amounts of amorphous content can be dramatic, resulting in reduced flow, increased hygroscopicity and the potential of the material to revert to the more stable crystalline state over time, causing agglomeration and increased particle size. It is therefore a necessity to be able to detect and quantify this material in order to achieve process control and consistency of product behaviour. Often however, this amorphous phase may occur at only a few percent of the total weight by mass, and is thus difficult to detect.

Until recently, the lower detection limit for amorphous content lay in the region of approximately 10% w/w, with X-Ray Powder Diffraction and Differential Scanning Calorimetry being among the most widely used techniques in the quantification of amorphous content (Saleki-Gerhardt et al., 1994). Density (Duncan-Hewitt and Grant, 1986), enthalpy of solution (Pikal et al., 1978), infrared spectroscopy (Black and Lovering, 1977) are among the other techniques that have been exploited in order to ascertain amorphous content, and FT-Raman Spectroscopy (Taylor and Zografi, 1998) has been found capable of quantifying the degree of crystallinity of

indomethacin to a lower limit of detection of either 1% w/w amorphous or crystalline content.

Sebhatu et al. (1994) looked at the application of isothermal microcalorimetry to assess the degree of disorder in crystalline solids, and determined that the technique was capable of detecting at least 2% w/w amorphous material in α-lactose monohydrate. A similar study (Briggner et al., 1994) reported that it should be possible to quantify the amorphous content of a partially amorphous lactose sample by isothermal microcalorimetry with a resolution of at least 1% w/w, down to a level of 1% w/w amorphous content, although a full calibration was not carried out, and the lowest amorphous content investigated was 3% w/w. A further study (Buckton et al., 1995) attempted to determine the lower limits of detection of the technique, and illustrated that it is possible to detect 0.313% w/w amorphous content (again in lactose). Quantification of low amorphous content by isothermal microcalorimetry has been impeded by several factors. In such small incidences of amorphous content, the crystallisation event commences before system equilibration, which prevents accurate integration of the peak and determination of enthalpy of crystallisation. In order to overcome this, increased sample loading has been investigated. However it would seem that when sufficient sample is present to prevent premature crystallisation, the events which together make up the crystallisation process (*e.g.* water uptake, molecular reorganisation, expulsion of plasticising water and mutarotation) become prolonged and extracted, resulting in a peak with several phases and which results in an enthalpy of crystallisation which is not comparable with those peaks of samples of greater disorder.

Gravimetric studies have also been undertaken in order to ascertain the lower limit of detection of amorphous content. Buckton and Darcy (1995) found that as little as 0.05% w/w amorphous lactose could be detected, and they suggested that it would be possible to correlate residual weight change (due to the inclusion of a hydrate molecule into the crystallised material) with the original amorphous content of the

material, although subsequently it has been shown that this relationship is not linear, due to the crystallisation the amorphous phase to varying proportions of both the α-monohydrate and β-anhydrous species (Buckton and Darcy, 1999).

3.2.1.2. The Use of Gravimetric Vapour Sorption in Quantitative Analysis

Quantification of amorphous content has been attempted by gravimetric vapour sorption. As has already been stated, Buckton and Darcy (1995) found that amorphous material crystallised to form hydrate water, the amount of which is measurable by mass increase. However this relationship is not linear for lactose, due to the formation of both the α-monohydrate and β-anhydrate forms in varying proportions. Saleki-Gerhardt et al. (1995) found a degree of correlation between water loss on drying by raffinose pentahydrate (attributed to loss of hydrate water) and estimated amorphous content. They also investigated water vapour sorption by amorphous/crystalline mixes, finding that a linear relationship between increased water uptake and degree of disorder exists, although at amorphous contents of less than 20% and greater than 80% w/w, a deviation from linearity is observed. Since these initial investigations there has been little progress in using gravimetric vapour sorption to quantify amorphous content. Therefore another approach is required in order to accurately quantify disorder, particularly in predominantly crystalline samples.

3.2.1.3. The Use of Near Infrared Spectroscopy in Quantitative Analysis

The applications of NIRS in quantitative analysis are wide and varied. Moffat et al. (2000) have used NIRS to determine the water content of intact paracetamol tablets, whilst the technique has also been used to determine the residual moisture content of lyophilised sucrose (Kamat et al., 1989). Lonardi et al. (1989) employed NIRS to determine the concentration of active ingredient and the moisture content of antibiotic powders. Seyer et al. (1997) have used second derivative NIR spectra to quantify small amounts of amorphous material in crystalline samples.

3.2.2. AIMS OF THIS STUDY

Through the recording of NIR spectra of dried partially amorphous samples, this study aimed to establish the limits of NIRS in quantifying the amorphous content of predominantly crystalline samples. A further objective of this work was to determine the extent of water sorption and desorption by such samples in the DVS and to correlate those values with the amorphous content of the samples

3.2.3. EXPERIMENTAL

3.2.3.1. Preparation of Partially Amorphous Lactose Samples

Partially amorphous samples of between 0-10% w/w amorphous content were prepared as described in Section 2.10, increasing in increments of 1% w/w. They were stored over phosphorous pentoxide at room temperature prior to use, to ensure the absence of large quantities of water vapour and prevent changes occurring in the amorphous material.

3.2.3.2. Dynamic Vapour Sorption

Gravimetric studies of the amorphous lactose mixes were carried out in a DVS apparatus (Surface Measurement Systems, UK) (Section 2.3.). Samples of approximately 35-40 mg were dried at 0% RH and 25 °C. Complete drying of samples was generally achieved within six hours, although it was possible to monitor and adjust this drying time as required. Following drying, samples were exposed to an elevated RH of 75% at 25 °C, so as to induce crystallisation.

In order to quantify the amorphous content of predominantly crystalline samples, the mass change during the water sorption phase at 75% RH was recorded as rate of change of mass (dm/dt) as a function of time. The area under the curve was calculated and recorded as the mass of water sorbed. As crystallisation progressed, water was rapidly expelled from the sample. This water desorption was also recorded as dm/dt against time and the mass of water desorbed determined. A total of 28 samples were used in this study.

3.2.3.3. Near Infrared Spectroscopy

When no further mass loss could be recorded for the partially amorphous samples, a NIR spectrum was recorded (Foss NIRSystems, Maryland, USA) (see section 2.3.), whilst still exposed to 0% RH. NIR spectra typically contain broad, overlapping bands that cannot always be ascribed to an individual sample component. Therefore, a calibration sample set must be selected which is representative of the entire sample set. Mathematical processing of all the spectra in the set is carried out in order to eliminate multiplicative interferences and determine any correlation that exists between the samples and, in this instance, their known amorphous contents. The multiple linear regression (MLR) technique for generating the calibration equation was selected for this purpose. It is an effective calibration approach when the relationship to be established is linear, spectral noise is low and there is no interaction between sample components. The calibration model established must then be validated by applying it to the spectra of a different set of samples.

A NIR absorbance spectrum for each dry sample was entered into the Vision® database along with its actual amorphous content (termed the reference value) known from sample preparation. These were treated mathematically by performing a Standard Normal Variate (SNV) transformation to remove multiplicative interferences of scatter and particle size. The first derivative was then calculated, which enabled enhancement of peak resolution (segment size of 10 nm and a gap size of zero data points). The spectra of the 28 dried amorphous samples used in this study (taken at the end of the drying step at 0% RH in the DVS) were randomly assigned to two groups in a 60:40 ratio - the former group forming the calibration set from which the model was to be built, and the latter the validation set upon which the model was to be tested. A forward search MLR was applied to the data in the calibration set using the Vision® software. It is designed to scan all wavelengths and select the one at which the best correlation for the samples between their actual amorphous contents (reference values) and SNV first derivative NIR absorbance. Due to the number of samples included in the study, it was possible to use up to

three individual wavelengths to establish the calibration model, since one wavelength may be selected per ~10 samples available (in both groups). Using more than three wavelengths in the calibration equation would have increased the risk of overfitting the data. The model built formed a calibration equation, the reliability of which was tested upon the validation set. In addition, in order to ascertain the effect, if any, of different batches of spray dried material, a third external batch of 10 samples was prepared in the same range of amorphous contents as the original samples, and calibration equation was applied to those samples.

3.2.4. NIRS QUANTIFICATION OF AMORPHOUS LACTOSE

3.2.4.1. Establishing the Calibration Equation

As has already been outlined, all spectra were mathematically treated by performing a SNV transformation and calculating their first derivative (Figure 3.7). The forward search MLR applied to the treated spectra of the calibration set established that the wavelength of 2024 nm was that at which the greatest correlation could be found between known amorphous content (reference values) and SNV first derivative absorbance. A multiple correlation coefficient (R^2) between the actual amorphous contents and the NIRS values was found to be 0.927 at this wavelength. When a second wavelength (1970 nm) was added to the calibration, this value improved to R^2 = 0.973. A third wavelength of 1994nm was added to further improve the correlation to R^2 = 0.991. The residual sum of squares (RSS) of the three wavelength calibration fit was found to be 1.47 (equation 3.3), resulting in a standard error of calibration (SEC) of 0.350% w/w amorphous content (equation 3.4) (Figure 3.8).

$$RSS = \sum_{i=1}^{n} (y_i - Y_i)^2 \qquad \text{.....Equation 3.3}$$

$$SEC = \sqrt{\frac{RSS}{n-p}} \qquad \text{.....Equation 3.4}$$

Where:

y = the actual amorphous content (known from preparation),

Y = the NIRS calculated amorphous content,

n = the number of samples

p = the number of coefficients in the calibration equation.

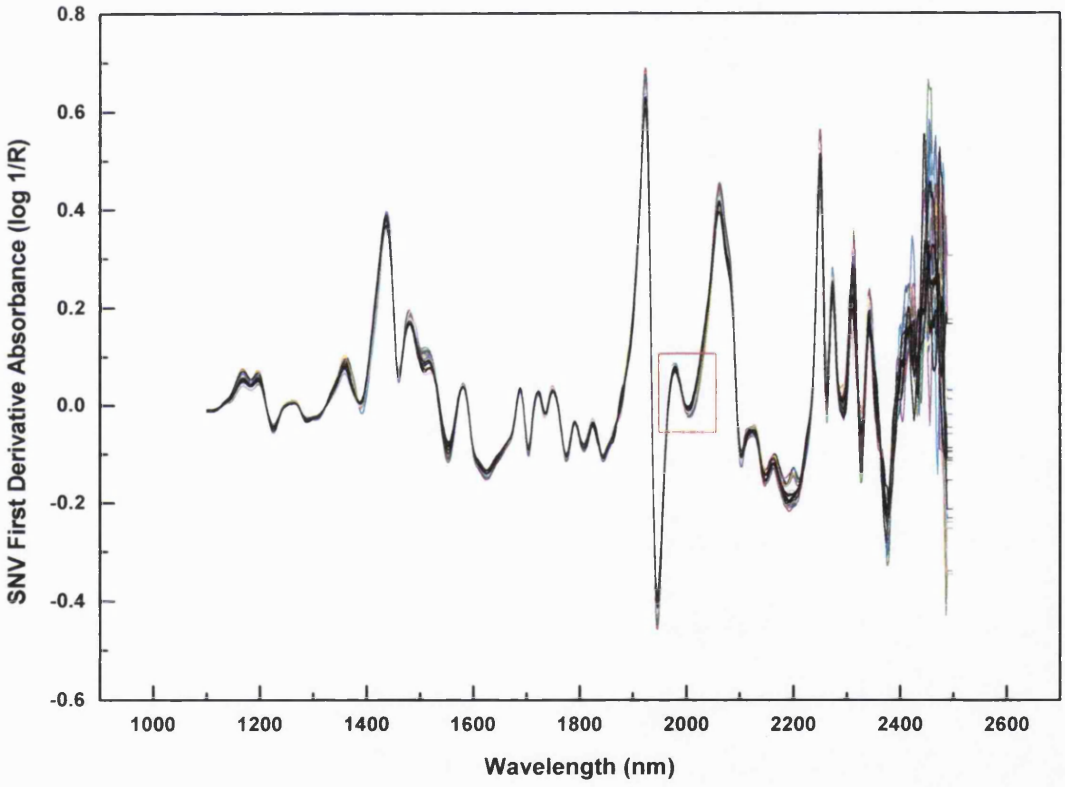

Figure 3.7 *SNV first derivative NIR absorbance spectra for all 28 partially amorphous lactose samples. The area highlighted is that which includes the wavelength (2024 nm) at which the greatest correlation between known amorphous content and absorbance was found.*

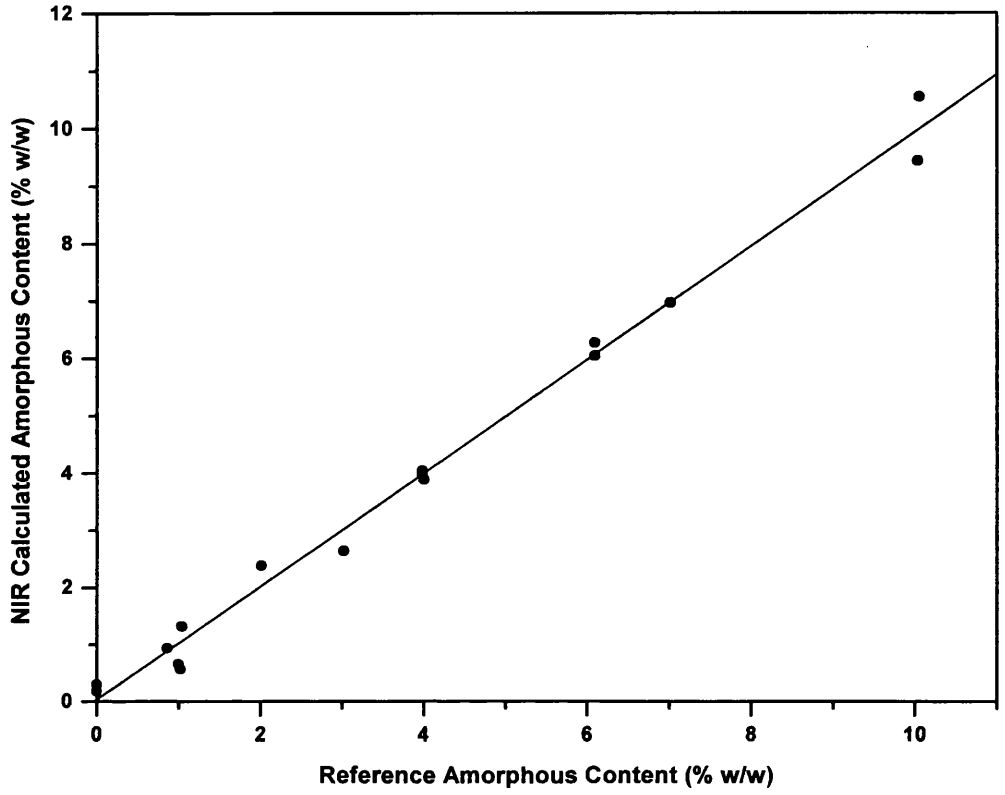

Figure 3.8 *The actual versus NIRS absorbance calculated amorphous content for the calibration set. The line of best fit is used to build the calibration equation, from which the quantification of the amorphous content of other samples can be carried out. A standard error of 0.35 % w/w amorphous content was achieved.*

3.2.4.2. Validation of the Calibration Equation

In order to validate the calibration equation, it was applied to those samples contained within the validation set. From the 1st derivative absorbance values at the wavelengths previously chosen, the amorphous contents of the validation samples were calculated. In Figure 3.9 these calculated amorphous content values have been plotted against their actual amorphous contents. The standard error of prediction (SEP) of this set was found to be 0.84 % w/w (equation as for SEC where $p = 0$).

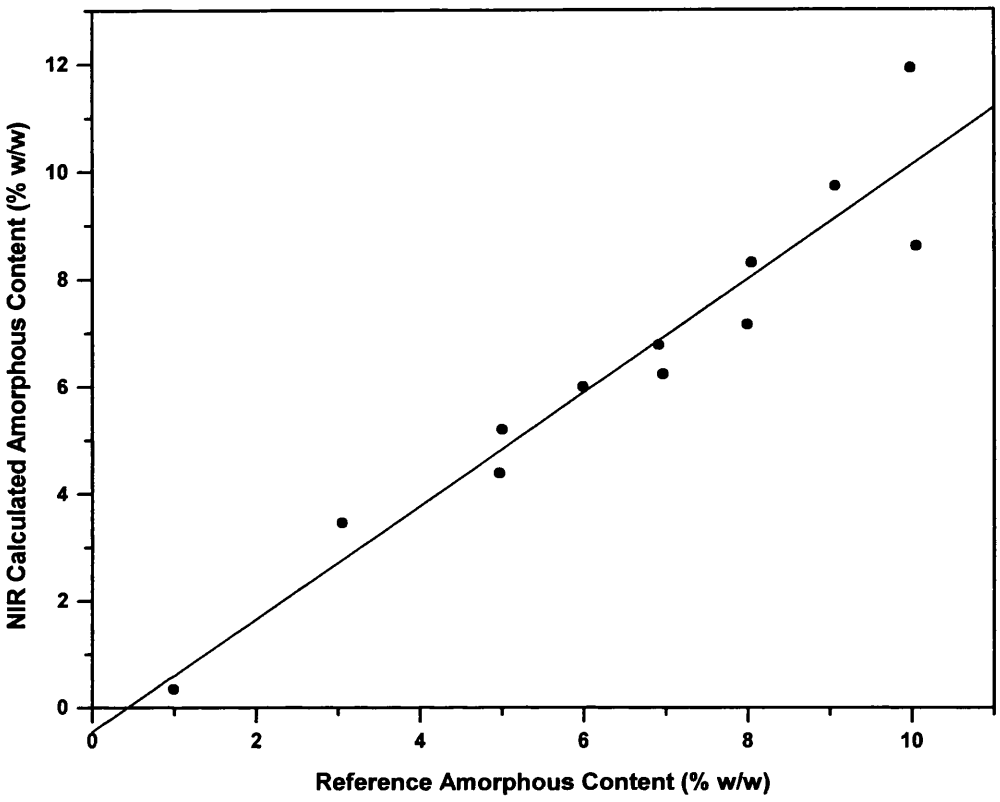

Figure 3.9 *The actual versus NIRS absorbance calculated amorphous content for the validation set, calculated from the calibration equation. A standard error of 0.84 % w/w amorphous content was achieved.*

Initial sample preparation was carried out before any of the quantification work began, which means that some samples were used fresh whereas others had been stored for several weeks before being studied, albeit under controlled conditions. The results obtained would indicate that this prolonged storage period did not prove problematic for NIRS (as data for the same sample measured at the start and end of the process were the same within experimental error). Experimental design also meant that repeat runs on the same sample were carried out on different days. Any slight variation between those runs was within that which would be expected of both techniques. The original samples were prepared from two different spray dried

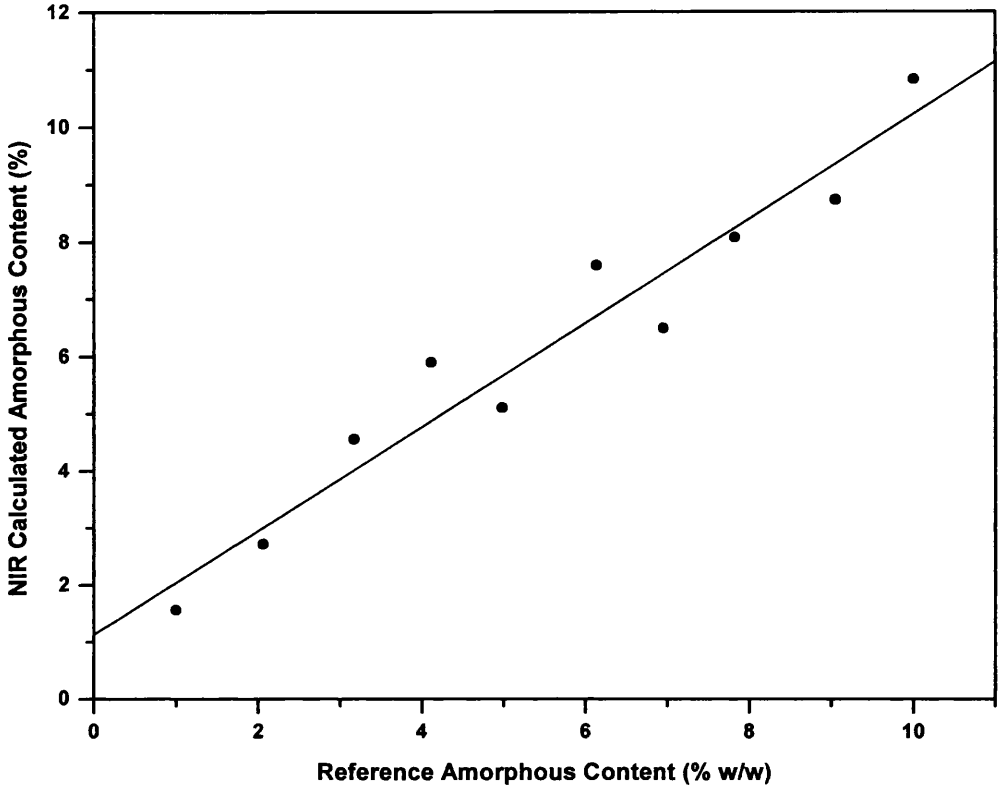

Figure 3.10 *The actual versus NIRS absorbance calculated amorphous content for the external sample set, calculated by the calibration equation. A standard error of 0.99% w/w amorphous content was achieved.*

batches, and no differences were detected due to inter-batch variation. Only one batch of crystalline lactose was used. Different batches of crystalline material are not expected to yield different results as the amorphous lactose peaks are the key areas of interest. It can be seen therefore that NIRS allows reproducible data to be generated on different samples at different times.

3.2.4.3. External Confirmation of the Robustness of the Calibration Equation

As a further test of the reliability of NIRS, a third (external) batch of amorphous lactose was prepared and from this, mixtures were formed with crystalline lactose.

These new mixtures were used to test the existing calibrated equation that had been derived from NIRS (Figure 3.10). This was done to ensure that it was able to cope with entirely new samples. The SEP achieved by the technique was found to be 0.99 % w/w amorphous content, thus demonstrating the validity of the equation.

3.2.4.4. Interpretation of Errors

An indication of the accuracy of this technique can be gained from the standard error of calibration (SEC) and standard error of prediction (SEP) values calculated for the calibration, validation and external sample sets (0.35 % w/w, 0.84 % w/w and 0.99% w/w amorphous content respectively), which show how closely the NIRS results correlate with the known amorphous contents of the samples from preparation. Obviously the lower these values are, the better the calibration model. It would be expected that the SEP value be greater than the SEC values, since the calibration equation is based only on those samples in the calibration set. In fact, to achieve a smaller SEP value than the SEC value would imply that the calibration equation was unreliable.

The percentage error of the calculated amorphous contents decreases with increasing amorphous content (the absolute error staying the same). However, the error is sufficiently small that this technique offers the capability of quantifying amorphous contents to a high degree of accuracy, even if the amorphous content drops to around 1% w/w. Bearing in mind the limitations of quantification with other techniques, as already discussed, and the speed, ease and accuracy of NIRS, this spectroscopic technique could compete with, or even replace techniques such as differential scanning calorimetry in the quantification of low amorphous contents.

NIRS does not appear to suffer from a lower limit of quantification. At a sample mass of 50 mg the technique is able to differentiate between samples of 0% and 1% w/w amorphous content. The ability of NIRS to differentiate between even more similar samples is an area for further work. In addition, the effect of sample size on

NIR spectra requires further investigation, since it is likely that the powder bed contained within the sample pan allows some light to pass through it. Were the sample size to be increased such that the powder bed became deeper, it is possible that this transmission could be reduced, thus leading to a stronger signal being recorded.

3.2.4.5. Transferability of NIRS Quantification

A major hindrance of quantitative NIRS analysis is the difficulty of transferring calibration models between instruments. Because detector responses are not uniform, the signals recorded by two instruments may differ owing to wavelength shifts and/or changes in measured intensities. This therefore prevents the use of a calibration model generated on one instrument being used on another instrument. However, since the recording of NIR spectra is so rapid, it is possible to overcome this problem by recording spectra for calibration samples on each instrument and constructing independent calibration equations for each apparatus. Calibration transfer methods do exist to facilitate the transfer between instruments (*e.g.* Wang et al., 1991), which usually involve either the use of wavelengths which are known to remain unchanged relative to spectral shift, or wavelength correction and adjustment of spectral intensity.

3.2.5. DVS Quantification of Amorphous Lactose

3.2.5.1. The Crystallisation of Partially Amorphous Lactose

Following the recording of the NIR spectrum of each dry sample, it was possible to increase the humidity of the environment to which the samples were exposed to 75% RH. In Figure 3.11 a typical DVS plot for a sample of 5% w/w amorphous content is shown. After 260 mins of drying at 0% RH, a swift mass increase was observed due to vapour sorption at the elevated RH, followed very quickly (approximately 3 minutes) by a mass loss whilst the sample was still maintained at the elevated RH. This mass loss was due to crystallisation, which is a consequence of the sorbed water

plasticising the amorphous material such that its glass transition temperature is reduced to below that of the environment at which the experiment is being performed (Buckton and Darcy, 1995). The expulsion of water during crystallisation is not complete, as some of the water is retained as a partial monohydrate (some of the material crystallises as an anhydrous form). The changes in mass ensuing from this event have been explored in order to attempt the quantification of amorphous content by this gravimetric method.

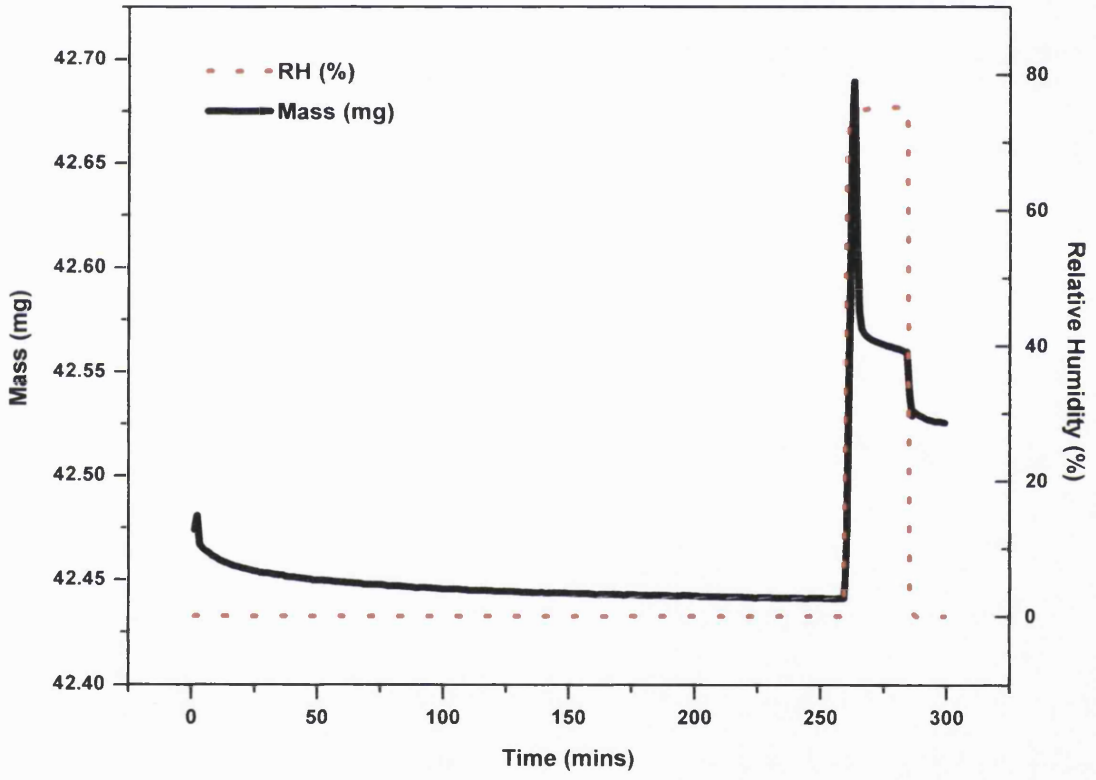

Figure 3.11 *Plot of mass against time for a 5% w/w amorphous lactose sample being dried at 0% RH for 260 mins, followed by exposure to 75% RH in order to induce crystallisation.*

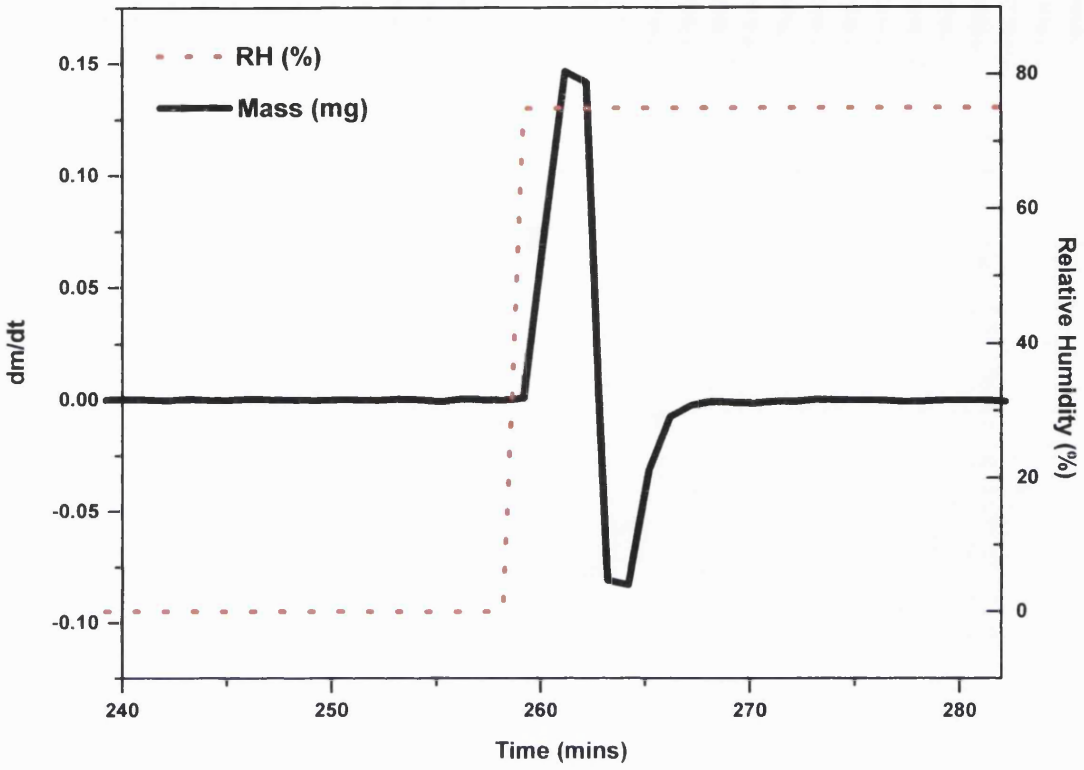

Figure 3.12 *Rate of change of mass (dm/dt) against time for a 5% w/w amorphous sample. Before the mass increase, the sample was being exposed to a 0% RH drying step. Following the increase to 75% RH, the sample was observed to initially gain mass, in association with water sorption and plasticisation. There was a subsequent loss of mass as the plasticising water was expelled from the sample as it crystallises.*

3.2.5.2. The Rate of Change in Mass Against Time Plot

From the DVS data it was possible to calculate the rate of change in mass (dm/dt) as a function of time for each amorphous mixture, starting from the point of exposure to 75% RH, by calculating the first derivative of the mass against time data. This produced a two-phase response (Figure 3.12). The first phase of this plot, which involved an initial positive peak, represented the mass uptake by the sample as it sorbed water and was being plasticised. The point at which the plot crossed the x-axis was equivalent to the top of the peak of the sorption response in Figure 3.11, when the rate of change of mass was momentarily zero. Subsequent to this (Figure 3.12) there was a negative peak, which represented a mass loss in association with

the expulsion of plasticising water. Integration of the positive peak of the dm/dt plot calculated the area under that peak, and gave the quantity of water sorbed during the sorption region of the response. The area of the negative region of the dm/dt plot was the quantity of water desorbed.

3.2.5.3. Quantification of Amorphous Content by Water Sorption

A linear relationship was obtained between the mass of sorbed water and the original amount of amorphous material within the sample (but not amorphous content expressed as % w/w) (Figure 3.13). Performing a linear regression on these data yielded a correlation (R^2) of 0.863. The equation for the line of best fit was:

$$y = 0.330x - 0.102 \qquad \text{.....Equation 3.5}$$

Where:

y = the mass of water sorbed

x = the amorphous content.

This line did not cross the x-axis at zero (intercept 0.309). In Figure 3.13 it is shown that quantification by this method was accurate to approximately ± 0.5 mg amorphous content. It can also be seen that a lower limit of detection at around 1 mg amorphous content was found, where the technique became less accurate. As a result of this, samples with amorphous contents at or below this level did not yield a reliable result. There are a number of factors which may contribute to this. Primarily, at these very low amorphous contents, the water sorption response due to the crystalline portion of the sample may have become significant. In addition, since quantification was based upon the original amorphous content, it did not reflect sample composition. For example, a 40 mg sample with an amorphous content of 8% w/w contains the same amount of amorphous material as 80 mg of a 4% w/w sample. However the crystalline portion of the sample adsorbs a certain, although small amount of moisture, which may interfere with the results. As the amorphous

content of the sample decreases, this error will have a greater impact on the accuracy of the quantification, so that at very low amorphous contents, its effect is greatest. In addition, as amorphous content decreases, errors arising from the preparation of the samples, such as the accuracy of weighing out small amounts of amorphous material, and the difficulty in achieving a uniform powder blend, will have a greater impact upon the model used.

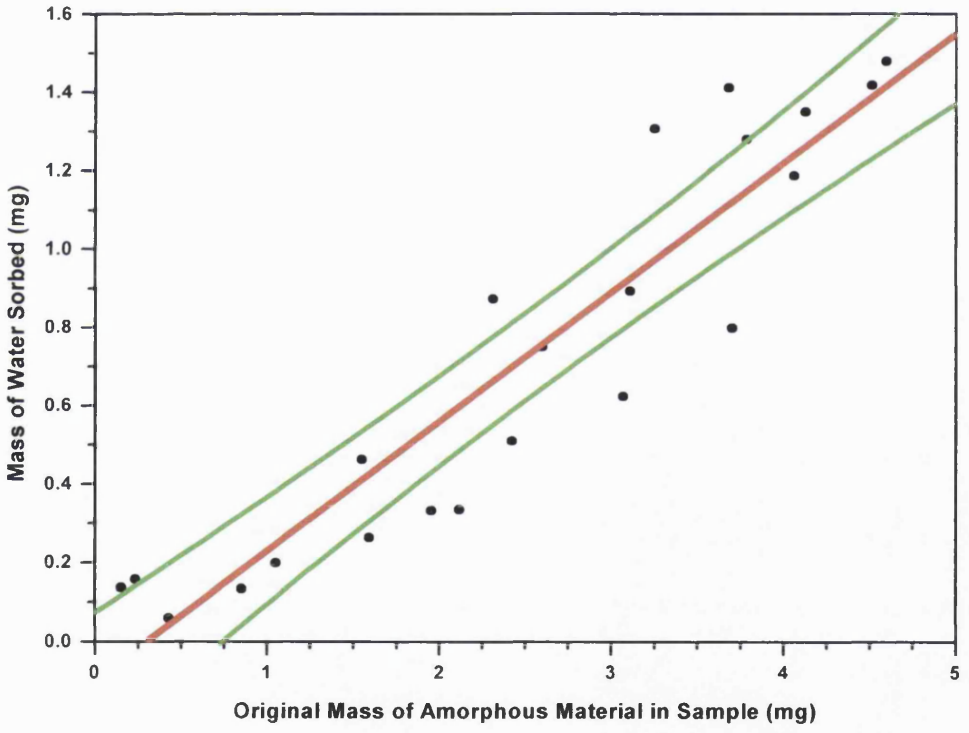

Figure 3.13 *Plot of water sorbed against the mass of amorphous material in the samples. The line of best fit is shown in red, with the 95% confidence intervals represented by the green lines. It can be seen that quantification to within approximately ± 0.5 mg amorphous content was achieved, corresponding to a level of accuracy of ca. 1% w/w amorphous content for a 40 mg sample.*

3.2.5.4. Quantification of Amorphous Content by Water Desorption

The area of the (negative) peak below zero of the same dm/dt against time plot (Figure 3.12) represented the amount of water that was expelled from the sample. The mass as a function of time data (Figure 3.11) showed that mass loss continued long after the dm/dt as a function of time peak (Figure 3.12) had ended, indicating that this water loss continued at a steady rate after the initial fast expulsion (*i.e.* the rate of change in mass loss was zero). Despite the fact that the quantity of water that was desorbed was limited due to the formation of a partial hydrate, a correlation was found between the amount of water expelled from the sample and the original amorphous content. The assumption in this case is not that the total amount of desorbed water has been accounted for, but that some instantaneous process at the onset of crystallisation involves the expulsion of water in a quantity directly proportional to the amount of amorphous lactose originally contained within the sample. These data have been plotted in Figure 3.14, and in this case the linear regression performed on the data gave a correlation (R^2) of 0.808, implying that desorbed water is not as good an indicator of amorphous content as sorbed water. Again quantification with an accuracy of approximately ± 0.5 mg amorphous content was found. However samples containing less than approximately 1 mg amorphous content were not seen to desorb detectable amounts of water, and therefore their amorphous contents were not quantifiable by this method.

3.2.5.5. Determination of Errors

As has already been stated, initial sample preparation was carried out before any of the quantification work began. The results obtained for gravimetric quantification of amorphous content would again indicate that prolonged storage (under controlled conditions) does not prove problematic for the technique, with any variation between results obtained from runs on different days remaining within that which would be expected. Amorphous lactose from two different spray dried batches was also used in the original study and did not show any differences.

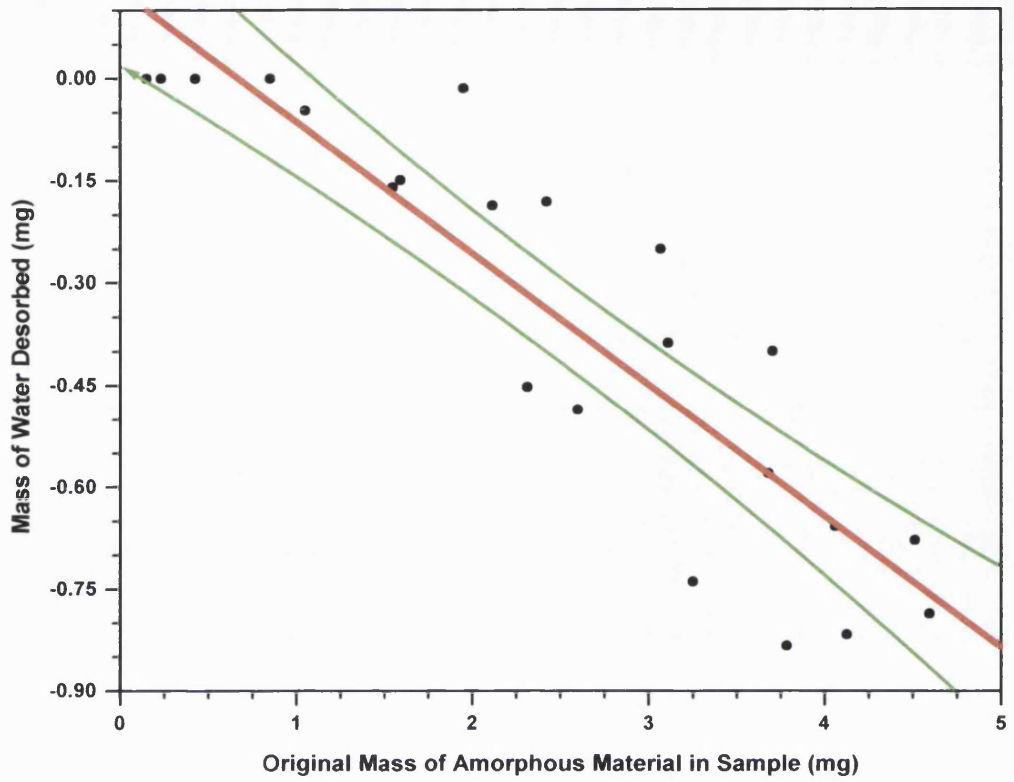

Figure 3.14 *Plot of mass of water expelled against the original mass of amorphous material within the sample. The red line represents the line of best fit for the data, whilst the green lines represent the 95% confidence intervals of the line of best fit. Again it can be seen that quantification to within ca. ± 0.5 mg was achieved.*

The external batch which was used as a further validation of the reliability of the NIRS technique was also quantified using DVS, and the data on this new series of mixtures were identical to the originals within experimental error.

As already mentioned, DVS quantification had been shown to be subject to a lower limit of reliability, which falls at approximately 1 mg amorphous content (although this may be dependent on the material being quantified). The lower limit of quantification for this technique is therefore sample mass dependant. Assuming a sample mass of 50 mg, a 2% w/w amorphous content would be the lower limit. However, if that were increased to 150 mg, which is within the capability of the technique, then the best detection would be 0.7% w/w.

3.2.6. CONCLUSIONS

It has been shown that NIRS and DVS are both capable of quantifying the amorphous content of lactose below 10% w/w. It is clear that at degrees of disorder as low as 1% w/w, either technique is capable of achieving a previously unattainable level of accuracy for quantification, NIRS achieving an accuracy of ± 1% amorphous content, and DVS achieving quantification limits of ± 0.5 mg amorphous content. Each technique has its own particular advantages. Recording a NIRS spectrum takes only a few seconds and complete recovery of the sample is also possible. DVS on the other hand provides more tangible information in the form of mass change. There are obvious advantages to having both techniques operating in combination as an immediate check of the NIRS data can be obtained from the DVS sorption response. Near infrared spectroscopy is known to be sensitive to the presence of water, as it has been used to determine the moisture content of solids (Kamat et al., 1989, Buice et al., 1995). Recording NIRS data in the DVS apparatus provides complete control of the environment, and thus control of the water sorption peaks that would otherwise make a major contribution to the NIRS response and possibly interfere with the accuracy of the NIRS quantification.

The development of non-destructive *in situ* analysis of materials, as well as on-line monitoring of pharmaceutical processes is of growing interest, and NIRS is a leading candidate for such applications with the availability of fibre-optic probes (Hailey et al., 1996). This work further extends the uses of NIRS.

The use of two methods in series on the same sample (the first being non-destructive) provides an instant check for internal consistency, which is very appealing. The NIRS-DVS data presented here include spectra and mass changes for samples containing amorphous material originating from different spray-dried batches. This indicates that when a calibration has been established it is applicable to different batches.

This study has developed quantification methods based on calibrations established with binary amorphous/crystalline mixtures, which represent a two state model, *i.e.* each particle is either amorphous or crystalline. Further work is required in order to determine the applicability of such calibrations to materials composed of mechanically processed samples which contain individual particles which are partially amorphous, *i.e.* one state models.

CHAPTER FOUR

THE QUANTIFICATION OF SMALL DEGREES OF DISORDER IN LACTOSE BY SOLUTION CALORIMETRY

4.1. INTRODUCTION

The occurrence and impact of amorphous material in predominantly crystalline materials has already been discussed at length (Chapter 1, Chapter 3). The accurate quantification of amorphous material in "crystals" has been the goal of many workers. Long-standing techniques such as X-Ray Powder Diffraction (XRPD) and Differential Scanning Calorimetry (DSC) are known to be capable of quantifying amorphous contents at 10% w/w and above (Saleki-Gerhardt et al., 1994). However, processing-induced material regularly comprises only a fraction of that amount, and as such, techniques with much lower detection limits have been sought. Possible alternatives for detection and quantification of amorphous content include gravimetric vapour sorption and near IR spectroscopy (see Chapter 3). In addition, isothermal microcalorimetry offers the ability to quantify amorphous content (Sebhatu et al., 1994, Briggner et al., 1994), however it is limited to those amorphous materials which undergo spontaneous crystallisation under certain relative humidity or organic vapour conditions. One method that has not been studied to any great extent is solution calorimetry.

Solution calorimetry offers an alternative thermal analysis technique with which to attempt the quantification of these problematic partially amorphous samples. First applied pharmaceutically in the 1970's (Pikal et al., 1978), the principle of the technique is to create an isothermal system within which very small enthalpy changes due to physical (*e.g.* dispersion or dissolution) or chemical interactions during the mixing of two solutions or a solid and a liquid may be recorded as a function of time. The principles of isoperibol solution calorimetry has been outlined by Gao and Rytting (1997), based on the following equation:

$$S + L \leftrightarrow SL_1 \qquad \text{..... Equation 4.1}$$

where S and L are the amount of free substrate and ligand respectively.

In an equilibrium system, the enthalpy change is defined as ΔH^o and the total heat evolved, Q, is related to the number of moles of SL_1 produced and ΔH^o (Tong et al., 1991), *i.e.:*

$$Q = SL_1 * \Delta H^o \qquad \text{..... Equation 4.2}$$

Since the technique measures the heat generated during substrate dissolution, SL_1 becomes the total amount of sample (since equilibrium is achieved quickly) and ΔH^o is the heat of solution to infinite dilution in any fixed solvent L. Therefore the heat of solution could be obtained through the measurement of the total heat generated during the process. In a non-interacting binary system, the total specific heat of solution (ΔH^o_t) is the weight sum of the specific heats of the individual components (Craig and Newton, 1991, 1991a) such that:

$$\Delta H^o_t = X_a \Delta H^o_a + X_b \Delta H^o_b \qquad \text{..... Equation 4.3}$$

where X and ΔH^o are the weight fractions and heats of solution for two non-interacting substances.

The heat of solution method to quantify amorphous content is based on the energy difference between the amorphous and crystalline species, since the energy of the amorphous form is for many solids significantly higher than that of the crystalline form. Pikal et al. (1978) defined the percent crystallinity as:

$$P_c = 100\left[\frac{\Delta H^o_s - \Delta H^o_a}{\Delta H^o_c - \Delta H^o_a}\right] \qquad \text{..... Equation 4.4}$$

Where ΔH^o_s, ΔH^o_c and ΔH^o_a are the heats of solution to infinite dilution (in any fixed solvent) of the sample, the 100% crystalline standard and the 100% amorphous standard, respectively.

The enthalpy of solution of any particular solute in one of its solvents can be measured. The two-phase system in the set-up used in this investigation comprises 100 ml of solvent and a known amount of solute (solid or liquid), which are housed together in the reaction vessel and equilibrated to the temperature at which the reaction is to take place. The solute is sealed in a small fragile glass ampoule and this is immersed into the solvent. The glass ampoule prevents dissolution until thermal equilibrium has been established. Following equilibration the glass ampoule may be broken, thus initiating the reaction and allowing the enthalpy of solution to be measured.

Solution calorimetry is a suitable technique for the study of liquid-liquid and solid-liquid interactions. It has been used pharmaceutically to differentiate between micronised and crystalline salbutamol sulphate (Ward and Schultz, 1995) and between drug samples of different crystallinity (Thompson, 1994). Pikal et al. (1978) used the technique to correlate the extent of crystallinity with chemical stability in β-lactam antibiotics. Salvetti et al. (1996) measured heat of solution in order to discriminate between different physical forms of carbohydrates whilst Grant and York (1986) have also assessed solid state disorder with the technique. Quantification work has also been carried out and the technique has been shown capable of quantifying the crystallinity of sucrose between 0 – 100% w/w (Gao and Rytting, 1997). However, the suitability of this technique for the quantification of small amounts of amorphous content has yet to be reported.

4.2. AIMS OF THE STUDY

For the purposes of this work, the solution enthalpies of samples of less than 10% w/w amorphous content have been studied in order to establish the resolution which solution calorimetry offers in studying materials of small degrees of disorder. Furthermore, the impact of sorbed water on the measured enthalpy of solution has been investigated.

4.3. EXPERIMENTAL

4.3.1. PREPARATION OF 100% AMORPHOUS LACTOSE

100% amorphous lactose was prepared by spray drying, as outlined in Section 2.5.3.1. Confirmation of the amorphous nature of the yield was obtained from XRPD (method outlined in Section 2.7.2.).

4.3.2. PREPARATION OF PARTIALLY AMORPHOUS LACTOSE MIXES

Samples were prepared as described in Section 2.10. They were stored over Phosphorous Pentoxide at room temperature prior to use in order to ensure the absence of large quantities of water vapour and to prevent crystallisation of the amorphous portions of the samples.

In addition to this, water sorption studies were carried out which required the storage of some partially amorphous lactose samples under vacuum (-300 mbar) at 50 °C. This ensured the removal of all sorbed water, thus facilitating accurate gravimetric quantification of wetting.

4.3.3. SOLUTION CALORIMETRY

Enthalpies of solution of lactose mixes of various amorphous contents were measured using the Thermometric 2225 Precision Solution Calorimeter (Thermometric AB, Sweden), an instrument designed for use in conjunction with the air and water bath of a Thermometric 2277 Thermal Activity Monitor (TAM). Details of the experimental set-up are included in Section 2.2. Data were collected by measuring temperature offset (°C) from a predefined zero point (actually the temperature of the air bath of the TAM, in this case 298.000 ± 0.0001 K). In each experiment, before and after the dissolution reaction takes place, the system was calibrated using a heater (Figure 4.1).

A glass ampoule containing approximately 200mg of sample (accurately weighed) was sealed with a silicone bung and bees wax and loaded into the stirrer unit of the

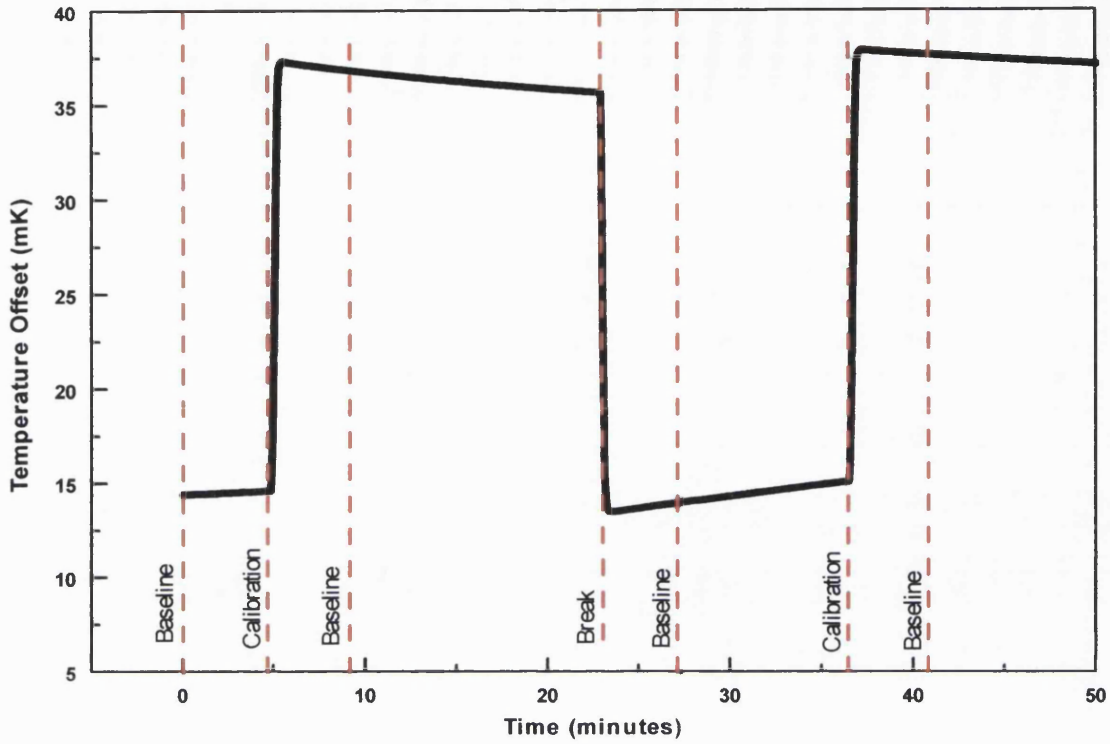

Figure 4.1 *Plot of temperature offset against time for a 5% w/w amorphous lactose sample, with a stirring rate of 600 rpm. This trace shows the calibration sections of the experiment, which occur before and after the ampoule is broken, as well as the baseline periods, which aid calculations to adjust for heat exchange between the solution calorimetry and the environment, as well as the heat generated by the stirrer. Following the breaking of the ampoule, a drop in temperature is seen, implying that the response in this case is endothermic.*

solution calorimeter. This unit was then lowered into the glass vessel containing exactly 100 ml of solvent (distilled water), the glass ampoule isolating the solute from the solvent. The combined unit was then lowered into the TAM channel for equilibration prior to the experiment.

4.3.4. Determination of Enthalpy of Solution

Data were analysed using the 'Software for Solution Calorimeter System' version 1.2 (Thermometric AB, Sweden). All data reported in this study are based upon calculations performed using the calibration carried out after the breaking of the

ampoule since there was little difference between the results based on either calibration. In addition, although the experimental set-up was such that 10 mins was allocated to the break event, during data analysis it was possible to move the event markers such that immediately following the end of the dissolution response, the event marker denoting the beginning of the baseline subsequent to the break event could be moved. By converting the temperature offset data to heat flow data using a facility provided in the software, it was possible to clearly see the end of each thermal event (Figure 4.2).

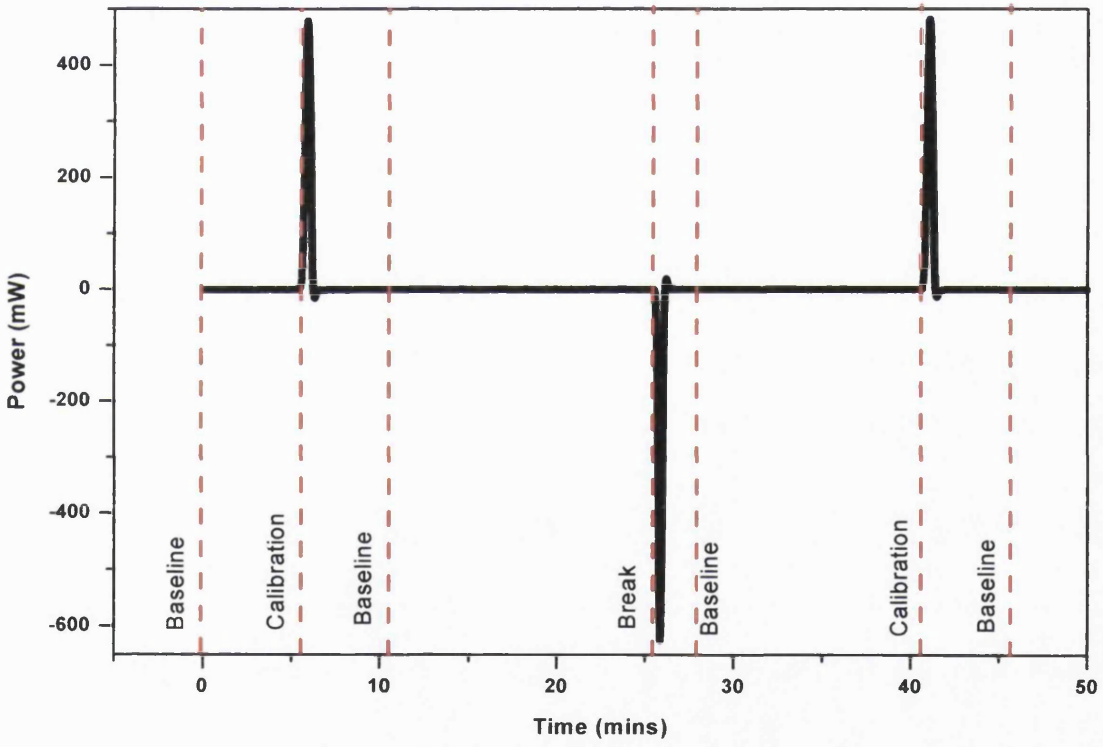

Figure 4.2 *Plot of power (heat flow) against time for a 5% amorphous lactose sample. Through magnification of the baseline subsequent to the break event, it is possible to move the event marker (shown in red) to that point where the heat response due to the break event ends. In this way it is possible to aid the software in calculating the enthalpy of solution by including only the data which is directly associated with the dissolution event itself.*

4.3.5. VAPOUR SORPTION STUDY

Four different storage conditions were employed in order to investigate the effect of residual moisture content on the enthalpy of solution obtained. Two supposedly dry conditions were used – in a vacuum oven (Sanyo-Gallenkamp) at 50°C and –300 mbar; at room temperature in a desiccator over Phosphorous Pentoxide. In addition, two elevated RH environments were created by storage in a desiccator (used as a humidity chamber) at 25 °C over saturated salt solutions - 33% RH was produced by Magnesium Chloride; 43% RH was produced by Potassium Carbonate. In all cases the storage period was for 72 hours. The filled ampoules were weighed (along with a sealing bung) immediately before storage and then at the end of storage the bung was inserted to seal the ampoule and the sample was weighed again to monitor the weight change. Subsequently the bung was double-sealed with bees wax.

4.4. RESULTS AND DISCUSSION

4.4.1. CHARACTERISATION OF THE ENTHALPIC RESPONSE

It can be seen from the results obtained in this study that the enthalpy of solution increases in a linear fashion with decreasing amorphous content (see discussion below). The heat of solution of 100% amorphous lactose exhibited an exothermic response (-56.50 J/g, equivalent to –19.32 J/mol), whilst the heat of solution of 100% crystalline lactose was endothermic (55.38 J/g, equivalent to 19.94 J/mol). When a mixture containing 50% w/w amorphous and 50% w/w crystalline lactose was dissolved, an initial exothermic response was observed, followed by an endothermic response (Figure 4.3). This was due to the fact that amorphous lactose is more readily soluble in water than the crystalline form, so the exotherm for dissolution of the amorphous form is seen before the endotherm for the dissolution of the crystalline material. The bulk of this study relates to samples with an amorphous content in the range 0-10% and for these samples only a net endothermic response was observed, since the majority of the sample was crystalline in nature.

The net measured response for the enthalpy of solution is a summation of numerous component parts. The first stage will be wetting of the powder, followed by dissolution, which will involve the disruption of the bonding between the solid molecules and the formation of bonds between the solute and the solvent. There will also be rearrangement of bonding within the solvent in order to accommodate the solute. Consequently the single number for the enthalpy of solution must be viewed with some caution.

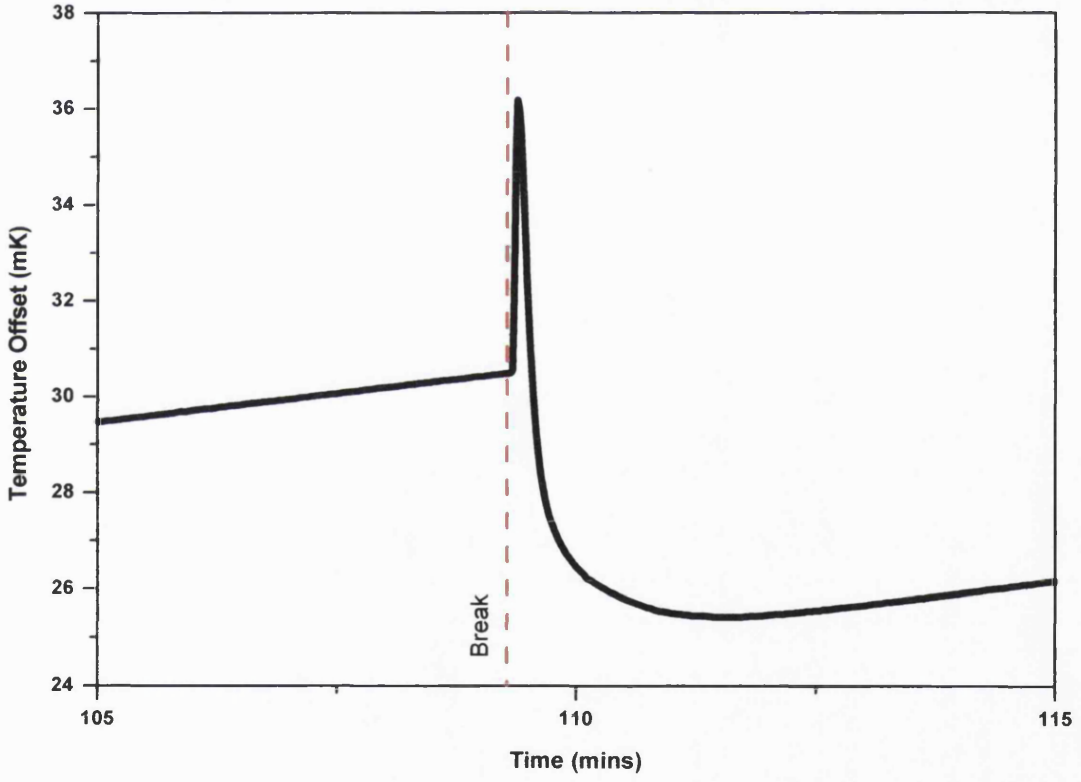

Figure 4.3 *Temperature offset against time for a 50% amorphous lactose sample, illustrating the initial exothermic response due to the faster dissolution of the amorphous portion of the sample, followed by the endothermic portion of the response for which the crystalline portion of the sample is responsible.*

4.4.2. SEALING OF AMPOULES

Preliminary observations showed that the results followed two trends (Figure 4.4). One trend was the expected notable decrease in enthalpy of solution with increasing amorphous content in the sample. However, some samples did not fit this trend, and tended to give responses closer to the enthalpy of solution which would be

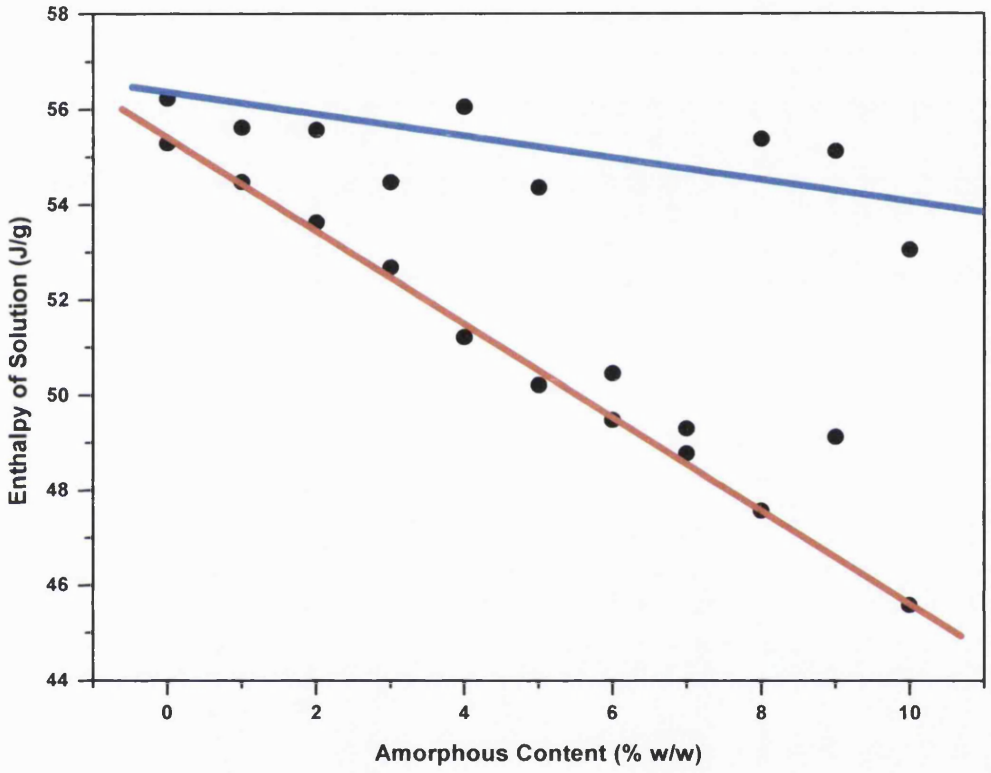

Figure 4.4 *Enthalpy of solution plotted against the original amorphous content of the samples, showing two distinct trends in the responses of the sample. The first trend, shown by the red line, follows the expected decrease in enthalpy with increasing amorphous content. However the blue line shows an altogether different response, which is thought to be due to the crystallisation of the amorphous portions of the sample inside the ampoule during equilibration, and is caused by the penetration of water vapour into the ampoule. In order to avoid this, all further samples were double-sealed with bees' wax.*

expected for the crystalline form. This response was more common in samples that had been equilibrated in the calorimeter overnight. There was no indication of penetration of liquid water into the ampoule even after overnight storage. However, it was concluded that such samples were tending to crystallise, since their appearance changed from that of a free-flowing powder to a fused solid. This was attributed to water vapour passing into the ampoule through the wax and bung seal of the ampoule. Subsequently all ampoules were sealed with wax twice, in order to eliminate water vapour penetration. The first layer of wax was allowed to set hard before the second layer was applied, resulting in satisfactory sealing. All data reported below were collected using this double sealing method.

4.4.3. Adjusting for Additional Heat Generation

The significance of the effect of the heat generated by the stirrer was studied. It was observed that when the stirrer was operating at 300 rotations per minute (rpm) the equilibration temperature of the vessel in the air bath was 25.0000 ± 0.0001°C, but if the stirring rate was increased to 600 rpm, that equilibration temperature was higher, at 25.0259 ± 0.0001°C. It was necessary to adjust for this raised equilibration temperature, ensuring that all calibrations were commenced from the correct point so as to cross the equilibration point.

The impact of this raised equilibrium temperature was investigated by using both stirring rates on the same samples. In Figure 4.7 it can be seen that the enthalpies of solution generated from stirring at 300 and 600 rpm followed the same line of best fit. For samples of 1% w/w amorphous content, at 300 rpm the average enthalpy of solution was found to be 54.70 J/g (standard deviation = 0.16 J/g, n = 3), whilst at 600 rpm it was found to be 54.46 J/g (standard deviation = 0.18 J/g, n = 2). This indicates that the calibrations and baselines included in the method were capable of adjusting for the additional heat generated by the stirrer. As expected the dissolution occurred much more quickly at the higher stirring speed (the average time of dissolution was approximately 8 minutes at 300rpm and less than 3 minutes at 600 rpm).

4.4.4. Effect of Sample Mass

The effect of sample size has also been investigated. Samples masses of between 100 – 350 mg were used in order to ascertain the influence of fill mass and/or volume on the enthalpies recorded. No effect at all was detected, indicating that as long as the solute is freely soluble in the solvent in the quantities being used, uniformity of sample size is not paramount. Obviously, if the solute were found to be sparingly soluble, this issue would be of greater importance.

4.4.5. Effect of Water Sorption on Enthalpy of Solution

All calorimetric experiments have the potential to measure processes other than the one which is the intended subject of investigation. In the case of enthalpy of solution measurement, there is inevitably a contribution due to the initial wetting of the powder surface prior to dissolution. It is indeed possible to use a non-solvent system in order to measure the enthalpy of immersion (powder wetting) in a solution calorimeter. Hollenbeck et al. (1978) have shown that the measured enthalpy of immersion of microcrystalline cellulose changes depending on the extent of sorbed water in the sample prior to sealing the ampoule. The sorption of water by a powder is the first stage of wetting, indeed it is argued that the sorption of the first few layers of molecules on the surface is the greatest part of the overall wetting response.

Amorphous lactose is able to sorb substantial amounts of water and this would be expected to alter the initial wetting (immersion) response and thus change the net enthalpy of solution value. It is important to know to what extent the enthalpy of solution may change as a function of water content, as this will influence the confidence in data that are generated for partially amorphous samples, that potentially have different water contents.

Individual ampoules were filled with 100% amorphous material that had been stored desiccated over phosphorous pentoxide at 20 °C. The filled ampoules, each with an identified weight of amorphous lactose, were then stored for a further period of 72 hours either in a vacuum oven (-300 mbar) at 50°C, desiccated over phosphorous

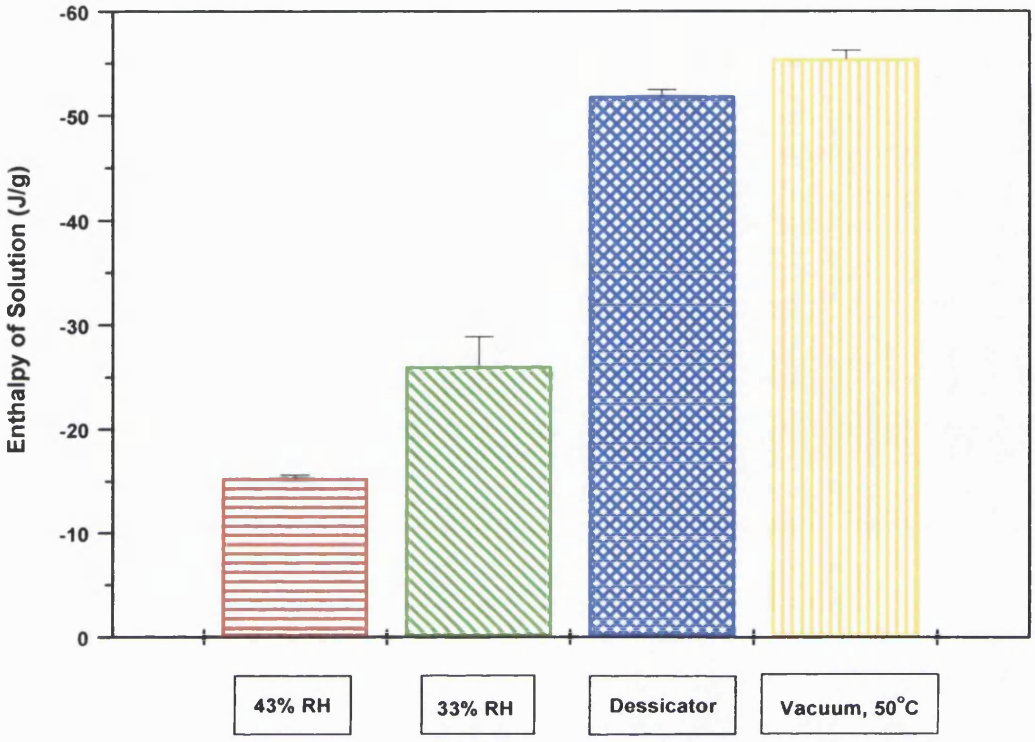

Figure 4.5 *Enthalpies of solution for samples of 100% amorphous lactose stored under different conditions for 72 hours.*

pentoxide at 20°C, or in desiccators (humidity chambers) at either 33% RH or 43% RH at 20 °C. These humidities were selected as they are high enough to cause substantial water sorption into an amorphous material, but not high enough to induce crystallisation over the time of storage used (for the given sample mass in the given container geometry). Some ampoules were then rapidly double sealed with wax as described previously and their enthalpies of solution were then recorded (Figure 4.5). The effect of water sorption was seen as a dramatic increase in the enthalpy of solution, the trend of which was in keeping with the sample having been progressively more wetted during storage at the more elevated humidities. Wetting is an exothermic response, and in a sample that has already sorbed some moisture from the environment, the enthalpy of solution will be significantly different. Sorption of water prior to enthalpy of solution measurement results in a less

exothermic (*i.e.* less negative) response than would be observed for a completely dry sample.

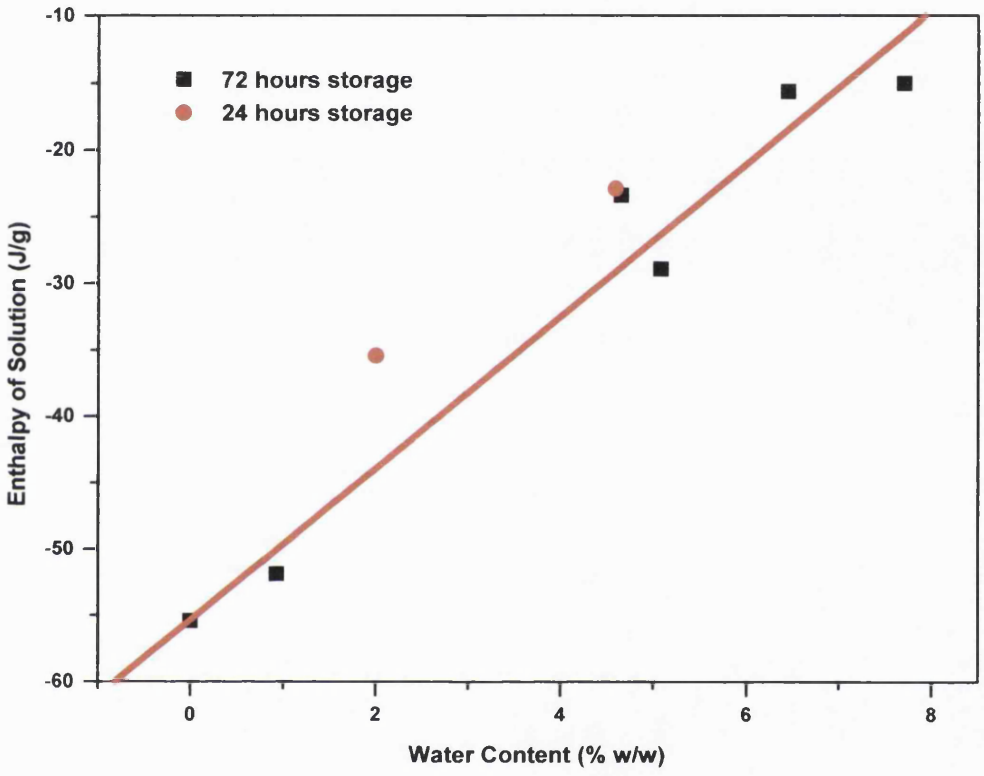

Figure 4.6 *Water content of 100% amorphous lactose stored under different conditions, against enthalpy of solution.*

Upon storage in the vacuum oven for 72 hours, samples were seen to have undergone a reduction in mass of approximately 0.91%, which would indicate that the vacuum oven displaced more water than storage in a desiccator. This enabled adjustment of the original 'dry' masses, and re-weighing of the other samples after storage at elevated RH facilitated the quantification of sorbed water under these conditions. At 33% RH, a 4.87% w/w increase was observed, whilst at 43% RH, a 7.08% w/w mass gain was noted. The relationship between water content of the

amorphous sample and the measured enthalpy of solution is shown in Figure 4.6. There is approximately a 5 J/g reduction in the net response for each 1% of water that is absorbed. Additional samples were stored at 33% and 43% RH for 24 hours. Although they absorbed less water than those samples stored for 72 hours (as would be expected) and had not achieved equilibrium with their environment, they still fit with the linear relationship shown in Figure 4.6.

It is often assumed that the wetting of amorphous materials by vapours is reasonably similar to the enthalpy of condensation of water. The enthalpy of vapourisation of water (numerically the same as the enthalpy of condensation, except with a changed sign) is 40.66 kJ/mol (CRC Handbook). The total enthalpy change expected for sorption of 7.08 % water content in 1 g of powder (0.0708 g or 0.0040 mol of water) would be –163 J. As the total change in enthalpy of solution following the sorption of 7.08 % water was 40.1 J/g between the dry and the most wetted sample, this is about one quarter of the equivalent enthalpy of condensation. This apparent difference requires further investigation.

4.4.5. Quantification of Amorphous Content in Predominantly Crystalline Samples

In order to establish a quantification calibration, the enthalpies of solution of samples of between 0-10% w/w amorphous content were calculated (Figure 4.7). Several observations can be made from Figure 4.7. Firstly, it is possible to differentiate between the enthalpies of solution of samples with amorphous contents ranging from 0-10 %. It is also evident that the stirring rate employed does not affect the enthalpy of solution measured (as stated in section 4.3.3.), as data from desiccated samples stirred at both rates are included here, and they can be seen to overlay.

In addition to the desiccated samples, Figure 4.7 also includes samples which were stored in a vacuum oven prior to being run in the solution calorimeter. It can be seen that the enthalpies of solution calculated for these samples are in good agreement

with those calculated for the desiccated samples. Although the effect of residual water has been shown to have a considerable impact on the enthalpy of solution calculated for 100% amorphous lactose, the crystalline form is less hygroscopic and is therefore less likely to require more extreme drying conditions to remove remaining adsorbed water. Samples of between 0-10% amorphous content are therefore less likely to show the effects of residual water, and for this reason little difference is observed between those samples stored in a vacuum oven or in a desiccator.

In order to ascertain the quantification limits of the technique, the line of best fit has been included, based on the desiccated samples only. It has a correlation (R^2) of 0.983. In addition, the 95% confidence intervals for that line have been included, and can be seen to shadow the original line. If such a calibration were used to quantify the amorphous content of a sample of unknown disorder, it can be seen such quantification would be accurate to within 1% w/w amorphous content.

In addition to this, Figure 4.8 shows the line of best fit for the vacuum oven dried samples, which has a correlation (R^2) of 0.986. Again the 95% confidence intervals have been included, but there is little difference between the quantification capabilities with desiccated or vacuum-dried samples in this amorphous content range.

Quantification by solution calorimetry has been shown to be independent of sample mass, although the minimum sample requirement certainly depends upon the magnitude of the dissolution/dispersion reaction involved, and the rate at which that reaction occurs.

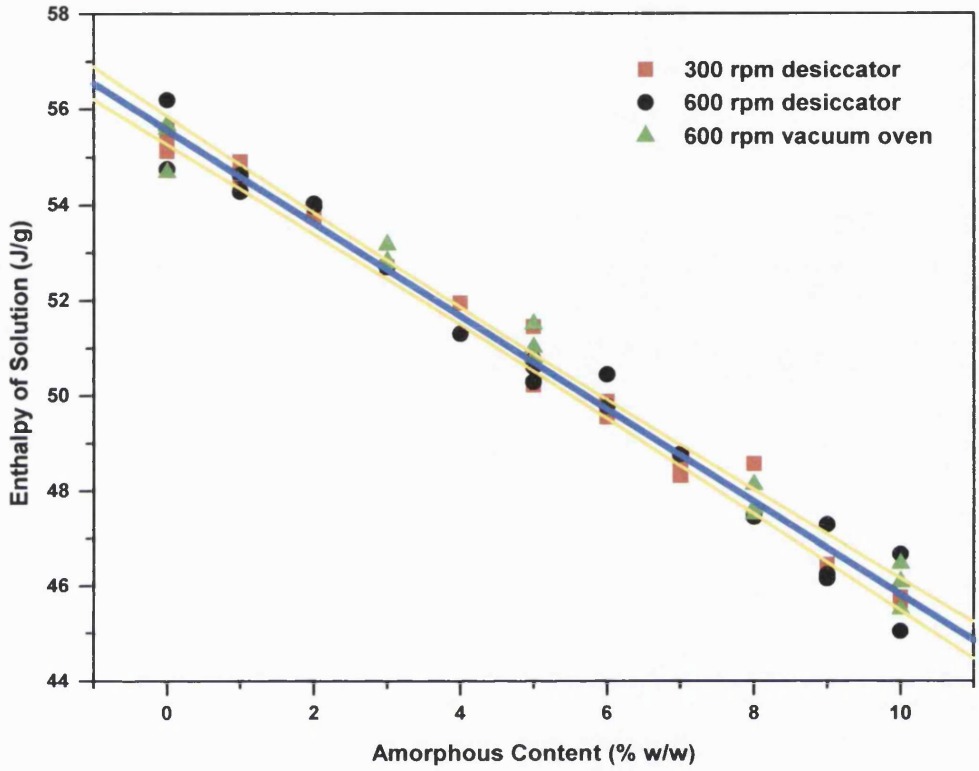

Figure 4.7 *This plot shows the line of best fit (the blue line) for the desiccated samples run at both stirring rates (R^2 = 0.983). It can be seen that stirring rate does not affect the enthalpy calculated. The 95% confidence intervals for the line of best fit are also shown (in yellow) and can be seen to fit very closely to the original line. Quantification would be accurate to ± 1% w/w amorphous content, based upon this calibration. Overlayed are those samples (green triangles) which were stored in a vacuum oven at 50 °C and –300 mbar.*

It should be remembered that a proportion of the error inherent in the establishing of such a quantification calibration in this low amorphous content region will be due to weighing errors and the difficulties involved in preparing a uniform mix containing such small amounts of the amorphous material. In addition, the quantification limits

calculated here for lactose will not be the same for all materials, as the sensitivity will depend upon the difference in enthalpy of solution between the amorphous and the crystalline forms. Obviously the larger the difference the greater will be the sensitivity for quantification and vice versa.

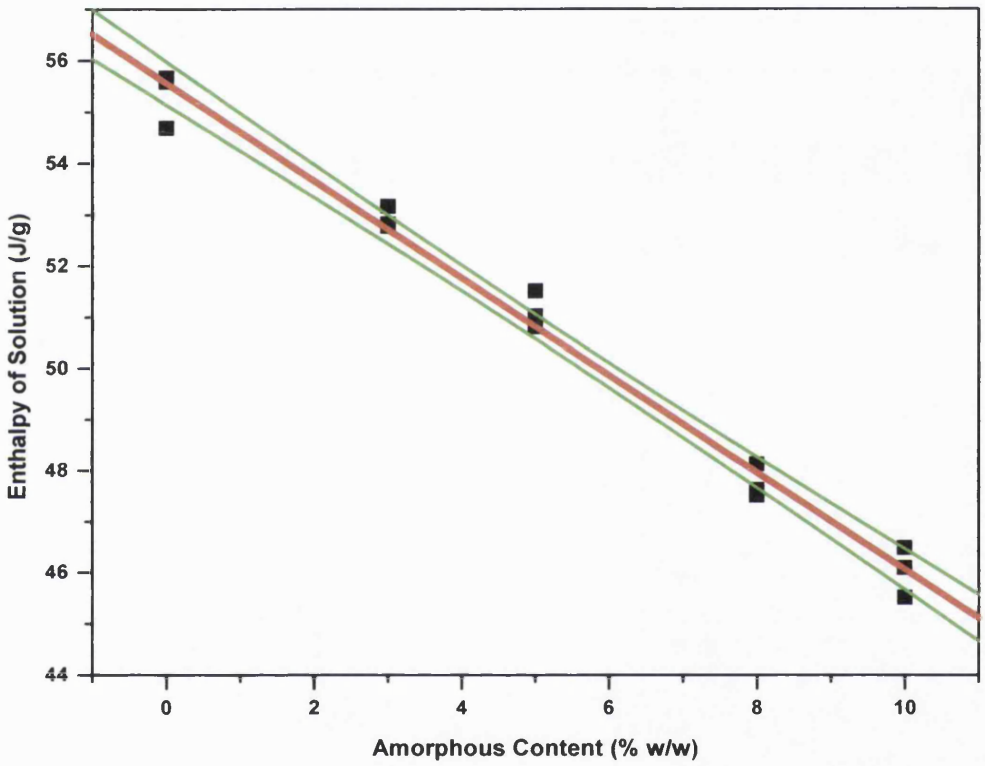

Figure 4.8 *The line of best fit for those samples which were dried in a vacuum oven at 50 °C and –300 mbar. The correlation (R^2) has been found to be 0.986, which is almost identical to that found for the desiccated samples. This is due to the fact that samples in this range of amorphous content are predominantly crystalline and therefore residual water will have less of an impact on the enthalpy of solution calculated. However, for samples of greater amorphous content this effect would be increasingly noticeable, and the issue of residual water content is very important in such cases.*

4.5. CONCLUSIONS

Solution calorimetry has been found to provide a reliable method by which to detect and quantify the amorphous composition of materials of small degrees of disorder. Upon building a calibration model, it offers a calorimetric technique with which quantification can be carried out quickly and reliably. This work has shown that in the case of lactose, a calibration model has been established which provides accurate quantification of disorder to within ± 1% w/w amorphous content, in the range of 0 – 10% amorphous content. These limits were achieved with both desiccated and vacuum oven stored samples. However, above this range the effects of vapour sorption by the amorphous portion of the sample would become increasingly important, requiring the removal of all residual moisture.

Solution calorimetry has also been shown capable of differentiating between samples of varying moisture content and providing an indication of how moisture sorption contributes to the thermodynamics of the solution process. Further work is required in order to explain the underlying processes involved.

The results obtained have illustrated that sample storage is capable of impacting greatly upon the enthalpy of solution obtained. It is clear that hygroscopic materials such as lactose are liable to produce erratic results if storage conditions are not controlled. Residual water is capable of distorting results, and the greatest accuracy in quantification of amorphous content can only be achieved if samples have been maintained in an extremely dry environment. This work highlights the difficulty involved in removing residual water from a hygroscopic amorphous material, which is a serious stability issue particularly if the glass transition temperature of that material is close to the storage temperature.

It is also important to note that the suitability of solution calorimetry to such quantification work relies upon a large difference between the energies of the amorphous and crystalline forms, and the availability of 100% amorphous and crystalline standards. Different materials will exhibit different enthalpies of solution

in the amorphous and crystalline forms. Indeed further work is needed in order to establish whether amorphous forms of the same material, generated by different techniques, have the same enthalpies of solution.

CHAPTER FIVE

ISOTHERMAL MICROCALORIMETRY TO QUANTIFY SMALL DEGREES OF AMORPHOUS CONTENT

5.1. The Use of Batch Isothermal Microcalorimetry to Determine the Amorphous Content of Predominantly Crystalline Samples

5.1.1. Introduction

The accidental introduction of disorder into crystalline materials during processing has already been discussed at length (Chapter 1). This material can have a detrimental effect on product behaviour, such effects including increased chemical instability (Pikal et al., 1978) and hygroscopicity (Kontny et al., 1987) and reduced powder flow. However, it is often the reversion of this unstable amorphous material to the lower energy state crystalline form on storage that has the most dramatic effect, bringing about particle aggregation. Despite this accidentally introduced amorphous material often occupying only a few percent of the bulk, its location on particle surfaces gives it a disproportionate control over the surface interactions of the predominantly crystalline powder. In Chapters 3 and 4 the development of new vapour sorption, spectroscopic and solution calorimetry methods to enable the quantification of this small degree of disorder has been outlined. Here, the use of isothermal microcalorimetry to study crystallisation and materials of low amorphous content is investigated.

The transition of material from the unstable amorphous state to the crystalline form is accompanied by a heat exchange. Early microcalorimetric work outlined the sensitivity of the technique, *e.g.* detecting crystal changes in pre-stored anhydrous lactose samples due to the incorporation of water (Angberg et al., 1991). The technique was further developed (Byström, 1990, Angberg et al., 1992) to show that sealing a hydrophilic amorphous sample in a glass ampoule containing a reservoir of saturated salt solution (to produce an atmosphere of specified relative humidity) in effect produced a mini humidity chamber in which reactions involving water sorption could be monitored by recording heat flow against time. Subsequent to this, Sebhatu et al. (1994) showed that this set up could be employed to induce spontaneous crystallisation in amorphous lactose samples, facilitating the detection

and measurement of the crystallisation process. The crystallisation of other materials has also been followed, including salbutamol sulphate (Buckton et al., 1995) and nifedipine (Aso et al., 1995). Ahmed et al. (1996) showed that a similar set up, replacing the saturated salt solution with an organic solvent, *e.g.* ethanol, enables the crystallisation of a hydrophobic amorphous material to be studied.

The suitability of isothermal microcalorimetry to detect low levels of amorphous content has also been investigated. Sebhatu et al. (1994) showed that it is possible to detect as little as to 2% disorder in samples containing milled amorphous lactose, by inducing crystallisation through exposure to elevated relative humidity. A later study by Buckton et al. (1995) detected crystallisation in a 0.313% w/w amorphous lactose sample. However, they stated that at very low amorphous contents, the crystallisation response of the samples was less reproducible. At the lowest levels of amorphous content investigated (0.313% and 0.625% w/w) a multiple peak was obtained. In the case of such samples, crystallisation occurs within an hour of the start of the experiment. It is possible that the crystallisation response for such samples coincides with the wetting of the sample, or that the events which together contribute to the crystallisation response become separated, thus resulting in a multi-phase peak.

5.1.2. Aims of this Study

Through the investigation of the crystallisation response for totally and partially amorphous lactose samples at different relative humidities, it was hoped that a method for the quantification of amorphous content by isothermal microcalorimetry could be developed.

5.1.3. Experimental

5.1.3.1. Preparation of 100% Amorphous Lactose

100% amorphous lactose was prepared by spray drying as outlined in Section 2.5.3.1. Confirmation of the amorphous nature of the yield was obtained from XRPD.

5.1.3.2. Preparation of Partially Amorphous Lactose Samples

Samples were prepared as described in Section 2.10. They were stored over phosphorous pentoxide at room temperature prior to use to ensure the absence of large quantities of water vapour and prevent crystallisation of the amorphous portions of the samples.

5.1.3.3. Batch Isothermal Microcalorimetry

Details of the Thermal Activity Monitor (TAM) 2277 (Thermometric AB, Järfälla, Sweden) can be found in Section 2.1. Samples were weighed accurately into 3 mL glass ampoules. Into both the sample and reference ampoules was placed a mini-hygrostat containing a saturated salt solution to produce the desired relative humidity. Magnesium nitrate ($Mg(NO_3)_2,6H_20$) was used to produce an atmosphere of 53% RH, whilst Sodium Chloride (NaCl) was used to produce 75% RH. All experiments were to be carried out at 25 °C, therefore pre-equilibration of samples, ampoules and salt solutions (the individual components before assembly and sealing) to that temperature for 30 mins was carried out prior to all experiments. The method followed for experiments and calibrations is outlined in Section 2.1. All data were analysed using Origin 3.0 ™ software.

5.1.4. Results and Discussion

5.1.4.1. Processes Involved in the Crystallisation of 100% Amorphous Lactose

In Figure 5.1 the crystallisation response of a 33.0 mg sample of 100% amorphous lactose at 75% RH in the TAM is illustrated. It can be seen that several phases are involved in the response. Having kept the ampoules in the upper equilibration position for approximately 20 mins (until a baseline had been achieved) they were then lowered to the measuring site, resulting in a sharp exothermic electrical spike (due to the friction of lowering) and a more prolonged exothermic peak lasting almost one hour, denoted peak A in Figure 5.1 and highlighted in Figure 5.2. This initial exothermic peak results from a combination of evaporation of the salt solution in order for the atmosphere in the ampoule to reach the specified RH (an endothermic response), and from wetting of the amorphous lactose sample as it

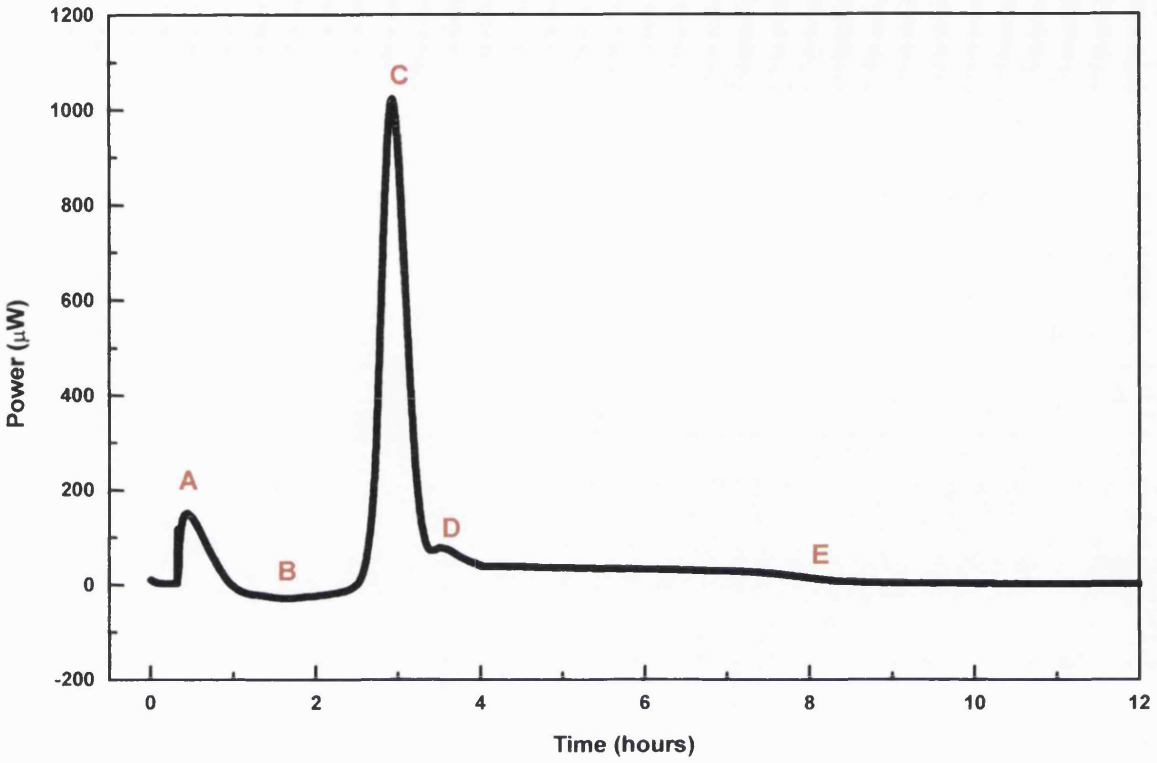

Figure 5.1 *The typical crystallisation response for a 33 mg sample of 100% amorphous lactose at 75% RH, as recorded by isothermal microcalorimetry.*

absorbs the water (an exothermic response) (Sebhatu et al., 1994, Ahmed et al., 1995, Darcy and Buckton, 1998). In addition, it has been suggested (Buckton and Darcy, 1996) that this response may be due, in part, to the structural collapse of the amorphous phase.

The decay of peak A may be attributed to a reduction in the magnitude of the exothermic water sorption response, an increase in evaporation from the hygrostat, or a combination of these effects. A short baseline can be clearly seen (denoted B), although it's location at –30 μW implies that the majority process continues to be endothermic.

Previously, a lag time has been noted after the initial exothermic peak A, where a flat baseline response has been obtained. This response has been attributed to the

endothermic vapourisation of the salt solution and the exothermic vapour sorption by the sample being equal and opposite in magnitude and therefore cancelling each other out (Angberg et al., 1992, 1992a). In this instance, magnification of events show that this is not the case (Figure 5.2). However it is possible that the new data analysis packages available, which allow greater magnification of data, show events in greater detail.

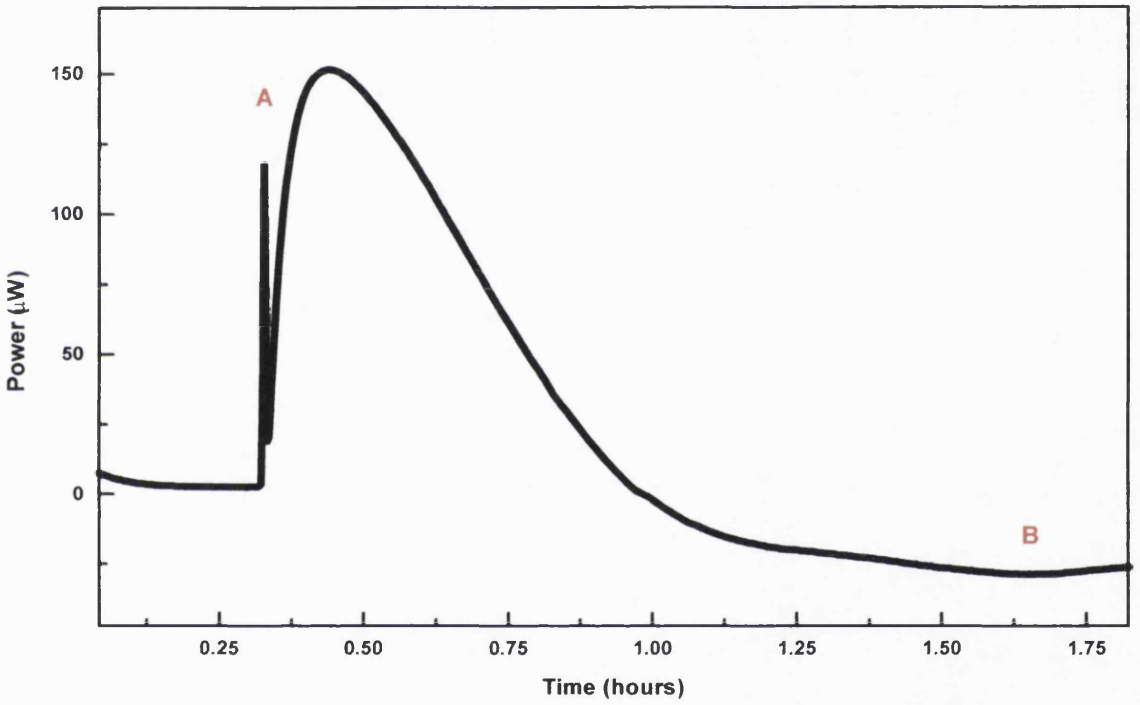

Figure 5.2 *Magnification of the early exothermic peak observed for 100% amorphous lactose at 75% RH. Contributing to this peak are the friction created by the lowering of the ampoules to the measuring site of the channel, the evaporation of the salt solution and the wetting of the sample.*

After just over 150 mins, the main crystallisation event gets underway (denoted C) and a swift exothermic response is observed. The shape of this peak indicates a very rapid process. Previous work has shown that samples removed immediately after this large exothermic peak are crystalline in nature (Briggner et al., 1994). In

addition, examination of the sample after the peak reveals that it has changed from a flowing particulate material to a hard, fused, solid mass.

It has been observed (Makower and Dye, 1956) that subsequent to crystallisation carbohydrates expel the previously absorbed plasticising water. Indeed this effect may be observed gravimetrically (Chapter 3). Whilst the crystallisation event itself is exothermic, this expulsion of water from the sample will be an endothermic event. Figure 5.3 shows that magnification of the crystallisation event reveals a clear shoulder peak (denoted D) to the main crystallisation peak (C). This event has been observed previously. Sebhatu et al. (1994) suggested that it should not be attributed to the expulsion of plasticising water as a consequence of crystallisation, since that event should be cancelled out by the exothermic condensation of that water back into the mini-hygrostat, in a manner similar to that suggested by Angberg et al. (1992, 1992a) to explain the lag phase between the original peak and the main crystallisation event. However since it has now been shown that this lag phase is in fact an endothermic event, the expulsion and condensation of water could be a possible explanation for this exothermic shoulder.

Sebhatu et al. (1994) suggested that this event, D, should be attributed to the incorporation of water into the anhydrous α-lactose formed after crystallisation to form α-lactose monohydrate. Briggner et al. (1994) attributed the event to the mutarotation of β-lactose to α-lactose monohydrate. Angberg et al. (1991) showed that this mutarotation process can be followed by microcalorimetry, and that it occurs as an extensive process only at the highest relative humidities (94% RH), although it does occur at lower relative humidities to a lesser extent.

Subsequent to this relatively fast co-operative crystallisation process, a final long, slow exothermic process may be observed upon close examination (Figure 5.3). This event has never previously been noted, and therefore no explanations for its existence have been offered to date. It is possible that it may be attributed to water movement within the ampoule, either between the sample and the mini-hygrostat, or

within the sample itself. However, it may represent a mutarotation process. Angberg et al. (1991) used microcalorimetry to investigate mutarotation in anhydrous crystalline lactose, and found that it was possible to detect a process after sample storage for 112 days at 94% RH. This would indicate that the process is in fact of a long, slow nature. It would therefore be surprising if the mutarotation event goes to completion over just a few hours. However, it is possible that immediately after crystallisation the sample is sufficiently wet that some mutarotation does occur over several hours.

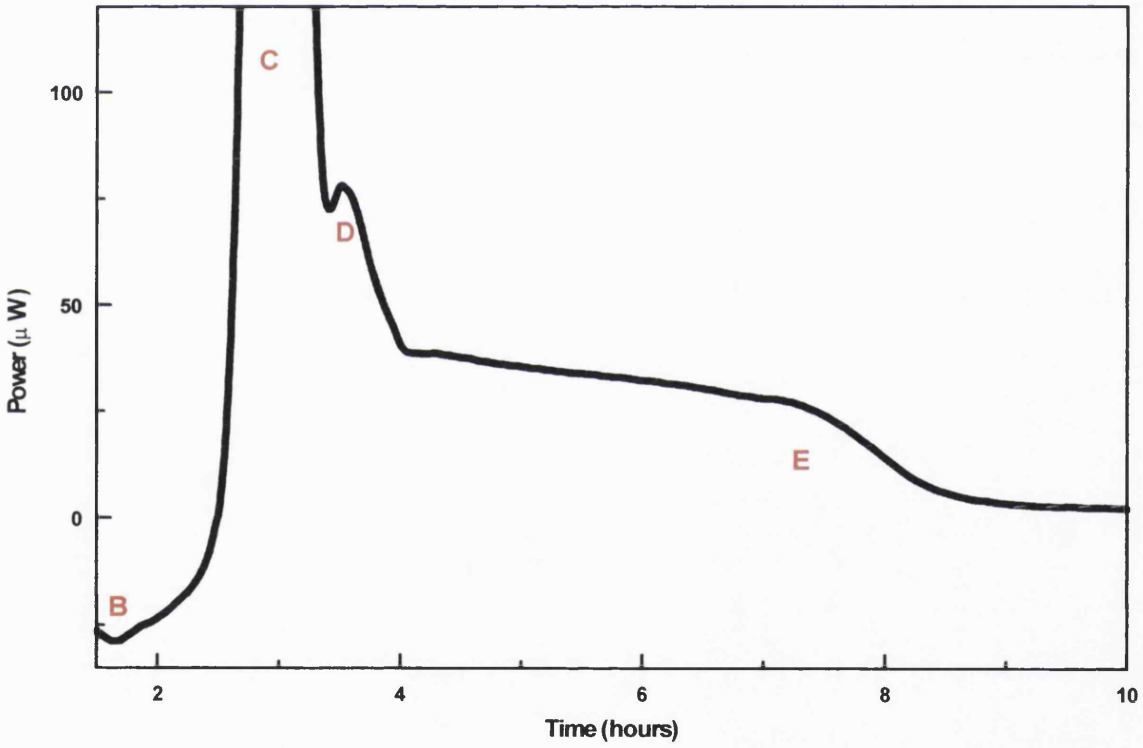

Figure 5.3 *Magnification of the crystallisation of 100% amorphous lactose at 75% RH. The existence of a shoulder (denoted D) and a low slow exothermic event (denoted E) subsequent to the main peak is clear.*

5.1.4.2. Determination of the Enthalpy of Crystallisation of 100% Amorphous Lactose

From the above discussion, it can be concluded that determining the enthalpy of crystallisation for amorphous lactose is a complicated procedure. Due to the multi-phase response in the microcalorimeter, it is difficult to assign a start- and end-point to the event. In addition, different workers seem to use different approaches to calculate the enthalpy. Sebhatu et al. (1994) first reported a method for the determination of the enthalpy of crystallisation of amorphous lactose, having assigned three main phases to the crystallisation response observed in the isothermal microcalorimeter. For their determination of crystallinity, only the integration of the main crystallisation peak (which they termed phase II, termed phase C in Figure 5.1) was carried out. The 'third phase' of the process (phase D in this study), was not included in their calculations. The integration of the main crystallisation peak gave a specific heat of crystallisation of 32 J/g, ± 4%.

Further publications reported values for the enthalpy of crystallisation of lactose, however there is less clarity in terms of what was actually measured. Briggner et al. (1994) stated that "if the areas under the curve are measured for each peak" the enthalpies recorded were between 44.9 and 47.8 J/g. Chidavaenzi et al. (1997) found that for 100% amorphous lactose a value of 50 mJ/mg "was obtained by integrating the area under the crystallisation peak".

Darcy and Buckton (1998) returned to the three phase crystallisation process in which it was stated that "the area under the curve for the sum of parts 2 and 3 has proved to be reproducible for spray-dried amorphous lactose samples... amounting to a mean net heat change of 48 J/g when measured at 25 °C".

Originally, many of these published enthalpies (Briggner et al., 1994, Buckton and Darcy, 1995) were deduced from peak areas which had been directly calculated using the Digitam 3.0® software (Thermometric AB, Sweden) used to record experimental data. However with specific peak analysis programs such as

Origin™© (Microcal Software, Inc.) we are better equipped to analyse data, with various choices of baseline and peak analysis packages, aided by the ability to magnify curves. This has led to the observation that certain previously ignored artefacts associated with crystallisation are in fact of a magnitude significant enough to have a notable impact on calculated enthalpies.

In addition to these issues it has been suspected that slight alteration of experimental conditions can have a disproportionate impact on the observed response in the isothermal microcalorimeter. It has been shown that alteration of temperature and relative humidity can have a dramatic effect on the recorded enthalpy of crystallisation for amorphous lactose (Buckton and Darcy, 1998). Increasing temperature from 25 to 60 °C was found to result in a larger calculated crystallisation enthalpy (attributed to the fact that less plasticising water would be required to induce crystallisation, and therefore the amount of expelled water subsequent to crystallisation (an endothermic event) would be reduced). Increasing relative humidity was found to result in a smaller value, especially at higher temperatures.

Due to the fact that the information gained from isothermal microcalorimetry does not provide any chemical data, it is very difficult to determine which processes are occurring during the various stages of the crystallisation experiment. In determining the enthalpy of crystallisation of 100% amorphous lactose, the aim is to provide a standard value from which the amorphous content of partially amorphous samples may be calculated. It is therefore essential that a reproducible technique be established for the assignment of start- and end-points of the peak to be integrated. It is obvious that the processes occurring in a sealed ampoule during the crystallisation of amorphous lactose overlap, and since they cannot be distinguished from each other it is not possible to draw a line between them and therefore difficult to omit one or other of them. It should also be noted that to term the area under the peak as an enthalpy of crystallisation is, in fact, a simplification, since various events are occurring simultaneously.

5.1.4.3. Assigning a start- and end-point to the peak

It would seem that in most cases an endothermic event precedes the main crystallisation peak, so that the start-point of the peak occurs at a negative power value. The extent of this event seems variable (compare Figure 5.1 with Figure 5.4). It must be decided whether an area should be taken from the minimum point of this endotherm, or perhaps from the point at which the peak crosses the x-axis (at $y = 0$). In any case, having decided upon the appropriate x-coordinate, most peak analysis packages allow the choice between integration from $y = 0$ or from the y-ordinate itself. If this endotherm is ignored, it is possible that an event which sometimes occurs during the main crystallisation peak (phase C), and as such is otherwise included in calculations, is being omitted. This could lead to greater enthalpies being calculated than would be expected, since the main peak would be larger than in other instances.

The final long exothermic event (E) subsequent to crystallisation is observed in all experiments, and gives rise to a difficulty in assigning the endpoint of the area to be integrated. Without a greater understanding of the processes involved in the late stages of the crystallisation of amorphous lactose, it is not possible to know if this artefact should be regarded as an extension of the main crystallisation event, or if it is another process altogether. As already mentioned, it is likely that water movement within the sample, as well as mutarotation, is mainly responsible for this event.

Inclusion of the final exothermic process mentioned above (which can continue for many hours) can have a huge impact on the enthalpy calculated since the average enthalpy of this area alone has been found to be as large as 25 J/g, depending upon the method used to determine enthalpy of crystallisation (see Figure 5.5, Table 5.1). To omit it, another question is raised regarding the attribution of an end point to some coordinate following the main crystallisation peak. This is of importance since the main peak does not return to baseline. Therefore it is necessary to decide if a sloping baseline from the start-point (*e.g.* as illustrated in Figure 5.5) is suitable for

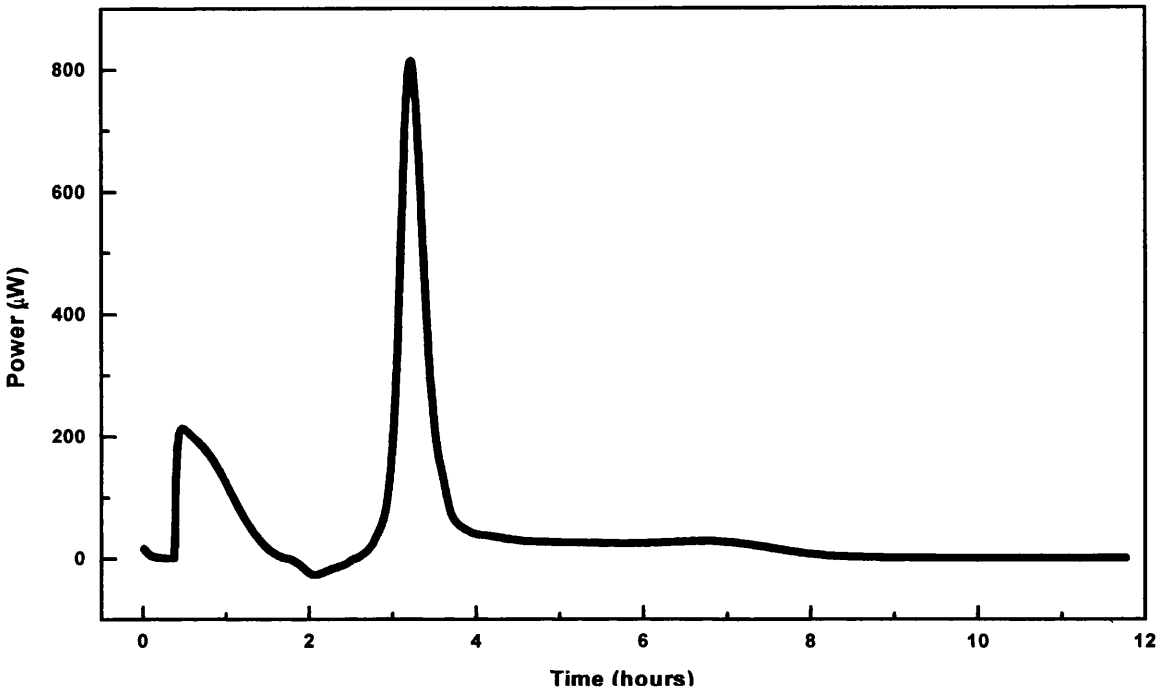

Figure 5.4 *The crystallisation of 100% amorphous lactose at 75% RH. In this instance a clear endothermic event immediately prior to the main crystallisation event is observed. This adds to the difficulty in assigning a start point from which to integrate the peak. It should also be noted that the shoulder often seen during crystallisation at 75% is absent.*

calculations or if integration from a constant y-value (*e.g.* y = 0 or the y-ordinate consistent with the start point) is preferable. This altered baseline value could reflect a change in the heat capacity of the sample, which is reasonable since the sample has changed physical form. One possible solution is to extrapolate the endpoint to the y-ordinate which corresponds to that of the starting point.

In order therefore to determine the best method by which to calculate the enthalpy of crystallisation, several different techniques were used to assign start- and end-points of crystallisation. This was in order to establish which, if any, provided good reproducible enthalpies of crystallisation, and each method was applied to 18 different crystallisation responses of 100% amorphous lactose at 75% RH and 25 °C. These methods were as follows:

- Method 1a: Determination of enthalpy based upon the inclusion of phase C only. Integration of data from y = 0.

- Method 1b: As method 1, but with the integration of both phases C and D. If a separate phase D is not visible, it is assumed that it is included in the entire enthalpy of the main crystallisation peak (phase C).
- Method 1c: Determination of enthalpy by the integration of phases C, D and E from y = 0.
- Method 2a: Determination of enthalpy based upon the inclusion of phase C only, integrated with a sloping baseline, from the lowest point during phase B to the endpoint of phase C.
- Method 2b: As method 2a, but with data from phase D included in the integration. Again, if a separate phase D is not observed, it is assumed that it is included in the main crystallisation peak.
- Method 2c: Again as method 2a, but with the integration including phases C, D and E.
- Method 3a: Determination of enthalpy based upon the integration of phase C only, taking the start-point as the lowest enthalpy observed in phase B, and integrating with a flat baseline from this point.
- Method 3b: As method 3a, but including phases C and D.
- Method 3c: Again as method 3a, but including phases C, D and E.
- Method 4a: Determination of enthalpy includes all of phases B and C, with integration from y = 0 (*i.e.* areas of negative peaks are subtracted from the total area).
- Method 4b: As method 4a, but integration of phases B, C and D is performed.
- Method 4c: Again as method 4a, but integration of phases B, C, D and E is performed.

A further explanation of these methods is shown in Figure 5.5. These data are summarised in Table 5.1.

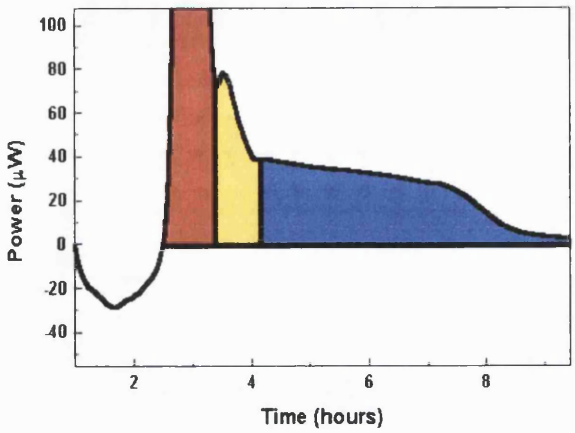

Methods 1a, b, c.

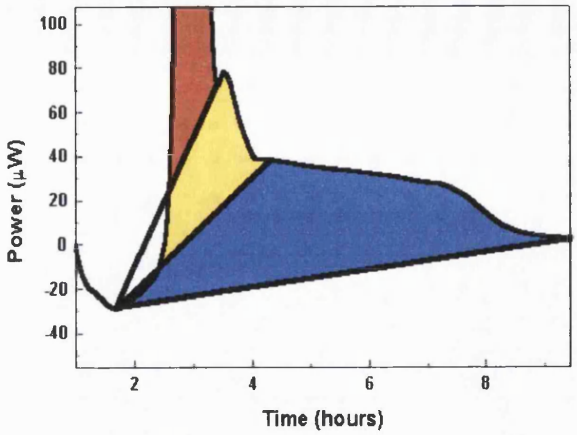

Methods 2a, b, c.

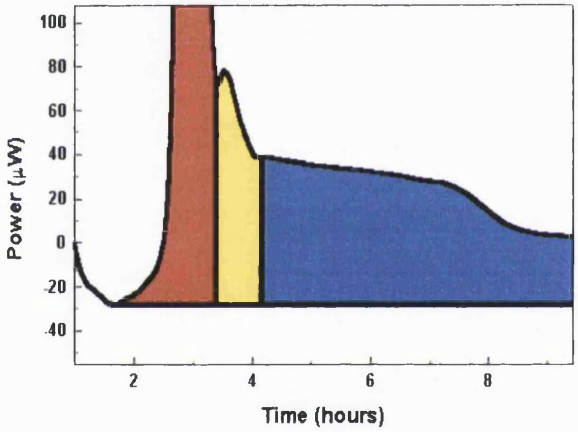

Methods 3a, b, c.

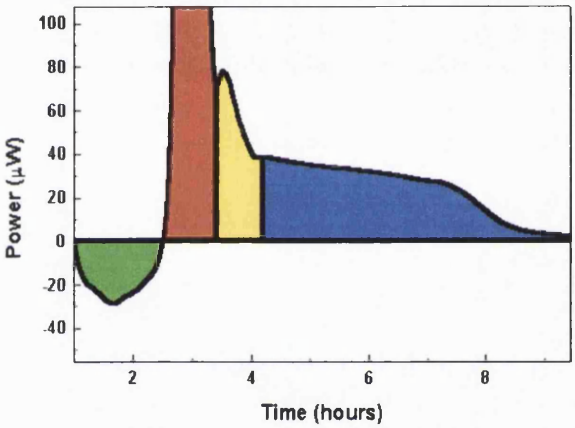

Methods 4a, b, c.

Figure 5.5 *The 12 different methods for integration of peak area used are illustrated above. Methods (a) integrate the area coloured red, (b) the red and yellow areas and (c) the red, yellow and blue areas respectively. Methods 1 and 4 are integrated from y = 0, Methods 2 are integrated with a sloping baseline from the minimum point prior to the crystallisation peak and Methods 3 with a flat baseline from that point. Methods 4 differ from Methods 1 as the event immediately prior to the large crystallisation peak (coloured green) is included in all calculations, and is, in effect, subtracted from the total area since in the case shown here it is endothermic. It should be noted that in Method 2a the baseline intersects the actual data, and as such it would not be a suitable method to use in this case.*

Table 5.1 *The enthalpies of crystallisation for 18 different 100% amorphous lactose samples crystallised at 75% RH, as calculated by 12 different integration methods.*

Sample Mass (mg)	Enthalpy of Crystallisation (J/g)											
	Method of Integration											
	1a	1b	1c	2a	2b	2c	3a	3b	3c	4a	4b	4c
31.3	42.56	51.08	59.45	-	49.41	64.99	44.04	55.10	72.43	41.80	50.49	58.27
31.6	41.27	48.24	58.51	-	46.07	60.90	41.86	49.68	64.73	40.40	47.97	57.88
35.6	-	46.27	54.53	-	43.10	48.77	-	44.00	-	-	47.63	56.27
38.6	-	45.03	50.81	-	41.35	48.74	-	43.57	-	-	44.53	51.45
58.0	-	42.10	49.82	-	39.44	43.40	-	39.88	-	-	43.54	50.74
81.4	-	43.73	52.23	-	40.80	44.38	-	41.16	-	-	46.34	54.31
33.2	39.85	43.54	51.66	-	41.89	54.68	41.10	45.79	60.11	39.21	43.40	51.15
33.0	41.22	45.55	59.94	-	-	70.31	44.89	51.27	84.30	37.88	42.78	56.66
30.7	40.90	45.51	59.04	-	42.99	69.55	44.73	51.99	83.82	37.53	42.69	55.57
34.0	47.36	54.55	63.13	-	52.45	69.41	48.74	58.27	76.33	46.46	53.03	61.87
30.83	-	44.92	52.33	-	41.63	49.68	-	43.49	-	-	45.31	52.66
38.23	44.28	47.11	52.63	40.52	43.51	52.21	44.01	46.66	-	38.81	45.02	52.67
40.80	-	46.22	53.41	-	42.19	-	-	43.97	-	-	46.88	53.92
30.53	36.71	40.51	47.11	32.64	38.61	49.97	37.90	42.74	54.22	36.51	40.37	47.18
38.23	-	42.33	48.28	-	39.94	47.59	-	42.14	47.59	-	42.36	48.18
40.63	-	44.11	47.24	-	41.28	47.33	-	43.21	-	-	44.98	49.91
29.4	40.54	42.75	53.29	38.14	41.53	64.88	46.11	50.06	78.27	39.10	43.12	51.84
34.1	38.33	43.36	53.30	33.53	41.60	60.71	41.78	49.54	70.52	36.40	41.33	51.43
Average	41.30	45.38	53.82	36.21	42.81	55.74	43.52	46.81	69.23	39.41	45.09	53.44
n	10	18	18	4	17	18	10	18	10	10	18	18
SD	2.83	3.27	4.34	3.25	3.42	9.11	2.85	4.96	11.75	2.83	3.13	3.66
% error	6.85	7.21	8.06	8.98	7.99	16.34	6.55	10.60	16.97	7.18	6.94	6.85

From the data shown in Table 5.1, it can be seen that a large difference in the standard deviation achieved by the different quantification methods was achieved. Furthermore, this standard deviation (as expressed in J/g) required conversion to a percentage of the total average enthalpy calculated in order to ascertain the best method for the determination of enthalpy of crystallisation. It must also be considered that certain integration methods were not applicable to all samples. There are several reasons for this. For example, not all samples illustrated a clear shoulder (phase D) subsequent to crystallisation. In addition, in some cases where a sloping baseline was employed for the integration, the baseline itself intersected the data (as illustrated in Figure 5.5 (Method 2a)), therefore invalidating the method. Subsequently, although Method 3a achieved the lowest percentage error in the calculation of the enthalpy of crystallisation of 100% amorphous lactose, it was only applicable to 10 of the 18 samples and was therefore not be a suitable choice.

In selecting a method to be used as the standard for integrating data, it must be remembered that partially amorphous samples may not always demonstrate the same crystallisation profiles as totally amorphous material. Therefore, selection of an easily applicable technique was necessary. For this reason Methods 1b and 4c were chosen for the integrations involved in determining the enthalpies of crystallisation of predominantly crystalline samples exposed to 75% RH.

5.1.4.4. Quantification of Amorphous Content in Predominantly Crystalline Lactose by Batch Isothermal Microcalorimetry at 75% RH.

Assuming a linear relationship between enthalpy of crystallisation and amorphous content, samples of 1-75% w/w amorphous content were crystallised at 75% RH and 25 °C, and the areas under their crystallisation peaks integrated, using Methods 1b and 4c (see section 5.3.2.1.). A reference enthalpy of crystallisation value for 100% amorphous content was taken as the average enthalpy of crystallisation for each method, as shown in Table 5.1. The original amorphous contents against those calculated using Method 1b are plotted in Figures 5.6a and 5.6b. It can be seen that a linear relationship was achieved although the amorphous content calculated was

usually less than that which was actually contained within the sample, indicating that there may be a standard error relating to the technique. It can also be seen clearly in Figure 5.6a that a great deal of scatter in the data in the 1-10% amorphous content range was obtained. A correlation (R^2) of 0.769 was achieved in that range, and 0.986 in the 1-75% amorphous content range. It should be noted that in the 1-75% amorphous content range, only the 5% and 10% amorphous content samples are included from the lower range. Also, due to the presence of fewer samples of greater than 10% amorphous content, the correlation value in the 1-75% range is not a good reflection on the capabilities of the method. It is also apparent that the calculated amorphous contents are much lower than the actual values. It is possible that a degree of error using this integration method is due to difficulties in assigning the point at which phase D ends. This error may have become more significant with decreasing amorphous content.

In Figures 5.7a and 5.7b the data calculated by Method 4c for the same samples are shown. Again a linear relationship was achieved, with a correlation (R^2) of 0.974 in the 1-10% region, and 0.984 for the 1-75% amorphous content range. For those samples of greater than 10% w/w amorphous content, Figure 5.7b illustrates that the technique consistently quantifies amorphous content at a value of ca. 20% less than the actual figure. One possible explanation is that the reference 100% amorphous lactose value is inappropriate. However, as shown in Figure 5.10, samples of as little as 7% w/w amorphous content display an event which corresponds to that denoted 'phase E' in Figure 5.3. It therefore seems logical to include this event in calculating the enthalpy of crystallisation of partially amorphous samples. It is possible that this error arises from the effect of the crystalline portion of the sample having an effect on the behaviour of the bulk.

When samples of very low amorphous content are exposed to elevated relative humidities (*i.e.* once the ampoules are sealed) their crystallisation response is much smaller, and is observed much more quickly than is the case for samples of greater disorder. This effect has been previously noted (Buckton et al., 1995). And in such

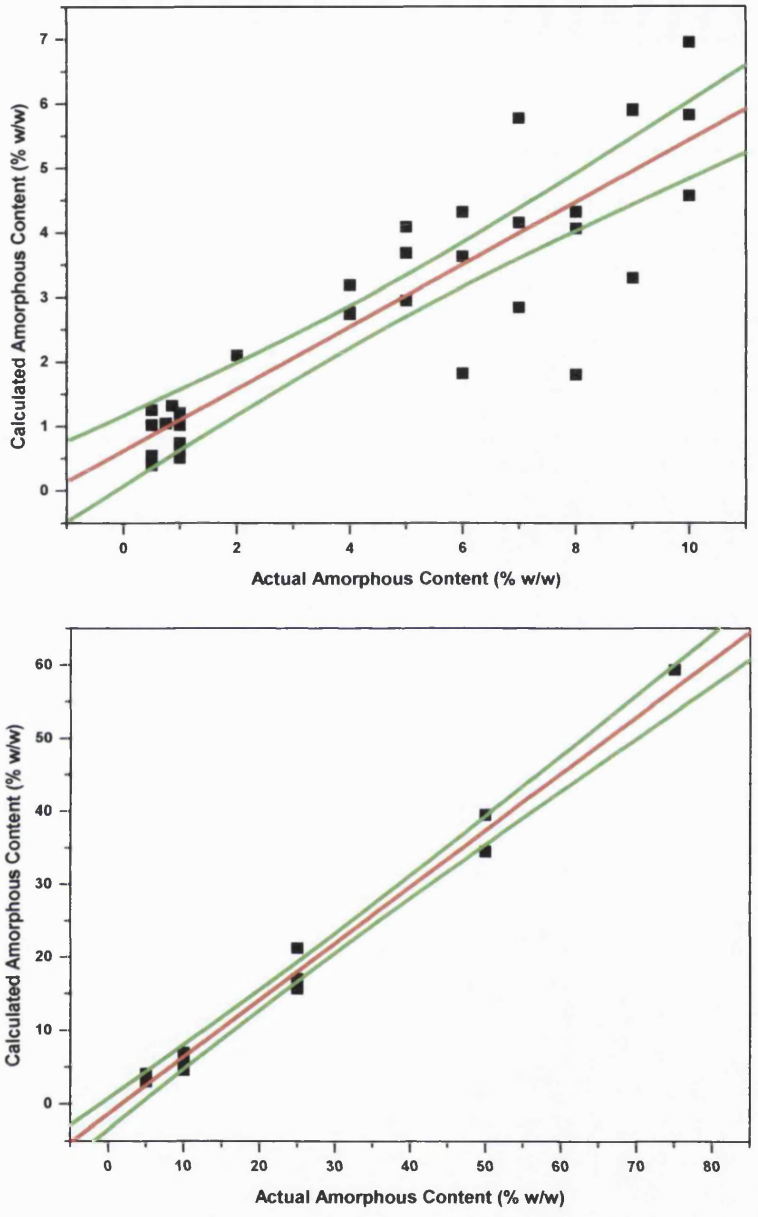

Figure 5.6a and b *The actual versus Method 1b-calculated amorphous contents of 1-10% and 5-75% w/w amorphous lactose samples crystallised at 75% RH. It should be noted that the calculated values are lower than the actual amorphous contents known from sample preparation. Green lines indicate the upper and lower 95% confidence intervals in the line of best fit. Correlation (R^2) was found to be 0.769 (1-10%) and 0.986 (1-75%) respectively.*

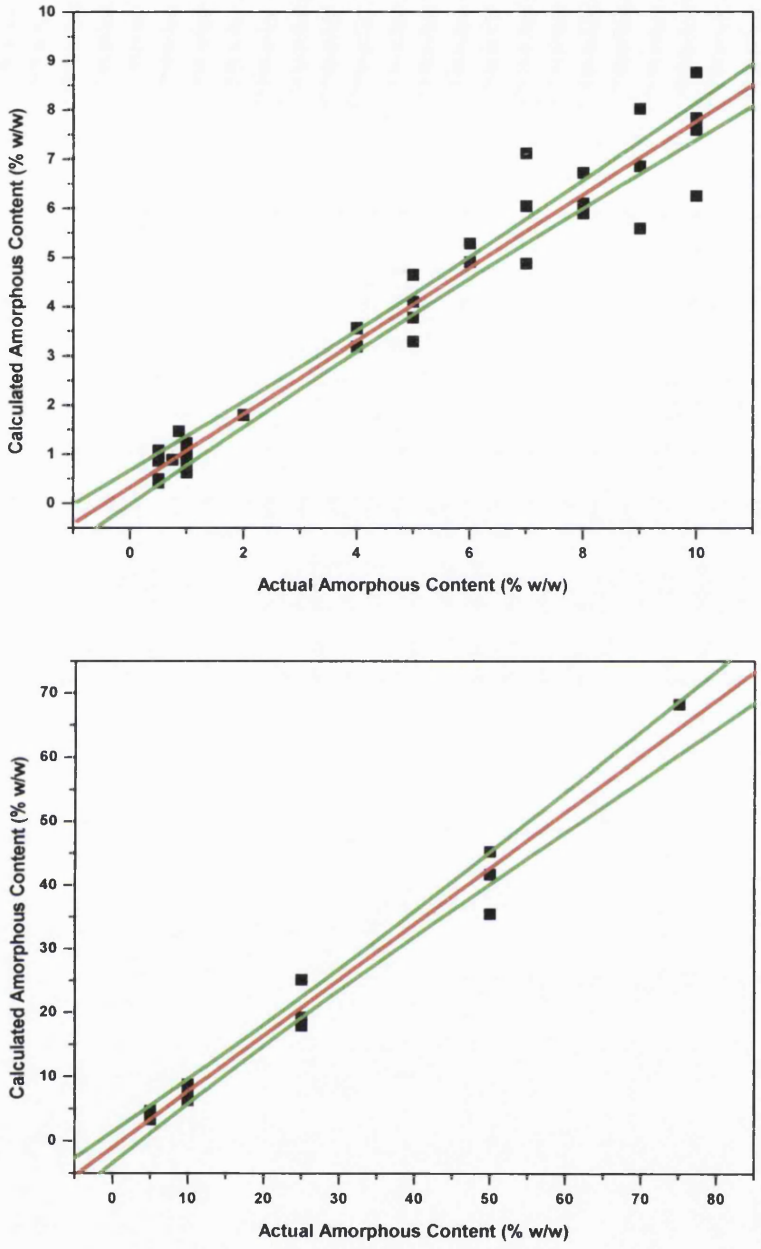

Figure 5.7a and b *The actual versus Method 4c-calculated amorphous contents of 1-10% and 5-75% w/w amorphous lactose samples crystallised at 75% RH. It should be noted that the calculated values are lower than the actual amorphous contents known from sample preparation. Green lines indicate the upper and lower 95% confidence intervals in the line of best fit. Correlation (R^2) was found to be 0.974 (1-10%) and 0.984 (1-75%) respectively.*

cases, the crystallisation response often commences before a baseline has been achieved following the lowering of the ampoules (Figure 5.8). In addition to this it is possible that it overlaps with the wetting response. These occurrences lead to problems in determining the area under the crystallisation peak, since the starting point of the response has been lost. Hence, inaccuracies are introduced.

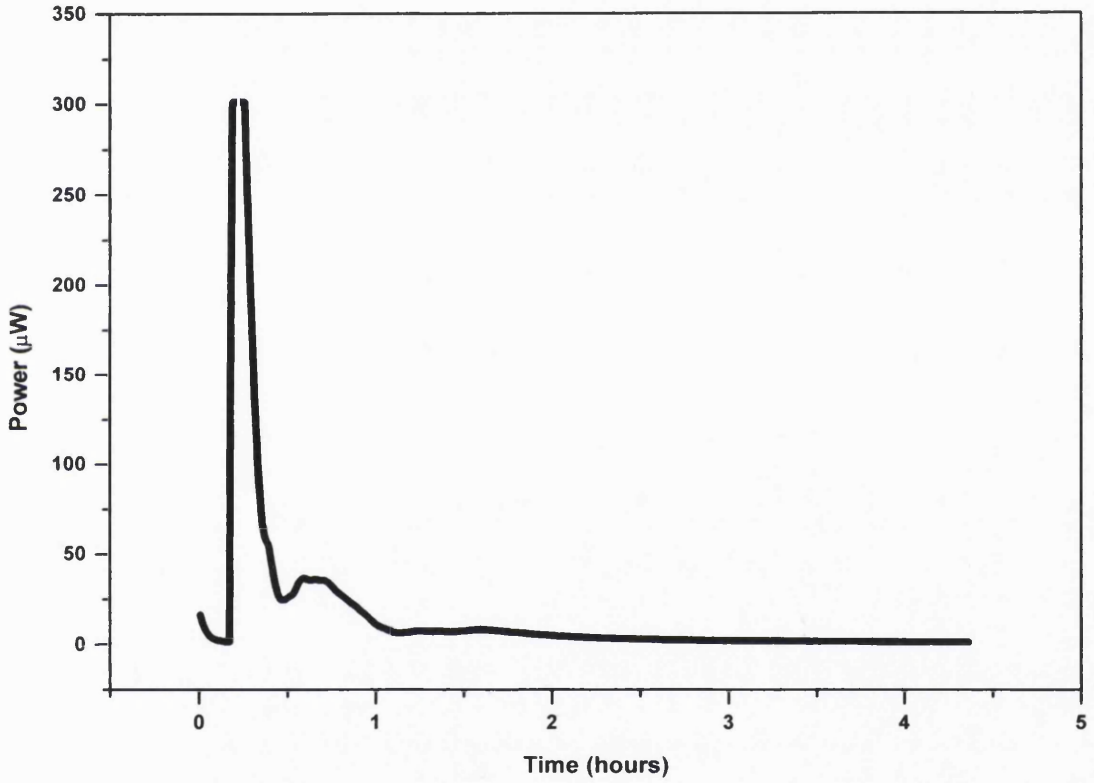

Figure 5.8 *The crystallisation response for a 660 mg sample of 0.5% w/w amorphous lactose at 75% RH by isothermal microcalorimetry, showing that the main crystallisation peak is lost in the initial friction response due to the lowering of the ampoules. The initial sharp peak, being caused by both the lowering of the ampoules and the fast crystallisation peak, is seen to go off scale (*i.e. *above 300 μW).*

In order to overcome this effect, sample masses were increased in order to increase the amorphous content within the ampoule. In the case of 1% w/w amorphous content, sample masses in excess of 800 mg have been used. This serves to prolong the time taken for crystallisation to commence, although it also impedes the absorption (and expulsion) of moisture by the sample. Subsequently, the resulting crystallisation responses often show multiple phases instead of one co-operative crystallisation peak (Figures 5.9 and 5.10). Therefore, determination of enthalpy of crystallisation in materials that crystallise quickly is possible if large quantities of sample are available in order to delay the onset of the event.

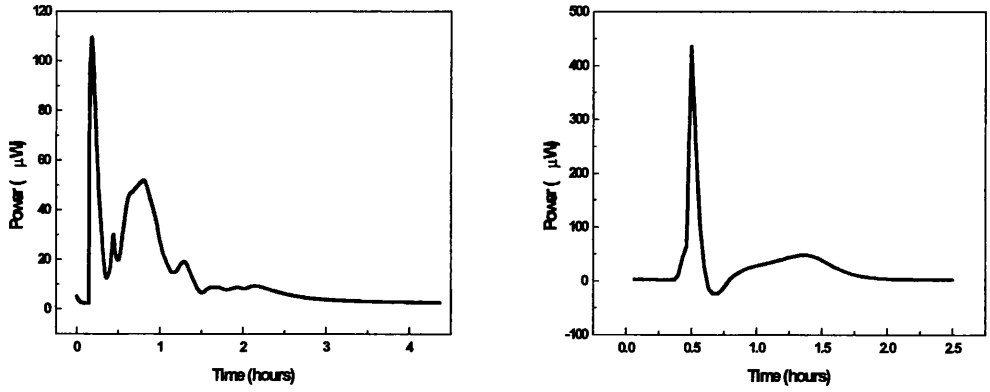

Figure 5.9 and 5.10 *The crystallisation response of 1% (left) and 7% (right) amorphous lactose at 75% RH, respectively. The 1% amorphous sample illustrates the effect of increased sample mass, demonstrating a prolonged and multi-phase crystallisation response. The 7% amorphous lactose sample clearly shows a large exothermic event after the main crystallisation peak, in addition to an endothermic event between the two exotherms. This is not seen for totally amorphous samples.*

5.1.4.5. Quantification of Amorphous Content in Predominantly Crystalline Lactose Samples by Isothermal Microcalorimetry at 53% RH.

In order to overcome the problems encountered determining the enthalpy of crystallisation of predominantly amorphous lactose samples at 75% RH, a quantification calibration was also performed at a lower relative humidity. Crystallisation at 53% RH and 25 °C was selected since previous work has illustrated that amorphous lactose still crystallises under these conditions, but with a greater lag time than at higher relative humidities (Briggner et al., 1994).

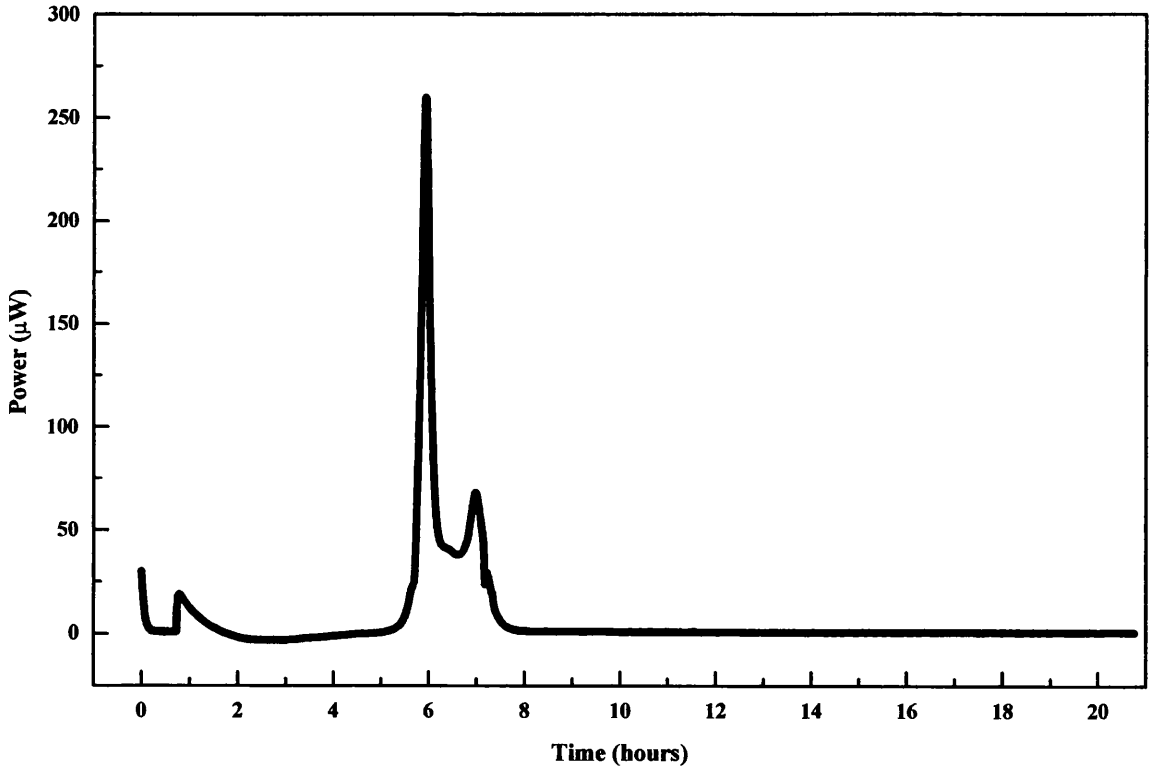

Figure 5.11 *The crystallisation of 100% amorphous lactose at 53% RH, showing clearly the second exothermic peak subsequent to the main crystallisation event. The absence of the long, slow exothermic event after the main peak is evident.*

The response for the crystallisation of 100% amorphous lactose under these conditions is shown in Figure 5.11. Integration of the crystallisation peak (using method 4c) revealed that the average enthalpy determined at the lower relative humidity was 57.28 J/g, which is greater that that calculated at 75% RH (53.44 J/g). Darcy and Buckton (1998) previously reported that RH does not affect the enthalpy of crystallisation of amorphous lactose at 25 °C, although they did observe this effect with crystallisation at higher temperatures. However, it should be noted that at that time integration of the exothermic peak post crystallisation was not carried out.

There are several reasons for the crystallisation response at lower RHs to result in the calculation of a greater enthalpy. The lower RH means that the supply of water vapour to the amorphous sample will be slower, thus delaying the entire crystallisation process and resulting in a protracted crystallisation peak. A greater separation of the individual components of the crystallisation response can be seen clearly in Figure 5.11, especially in the evidence of a second smaller exothermic peak after the initial large response, which corresponds to the shoulder which was sometimes present in the crystallisation response at 75% RH. However, this separation cannot be responsible for the larger enthalpy value obtained, since the overall value calculated for the process is independent of kinetics. The crystallisation response shown in Figure 5.1 for 100% amorphous lactose at 75% RH reveals that the slow exothermic event post crystallisation is completed after 8 hours exposure to the elevated RH. In comparison, from Figure 5.11 it is clear that the exothermic event seen at 75% RH is not observed at 53% RH. This would suggest that the event does not occur at lower RHs, which would support that argument that mutarotation is at least in part responsible for that event, as Angberg et al. (1991) showed that mutarotation is impeded at lower RHs. Another potential reason for greater enthalpies to be calculated at lower RHs is that amorphous lactose will absorb less water at lower RHs, and therefore, following crystallisation less plasticising water will be expelled. Since this expulsion process is an endothermic event, its reduction will result in a smaller negative contribution to the overall value, thus giving rise to a larger overall net enthalpy of crystallisation being calculated.

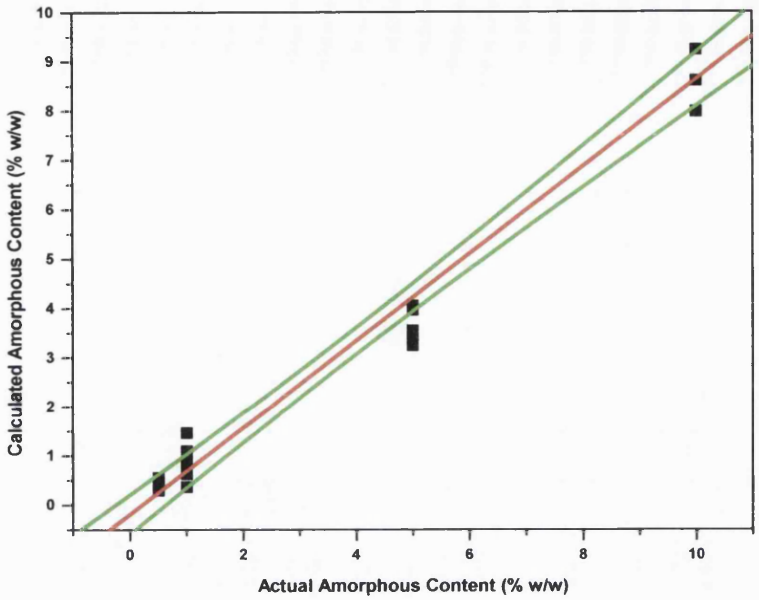

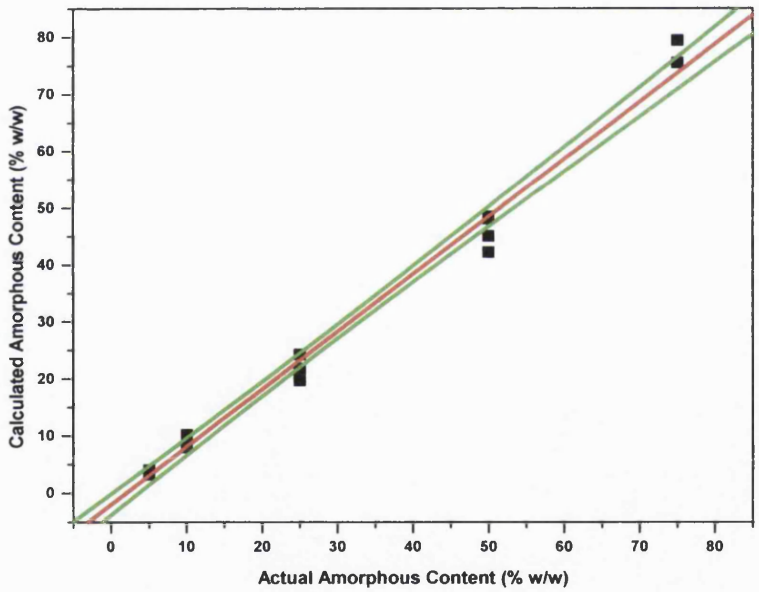

Figure 5.12 and 5.13 *The actual versus calculated amorphous contents of 1-10% and 5-75% w/w amorphous lactose samples crystallised at 53% RH. Again the calculated values are lower than the actual amorphous contents known from sample preparation , although it can be seen that determinations are closer to the actual values, and standard deviations are considerably reduced. Green lines indicate the 95% confidence intervals of the line of best fit.*

Gravimetric data have shown (Chapter 3) that the mass increase subsequent to the crystallisation of amorphous lactose is usually in the region of 3% w/w, as opposed to the 5% necessary for complete α-monohydrate formation. It is likely that different RH conditions result in different proportions of α-monohydrate and β-anhydrous lactose being formed, and that this may be responsible for higher enthalpies of crystallisation being obtained subsequent to crystallisation at lower RHs.

A linear relationship between the original and calculated amorphous contents determined at 53% RH was still achieved (Figures 5.12 and 5.13). Correlation (R^2) was found to be 0.968 between 1-10% amorphous content, and 0.991 between 1-75% amorphous content, showing that at the lower RH, the technique seems equally capable of quantifying amorphous content in lactose samples. However, the calculated values were still consistently approximately 10% lower than the actual values (except for the 75% amorphous sample). It is possible that these lower than expected enthalpies were related in some as yet unexplained way to the presence of crystalline material in the sample, and its effect on the crystallisation process. Although a portion of the error involved in the determination of amorphous content can be attributed to inconsistencies in the amorphous content of the samples from preparation (due to weighing errors and mixing), this cannot be attributed to the consistently low amorphous contents calculated, since other quantification techniques (*e.g.* DVS/NIRS in Chapter 3) did not experience the same errors, despite being developed with samples prepared by the same method.

5.2. The Use of Isothermal RH Perfusion Microcalorimetry to Determine the Amorphous Content of Predominantly Crystalline Samples

5.2.1. Introduction

The disadvantages of determining the enthalpy of crystallisation of amorphous and partially amorphous samples have been outlined in section 5.1, and have in part been

found to relate to the fact that upon sealing the sample and mini-hygrostat in the ampoule, the crystallisation of the sample cannot be halted or slowed. In order to overcome the problems which arise from this, a gas-flow set-up has been devised which allows for a dynamic system to be used, providing external control of the relative humidity to which the sample is exposed. This facilitates the alteration of RH throughout the duration of an experiment, thus providing control over the behaviour of the sample. Such a set-up allows for the establishment of a steady baseline whilst the sample is exposed to 0% RH, so that the amorphous material may be dried prior to the crystallisation step and the effects of lowering the apparatus into the channel can dissipate without any risk of crystallisation in the sample. Once a baseline has been achieved, the sample may then be exposed to elevated RH in order to induce crystallisation, and the heat flow generated recorded simultaneously.

In comparison with batch isothermal microcalorimetry, little work has been published on the use of the RH perfusion unit. One of the earliest published studies (Bhatt and Rubenstein, 1983) used the system to measure the interaction of water vapour with various crystalline and amorphous solids, showing that the technique is capable of detecting very small quantities of contaminants in a crystalline material. However, this early work relied on the used of saturated salt solutions to generate the required RH, and it highlighted the difficulties of this set-up to control the flow of gas through the solutions. From this, the current gas flow system was developed, where the vapour pressure (relative humidity) of the solvent is controlled through accurate mixing of two different gas flows (0% and 100% RH, respectively). This system offers a very sensitive and extremely reproducible technique, which was employed to probe the powder surface energetics of α-lactose monohydrate sourced from three suppliers in order to differentiate between them when contact angle measurements could not (Sheridan et al., 1995). This study showed that one supplier's product had different surface energy, thus explaining its different performance in a solid dosage form. The RH perfusion system has also been used to determine the hygroscopicity of drug substances (Jakobsen et al., 1997), as well as generating a calorimetric adsorption isotherm of water vapour on sodium benzoate

(Pudipeddi et al., 1996). Bakri et al. (1988) used the technique to ascertain the chemical stability of organic compounds, whilst more recently it has been used to characterise the physical and chemical interactions of a freeze-dried peptide (Sokoloski and Ostovic, 1997).

Isothermal RH perfusion microcalorimetry has also been used to investigate the crystallisation of a micronised drug substance. Using a ramping method (whereby the sample is exposed to continually changing RH at a defined rate), Briggner (1983) showed that the heat flow curve recorded could be divided into three distinct regions. The first region (exothermic) represented wetting of the drug substance, which was followed by a further exothermic response due to crystallisation itself, before a final endothermic region attributed to the evaporation of excess moisture from the sample following structural collapse and subsequent crystallisation. The area under the crystallisation curve could be integrated and related to the original amorphous content of the micronised solid, showing that the RH perfusion technique would be a suitable for the quantification of amorphous content.

However, several differences exist between the crystallisation response obtained in the static ampoule experiment and the gas flow system. Firstly, since the solvent vapour is generated outside the sample ampoule, the wetting and sorption by the sample can be detected. It has been suggested (Angberg et al., 1992, 1992a) that in the static ampoule set up this is not seen (or is at least diminished) due to the fact that the generation of solvent vapour (*i.e.* evaporation from the salt solution reservoir within the ampoule) generates a heat flow which is equal but opposite to that of the wetting response. Additionally, the gas flow technique provides a dynamic flow of vapour to the sample, and this facilitates much faster wetting and crystallisation responses, so that, for example, the time taken to the onset of crystallisation in the RH perfusion apparatus will be much less than that observed in a batch calorimetric experiment at the same RH. Care must be taken in the design of an RH perfusion experiment, since it is difficult to determine the point at which an equilibrium has been achieved following water sorption onto a thermodynamically unstable material.

This is due to the fact that a lag time often exists between establishing an environmental condition and achieving a change in solid state. This is particularly a problem in experiments where the RH is increased or decreased at a constant rate throughout the experiment (*i.e.* ramping). For this reason, the experimental set up in this section does not employ ramp experiments.

5.2.2. AIMS OF THIS STUDY

This work intended to investigate the crystallisation response of 100% amorphous lactose using isothermal RH perfusion microcalorimetry, in order to develop a technique for the quantification of amorphous content occurring at 1-10% w/w.

5.2.3. EXPERIMENTAL

5.2.3.1. Preparation of 100% Amorphous Lactose

See section 5.1.3.1.

5.2.3.2. Preparation of Predominantly Crystalline Lactose Samples

See section 5.1.3.2.

5.2.3.3. Isothermal RH Perfusion Microcalorimetry

Details of the experimental set-up can be found in Section 2.1. Samples of between 25-300 mg were loaded into the 4 mL stainless steel sample ampoule. The reference used in all cases was an identical empty 4 mL stainless steel ampoule, held on an ampoule lifter. The humidifying chambers were each loaded with 0.5 mL of water. A nitrogen gas flow of 2 - 4 mL/min was employed and this flow was directed down either the wet line (to become 100% RH) or the dry line (0% RH) in varying proportions in order to achieve the desired RH. The flow switch heater was set to 40 ^{o}C in order to prevent condensation of water within the unit. Calibrations were carried out after every three experiments, using empty sample and reference ampoules.

Since empty RH perfusion units contribute a heat flow upon changes in RH, 'blank' experiments, whereby both the sample and reference ampoules were empty, were carried out for each unit in duplicate using the same experimental method as for the actual sample experiments. The responses obtained were averaged for each unit, and then subtracted from the actual sample response before data analysis. All data were analysed using Origin 3.0 ^{TM} software.

5.2.4. Results and Discussion

5.2.4.1. Examination of the blank responses

The average blank responses for both units at 75% RH (following equilibration at 0% RH) are illustrated in Figure 5.14. It can clearly be seen that they do not give identical responses. Whilst both units show a clear exotherm immediately following exposure to 75% RH, it is clear that the magnitude of the response of unit 1 is far greater than that of unit 2. Upon magnification it can be seen that both units require several hours to completely equilibrate at the elevated RH. Unit 2 has almost returned to a steady baseline after only 2.5 hours, although it has only completely returned to baseline after almost 17 hours. This is in contrast with unit 1, which goes on to demonstrate an endotherm subsequent to the initial exotherm (at approximately 5 hours) and fails to reach a steady baseline until approximately 14 hours exposure to 75% RH. Although it would be a reasonable assumption that the magnitude of the exotherm for unit 2 is less than that of unit 1 due to the superimposition of the endothermic event (as seen in the case of unit 1 as a separate event) over the initial exotherm, integration of the blank responses (from $y = 0$) shows that whilst the enthalpy of the response of unit 1 is 0.56 J, that of unit 2 is much smaller, at 0.21 J. These data highlight the need to exercise caution in considering the units as identical instruments, although in comparison with the magnitude of the reactions to be measured, these differences are very small. Several reasons could contribute to the apparent differences in the behaviour of the RH perfusion units, including slight differences in the gas flow rate for each instrument, since each relies on a different mass-flow controller. It is unlikely that such differences are caused by a leak, since both units are capable of achieving a baseline

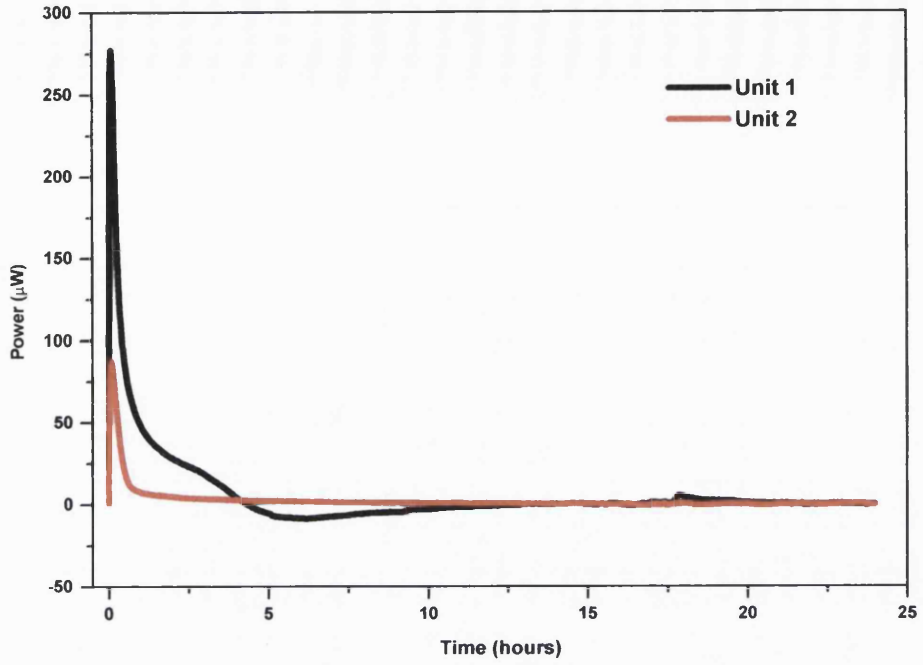

Figure 5.14 *The 'blank' (empty) responses of both RH perfusion units at 75% RH, following equilibration at 0% RH. It is clear that the instruments do not display identical behaviour under these conditions.*

within the specified noise limits (± 2 μW over 8 hours). A leak is usually observed as an endothermic response, due the heat of vapourisation of the escaping vapour. A further source of error lies in the flow switches themselves, which are capable of controlling humidity to ± 5% RH. Using saturated salt solutions (LiCl,H_2O and NaCl, 12% and 75% RH respectively at 25 °C), the capability of the flow switches to control RH has been validated for the units and appears to exceed the specifications, at ±2% RH. In order to eliminate any effects due to differences in the units themselves, the average blank responses were subtracted from all experimental results prior to data analysis.

5.2.4.2. Subtraction of blank responses from experimental data

In Figures 5.15 (a) and (b) are illustrated the responses of RH perfusion units 1 and 2 for samples of 1% w/w amorphous lactose crystallising at 75% RH, subsequent to equilibration and drying at 0% RH. It can again be seen that the units do not show

identical crystallisation profiles, even after subtraction of the blank responses. In the case of unit 1, it would seem that the endothermic response subsequent to the main exothermic peak is a longer process which results in a broader negative peak. Since the sample masses in both cases are very similar (0.27242 g and 0.26864 g respectively) it is interesting to note that the initial exothermic peak obtained from unit 1 reaches a maximum heat flow of 350 μW, as compared with the sample in unit 2 which achieves a value of 500 μW. This would imply that the reactions are occurring at different rates. It is possible that the endothermic event in unit 1 gets underway earlier than is the case of the sample in unit 2, thus reducing the maximum heat flow value achieved.

Since the crystallisation response involved both endo- and exothermic processes, a suitable method for achieving consistent determination of peak area, and thus enthalpy of crystallisation, was required. Since the systems achieve equilibrium at 0% RH prior to exposure to 75% RH means that in all cases the baseline determination is much simpler, as the start-point can always be taken as $y = 0$. However, the issue of what is to be included in the overall response still remains, as the duration of the exo- and endothermic portions of the experiments carried out in each unit are different.

It is also important to note that the enthalpy of crystallisation as determined by isothermal RH perfusion microcalorimetry will not be the same as those values calculated by batch isothermal microcalorimetry. This is for a number of reasons which have already been outlined (see section 5.2.1.). It is also possible that the constant availability to the samples of a humidified gas flow facilitates further reactions, most notably mutarotation, at 75% RH, and that in the case of crystallisation of amorphous lactose in the RH perfusion unit that process is able to continue to completion. In addition, since there is a constant flow of gas through the ampoule, once expelled, the plasticising water is removed from the ampoule and therefore a condensation response does not contribute to the overall response detected.

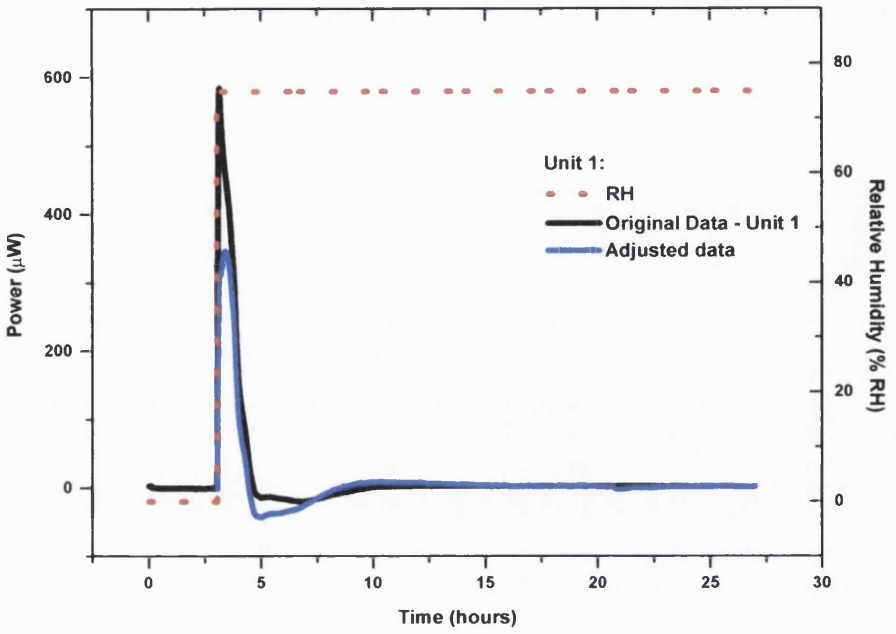

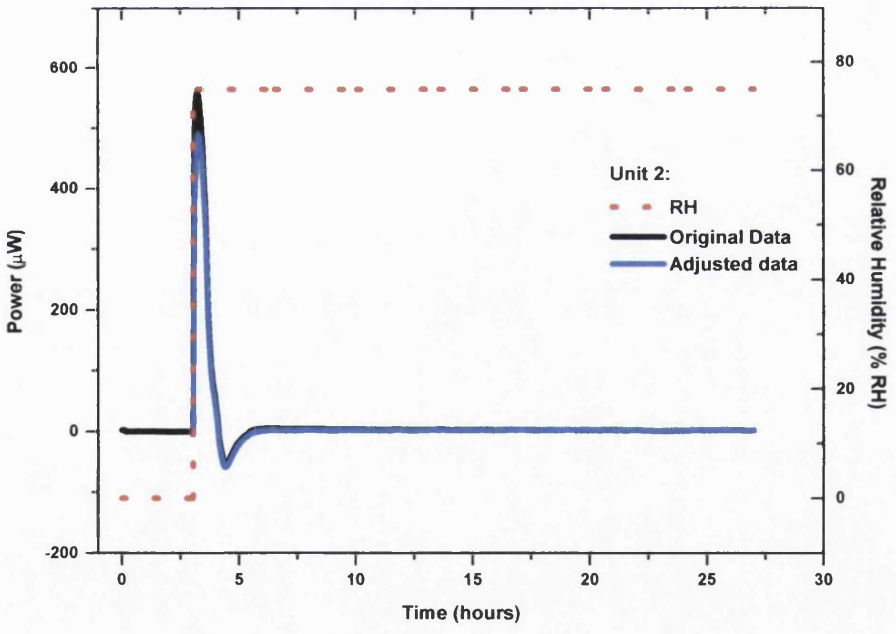

Figures 5.15 (a) and (b) *The raw and adjusted crystallisation responses of 1% w/w amorphous lactose samples are shown above in units 1 and 2, illustrating the different profiles obtained from each RH perfusion vessel.*

5.2.4.3. Determination of enthalpy of crystallisation by isothermal RH perfusion microcalorimetry

The responses of two 28 mg samples of 100% amorphous lactose in perfusion units 1 and 2 are shown in Figure 5.16. The samples were held at 0% RH until they were dry (dQ/dt = 0) and then exposed to 75% RH for 12 hours. It can be seen that although the rates of reaction were not the same, the processes occurring could be followed in either unit. Upon exposure to the elevated RH, an exothermic process began which is attributable to absorption of water by the sample. Initially there was a very sharp peak due to the fact that the sample had previously been held at 0% RH and was therefore extremely dry. Following 5.5 hours in unit 1, and 4.5 hours in unit 2 there was a second exothermic event which is represented by a sharp peak,

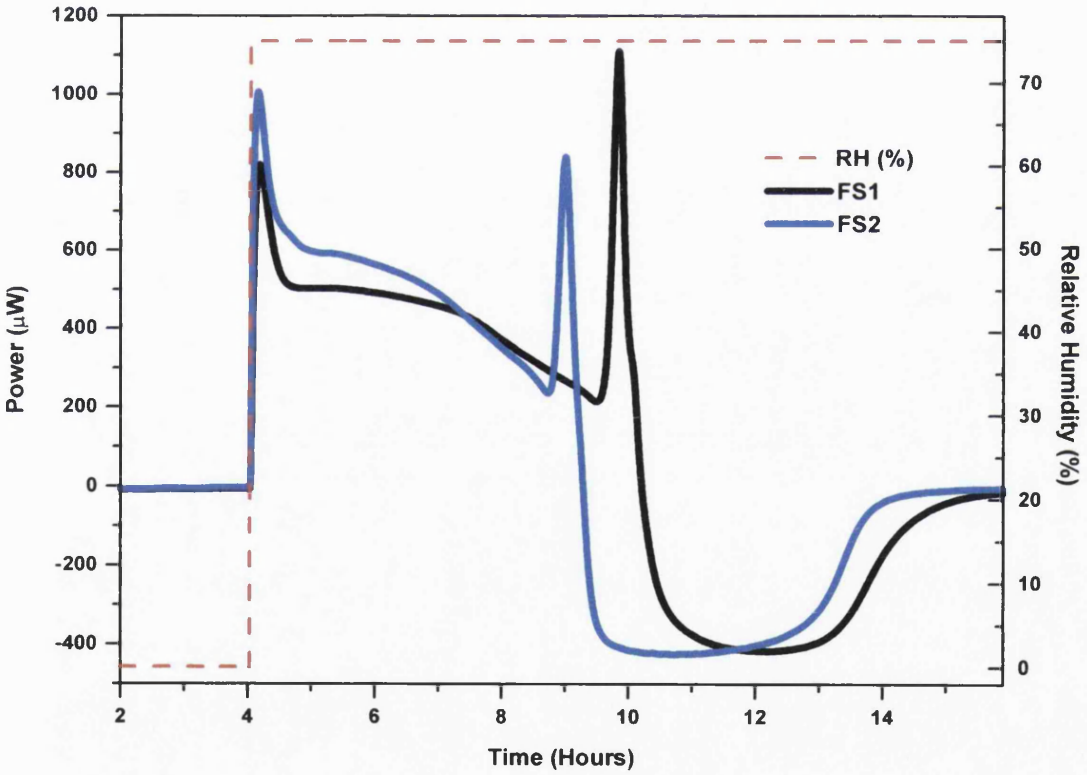

Figure 5.16 *The wetting and crystallisation responses of two 28 mg samples of 100% amorphous lactose in perfusion units 1 and 2 upon exposure to 75% RH.*

and this is due to the crystallisation of the sample. However the exothermic event was shortlived, and less than an hour later has been replaced by a long endothermic signal, which was caused by the expulsion of plasticising water by the sample, and lasted for 4 hours.

Integration of the total area of the events in Figure 5.16 resulted in an average enthalpy of crystallisation of 136.74 J/g (standard deviation = 26.94 J/g). The spread in the data seems to result from slightly different responses being obtained from each unit. However the issue of correlation of enthalpies between both RH perfusion units is addressed in Section 5.2.4.4.

5.2.4.4. Quantification of amorphous content in predominantly crystalline lactose by isothermal RH perfusion microcalorimetry

The crystallisation responses of partially amorphous lactose samples (between 1-10% w/w) were obtained from both RH perfusion units, and several methods were employed in order to ascertain the best determination of such levels of amorphous content (Figure 5.17). Due to the different forms of response obtained from each unit, initial approaches led to incompatible results from each unit. Figure 5.18 shows that when the total area of each reaction (following subtraction of the blank response) was integrated (Method A), two different trends were observed. The enthalpies of crystallisation calculated for samples crystallised in unit 1 followed a much inferior linear relationship with original amorphous content, as compared with those samples crystallised in unit 2. Since the crystallisation responses obtained from unit 1 include many events subsequent to crystallisation, an approach which excluded these events was investigated.

Integration of the crystallisation responses of all samples was carried out, including only the initial exothermic phase of the reaction and the subsequent endothermic peak, to the point at which it subsequently crossed the x-axis (Method B). This led to very little change in the enthalpies of crystallisation calculated for those samples crystallised in unit 2. However the values obtained from unit 1 were dramatically

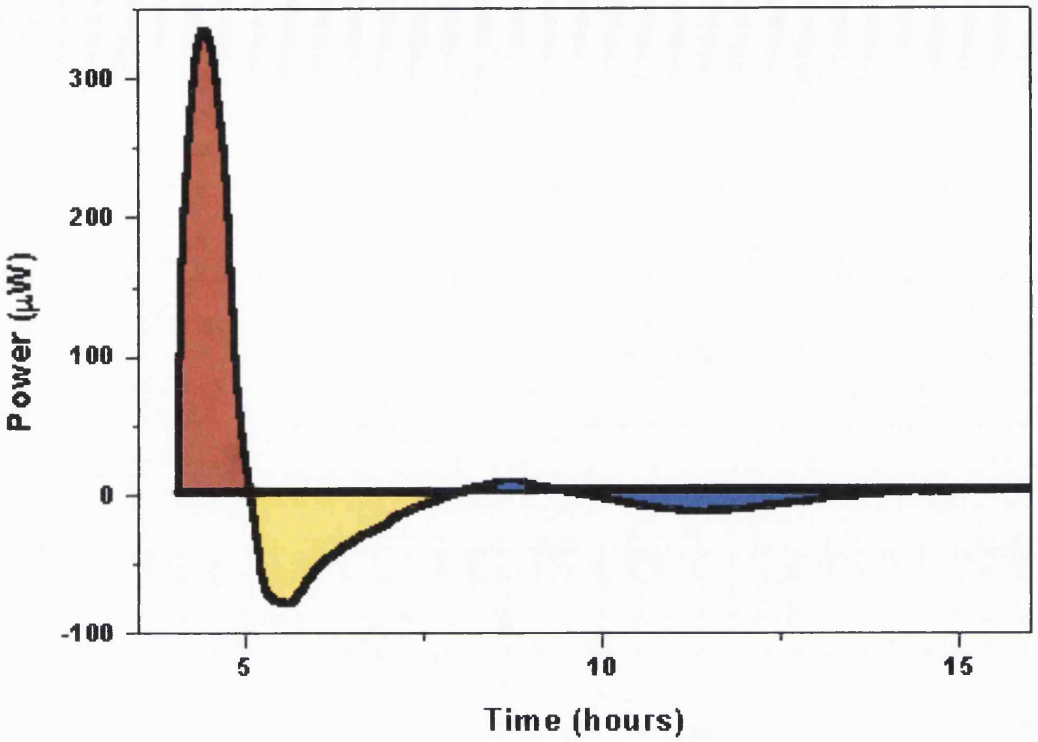

Figure 5.17 *Above, the crystallisation response for 4% amorphous lactose in RH perfusion unit 1 demonstrates the various methods of integration employed in this study. In the case of the integration of the 'total area' (Method A), all coloured areas above are included (it should be noted that since all integrations are carried out from the x-axis (y = 0), any areas which fall below that x-axis are automatically subtracted from the total area calculated). In the case of integrating the 'initial crystallisation response' (Method B), the red and yellow areas are included, whilst the 'positive exothermic peak' (Method C) is shown in red, and the 'negative endothermic peak' (Method D) in yellow.*

reduced, particularly in those samples of greater than 6% w/w amorphous content. It would appear that samples of less than 6% disorder do not exhibit any significant post-crystallisation event, as detectable by the perfusion unit. However, at amorphous contents greater than that level, the subsequent phases of crystallisation contribute much more greatly to the overall enthalpy calculated using Method A. From Figure 5.19 is can be seen that whilst a much improved agreement has been achieved between the two units, a degree of spread in the data still exists (R^2 =

0.851). Therefore, a further integration method was attempted in order to improve further the ability of RH perfusion mircocalorimetry in quantifying amorphous content in predominantly crystalline samples.

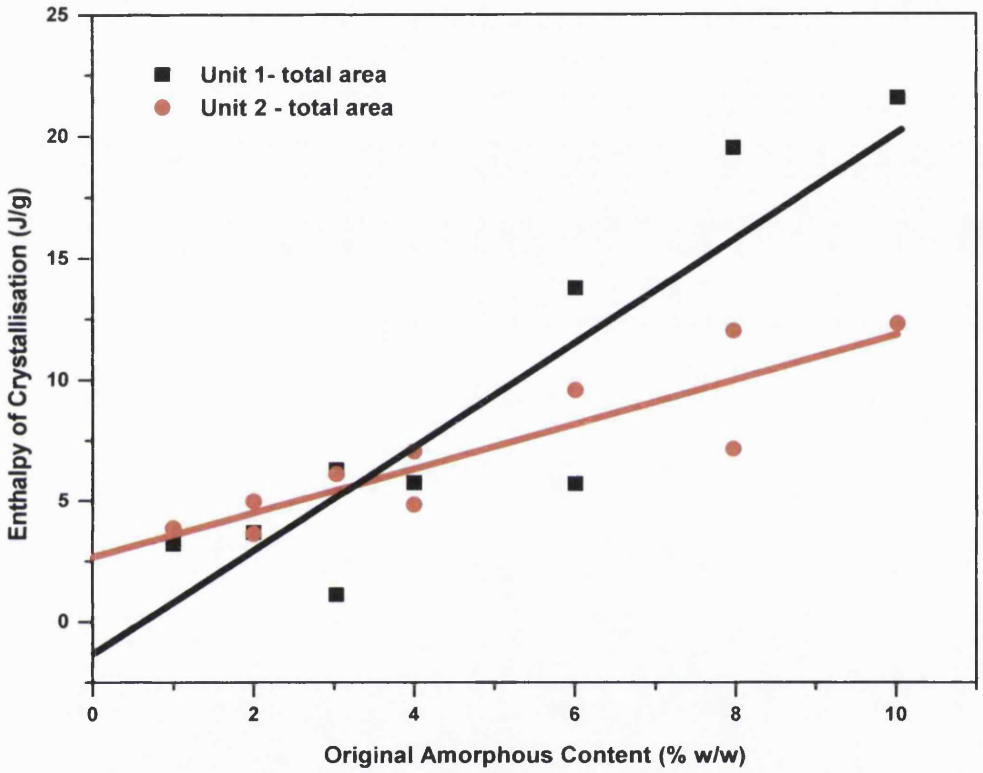

Figure 5.18 *The enthalpy of crystallisation of partially amorphous lactose samples (1-10% w/w) against original amorphous content, calculated by Method A. A clear difference between the values obtained from the two perfusion units is observed, indicating that the responses obtained are not identical. The black line represents the best linear fit for those samples crystallised in unit 1, whilst the red line represents the best linear fit for those samples crystallised in unit 2. It should be noted that by this method, unit 1 would expect to see a negative enthalpy of crystallisation for samples of less than approximately 0.5% w/w amorphous content.*

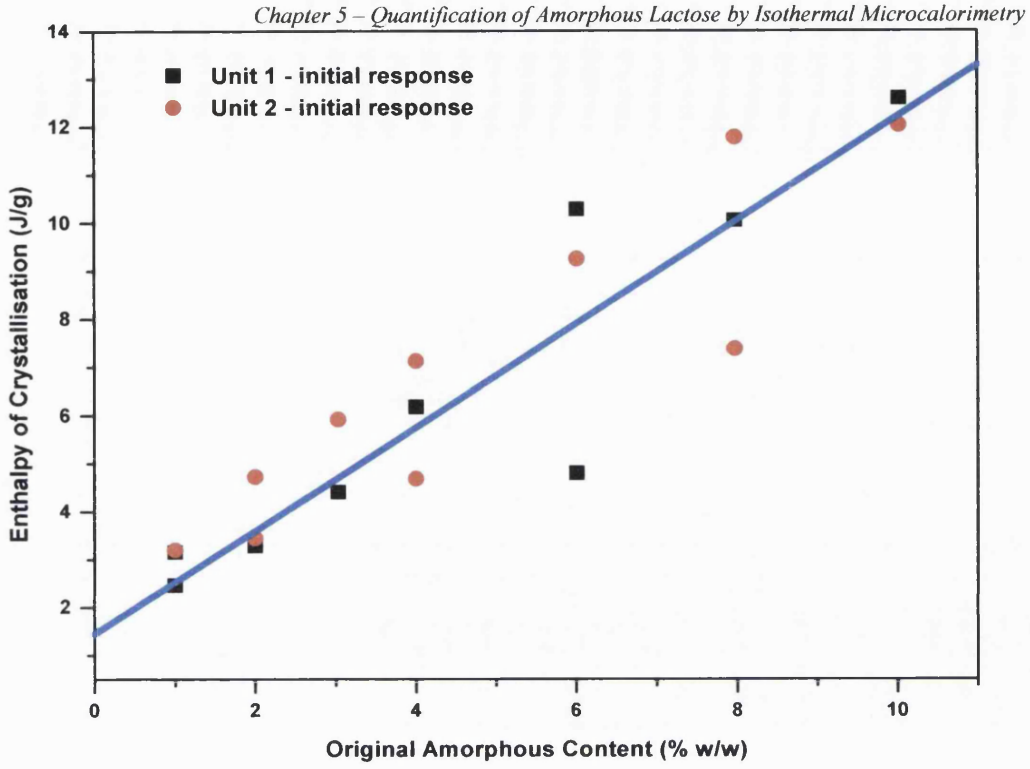

Figure 5.19 *Integration of only the initial exo- and endothermic phases of the crystallisation response (Method B) results in greater agreement between the enthalpy of crystallisation values of the two units (R^2 = 0.851).*

Integration of the positive exothermic peaks (Method C) only was carried out (Figure 5.20), and the results obtained show a further improvement in the ability to quantify amorphous content (R^2 = 0.943). It would seem that quantification can be carried out to approximately ± 1 % w/w, although for the samples of 6 % and 8 % w/w amorphous content this is not the case. However it should be noted in an effort to identify any problems with sample homogeneity, mixes were prepared in small quantities so as to enable the use of almost the entire sample throughout the course of this investigation. It would seem from the data presented here that sample mixing in these two cases was incomplete. In actual fact, if the enthalpies of crystallisation of the three experiments in each case are averaged, the new enthalpy of crystallisation sits very close to the line of best fit, implying that the amorphous content of the mixtures was not homogenous and that the limitation in this instance lies with the sample and not the method.

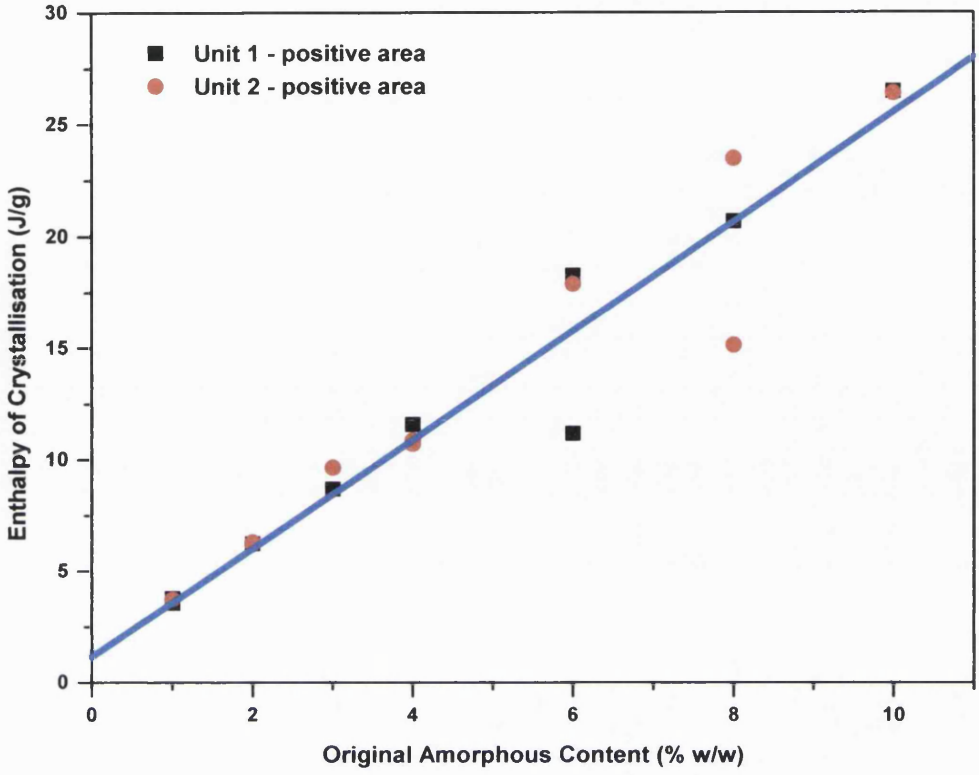

Figure 5.20 *Enthalpy of crystallisation, as determined by the positive exothermic peak only (Method C), illustrated an improved correlation between the perfusion units in determining the amorphous content of predominantly crystalline samples (R^2 = 0.943).*

In Figure 5.21 the enthalpy of crystallisation calculated from the area of the main endothermic peak (Method D) against original amorphous content is plotted. Surprisingly, this relationship shows the best correlation between enthalpy and amorphous content (R^2 = 0.978) and offers another method to quantify amorphous content, albeit a slightly unusual one. Since crystallisation is an exothermic process and is therefore represented mainly by the initial positive peak, in reality 'enthalpy of crystallisation' is an inaccurate term for these data, since the negative enthalpy measured is in fact related mostly to the heat flow resulting from the expulsion of plasticising water from the sample.

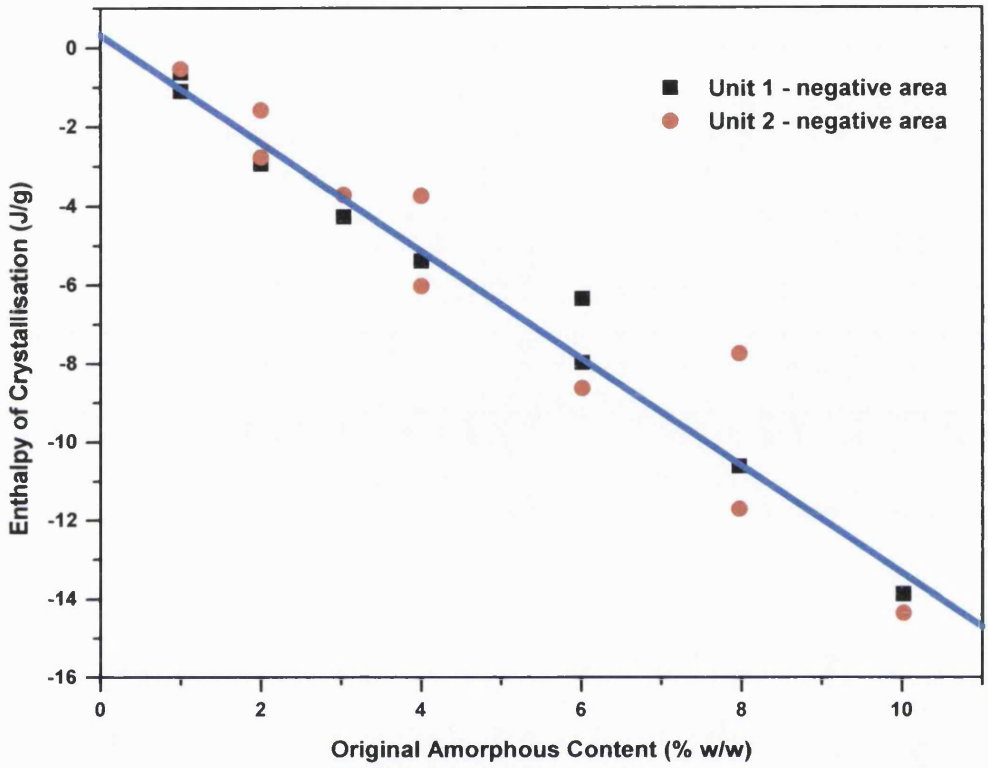

Figure 5.21 *The linear relationship between the enthalpy of crystallisation, as calculated by integrating the area of the negative endothermic peak, and the original amorphous content of the samples. This relationship has a correlation (R^2) of 0.978, which is the highest correlation obtained from any method used.*

5.3. CONCLUSIONS

From the investigations carried out using batch isothermal microcalorimetry, it was determined that quantification of amorphous content in the 0-10% w/w range was possible with the lactose. This work also highlighted the attention that is required when consistent integration of sample data is required, as obtaining reproducible results has been a disadvantage associated with the technique. Although both 53% and 75% RH respectively were found to be suitable for the quantification work, a

greater correlation was found when using the lower humidity. This could be related to the fact that at this RH, the onset of crystallisation is impeded, allowing more time for a steady baseline to be attained prior to the crystallisation event itself. Attention is required to the issue of the consistent underestimation of amorphous content by quantification at 75%, and to a lesser extent at 53% RH. It is possible that although it has previously been shown that 100% crystalline lactose does not show a heat flow by isothermal microcalorimetry at elevated RH, when a sample comprises some crystalline material, that material interferes with the total enthalpy recorded. Therefore, instead of basing a calibration on a 100% amorphous standard, since it is clear that a linear relationship exists between amorphous content and enthalpy of crystallisation, any such quantification work should be based upon the calibration established with partially amorphous samples.

The use of isothermal RH perfusion microcalorimetry was also investigated for this quantification work. Many issues were again highlighted, relating to the difference between the responses obtained from two supposedly identical perfusion units, and the efforts required in correlating the results obtained from each of them. It was found that several integration methods are capable of producing reproducible results, and that the quantification limits of the technique are ± 1% w/w amorphous content for lactose.

At this point, a discussion of the relative advantages and disadvantages of the techniques is relevant. It should be noted that the main advantage of the RH perfusion technique is the facility it provides the user of controlling the RH throughout an experiment, so that a particular reaction can be prevented or delayed. This has been put to use in this work, where samples are exposed to 0% RH until such a time as a steady baseline has been attained. However, due to the friction involved in lowering the perfusion unit into the measuring site of the calorimeter, and the increased number of components within the unit which take time to achieve equilibrium, a disadvantage of the technique is the prolonged period of time required for the system to achieve a steady baseline. In addition to this, when the RH within

the unit is increased, an exothermic response is obtained relating to the sorption of water within the ampoule, even if the unit is empty, although this is small in comparison to the response of a sample. Therefore the technique is not suited to the detection of amorphous material. In the case of batch isothermal microcalorimetry however, the presence of less than 0.5% w/w amorphous content can be confirmed by the presence of a crystallisation peak.

Although isothermal microcalorimetry is an extremely sensitive technique in measuring heat flow within the ampoule, it does not provide any chemical information. As such, the technique poses many questions as to the individual events which comprise the crystallisation process. Further work is required in order to provide a greater understanding of the events which contribute to the features seen in the crystallisation response.

CHAPTER SIX

THE USE OF CALORIMETRY, VAPOUR SORPTION AND NIR SPECTROSCOPY TO INVESTIGATE THE PROPERTIES OF AMORPHOUS AND CRYSTALLINE RAFFINOSE

6.1. INTRODUCTION

Some materials are known to exist in multiple hydrate levels, pharmaceutical examples including both drugs (*e.g.* nedocromil sodium, Khankari et al., 1998) and excipients (*e.g.* carbohydrates such as raffinose). Raffinose is of interest since recent developments in the ability to manufacture therapeutic macromolecules have led to a need for protein stabilisation in the solid state. Since certain carbohydrates have been shown capable of conferring stability to proteins, many researchers have concentrated on developing a greater understanding of the protein-carbohydrate interaction. Many of these investigations have focused on the behaviour of carbohydrates in the presence of elevated temperature and/or humidity (for example Green and Angell, 1989, Aldous et al., 1995 and Saleki-Gerhardt et al., 1995). The crystallisation of hydrate-forming carbohydrates is thought to be particularly relevant in the enhancement of physical and chemical stability since it will involve the removal of water from the remaining phase, thus raising its glass transition temperature. This is particularly relevant for materials which can form multiple hydrates in real time, *e.g.* trehalose and raffinose (Aldous et al., 1995).

Raffinose (β - D – fructofuranosyl – O - α - D – galactopyranosyl - (1 - 6) - α - glucopyranoside) is a trisaccharide which, as well as existing in a pentahydrate form, has been shown to form intermediates at lower hydrate levels (Saleki-Gerhardt et al., 1995; Kajiwara et al., 1999). The hydrogen bonding of raffinose is complex, since three of its water molecules are both proton donors and acceptors, whilst the remaining two will act only as donors (Jeffrey and Huang, 1990). The complexity of raffinose as a model is also useful as a way of understanding the value and limitations of analytical techniques such as gravimetric sorption, near-infrared spectroscopy (NIRS) and isothermal microcalorimetry.

6.2. AIMS OF THIS STUDY

The aims of this study were to follow the transitions of raffinose between the amorphous and crystalline states, using primarily the techniques of gravimetric sorption, NIRS, isothermal microcalorimetry and solution calorimetry, with a view to improving the understanding of both the methods of analysis and of the transitions that take place when complex materials crystallise.

6.3. EXPERIMENTAL

6.3.1. PREPARATION OF AMORPHOUS RAFFINOSE

6.3.1.1. Spray Drying

Amorphous raffinose was prepared by spray drying a 10% w/v aqueous solution as outlined in Section 2.5.3.2. All yields were confirmed amorphous by X-Ray Powder Diffraction.

6.3.1.2. Heat Drying

Raffinose pentahydrate was dried at 100 °C for 24 hours at –300 mbar in a vacuum oven, as outlined in Section 2.6.2. All yields were confirmed amorphous by X-Ray Powder Diffraction.

6.3.2. NEAR INFRARED SPECTROSCOPY/GRAVIMETRIC VAPOUR SORPTION

Gravimetric studies of amorphous raffinose samples were carried out in a humidity and temperature controlled microbalance DVS apparatus (Surface Measurement Systems, London, UK) as outlined in Section 2.3. Samples of approximately 20–70 mg were dried at 0% RH at 25 °C. Six to ten hours was generally sufficient for complete drying to be achieved. NIR spectra of the samples were simultaneously recorded (Foss NIRSystems, UK) using a fibre optic probe situated approximately 4 mm below the flat-bottomed quartz glass DVS sample pan (see Section 2.3.). After the initial drying step, the raffinose samples were exposed to elevated RH values at 25 °C, in order to induce crystallisation. NIR spectra were recorded throughout the

sorption/desorption processes. Dehydration of certain samples was also carried out by maintaining them at 0% RH post crystallisation.

6.3.3. Batch Isothermal Microcalorimetry

Heat flow consequent to water vapour interacting with amorphous raffinose was recorded using a 2227 Thermal Activity Monitor (TAM), (Thermometric AB, Järfälla, Sweden) at 25 °C (see Section 2.1.). Samples were accurately weighed into 3 mL glass ampoules, to which were added a hygrostat containing a saturated salt solution to produce a predetermined relative humidity (RH). sodium chloride was used to produce 75% RH and potassium carbonate to produce 43% RH. The influence of sample mass was investigated, between 15 mg and 150 mg. The ampoules were sealed so as to be air-tight, and lowered into the equilibration position in the TAM until dQ/dt (the rate of change of heat flow with time) was zero, then lowered into the measuring site of the channel. Due to the nature of the responses obtained, integration of peak areas was carried out from the baseline immediately prior to ampoule lowering. In order to correct for the disturbance due the lowering of ampoules, ampoules containing hygrostats but no powdered sample were lowered and the average heat flow from four experiments determined. This blank response was subtracted from all enthalpies calculated.

6.3.4. Isothermal Perfusion RH Microcalorimetry

Details of the experimental set-up are outlined in Section 2.1. Samples of 10 – 15 mg were loaded into the 4 mL stainless steel ampoule. The reference used in all cases was an empty 4 mL stainless steel ampoule on an ampoule lifter. The humidifying chambers were each loaded with 0.5 mL of distilled water. A nitrogen gas flow of 2 – 4 mL/min was employed and was directed down either the wet line (to become 100% RH) or the dry line (0% RH) in varying proportions in order to achieve the desired RH. The flow switch heater was set to 40 °C in order to prevent condensation of water within the unit. Calibrations were carried out prior to each experiment, using empty sample and reference ampoules.

'Blank' empty ampoule experiments were also run with each unit so as to be able to subtract the heat flow contribution of each unit from the experimental data.

6.3.5. Differential Scanning Calorimetry

Thermographs of raffinose samples (amorphous, pentahydrate (as purchased) and samples removed from the TAM) were obtained using a Differential Scanning Calorimeter (PerkinElmer DSC 7 or PerkinElmer Pyris 1) (see Section 2.4.). Samples of 1.5 - 3 mg were loaded into non-hermetically sealed aluminium pans and measurements were taken under a nitrogen atmosphere from 25–200 °C at a heating rate of 10 °C per minute using an empty pan as reference. Prior to measurements, calibrations using indium and zinc were carried out under the same conditions. Samples were run in triplicate unless otherwise indicated.

6.3.6. Solution Calorimetry

Enthalpies of solution for raffinose samples of approximately 200 mg were measured using the Thermometric 2225 Precision Solution Calorimeter (Thermometric AB, Järfälla, Sweden) and the water and air bath of the Thermometric 2277 TAM. Details of the experimental set up are included in Section 2.2. A stirring rate of 600 rpm was employed in all cases. The system was electrically calibrated before and after the dissolution reaction. All data reported here refer to the value calculated using the post-break calibration.

6.3.6.1. Vapour Sorption/Dehydration Study

Enthalpies of solution were determined following storage under several dry and humid conditions in order to determine the effect of vapour sorption, crystallisation and dehydration on amorphous and crystalline raffinose. Three 'dry' conditions were used - in a desiccator over silica gel at 25 °C and at 35 °C and in a vacuum oven at 50 °C and –300 mbar. In addition four elevated relative humidity conditions were created by storage in a desiccator (functioning as a humidity chamber) over saturated salt solutions (all at 25 °C), 11% RH was produced by lithium chloride, 43% RH was produced by potassium carbonate, 58% RH was produced by sodium

bromide and 75% RH was produced by sodium chloride. Storage was for various periods of time (see Section 6.4.4.). The samples were weighed immediately prior to and after storage in order to monitor any weight changes.

6.3.7. SCANNING ELECTRON MICROSCOPY

Samples were mounted onto adhesive carbon discs attached to Scanning Electron Microscopy (SEM) stubs, and coated with gold by sputtering (Emitech K550 sputter coater, Emitech, Kent, UK) for four minutes at 30 mA. Scanning electron micrographs were obtained using a Philips XL20 SEM (Philips, Eindhoven, Netherlands) (voltages displayed on micrographs).

6.4. RESULTS AND DISCUSSION

6.4.1. DVS/NIRS

Many amorphous materials are plasticised by absorbed water vapour. The glass transition temperature (T_g) then drops below the experimental temperature, thus giving the molecules of the sample sufficient mobility to allow rapid crystallisation. As the sample crystallises it is usual for the absorbed water to be displaced. Consequently, it now seems to have become accepted that a clear sign of the presence of amorphous material in a sample would be a loss of mass on exposure to increasing relative humidity (RH). Conversely the absence of this mass loss would be interpreted as the absence of a crystallisation event. The absence of a crystallisation event would not mean that there is no amorphous content, but only that the sample did not crystallise, for example some materials do not crystallise rapidly in the presence of humidity at ambient temperature (Ahmed et al., 1996); others may be protected from crystallisation (*e.g.* the interaction between a protein and a carbohydrate).

6.4.1.1. Crystallisation Without Mass Change

Despite the growing view that mass loss must occur as a consequence of crystallisation, raffinose provides a good example of a crystallising material which

does not give rise to such behaviour. The mass change following the exposure of spray dried amorphous raffinose to 75% RH at 25 °C is shown in Figure 6.1. Substantial water sorption gave rise to a mass increase of 13.8% w/w, which was sufficient to lower T_g below the experimental temperature (25 °C) and consequently gave the material sufficient mobility to allow crystallisation to occur. It can be calculated from the Gordon-Taylor Equation (Gordon and Taylor, 1952) (Equation 3.1) that such a water content is consistent with a glass transition temperature of 18.1 °C. For the purposes of the calculation, the density of raffinose was 1.46 (Merck Index 2000) and the T_g of raffionse was 376K (Saleki-Gerhardt et al., 1995). Despite this lowering of T_g, there was no obvious mass loss. The absence of a mass loss

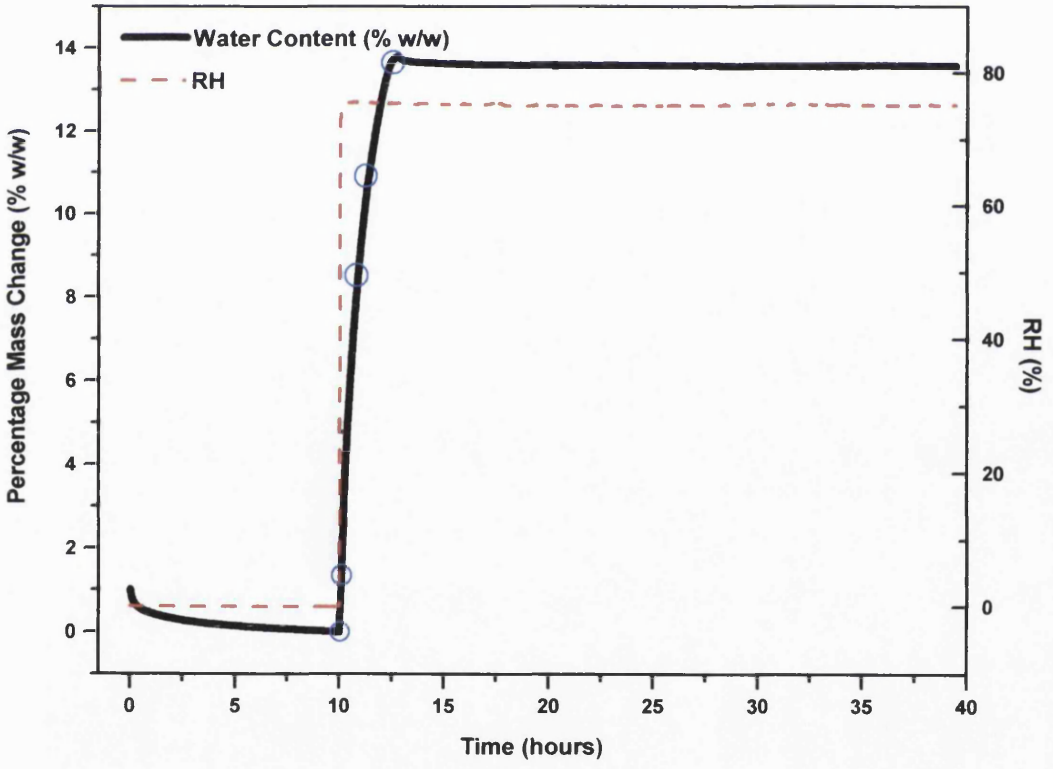

Figure 6.1 *DVS plot for 100% amorphous spray dried raffinose dried at 0% RH for 10 hours and then exposed to 75% RH for 30 hours at 25 °C in order to induce crystallisation. Circles indicate times when the spectra in Figure 6.2 were taken.*

would usually be interpreted as an absence of crystallisation, however, examination of NIR spectra taken during this process revealed that the sample started to crystallise after ca. 165 minutes at 75% RH (Figure 6.2). This is clear from the development of new peaks at both 1731 nm and 1779 nm, and also from the relocation of the dry amorphous raffinose peak at 1706 nm to 1702 nm. Furthermore it can be seen from the spectra that the solid state properties of the sample continued to change for ca. 1800 minutes (30 hours) despite no simultaneous changes in mass being observed (Figure 6.3).

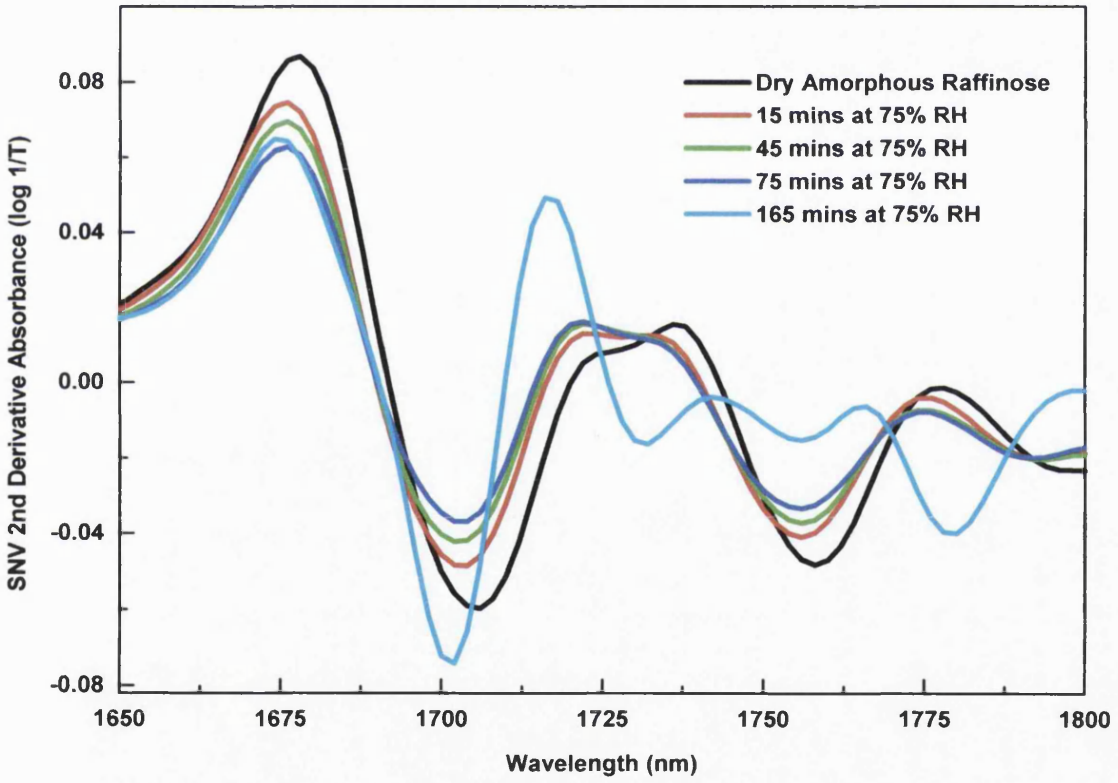

Figure 6.2 *SNV 2nd derivative NIR spectra for raffinose corresponding to different stages of the DVS plot shown in Figure 6.1. Spectra represent the amorphous form, and changes up to 165 mins exposed to 75% RH at 25 °C, at which point it would seem that a tetrahydrate has formed.*

The reason why there is a difference between this sample, showing no significant mass change throughout this long crystallisation process, and lactose, which shows substantial water loss, is that lactose is able to form a monohydrate (approximately 5% w/w water), however the amount of water sorption needed to cause rapid crystallisation is far greater than 5% w/w, hence there is free water to be desorbed. In fact lactose often retains less than 5% w/w water, due to the presence of some anhydrous crystalline form in the sample. The amount of water required to plasticise raffinose sufficiently in order for crystallisation to occur is similar to the amount of water which the molecule is able to incorporate as hydrate water. Raffinose is able to form different hydrates depending upon the conditions of temperature and

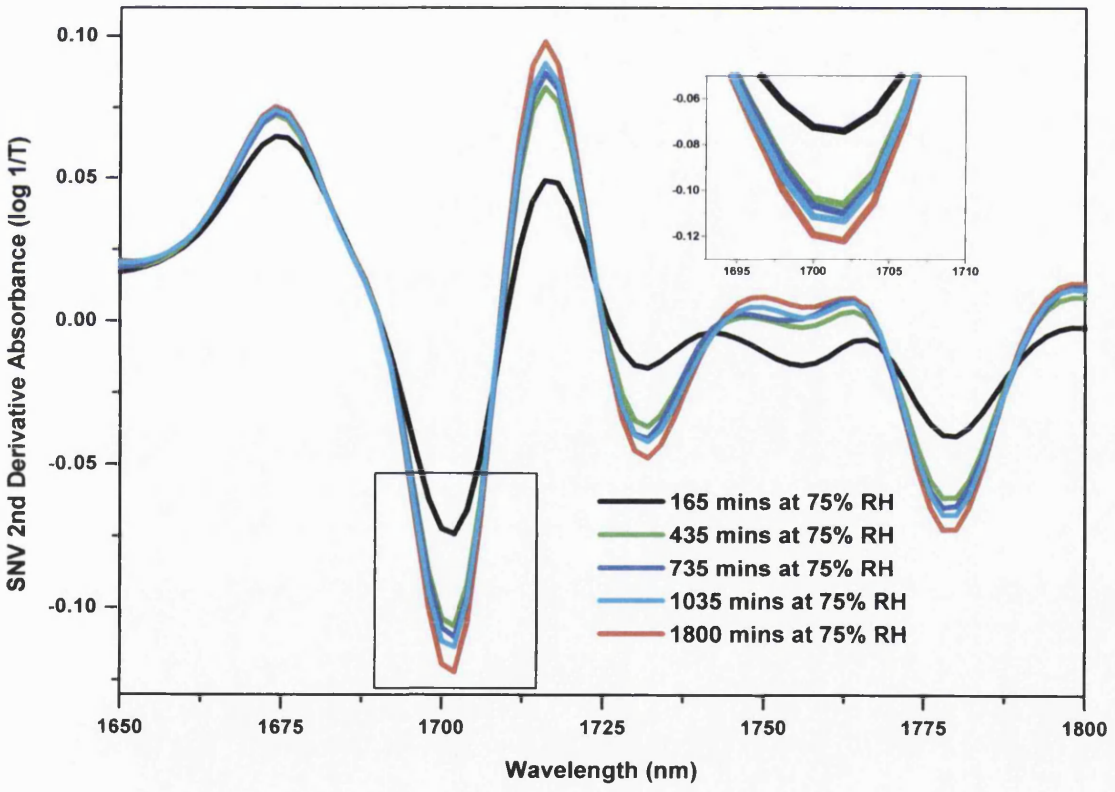

Figure 6.3 *SNV 2nd derivative NIR spectra representing the changes observed in the raffinose sample throughout approximately 30 hours exposed to 75% RH and 25 °C.*

humidity (Saleki-Gerhardt et al., 1995). At 75% RH and 25 °C, the sample seems to crystallise to the tetrahydrate (see further discussion below). It can be calculated that the tetrahydrate would show a 14.3% w/w mass gain over the anhydrous form, thus the mass required to form that hydrate is equivalent to that which was absorbed (15.0% w/w, n = 4, sd = 0.9% w/w). If mass change alone were relied upon to detect crystallisation of samples for which multiple hydrates can form, then it would be possible to miss the crystallisation event. It follows that the monitoring of the material using mass change alone would be an inadequate method of following changes within the sample. Although the absence of a mass change for the crystallisation of raffinose under these conditions is not surprising, these data do show the clear value of using more than just gravimetry as a method to assess onset of crystallisation.

6.4.1.2. Changes in Hydrate Level

Exposing the spray dried amorphous material to 75 % at 25 °C gave rise to significant variability in the extent of water sorption. Replicate experiments give peak weight gains within the range 13.7-16.0 % w/w (replicate data not shown). The higher end of these mass changes is in excess of that required to form the tetrahydrate, but somewhat less than that required to form a pentahydrate (17.9 % w/w). Equally the lower end of these mass changes was less than that needed for complete formation of a tetrahydrate (14.3 % w/w) but more than that required for the formation of a trihydrate (10.7 % w/w mass gain). It follows that the samples crystallise to mixed hydrates (for example some regions of trihydrate and some of tetrahydrate, clearly this is an example and other combinations are possible). This gives rise to the question of whether the formation of these mixed hydrate systems can be followed by use of NIR spectroscopy during the crystallisation process.

In order to form a pentahydrate, samples were crystallised at the increased relative humidity of 90% RH. In such instances it can be seen that the samples were seen to expel a quantity of water, although again much less than that which would be seen for 100% amorphous lactose (Figure 3.1). In addition, there was again a degree of

variability in the amount of water taken up by the samples. In one instance, for example, a 62 mg sample achieved a maximum mass equating to the uptake of 19.5% w/w (*i.e.* in excess of that required to form a pentahydrate) (data not shown). However, following the expulsion of plasticising water, and whilst still under elevated RH conditions, the sample's mass uptake fell to 17.4% w/w, which is slightly less than the 17.9% required of a pentahydrate. This is in contrast with a 26 mg sample (Figure 6.4) which achieved a maximum mass of 23.9% w/w and equilibrated at 90% RH to a mass of 17.9% w/w, which is exactly that required to form a pentahydrate.

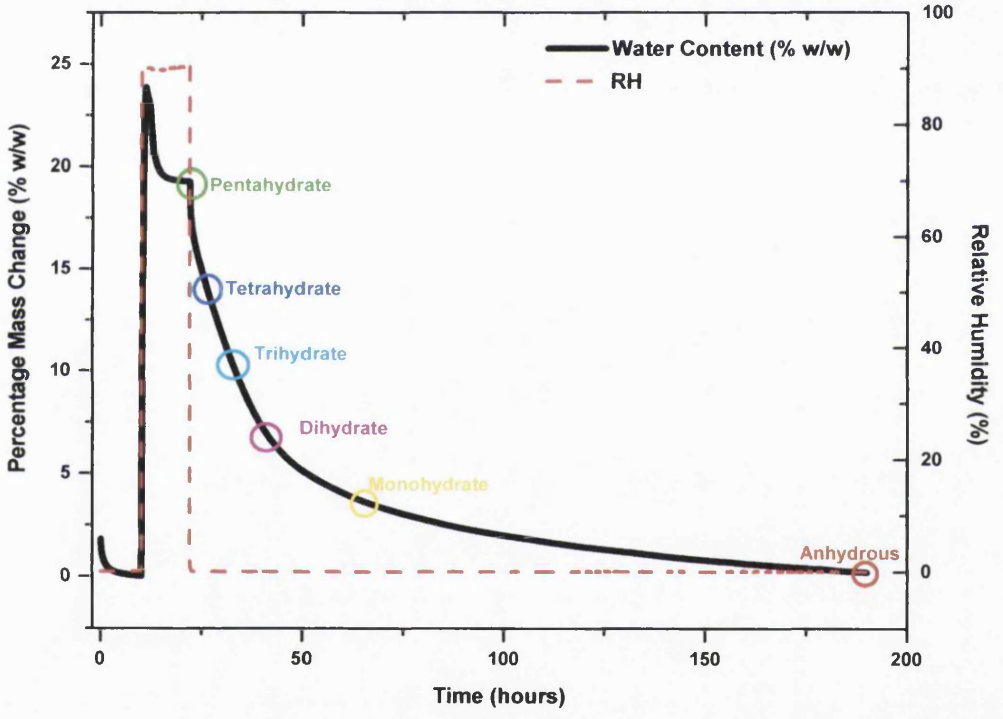

Figure 6.4 *The DVS plot for a 26 mg sample of 100% spray dried raffinose exposed to 90% RH. It can be seen that the sample expelled plasticising water prior to equilibrating at the mass uptake corresponding to the formation of a pentahydrate. In addition, upon subsequent exposure to 0% RH, the sample was dehydrated back to an anhydrous form. The circles correspond to the hydrate equivalents by mass, and are represented by NIR spectra in Figure 6.5.*

In Figure 6.5 the NIR spectra are shown for the same sample that has been dried until the measured mass equates to that of the different stoichiometric hydrates. Other workers (Saleki-Gerhardt et al., 1995; Kajiwara et al., 1999) have used this approach in order to isolate and test different stoichiometric hydrates of raffinose. Kajiwara et al. (1999) have studied the properties of raffinose during dehydration and commented on gradual amorphisation, but also showed evidence of minor changes in X-ray diffraction patterns that indicated the possibility that lower hydrates existed, this being confirmed by DSC such that sequential loss of water atoms was seen at least down to the trihydrate form. In common with the work of other authors (Saleki-Gerhardt et al., 1995; Kajiwara et al., 1999), there can be no guarantee that arriving at a sample that has a mass equivalent to a certain hydrate level equates to the existence of that hydrate form, for example a mass equivalent to a tetrahydrate could be achieved by having a mixture of tri- and pentahydrates present. Consequently the data are used in the same spirit as in previous reports using this methodology and do not prove the structures are present.

In the NIR region shown in Figure 6.5, it is observed that there is a substantial shift in the peak (the region is that associated with –OH group interactions) at masses equivalent to the different hydrate levels. To collect these spectra, an amorphous sample was crystallised in the DVS-NIR at 90% RH and then dried at 0% RH to gradually remove the water. At 90% RH the sample gained 23.9% w/w mass, which is more than that required to form a pentahydrate. The sample then crystallised, and the expulsion of plasticising water was observed (Figure 6.4). The sample equilibrated to a mass which corresponded to an increase of 17.9 % w/w (*i.e.* it had gained the equivalent of that required to form a pentahydrate), and the spectrum for that sample included in Figure 6.5 was taken following 16 mins exposure to 0% RH, in order to remove the interference of any adsorbed water at the higher RH. The NIR peak moved from 1437 to 1444 nm as a consequence of crystallisation to the pentahydrate form. Progression through the drying step facilitated the further removal of water, and the spectra in Figure 6.5 follow this process. The removal of the equivalent of one hydrate water to form the tetrahydrate results in a decrease in

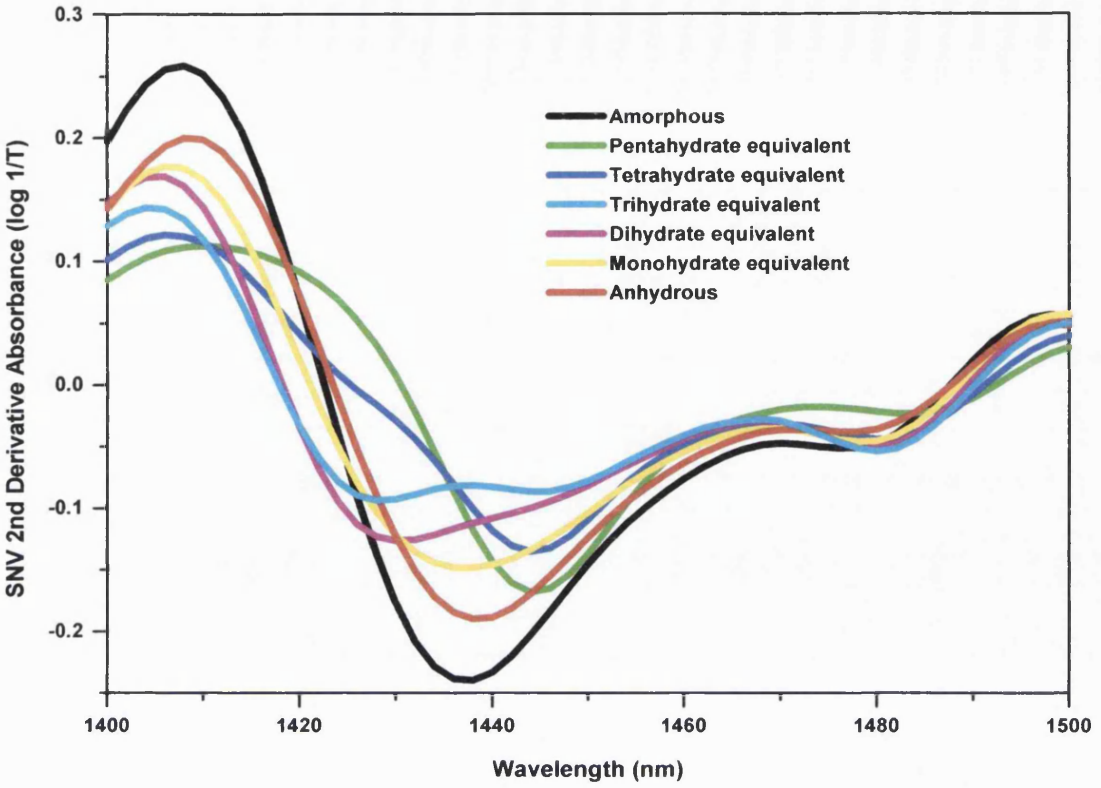

Figure 6.5 *2nd derivative NIR spectra corresponding to different hydrate levels by mass (calculated from DVS data) taken at 0% RH. (Note a mass equivalent to a certain hydrate level does not prove that the structure is that hydrate as it is possible that mixed hydrates could exist and give the same mass of material).*

the absorbance of the peak at 1444 nm. However, the most interesting stage of this peak development is that associated with the removal of sufficient water for the sample to have a mass equivalent to that of a trihydrate. In this instance the spectrum shows two peaks in the region, the original at 1444 nm, but also a stronger peak which occupies a wavelength of 1427 nm. This suggests that a hydrate mix may be present, or that some amorphous material has been generated. The lower peak for the sample of a water content equivalent to the dihydrate form is found at 1430 nm which is also consistent with a movement of the peak towards the position occupied by the amorphous form. Further dehydration (to the equivalent of monohydrate water content) results in the peak returning to the exact position which it had originally occupied in the amorphous form (1437 nm), and it does not shift

with the loss of the final hydrate water molecule (the size of the peaks differ due to the water content and possibly the changed geometry of the sample[1]). This is in keeping with observations made by Kajiwara et al. (1999) who could only find clear evidence of retained crystallinity when drying raffinose to the trihydrate level. Below the trihydrate water content it was felt that "sugar-water" hydrogen bonds were being replaced with "sugar-sugar" bonds which gave disorder in the long range packing (*i.e.* loss of crystallinity). It is important to stress again that it is not yet known if dehydration results in the sequential dehydration of raffinose, so that each hydrate species is present in turn, or if hydrate mixes form upon removal of hydrate water. As in the case of other studies (*e.g.* Kajiwara and Franks, 1997; Kajiwara et al., 1999; Saleki-Garhardt et al., 1995; Iglesias et al., 2000) the gravimetric data obtained cannot be interpreted with any more detail. The current study (Figure 6.5) supports the suggestion that hydrate mixes may be obtained with dehydration. The data are also compatible with the hypothesis that penta-, tetra- and tri- and perhaps even dihydrate forms exist, but that the sample becomes amorphous when the mass equates to the monohydrate.

There is a difference between the spectra for a sample of pentahydrate that was purchased and that produced in the DVS (Figure 6.6), particularly in the region of 1495 nm where the purchased raffinose has a peak which is totally absent in the DVS-produced material. It is believed that this is because the pentahydrate had not been given long enough to come to equilibrium (given that it has been shown above that changes in internal bonding continue for a long time after cystallisation has occurred). However, the shifts seen that have been tentatively ascribed to the various hydrate levels here (Figure 6.5) were also seen when the commercially available pentahydrate was dried in the DVS-NIR (data not shown).

[1] The NIR will penetrate throughout the entire sample. The basic NIR spectra are affected by sample geometry, however the data are used having been treated with standard normal variate and second derivative treatments, this results in spectra that show very minimal differences due to sample geometry.

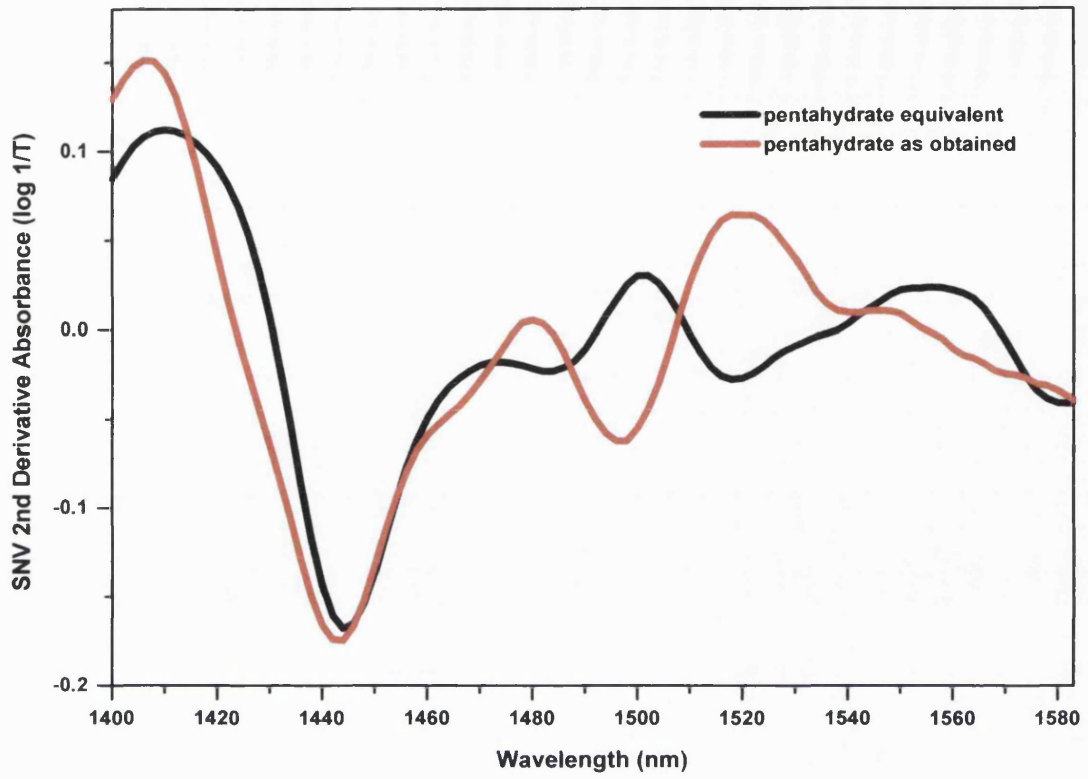

Figure 6.6 *SNV 2nd Derivative NIR absorbance spectra for a purchased raffinose pentahydrate sample and a sample crystallised in the DVS to form a pentahydrate equivalent. Differences between the spectra are observed in particular between 1460 – 1600 nm.*

From these data, the possibility of following the crystallisation of spray-dried raffinose upon exposure to both 75% and 90% RH was considered. In Figure 6.7 spectra taken during the exposure of an amorphous sample to 75% RH in the DVS-NIRS are illustrated (DVS data are shown in Figure 6.1). The first four spectra represent the amorphous material and its transitions throughout the first hour of exposure to elevated RH, which corresponds to the period of the experiment when the sample is seen to sorb significant quantities of water. The peak starts at 1436 nm and is seen to move slowly up to first occupy 1438 nm and to finally settle at 1442 nm when the sample crystallises. The final two spectra represent the remainder of the 11 hour exposure to 75% RH, and in this region there is no further change in the NIR spectra. These data indicate that the amorphous material crystallises to the

tetrahydrate (by comparison with Figure 6.5 and taking into account the mass change).

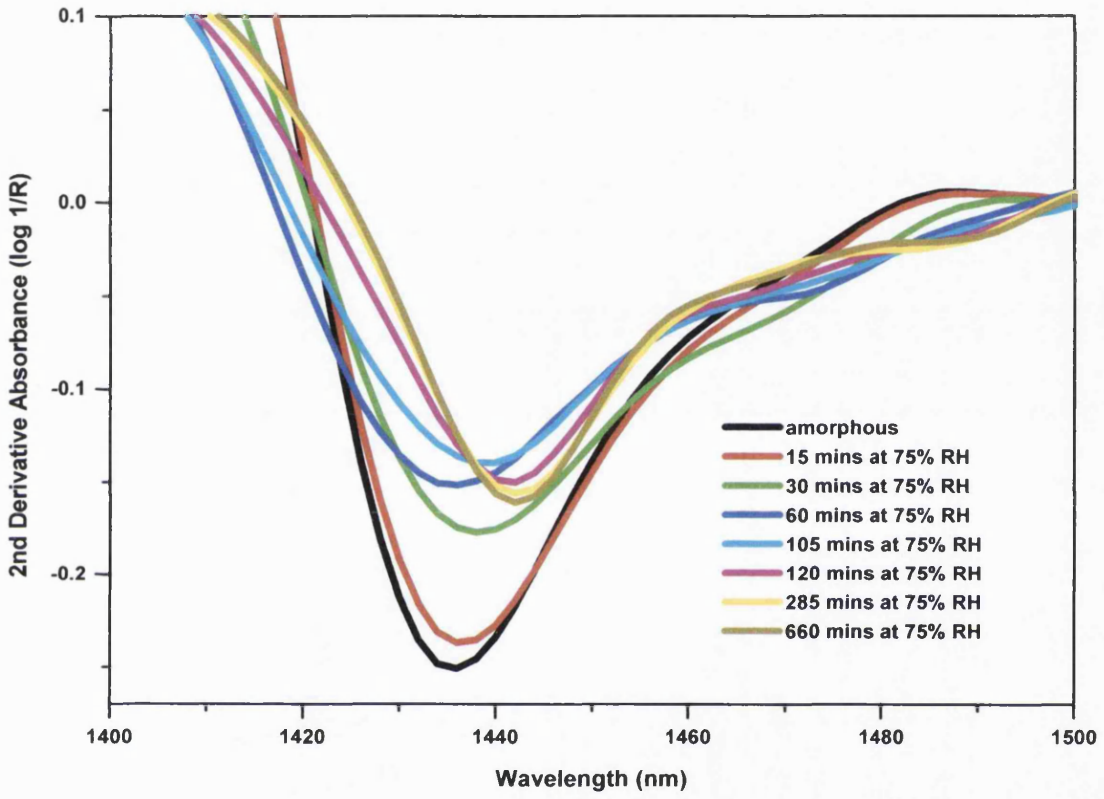

Figure 6.7 *SNV 2nd derivative NIR spectra in the 1400 – 1500 nm region, showing the progression of plasticisation and crystallisation at 75% RH and 25 °C for a spray dried amorphous raffinose sample.*

In Figure 6.8 the spectra of a spray dried amorphous raffinose sample undergoing crystallisation at 90% RH are plotted in the same region, and much the same transitions are seen, although they occur more quickly due to the greater availability of water under these conditions. Also, in this instance the spectra finally settle at 1444 nm, and from the data in Figure 6.5 and the mass change it would seem that a pentahydrate is formed. Interestingly, in this instance the sample continued to expel plasticising water to give an equilibrium mass corresponding to 17.4%. Therefore,

the sample taken after 331 mins at 90% RH actually had a lower water content than the pentahydrate-equivalent sample. Despite this, water movement in the sample shows that crystallisation had further progressed.

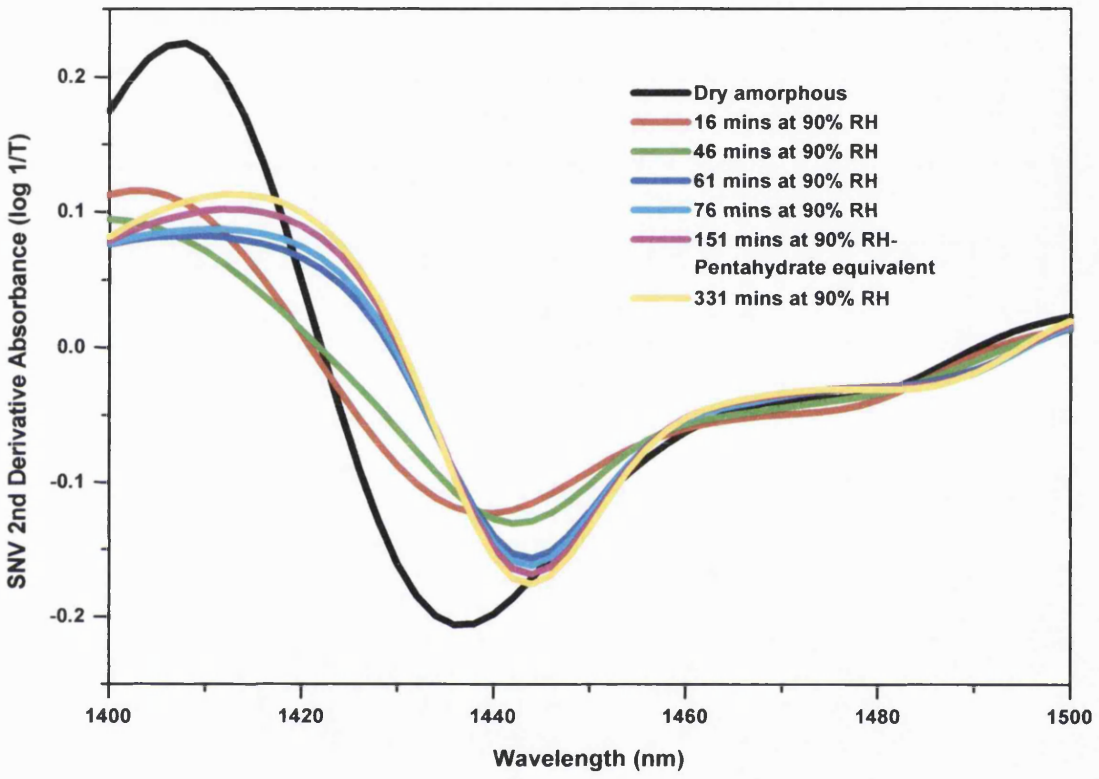

Figure 6.8 *SNV 2nd Derivative NIR spectra for the crystallisation of amorphous spray dried raffinose at 90% RH and 25 °C in the region of 1400 – 1500 nm.*

Although in Figure 6.7 the peak at 1442 nm does not change significantly after cystallisation has occurred, there are other portions of the spectra which do show changes post-crystallisation. The region around 1700 nm is one such region and this has already been discussed for a different sample (Figure 6.3). Furthermore, there are changes in the region of 1930 nm (which relates to the hydrate water content), where a marked deepening of the response is seen with time, despite the fact that the mass recorded by the DVS does not change, further indicating that water movement

within the sample continues long after the sample has ceased to take up or expel any further moisture. Figure 6.9 shows those spectra which were included in Figure 6.7 in the region of 1930 nm, and it can be clearly seen that the intensity of the peak at 1930 nm continues to deepen despite no corresponding mass uptake.

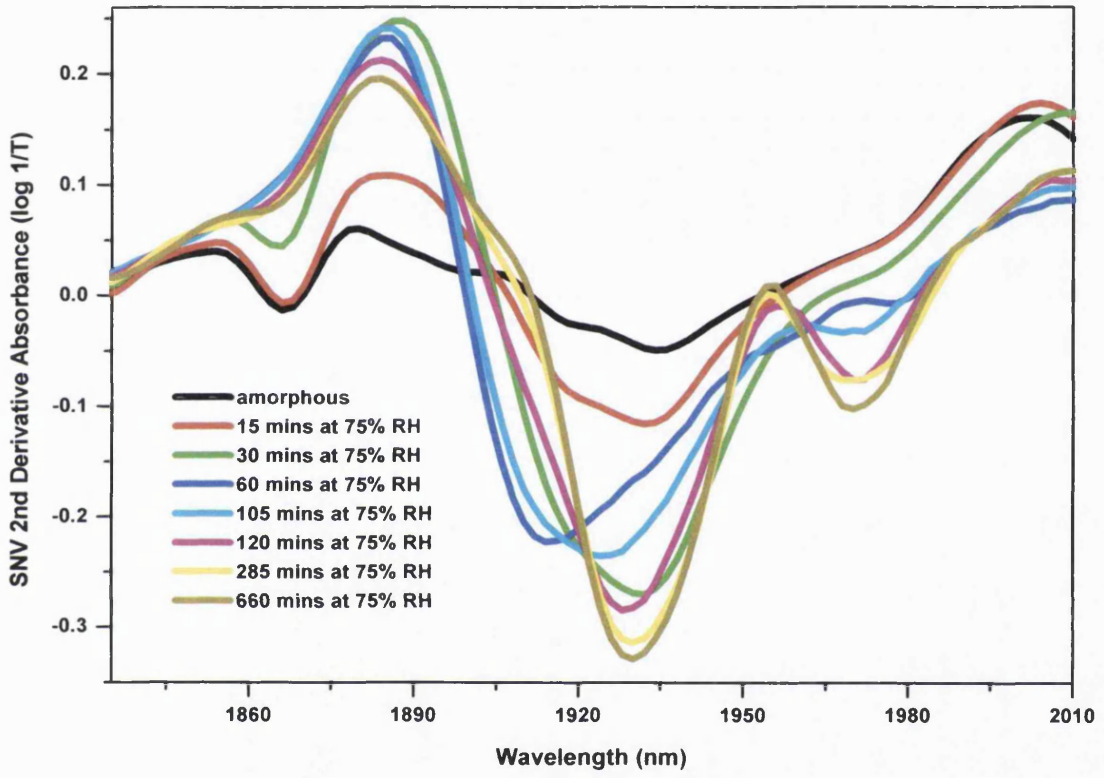

Figure 6.9 *SNV 2nd Derivative NIR spectra in the region of 1840 – 2010 nm, showing the development of the hydrate water peak at 1930 nm despite the lack of mass changes recorded by the DVS at 75% RH and 25 °C.*

One question which remains to be answered is that relating to why water uptake by samples is inconsistent under the same temperature and humidity conditions. It is possible that this relates to the fusion of the crystallising material. Taking two samples which were exposed to 90% RH, of 24 mg and 62 mg respectively, it has already been stated that whilst the smaller sample achieved a maximum water

content of 23.9 % w/w, the larger sample only gained 19.5% (Figure 6.10). Macroscopically it is clear that the sample's exterior fuses during crystallisation, and it is possible that the sample becomes impenetrable to the water in the atmosphere. This would also explain why the expulsion of plasticising water from the sample is so slow, as it is limited by a diffusion process. It is also interesting to note that despite the different quantities of water absorbed by the samples at 90% RH, they follow very similar water loss patterns at less than approx. 10% w/w water content when maintained at 0% RH.

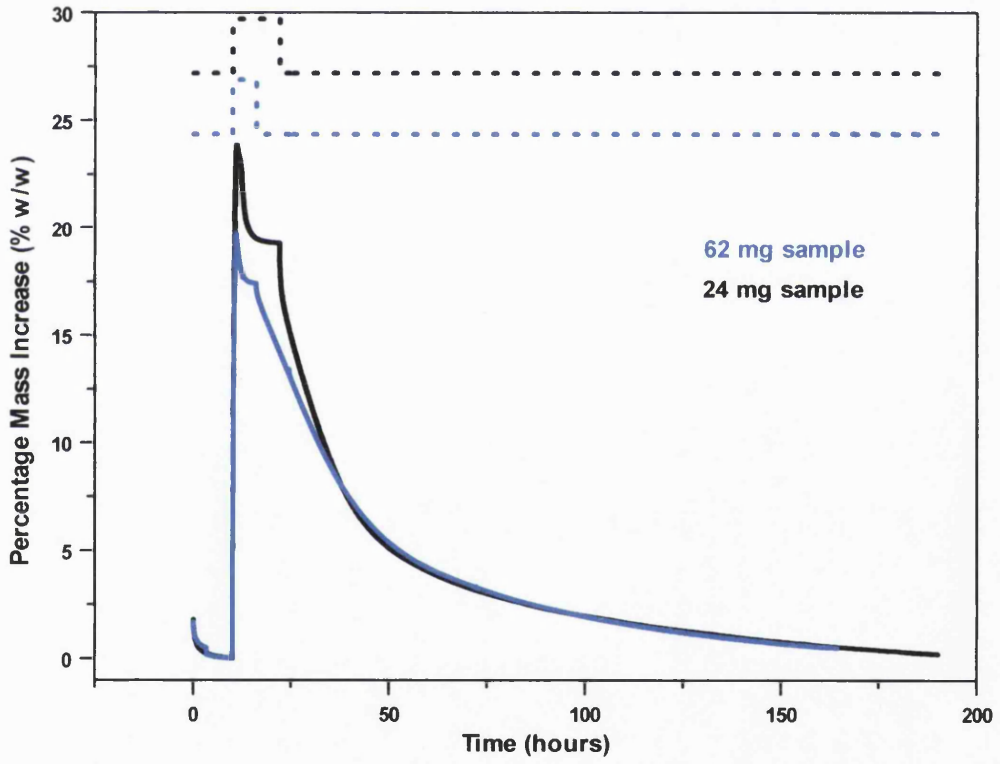

Figure 6.10 *The crystallisation of two samples of spray-dried raffinose (of 24 mg and 62 mg respectively) exposed to an initial 0% RH step, followed by a 90% RH step and then a final drying step at 0% RH.* _____ *= mass;* ..... *= RH.*

6.4.1.3. Heat Dried Raffinose

Amorphous raffinose was also generated by heat drying, which has been shown to induce molecular disorder whilst maintaining the external crystalline conformation (Saleki-Gerhardt et al., 1995). In order to ascertain the similarities between the behaviour of heat- and spray dried amorphous raffinose, heat dried samples were exposed to crystallisation in the DVS/NIRS at 75 % RH. The same trends were observed for the heat-dried samples as for the spray-dried, *i.e.* no mass loss was observed upon crystallisation, but NIR spectra confirmed the event. In addition, the samples were seen to absorb 14.9 % and 15.5 % w/w water respectively, which is again insufficient to form a pentahydrate. Crystallisation at 90% RH was carried out in order to produce a pentahydrate (Figure 6.11), however it resulted in a maximum

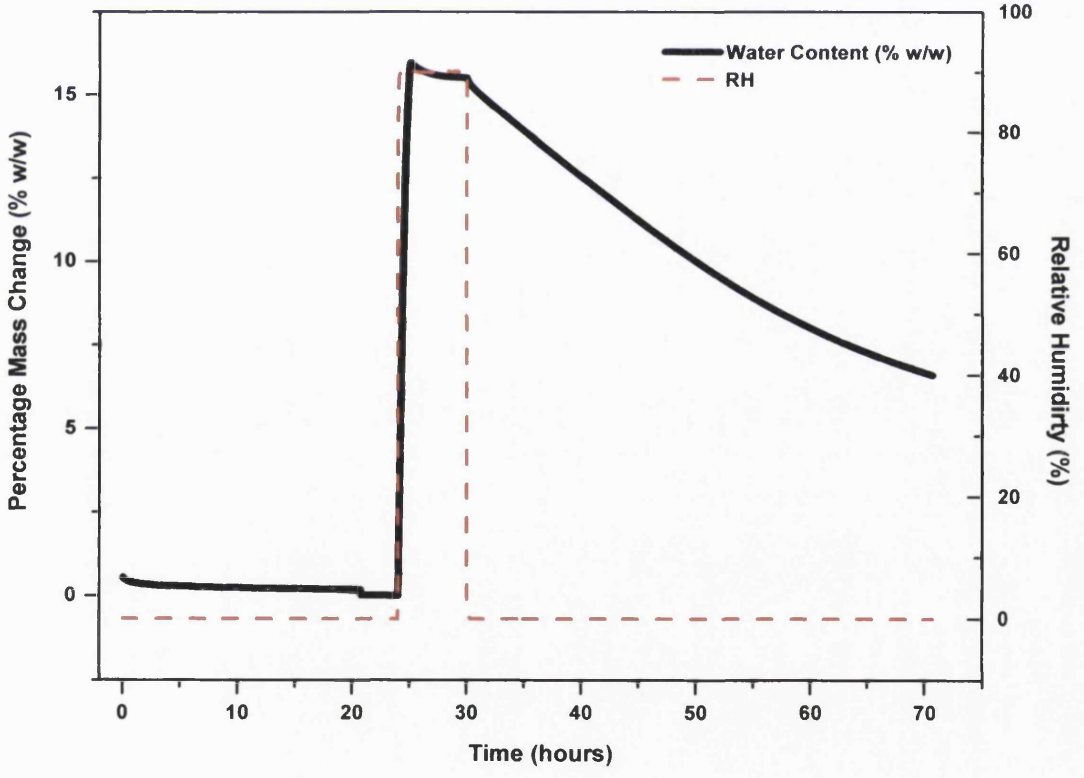

Figure 6.11 *The crystallisation of heat dried amorphous raffinose at 90% RH and 25 °C.*

water uptake of only 16.0 % w/w for a 46 mg sample, which is considerably less than that seen for the spray dried samples, and again less than the 17.9 % which corresponds to pentahydrate formation. It is noteworthy that subsequent to crystallisation the sample equilibrated to a mass uptake of 15.4 % w/w within six hours at the elevated RH, which is a much shorter time to equilibration than seen for the spray dried samples (the sample shown in Figure 6.4 required 11 hours to achieve equilibration). The amount of plasticising water expelled by the heat dried sample was also considerably less than by the spray dried samples, but that may be expected due to the reduced water uptake. It is interesting to note that exposure to 90% RH does not significantly increase the water uptake by heat dried raffinose

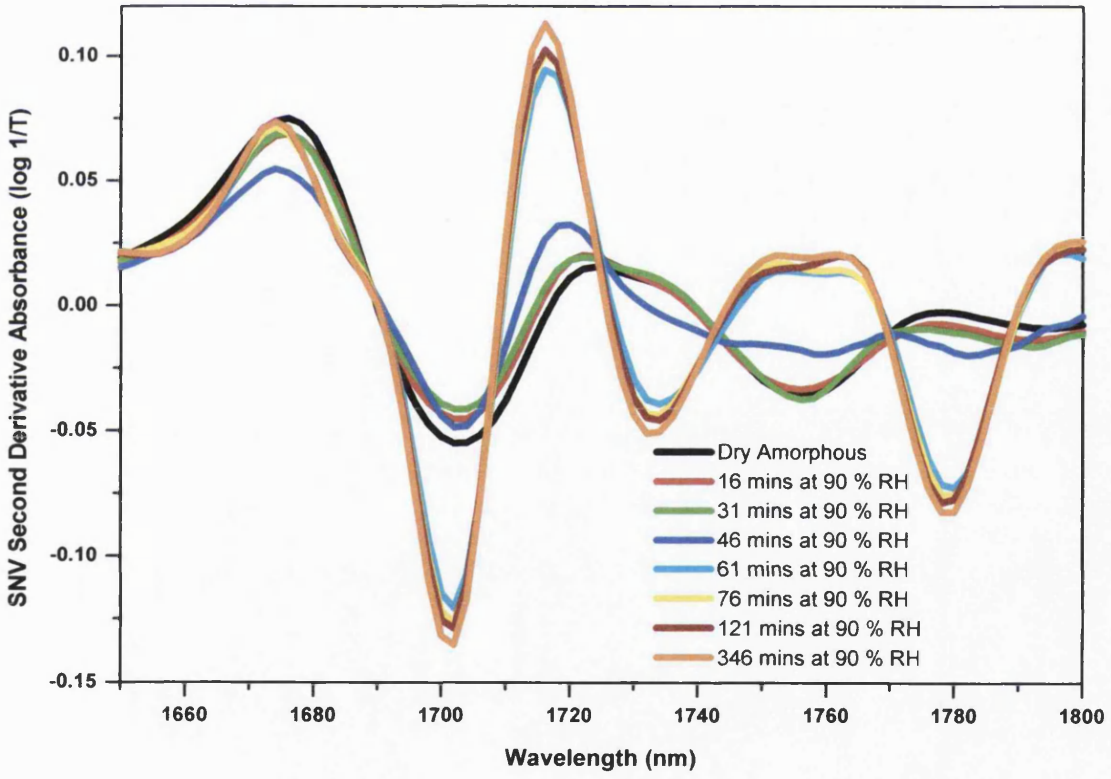

Figure 6.12 *SNV 2nd Derivative NIR spectra representing the crystallisation of amorphous heat dried raffinose at 90 % RH and 25 °C (corresponding DVS plot is shown in Figure 6.11).*

compared with that observed at 75% RH (15.3% at 75% RH, as compared with 16.0% at 90% RH). It is possible that the retention of the macroscopic crystalline appearance upon heat drying, which results in an amorphous material with a much smaller surface area as compared with the spray dried form, may be a limiting step in the absorption of water. The density of the material and its accessibility to water vapour penetration may also play an important role.

From the spectra in Figure 6.12, it is clear that the crystallisation process is more rapid for the heat dried material. This could again be due to the retention of the external crystalline appearance, which may in some way facilitate the crystallisation process. It is also possible that heat drying results in an amorphous form which more easily reverts to a crystalline conformation.

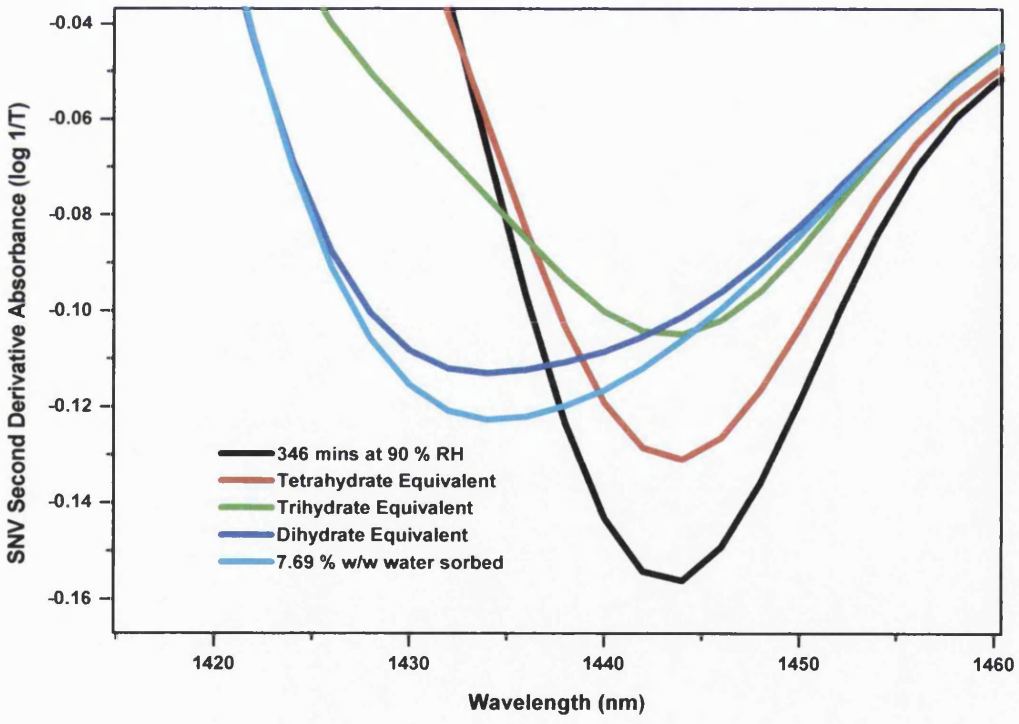

Figure 6.13 *SNV 2nd Derivative NIR spectra representing the dehydration of crystallised heat dried raffinose at 0 % RH and 25 °C.*

The dehydration of raffinose crystallised from the heat dried form is represented by the NIR spectra in Figure 6.13. It is clear that the process proceeds in much the same manner as in the case of raffinose crystallised from the spray dried form and it can be seen that the dry tetrahydrate-equivalent spectrum occupies the wavelength of 1444 nm, as previously shown in Figure 6.5. However, drying to a trihydrate equivalent mass does not result in a shift in the wavelength. The dihydrate spectrum occupies 1434 nm, in comparison with the spray dried dihydrate which is found at 1430 nm. The final spectrum which has been further dried to a residual water content of 7.7 % w/w.

Another interesting comparison to make between the spray and heat dried materials is the rate at which they absorb water. It can be seen from Table 6.1 that rate of absorption by the heat dried material is consistently slower than the spray dried material, which may again be due to a particle size effect. This slower rate of absorption may in turn limit the total amount of water sorbed, as crystallisation may get underway before the sorption process is complete, and this may prevent the absorption of further water.

Table 6.1 *The rates of water absorption by amorphous spray dried and heat dried raffinose upon exposure to elevated RH (percent mass increase with respect to dry amorphous mass per hour).*

	SPRAY-DRIED			HEAT-DRIED		
RH (%)	Mass Increase (%/hour)	Time to Maximum Absorption (mins)	Sample Mass (mg)	Mass Increase (%/hour)	Time to Maximum Absorption (mins)	Sample Mass (mg)
75	9.10	100	60.39	5.20	172	63.69
	9.09	106	45.15	5.63	165	56.89
	9.44	94	58.14			
	4.99	166	52.57			
90	20.79	57	61.31	14.31	67	45.74
	21.86	66	25.44			

6.4.2. BATCH ISOTHERMAL MICROCALORIMETRY

The enthalpy of crystallisation of many materials has been studied using batch isothermal microcalorimetry (e.g. Briggner et al., 1994, Aso et al., 1995, Ahmed et al., 1996, Lehto and Laine, 1998). It has been noted (Darcy and Buckton, 1998) that for lactose the measured enthalpy of crystallisation is significantly lower than would be expected (for example it is much smaller than the melting endotherm enthalpies measured by DSC, which should be equal and opposite to the enthalpy of crystallisation). Darcy and Buckton (1998) have argued that the small measured response is due to the fact that substantial water desorption (endothermic) occurs during crystallisation and that the net response is thus significantly smaller than the exotherm that would be expected for crystallisation alone. For raffinose, however, as discussed above, it has been seen that there is no significant water desorption when the material crystallises (Figure 6.1). In this instance then it would be expected that the net enthalpy of crystallisation would be similar to the enthalpy measured during melting.

6.4.2.1. Measured Enthalpies During Crystallisation and Melting

The crystallisation response of amorphous raffinose at 75 % RH and 25 °C as measured by isothermal microcalorimetry (Figures 6.14, 6.15) was found to have three distinct regions. The first exotherm is substantial and protracted, its duration depending upon sample mass, being around 8 hours for a mass of 100 mg (labelled A in Figure 6.14). The long duration of this region means that it cannot simply relate to thermal equilibration of the sample following lowering into the measuring site. It has been argued that the wetting response would be very small in this type of experiment, as the uptake of water by the sample (an exothermic response) would be approximately balanced by the generation of humidity from the saturated salt solution (evaporation being an endothermic response). Consequently the large and protracted initial phase of the reaction is likely to relate to processes other than just wetting, for example a reordering of molecules in the solid as a consequence of water sorption. After this initial exotherm there is a lag phase which again has been found to be sample mass related. This lag phase lasts ca. 6.5 hours for 100 mg

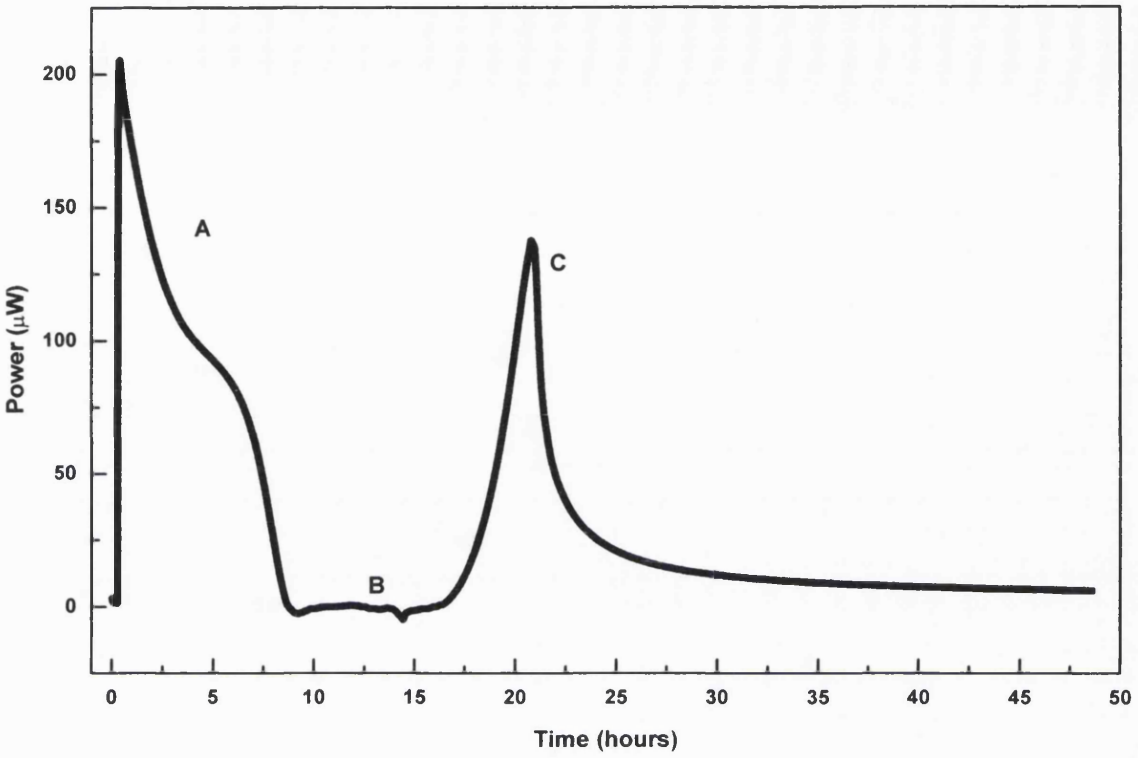

Figure 6.14 *Crystallisation of a 100 mg sample of spray dried raffinose in the TAM at 75% RH and 25 °C.*

sample load (shorter duration with a lower mass of sample), during which time the response is close to baseline. The shape of this lag phase response is different if the sample mass is changed, and for low loads (15 - 27 mg, *e.g.* Figure 6.15) a clear endothermic peak is seen in this region. This peak is less clear but still present for larger sample loads (labelled B on Figure 6.14). Following from this there is a further substantial exotherm (labelled C on Figure 6.14). It can be seen that this response is very protracted and does not return to baseline even for an experiment of 50 hours duration. This prolonged response is in keeping with the changes that are observed in the DVS-NIR experiments (see Section 6.4.1.) and indicates that the sample has crystallised but continues to undergo solid state transitions post crystallisation. As was discussed above, the solid state transitions may relate to transitions from whatever hydrates form during the initial crystallisation to the existence of the most stable form at the experimental conditions. This gives rise to a

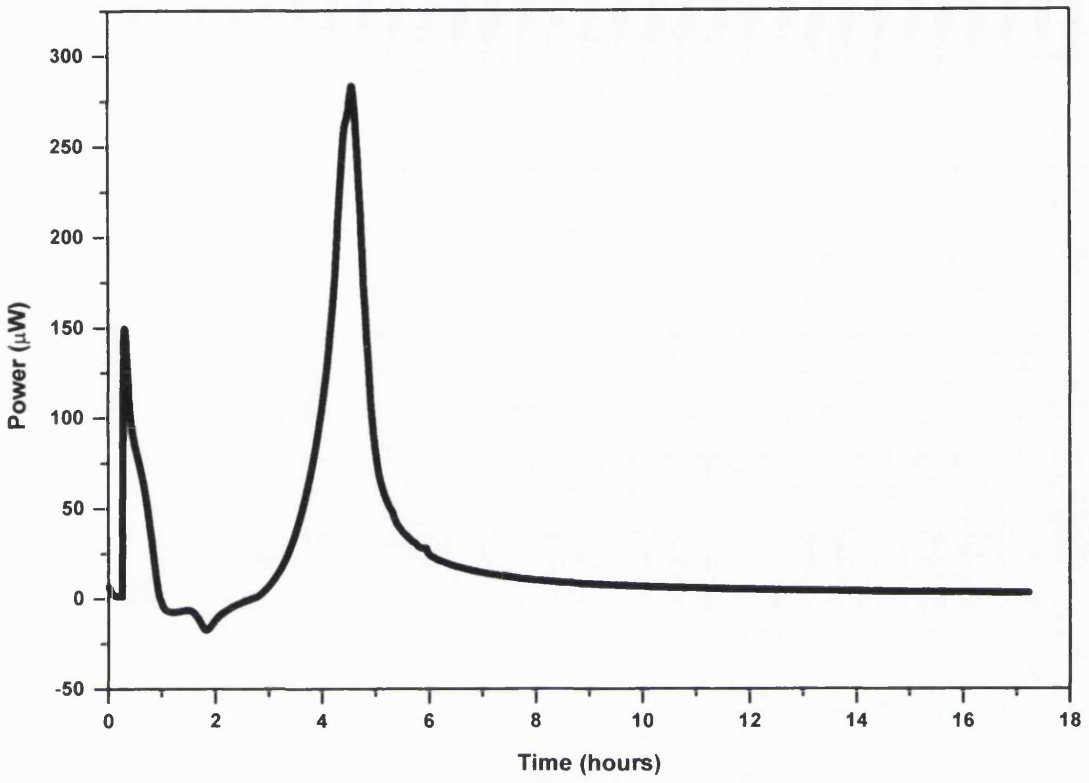

Figure 6.15 *The crystallisation of a 15 mg sample of spray dried amorphous raffinose at 75% and 25 °C RH in the TAM. It can be seen that the profile is very similar to that in Figure 6.14 of the crystallisation of a 100 mg sample, although the reaction occurs over a shorter time scale.*

problem with respect to defining the area under the power-time curve that best describes crystallisation. The lowest enthalpy values were obtained for large sample masses and the highest values for low sample mass (15 – 27 mg). This difference may reflect the fact that the tail of the experiment has not come close to completion for large sample masses, but the process is almost complete (however not truly back to baseline) for the small mass samples. Another important factor to consider is the availability of water vapour to the sample. As already discussed, amorphous raffinose requires a 17.9% w/w mass increase in order to form a pentahydrate, therefore a spray dried sample of 100 mg will require almost 20 mg of water vapour in order to completely crystallise. It is unlikely that a sealed ampoule/hygrostat

experiment would be capable of providing such quantities in the time scales used here. If Figures 6.14 and 6.15 are examined it can be seen that the maximum heat flow value achieved by the 100 mg sample is in the region of 150 μW, as compared to a value approaching 300 μW for the smaller sample.

This supports the argument that the reactions of larger samples are subject to a limiting step. Another factor to consider is the possibility that the samples are undergoing collapse, preventing the penetration of water vapour into the sample and thus inhibiting further crystallisation. Due to these factors it was assumed that the data for the large sample masses was restricted and that they were not able to form the higher hydrates. Consequently data for low sample masses were considered further.

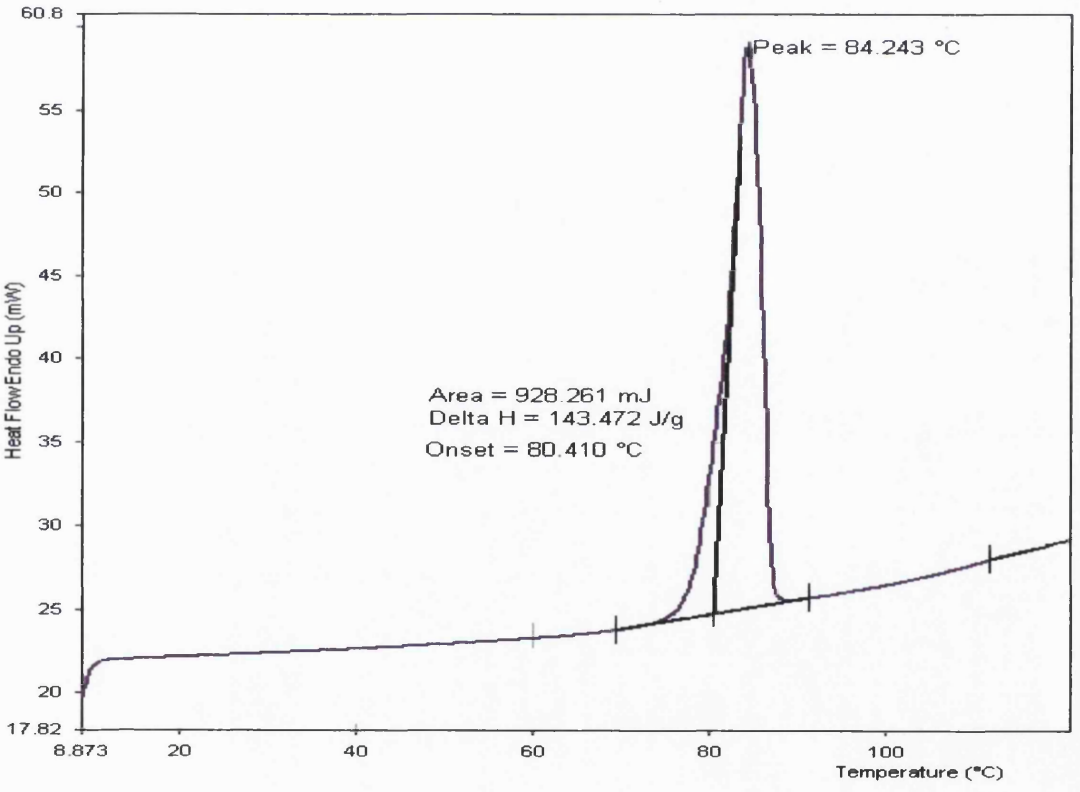

Figure 6.16 *The melting of raffinose pentahydrate (as obtained) as recorded by DSC.*

In order to make an accurate comparison of the enthalpies of crystallisation and fusion, it was necessary to correct the enthalpy of crystallisation values. This is due to the fact that there is a free energy change, ΔG, associated with crystallisation at temperatures other than the melting temperature. Hoffman (1958) described the following equation to calculate ΔG:

$$\Delta G = (\Delta H_f \Delta T/T_m)(T/T_m) \qquad \text{..... Equation 6.1}$$

Where: T = the crystallisation temperature, 298 K.

T_m = the melting point

ΔH_f = the enthalpy of fusion at T_m

ΔT = the difference between T_m and T.

The enthalpy measured for melting and dehydration of the commercially obtained pentahydrate using DSC was found to be 143 ± 7 J/g (Figure 6.16), this value being similar to the 149 J/g reported by Kajiwara et al., 1998. However the enthalpy of fusion of low mass samples previously crystallised in the TAM at 75% RH was found to be 74.2 (± 10.9 J/g). This is consistent with findings from DVS, which show that raffinose does not equilibrate to form a pentahydrate at 75% RH and 25 °C. The enthalpy of crystallisation (unadjusted) of those low mass samples obtained from the total AUC in the TAM (Figure 6.17) was found to be 80.6 (± 14.5) J/g (see further discussion), which, when adjusted using the Hoffman Equation results in a value of 89.5 J/g. Therefore, these samples show a good agreement between their enthalpies of crystallisation and fusion.

The mean DSC melt for ex- TAM high mass samples was 39 J/g, which was in keeping with the adjusted enthalpies of formation measured in the TAM for large mass samples (45.95 J/g). It is interesting to note that Kajiwara and Franks (1997) reported the enthalpy of fusion of raffinose trihydrate to be 85.3 J/g (the trihydrate

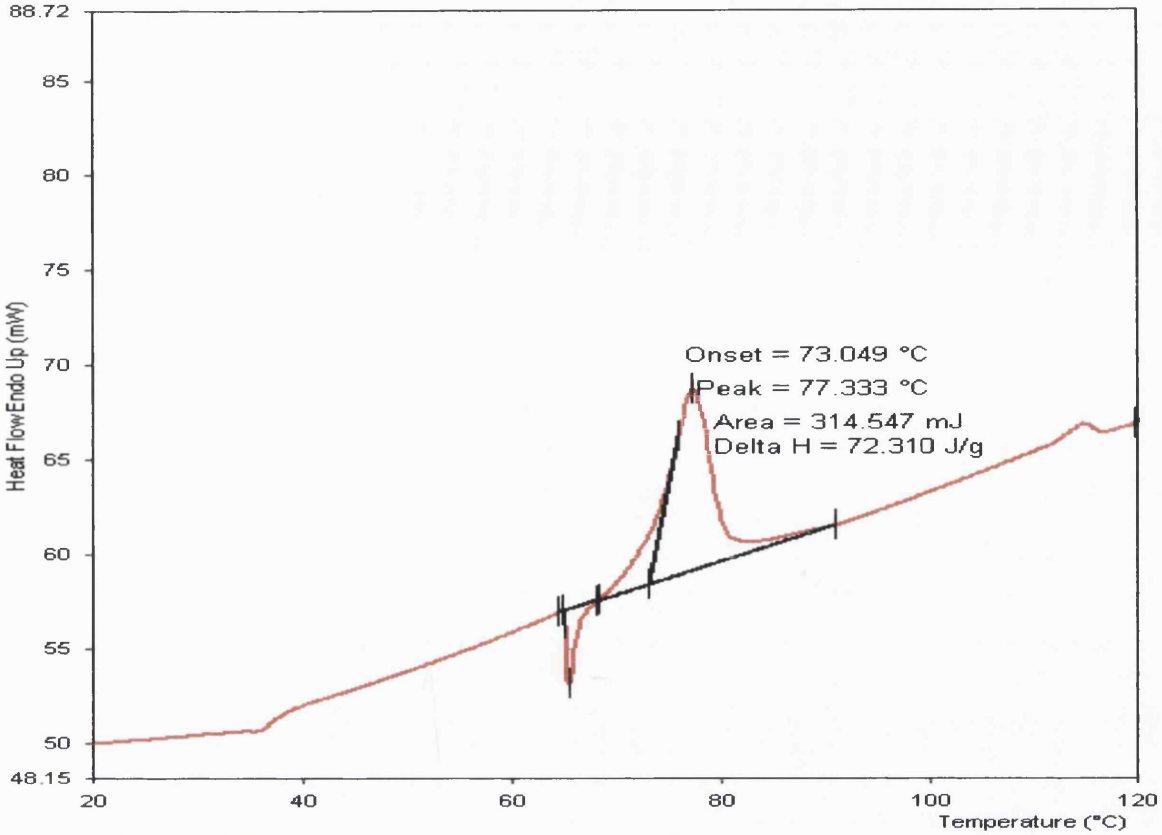

Figure 6.17 *The melting of a crystallised raffinose sample post-TAM (75%, 25 °C), as recorded by DSC.*

form was assigned to the dehydrated pentahydrate sample following Karl-Fischer determination of water content and calculation by molar ratio sugar:water).

From these data it can be seen that a good correlation between enthalpy of crystallisation and the enthalpy of melting was achieved, indicating that the hypothesis of Darcy and Buckton (1998) was correct in that water evaporation was the cause of differences between the DSC and TAM experiments for lactose. It is possible that the differences in the fusion and crystallisation enthalpies obtained can be attributed to several disadvantages in the measurement methods used. Chemical or physical changes (*e.g.* desolvation, polymorphic transitions or decomposition) in a sample upon heating to high temperatures in DSC can impact upon the determination of the enthalpy of fusion. These changes may occur prior to or in conjunction with the melting process (Ford and Timmins, 1989). Raffinose, however, has a relatively low melting point at 80 °C, thus limiting such effects. Crystallisation in the isothermal microcalorimeter is often, as in the case of raffinose, triggered by external stimulus (*e.g.* elevated relative humidity, exposure to

organic vapour). Under such conditions the effects of interactions between the external stimulus and the sample (*e.g.* wetting, hydration, swelling) may affect the enthalpy measured. It is important to note that if the crystalline solid produced in the microcalorimeter is a different form from that melted in the DSC, then the enthalpic changes which are recorded are not directly comparable, as shown above with different hydrates of raffinose.

6.4.2.2. Transitions Before Crystallisation

From the discussion above, the entire process recorded in the TAM must be measured as being related to crystallisation, with the first endotherm being due to an increase in the mobility of molecules as the T_g starts to drop, and the final phase being crystallisation followed by solid state transitions to optimise hydrate water distribution. If this division into two distinct regions of activity is true, then

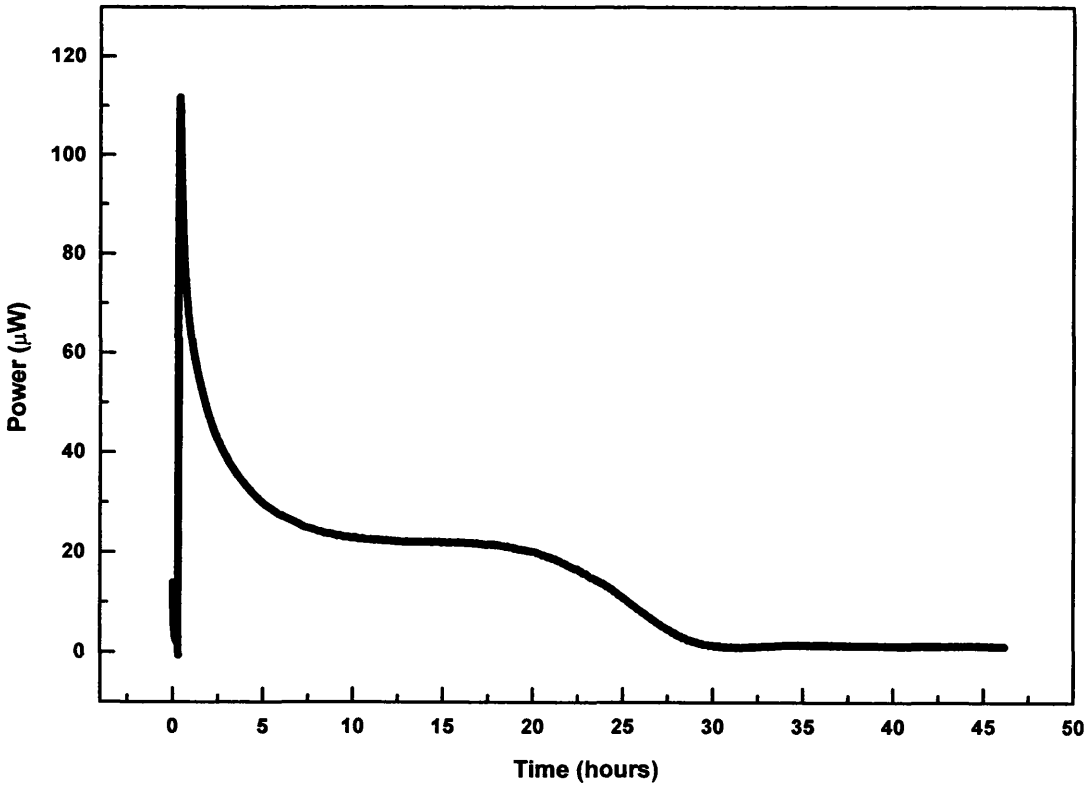

Figure 6.18 *Spray Dried raffinose exposed to 43% RH and 25 °C in the TAM.*

exposure of samples to an RH that does not give rise to crystallisation should produce a response similar to the first exotherm seen during exposure to 75% RH. It has previously been shown that at 30 ° C amorphous raffinose does not crystallise below 45% RH (Saleki-Gerhardt et al., 1995). In Figure 6.18 the response for a sample exposed to 43% RH and 25 °C is shown. The area under the curve in Figure 6.18 at 43% RH (25 J/g) is similar to that seen for peak A (28 J/g) in Figure 6.15 at 75% RH (both samples being of similar mass). If the experiment at 43% RH is stopped and the RH changed to 75% and the ampoule returned to the TAM, then the second exotherm is seen (Figure 6.19).

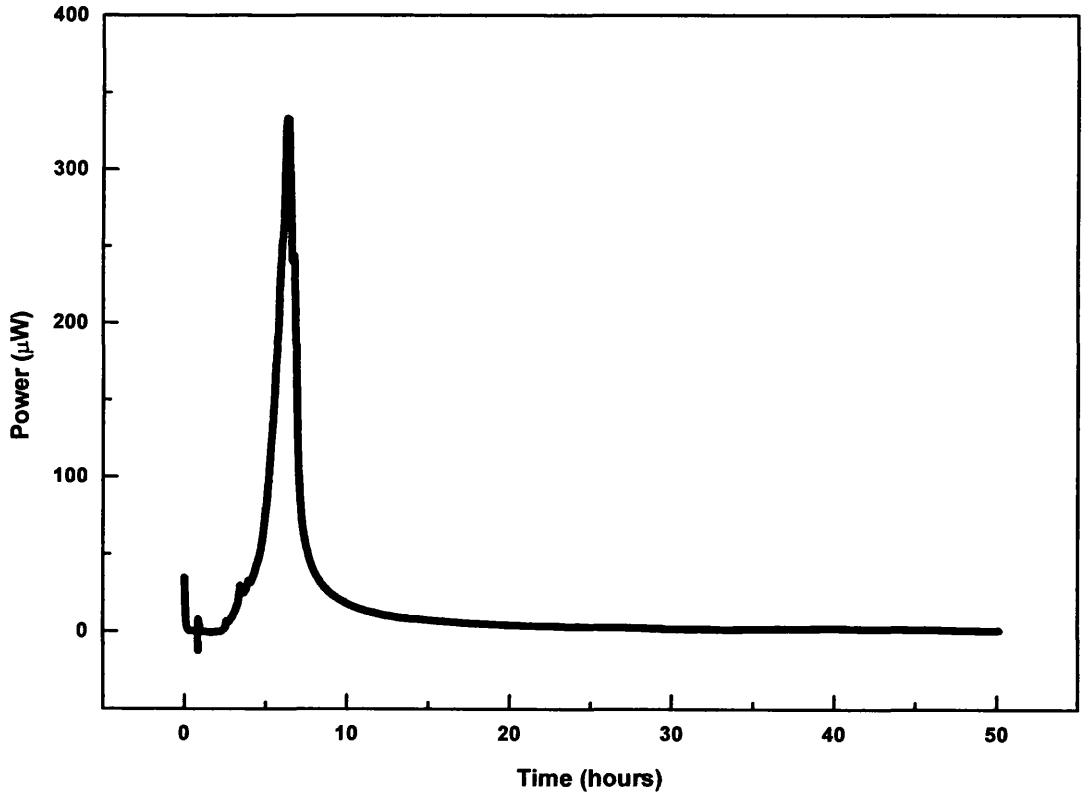

Figure 6.19 *The crystallisation at 75 % RH and 25 °C of the sample shown in Figure 6.18, which had previously been exposed to 43% RH and 25 °C in the TAM.*

A further check of what occurs during the first exotherm was made by exposing an amorphous spray dried sample to 43% RH and taking SEM photomicrographs. It can be seen (Figure 6.20 (a)) that the original spray dried material consists of spherical amorphous particles, but exposure to 43% RH for 5 weeks (Figure 6.20 (b)) causes major bulk changes to take place. It is obvious that the material is developing the external appearance of the crystalline state, although it does not have the properties of the crystal form (no crystalline melting point and amorphous by NIR spectroscopy) even after this period of storage. In principle, the material would be expected to crystallise following very long exposure to low RH, although at present the existence of an anhydrous crystalline form and indeed categorical proof of the existence of lower hydrates of raffinose remains absent. Hancock and Zografi (1997) have shown that materials must be stored 50 °C below their T_g for mobility to be sufficiently limited to prevent crystallisation over a multiple year shelf life that would be required for pharmaceuticals. In this instance raffinose at 43% RH has a T_g of ca. 27 °C which is in good agreement with the T_g of 28 °C reported by Iglesias et al. (2000) for a sample stored at this RH, so the softening that occurs here allows the formation of a different external morphology but not packing into the necessary long range order for molecules which would define crystallinity.

The observation reported here, that raffinose develops bulk crystalline appearance (sharp edges *etc*) without crystallising (in terms of long range order at the molecular packing level) is an extension of, but in keeping with, the observation by Saleki-Gerhardt et al. (1995) and Kajiwara et al (1999) who observed that heat dried raffinose hydrates became amorphous whilst retaining the external shape of the crystalline form.

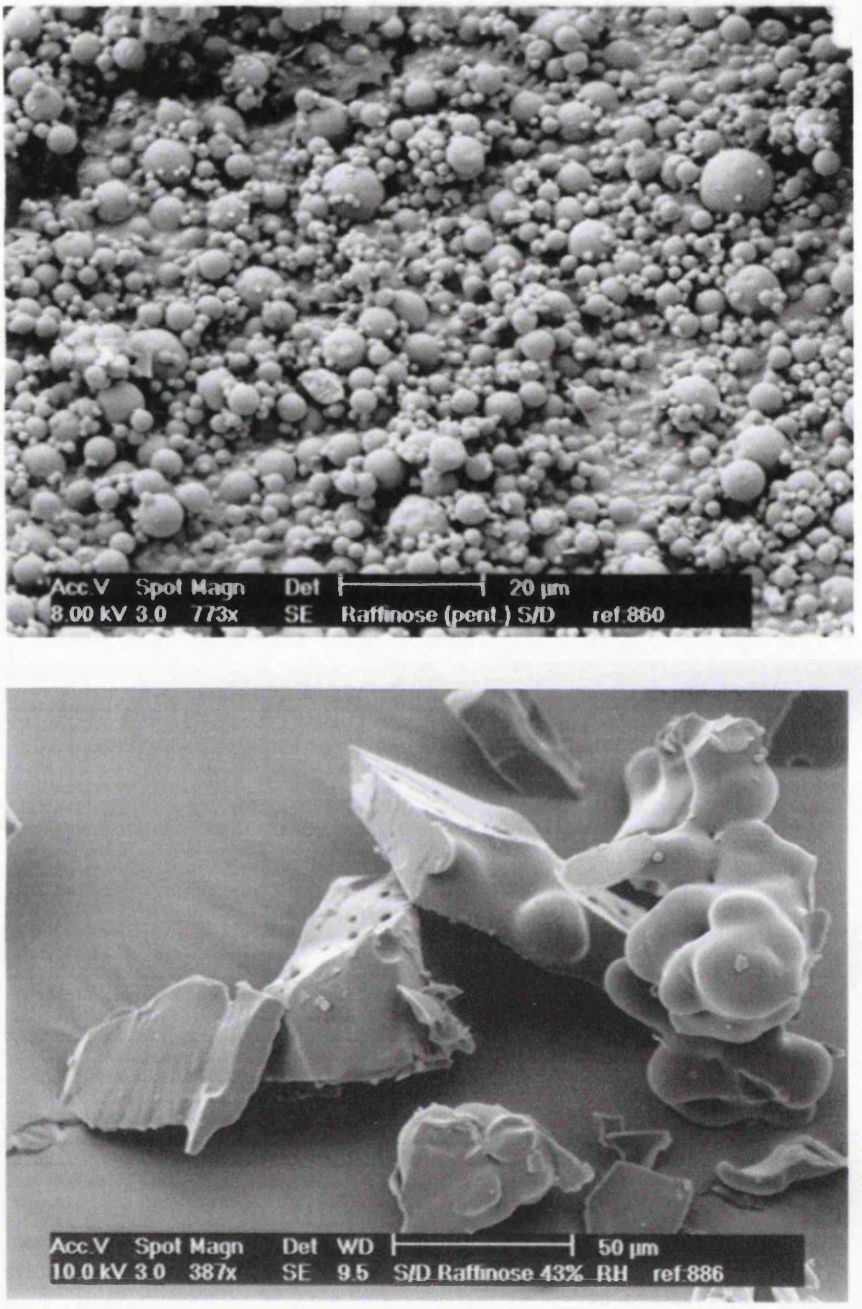

Figure 6.20 (a) and (b) *Scanning electron micrograph of (a) spray dried amorphous raffinose displaying the characteristic spherical appearance expected; (b) spray dried raffinose following exposure to 43% RH for 5 weeks. Evidence of the previous spherical morphology remains, however there has been significant agglomeration of particles and development of morphology similar to that seen with crystals.*

6.4.3. ISOTHERMAL RH PERFUSION MICROCALORIMETRY

It has been shown in Section 6.4.2. that it was not possible for crystallisation to go to completion in batch isothermal microcalorimetry, and as such it was not possible to determine the enthalpy of crystallisation of amorphous raffinose. Therefore the crystallisation of spray dried raffinose at 90 % RH and 25 °C using RH perfusion microcalorimetry was carried out, following from the findings from the DVS/NIRS work that crystallisation of spray dried raffinose does result in pentahydrate formation at 75% RH. In addition the dehydration of the crystallised material was also carried out (Figure 6.21).

In Figure 6.22 (a) a portion of the crystallisation of a 12 mg sample in the RH perfusion unit is shown. It can be seen that exposure to 90 % RH results in an immediate exotherm, as would be expected. This peak then beings to decay, and after approximately 2.5 hours exposure to 90 % RH, a second exothermic event occurs. It is probable that the first peak relates to the absorption of water by the sample, perhaps including some molecular rearrangements as have been seen in the batch microcalorimetry work. The second peak relates to the commencement of the crystallisation process itself. Close examination of the baseline following this peak reveals that the event does not come to completion for a further 104 hours (Figure 6.22 (b)). It is likely that water movement within the sample is responsible for this continued heat flow. Once a baseline had been achieved, the sample was exposed to 0% RH in order in bring about a dehydration of the crystalline material. This resulted in a prolonged response, as seen in Figure 6.23. Following 4 hours exposure to the drying environment, a secondary and much smaller endothermic peak can be seen. What this event represents is unclear, however it may be due to a change in energy level of the remaining hydrate material due to the removal of sufficient hydrate water. The total dehydration reaction continues for 165 hours.

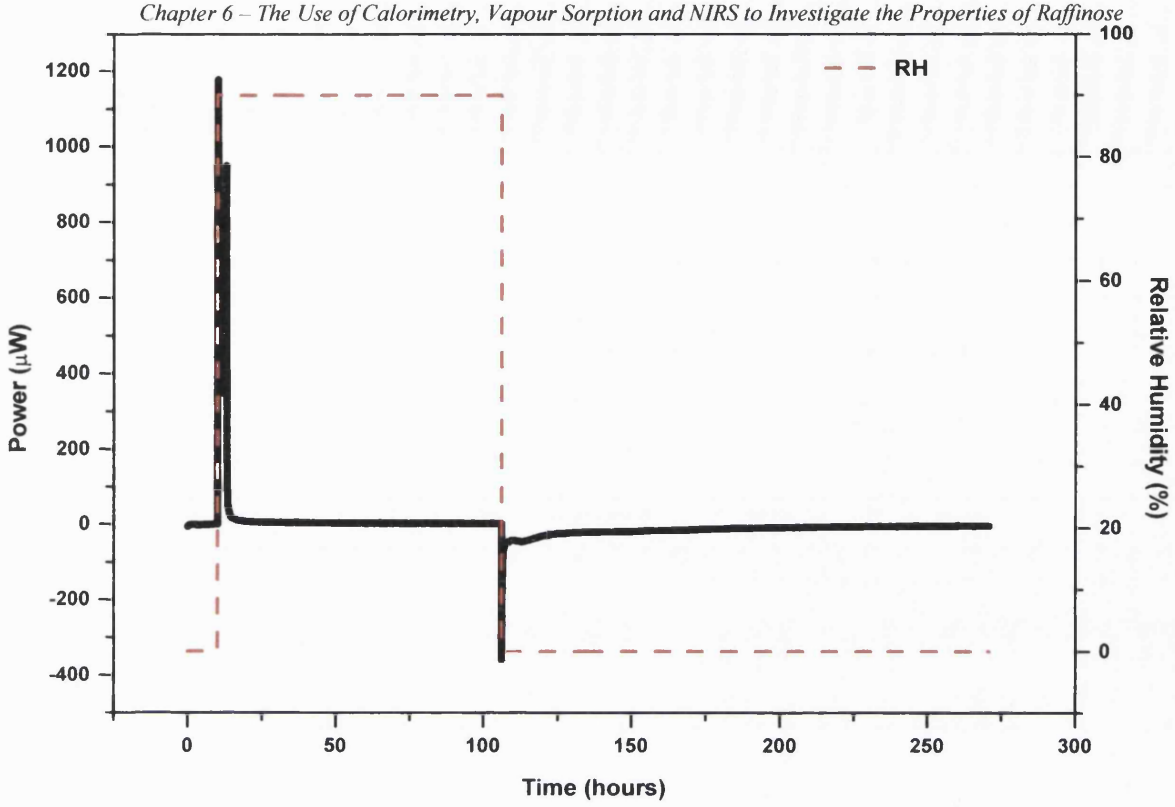

Figure 6.21 *The crystallisation and dehydration of amorphous spray dried raffinose at 90 % RH and 25 °C in the RH perfusion unit.*

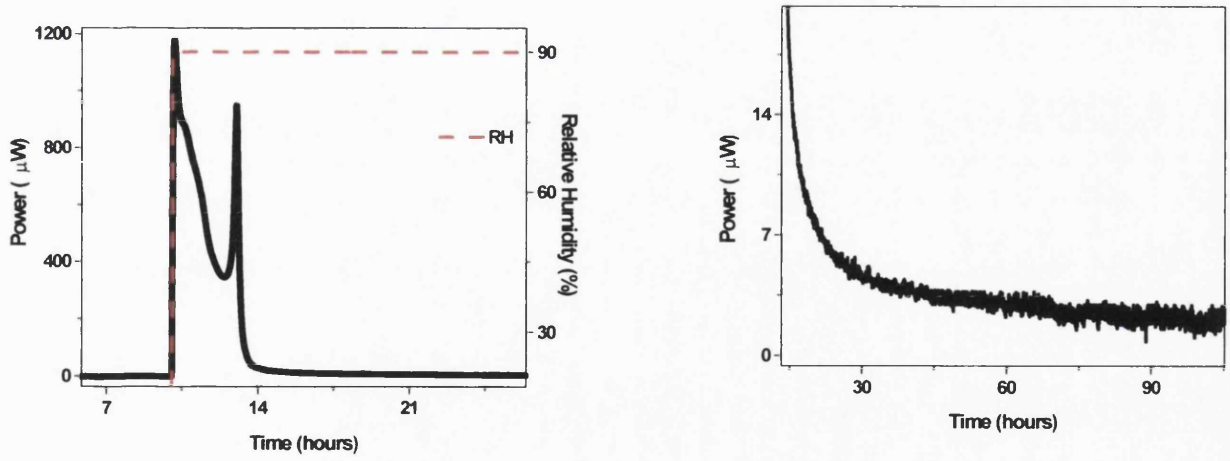

Figures 6.22 (a) and (b) *Magnification of phases of the crystallisation of amorphous raffinose as shown in Figure 6.21.*

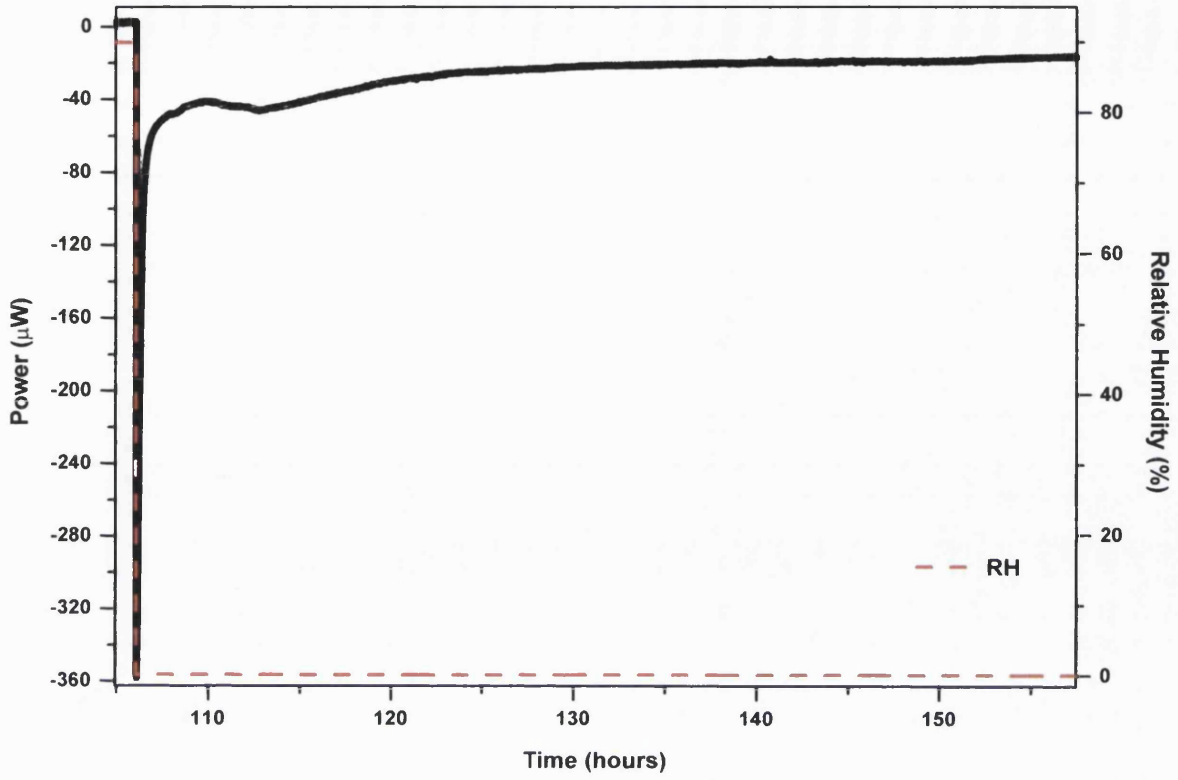

Figure 6.23 *The dehydration of crystalline raffinose at 0% RH and 25 °C in the RH perfusion unit.*

Integration of both the positive and negative peaks (following the subtraction of a blank *i.e.* empty experiment) was carried out. It was determined that the enthalpy associated with the absorption and crystallisation event (*i.e.* the positive peak) was 727.39 J/g. This value is surprisingly consistent with the value for the dehydration reaction (the negative peak), the integration of which resulted in an enthalpy of -713.03 J/g. It is possible that the difference between the two values is due to the latter reaction not running to completion. The similarity between the two values does lead to the conclusion that dehydration of crystalline raffinose is an amorphisation process which is very similar to a reversal of the crystallisation process.

6.4.4. SOLUTION CALORIMETRY

The use of gravimetry, NIRS and isothermal microcalorimetry to investigate the hydration and dehydration of raffinose has already been outlined. Solution calorimetry was also employed to examine the interaction of raffinose with water, since it has been previously shown that enthalpy of solution is affected by changes in the internal energy of a material (Pikal et al., 1978).

6.4.4.1. The Hydration of Amorphous Raffinose

In this study, empty solution calorimetry ampoules were weighed and then filled with approximately 200 mg amorphous raffinose (accurately weighed). These samples were then dried under vacuum at 50 °C in order to ensure the removal of residual water. The ampoules were then stored under four elevated relative humidity conditions at 25 °C for varying lengths of time as outlined in Section 6.3.6.1. The amount of water sorbed by the samples was calculated and correlated with their enthalpies of solution (enthalpies calculated for samples stored at 43%, 58% and 75% RH are based on the samples' wet mass to allow for the possibility that crystallisation had occurred *i.e.* that the additional mass is due to hydrate water). In conjunction with this, amorphous raffinose samples were also stored under identical conditions in vials and NIR spectra taken to confirm the amorphous/crystalline nature of the samples. The amounts of water sorbed by these samples differ from the values obtained for the samples stored in solution calorimetry ampoules due to the different geometry of the containers. It can be seen from Figure 6.24 that at 12% RH an amorphous spectrum was obtained, and that storage at 43% RH yielded a wet amorphous spectrum. However, storage at both 58 % and 75 % RH for 15 days resulted in the relocation of the peak to the wavelength of a mid-crystallisation material. Included is also the spectrum of a pentahydrate sample (as obtained) to illustrate that crystallisation was not complete. From the DVS/NIRS data included in Section 6.4.1. and observations reported by Kajiwara and Franks (1997) it is clear that the crystallisation of raffinose progresses very slowly. It is therefore not surprising that the spectra of the 58 % and 75 % RH stored samples are for partially crystallised samples.

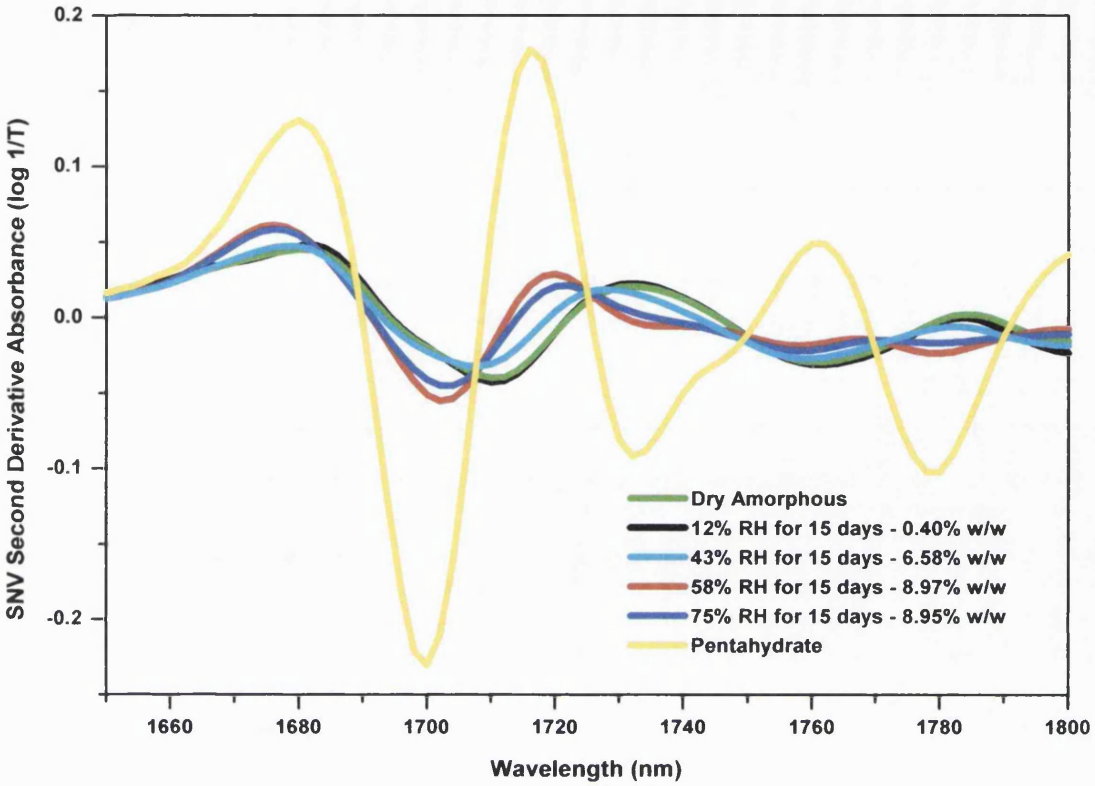

Figure 6.24 *The SNV 2nd derivative NIR spectra for vial stored spray dried amorphous raffinose at 25°C and the RH conditions shown. Also included are the spectra of amorphous and crystalline (pentahydrate, as obtained) samples for comparison.*

Several issues arise from the solution calorimetry results obtained. Firstly, it is clear that a general trend exists of increasing enthalpy of solution with increasing water sorption. However, Figure 6.25 does not contain sufficient data to ascertain whether this relationship is linear, as has been shown with lactose (Chapter 4). It is possible that water sorption by the amorphous material exhibits a linear relationship with enthalpy of solution at levels which do not induce crystallisation, however there are not enough data points to draw such a conclusion. In addition, from the SEM data in Section 6.4.2. it can be seen that particles appear to gain the external features of the crystalline form whilst remaining amorphous by DSC, NIRS *etc* and it is therefore not possible to ascertain whether or not crystallisation has taken place by macroscopic examination.

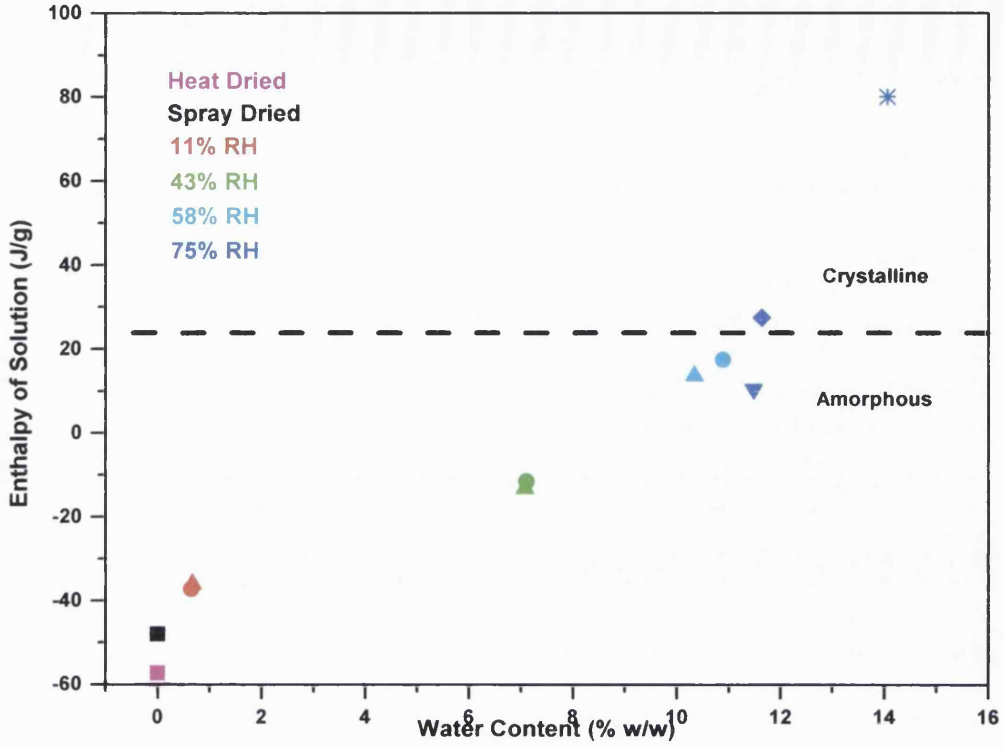

Figure 6.25 *Water absorbed against enthalpy of solution for amorphous raffinose. A general trend of increased absorption with increased enthalpy is observed. It is also interesting to note that despite a relatively small change in the quantity of absorbed water for those samples stored at 75% RH, the enthalpy of solution increased dramatically over time. The dashed black line represents the approximate location of the enthalpy of solution corresponding with the onset of order. It can also be assumed that above this line, increasing enthalpy of solution will correspond with increased hydrate content. (Storage times at elevated RH: ■ = 0 hours; ▼= 17 hours; ♦ = 8 days; ● = 11 days; ▲ = 15 days; * = 3 months).*

It is interesting to examine samples stored under just one condition. Looking at the responses of amorphous raffinose stored at 75% RH, it can be seen that over the first 17 hours of storage the sample had absorbed 11.5% w/w water, with a corresponding enthalpy of solution of 10.37 J/g. However, after 8 days, although water sorption had risen only to 11.6% w/w, its enthalpy of solution had increased to 27.52 J/g. It would seem that the extra water absorbed had a disproportionate effect on the

enthalpy of solution, implying that crystallisation occurred between 17 hours and 8 days at 75% RH. From the Gordon-Taylor Equation (Gordon and Taylor, 1952) (Equation 3.1), it can be calculated that raffinose must absorb 11.96% w/w water in order for its T_g to be lowered to 25 °C. Given the possibility of slight temperature fluctuations during storage, and the errors encountered in quantifying water sorption, this would support the possibility that crystallisation had occurred, and that an onset of molecular order within the sample was responsible for the increase in enthalpy of solution. It would also appear that a low (*e.g.* mono- or dihydrate) hydrate species was present after 8 days storage. A further sample was stored at 75% RH for three months, and with a corresponding mass increase of 14.1% w/w, which is slightly less than that required to form a pentahydrate. The enthalpy of solution of that sample was found to be 80.08 J/g, which further supports the findings that the crystallisation of raffinose is a prolonged process.

It is difficult to ascertain the enthalpy of solution of raffinose pentahydrate since any sorbed water might affect the accuracy of the result, and storage under 0% RH conditions has been shown capable of removing hydrate water from the crystal structure (Section 6.4.1.). Therefore varied enthalpies were recorded for the crystalline material, and the average value was found to be 88.82 J/g ± 0.96 J/g (n = 4). This would support the finding that the enthalpy of solution found for the sample stored at 75% RH for 3 months was indeed that of crystalline raffinose, and although the water uptake was less than the 14.9 % w/w required to form a pentahydrate, it is possible that a partial pentahydrate was formed. The samples were not dried before obtaining their enthalpies of solution, and therefore the contribution of a wetting response due to sorbed water (an exothermic effect) to the total enthalpy would have been to yield artificially high enthalpies. The effect of water sorption by the crystalline form is however much less significant than sorption by the amorphous form.

From the NIRS data in Figure 6.25 it can be seen that the 43 % RH sample has retained its amorphous form, whilst storage under 58 % RH for 15 days is sufficient

to induce crystallisation. It is interesting to note that a decrease in mass was observed in both the 43 % RH and 58 % RH stored samples at 15 days, as opposed to the levels of water sorption recorded after 11 days storage. This was most noticeable with the 58% RH stored samples, which saw a water content of 10.9% drop to a level of 10.3% w/w. In both cases a corresponding decrease in enthalpy of solution was also achieved. The amount of water absorbed was insufficient to reduce the T_g to 25 °C (according to the Gordon-Taylor Equation), so it would seem that the loss in mass cannot be attributed to the expulsion of plasticising water subsequent to a crystallisation event. It is probable that since the solution calorimetry ampoules are hand-made, slight differences in the geometry of the orifice through which the samples are normally filled, accompanied with different dry sample masses led to differences in water sorption by the samples.

It can be seen that the enthalpy of solution of the spray dried amorphous samples is higher than that obtained for the heat dried amorphous sample. Whilst it is possible that amorphous materials generated by different methods have different internal energies which affect the enthalpy of solution obtained, it is also possible that the difference between the two values is due to the fact that heat drying removes all residual water content, whilst the spray dried material still retains some moisture and thus the wetting response is reduced, leading to a higher enthalpy.

6.4.4.2. The Dehydration of Raffinose Pentahydrate

In order to assess by enthalpy of solution the effects of dehydration on raffinose pentahydrate, samples were stored in vials under three 'dry conditions'. These were at 25 °C and 35 °C over silica gel respectively, and in a vacuum oven at –300 mbar and 50 °C for two and four days respectively. The mass losses found are illustrated in Figure 6.26. Enthalpy of solution in each case was calculated based on the dehydrated sample mass. Again a general trend was observed of decreasing enthalpy of solution with decreasing mass. It would seem that samples stored at 25 °C over silica gel had not undergone any harsh drying process, as the mass losses observed were –0.2 % and –0.1 % w/w after two and four days respectively,

resulting in an average enthalpy of solution of 88.67 J/g ± 0.06 J/g. It is likely that variation in mass loss was due to slight water sorption during the ampoule filling subsequent to storage. Under the 25 °C conditions it would seem that only residual water was removed, with no effect on the pentahydrate itself.

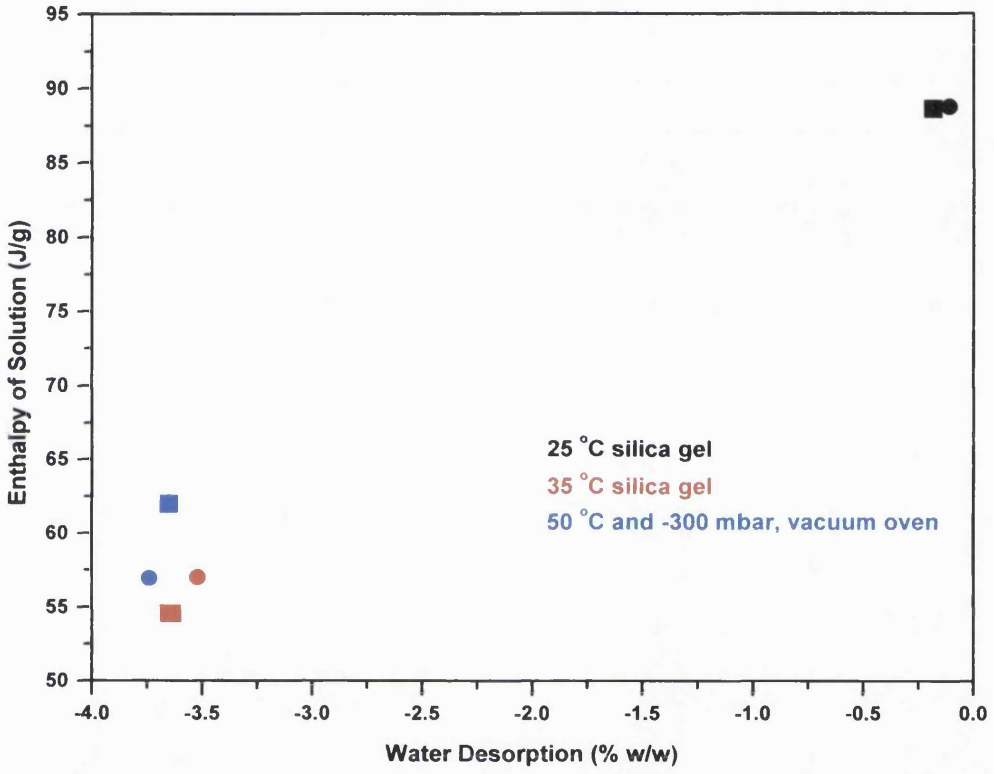

Figure 6.26 *Water desorption against enthalpy of solution for samples of raffinose pentahydrate stored under several 'dry' conditions (Storage times: ■ = 2 days; ● = 4 days).*

Little difference was observed between the mass losses under the two remaining storage conditions – mass losses ranged from –3.5 % w/w (35 °C over silica gel for two days) to –3.7 % w/w (vacuum oven at 50 °C for four days). Despite the reproducibility of degree of dehydration, a variation was recorded in the enthalpies of solution of 62.08 J/g (two days at 50 °C) to 54.49 J/g (four days at 35 °C). From

the enthalpies achieved and the degree of dehydration recorded, it is likely that under these two conditions the removal of hydrate water from the pentahydrate structure was facilitated. It can be calculated that raffinose pentahydrate undergoes a 3.03% w/w loss in losing one complete water molecule to form the tetrahydrate, and 6.06% w/w if dehydration to the trihydrate form occurs. It is possible that under the two higher temperature conditions a tetrahydrate is being formed, in addition to the loss of any residual water. Demertzis et al. (1989) stated that crystalline raffinose adsorbs 0.5 – 0.8 % moisture under relatively high humidity conditions. However it is unlikely that the residual moisture content of the raffinose pentahydrate in this study was of a similar level since the sample stored over silica gel at 25 °C did not show a similar mass loss. It is also possible that hydrate mixes are being formed, although the DVS/NIRS data in Section 6.4.1. suggest that this is not the case for higher hydrates.

6.4.4.3. Comparison of Hydration and Dehydration Data

Examination of the vapour sorption and dehydration data reveals good agreement between the findings. The samples stored at 58% RH for 15 days and 75% RH for 8 days showed mass gains approximately consistent with the formation of trihydrate-equivalent samples (10.7% w/w mass gain), with enthalpies of solution of 19.36 J/g and 27.52 J/g respectively. The dehydrated samples stored at 35 °C and 50 °C showed mass losses approximately consistent with the formation of a tetrahydrate (3.03% w/w mass loss), with corresponding enthalpies of solution of 54.49 – 62.08 J/g respectively. These preliminary results would indicate that enthalpy of solution increases with the formation of higher hydrates.

6.5. CONCLUSIONS

It has been reinforced that reliance on mass loss and the expulsion of plasticising water is not a reliable method of determining the occurrence of crystallisation. NIR has been found capable of detecting changes in raffinose during prolonged exposure to elevated RHs that are not associated with mass changes, indicating that water

movement continues in the sample long after the initial water sorption process. Furthermore the technique is able to follow changes in hydrate level and onset of amorphisation during the drying of crystalline raffinose.

Isothermal microcalorimetry has also indicated that the crystallisation of amorphous raffinose is a prolonged process. Ampoule crystallisation showed that, depending on the amount of water available to the sample, different hydrates or hydrate mixes are formed, which are characterised by different enthalpies of crystallisation (and fusion, determined by DSC). Since amorphous raffinose does not expel plasticising water during crystallisation, there appears to be much greater agreement between the enthalpies of crystallisation and fusion, compared with those figures in relation to lactose. RH perfusion microcalorimetry enabled the correlation of the enthalpy involved in the crystallisation of amorphous raffinose with that measured for dehydration and amorphisation, and showed that the heat flow resulting from both processes is very similar.

It has been seen that raffinose starts to take on the bulk external morphology of the crystalline form before developing the long range order of the crystalline state. It is argued (*e.g.* Kajiwara et al., 1999) that the amorphisation of raffinose during drying is due to the disruption of hydrogen bonding causing the formation of new "sugar-sugar" bonds to replace the "sugar-water" bonds giving rise to disruption and amorphous domains. In this study, not only has crystallisation at high humidity and the conversion of the crystalline to the amorphous form on drying been observed, but also the development of morphology (but not long range molecular order) at low RH.

And finally solution calorimetry has enabled the study of the effects of water sorption and desorption on amorphous and crystalline raffinose, and has again shown that water movement within the sample can result in a restructuring of the internal bonding, resulting in changes in the enthalpy of solution with only very small corresponding mass changes.

CHAPTER SEVEN

CONCLUSIONS AND FUTURE WORK

This thesis set out to develop techniques by which the quantification of amorphous material occurring at less than 10% w/w in the bulk would be possible. In conjunction with this, an investigation of the suitability and applicability of the same techniques to study the amorphous and crystalline behaviour of raffinose at various relative humidities was undertaken.

Using lactose as a model, the quantification of disorder in samples of 0-10% w/w amorphous content was undertaken. The combination technique of Dynamic Vapour Sorption and Near Infrared Spectroscopy (DVS/NIRS) was used to build two independent quantification calibrations simultaneously from the same samples. The environmental control offered by DVS (*i.e.* controlled temperature and relative humidity (RH) conditions) facilitated the gravimetric determination of water vapour sorption and desorption by the predominantly crystalline samples during crystallisation at 75% RH, and these data were correlated with the amount of amorphous material originally contained within the samples. It was found that water sorption provided a quantification accuracy of approximately ± 0.5 mg amorphous content (the absolute quantification limits are determined by the total sample mass), with a lower limit of detection lying at 1 mg amorphous content. Water desorption was found to offer a similar degree of accuracy, again with a lower limit of detection to be found at 1 mg amorphous content. Below this lower limit, neither vapour sorption or desorption could be accurately correlated with amorphous content, perhaps due to interference by the crystalline material present. Since the crystallisation process usually involves both the uptake and expulsion of water, it provides two values with which to determine amorphous content, thus facilitating an internal check for consistency.

The combination DVS/NIRS technique allows the spectroscopic method to maximise upon the environmental control offered, by facilitating the removal of all residual moisture (water being a contaminant of NIR spectra) from the predominantly crystalline samples prior to crystallisation. The NIRS quantification involved establishing a calibration model based upon the mathematically treated

NIR spectra of dry partially (0-10% w/w) amorphous samples. By correlating the amorphous contents of the samples with their absorbance at three wavelengths (selected by the software for their high correlation), a calibration equation was established which was applicable to other samples. It was found that quantification with an accuracy of ± 1% w/w amorphous content was achievable. In addition, NIRS was not found to be limited by a lower limit of detection. There are obvious advantages pertaining to having both techniques operating in combination. Primarily, the accuracy of the NIRS method relies upon the environmental control offered by the DVS. Using both quantification methods simultaneously also offers an immediate confirmation of the results obtained. There is much scope for future work in this field. It is important to note that these methods were developed with binary amorphous/crystalline mixtures, and their applicability to processed samples (where individual particles are composed of amorphous and crystalline regions) remains to be seen. The suitability of these techniques to quantification work in other materials is also yet to be investigated. It may also be possible to use these techniques to gain information about the interactions between binary systems.

Further techniques to quantify amorphous content were sought from calorimetric methods, again using lactose as a model material. Solution Calorimetry was found to show a linear relationship between amorphous content and the enthalpy of solution obtained from dissolving the lactose samples in 100 mL of water at 25 °C. Between 0-10% w/w amorphous content, quantification to ± 1% w/w was achieved. However, is it important to note that the ability of the technique to quantify amorphous content accurately relies upon the difference between the enthalpy of solution of the amorphous and crystalline forms, which in turn differs with each material. If these values are similar for a given material, the quantification accuracy will be compromised.

It was also found that a sample's residual water content can dramatically decrease the enthalpy of solution measured. This is particularly important in hygroscopic samples, and as such this effect was noted in studies on totally and predominantly

amorphous lactose samples. It is thought that this effect is due to the sorbed water reducing the overall wetting response (which is exothermic), thus reducing its contribution to the overall enthalpy of solution measured.

Further work is required to determine the applicability of Solution Calorimetry to quantification work in other materials. It may also prove possible to use the technique to investigate interactions between components in binary or multi-component systems.

Batch Isothermal Microcalorimetry was used to carry out amorphous content quantification at 25 °C and both 53% and 75% RH, by determining the enthalpy of crystallisation relating to the amorphous portion of each sample. It was found that a barrier to quantification with the technique was the difficulty encountered in accurately and reproducibly determining the area under the crystallisation peak, required to calculate the enthalpy of crystallisation. It has been found that the rate at which crystallisation proceeds is easily altered by sample mass, sample geometry and residual moisture content within the sample. This rate can lead to changes in the shape of the crystallisation peak, due often to the commencement of crystallisation before a steady pre-reaction baseline has been established. These changes in the shape of the crystallisation peak have made it difficult to achieve consistent enthalpy determination. Several integration methods were undertaken to determine the area under the crystallisation peak, and the best method applied to the determination of enthalpy of crystallisation for samples of 0-10% w/w amorphous content. Quantification at both RHs was achieved with a level of accuracy of ± 1 % w/w amorphous content.

Isothermal Perfusion Microcalorimetry was also employed to quantify amorphous contents occurring at less that 10% w/w in the bulk. At 25 °C, samples were dried at 0% RH to establish a baseline and subsequently crystallised at 75% RH. Again, different methods for determining the area under the crystallisation peak were studied, and it was found that several integration methods were capable of producing

reproducible enthalpies of crystallisation. Quantification to ± 1% w/w amorphous content was achieved. The main advantage of the RH perfusion unit is the control of RH environment it provides the user. This enables the drying of samples at 0% RH prior to inducing crystallisation, and it also ensures that the experiment commences from a steady baseline. This flexibility could also be manipulated to delay the onset of other reactions, highlighting the applicability of the technique in the study of more complicated systems. Currently, the main disadvantage of Isothermal Microcalorimetry is seen to lie in the fact that no chemical data is provided. As such, the crystallisation process itself is not fully understood, and future work is required in order to bring about an understanding of the many events which comprise the crystallisation process and contribute to the features observed in the crystallisation response in the microcalorimeter.

Each quantification method outlined has its own advantages and disadvantages, and it would be impractical to consider one technique as the most appropriate for every circumstance. It is possible that NIRS would achieve insufficient resolution for the quantification of the amorphous contents of some materials. And as already mentioned, the enthalpies of solution of the amorphous and crystalline forms of certain materials may be too similar to construct a reliable calibration. Furthermore, some materials do not undergo spontaneous crystallisation at elevated RH conditions, or in the presence of organic vapours, thus rendering them unsuitable for analysis via enthalpy of crystallisation determinations. In such cases DVS would also be an inappropriate method unless a correlation between mass absorbed and amorphous content existed. Therefore, in selecting a method for the quantification of amorphous content, it would be advisable to adopt the most suitable method for the circumstances, depending upon the relevant criteria.

Each of the techniques used in determining the quantification of amorphous lactose was found capable of differentiating between samples of only very slightly different crystallinity. As such, it was expected that each technique would be useful in examining the behaviour of other carbohydrates. Raffinose was selected as a

suitable candidate to challenge the applicability of these techniques since it is known to exhibit unusual characteristics, such as its existence as a crystalline pentahydrate and its ability to be rendered amorphous by dehydration. Amorphous raffinose was found to deviate from the anticipated gravimetric response for the crystallisation of carbohydrates, since it was observed to undergo crystallisation without the expulsion of water. This was noted as an absence of mass loss upon crystallisation. Confirmation of the crystallisation event was obtained from NIRS. The lack of expulsion of water by raffinose was related to the fact that at 75% RH and 25 °C it equilibrated to a crystal form which had taken up less than the quantity of water required to form a pentahydrate. Subsequently there was no surplus moisture present to be expelled from the material. Additional work is required to establish why raffinose is prevented from forming a pentahydrate under those conditions.

The combined DVS/NIRS technique facilitated the recording of NIRS spectra during the crystallisation process itself. These spectra revealed that, subsequent to the crystallisation event, changes were occurring in the sample in the absence of any simultaneous mass changes. This would imply that water movement within the sample continues after crystallisation in order for the material to achieve its equilibrium state under the given conditions. NIRS was also used to follow the dehydration of the crystalline pentahydrate, revealing that amorphisation did not commence until the sample had reached a hydrate water content consistent with the presence of a dihydrate form. Another area requiring future attention is to ascertain whether raffinose forms hydrate mixes upon crystallisation or dehydration (*e.g.* the presence of pentahydrate and trihydrate) or simply equilibrates to one crystal form.

Using Batch Isothermal Microcalorimetry and Differential Scanning Calorimetry (DSC) it was found that the enthalpy of crystallisation of raffinose showed a good correlation with the enthalpy of fusion determined by subsequently melting the same sample. For previously investigated materials, *e.g.* lactose, such a correlation has not been achieved due to the endothermic expulsion of water from the sample upon crystallisation reducing the overall enthalpy measured. However, since amorphous

raffinose has been shown to crystallise without the expulsion of water this problem was overcome. It was also noted that, as would be expected from the DVS data, samples crystallised at 75% RH and 25 °C in the microcalorimeter did not form a pentahydrate. The enthalpies of fusion of such samples were less than those obtained for the raffinose pentahydrate standard. Furthermore, the microcalorimetry data revealed that the crystallisation of raffinose is a prolonged event. Isothermal Perfusion Microcalorimetry was employed to monitor the crystallisation of amorphous raffinose at 90% RH and 25 °C, and the sample's subsequent dehydration at 0% RH and 25 °C. It was shown that the samples required approximately 4 days to crystallise under those conditions, and 8 days to fully dehydrate and become amorphous.

Solution Calorimetry facilitated the study of water sorption and desorption by amorphous and crystalline raffinose, further supporting the DVS/NIRS data by showing that very small changes in mass resulted in large changes in the enthalpy of solution measured.

The applicability of these techniques to study the physical properties of carbohydrates has been demonstrated. Further work is required in order to determine the exact mechanisms by which raffinose undergoes crystallisation, hydrate formation, dehydration and amorphisation. Raffinose itself has been shown to be an excellent model with which to test the applicability of such techniques, since its behaviour is so complex. Since raffinose has been shown capable of conferring stability to macromolecules there is scope for extending the use of such techniques to examine the nature of the carbohydrate-macromolecule interaction, thus elucidating the mechanism of stabilisation of raffinose and other such sugars.

REFERENCES

Ahlneck, C., 1993. Chemical and physical stability of drugs in the solid state. In Industrial Aspects of Pharmacy, Sandell, E. (ed.), Swedish Pharmaceutical Press.

Ahlneck, C. and Alderborn, G., 1989a. Moisture sorption and tabletting. I. Effect on volume reduction properties and tablet strength for some crystalline materials. Int. J. Pharm. 54, 131-141.

Ahlneck, C. and Alderborn, G., 1989b. Moisture sorption and tabletting. II. The effect on tensile strength and air permeability of the relative humidity during storage of tablets of three crystalline materials. Int. J. Pharm. 56, 143-150.

Ahlneck, C. and Zografi, G., 1990. The molecular basis of moisture effects on the physical and chemical stability of drugs in the solid-state. Int. J. Pharm. 62, 87-95.

Ahmed, H., Buckton, G. and Rawlins, D.A., 1996. The use of isothermal microcalorimetry in the study of small degrees of amorphous content of a hydrophobic powder. Int. J. Pharm. 130, 195-201.

Aldous, B.J., Auffret, A.D. and Franks, F., 1995. The crystallisation of hydrates from amorphous carbohydrates. Cryo-Letters 16, 181-186.

Aldridge, P.K., Evans, C.L., Ward, II, H.W., Colgan, S.T., Boyer, N. and Gemperline, P.J., 1996. Near-IR detection of polymorphism and process-related substances. Anal. Chem. 68, 997-1002.

Angberg, M., Nyström, C. and Castensson, S., 1991. Evaluation of heat-conduction microcalorimetry in pharmaceutical stability studies. III. Crystallographic changes due to water vapour uptake in anhydrous lactose powder. Int. J. Pharm. 73, 209-220.

Angberg, M., Nyström, C. and Castensson, S., 1992. Evaluation of heat-conduction microcalorimetry in pharmaceutical stability studies. V. A new approach for continuous measurements in abundant water vapour. Int. J. Pharm. 81, 153-167.

Angberg, M., Nyström, C. and Castensson, S., 1992a. Evaluation of heat-conduction microcalorimetry in pharmaceutical stability studies. VI. Continuous monitoring of the interaction of water vapour with powders and powder mixtures at various relative humidities. Int. J. Pharm. 83, 11-23.

Aso, Y., Yoshioka, S., Otsuka, T. and Kojima, S., 1995. The physical stability of amorphous nifefipine determined by isothermal microcalorimetry. Chem. Pharm. Bull. 43 (2), 300-303.

Aucott, L.S., Garthwaite, P.H. and Buckland, S.T., 1988. Transformations to reduce the effect of particle size in near-infrared spectra. Analyst 113, 1849-1854.

Bakri, A., Janssen, L.H.M. and Wilting , J., 1988. Flow microcalorimetry applied to the study of chemical stability of organic compounds. J. Therm. Anal. 33, 1193-1199.

Bell, J.H., Hartley, P.S. and Cox, J.S.G., 1971. Dry Powder Aerosols I: A new powder inhalation device. Pharm. Sci. 60, 1559 – 1564.

Berlin, E., Kliman, P.G., Anderson, B.A. and Pallansch, M.J., 1971. Calorimetric measurement of the heat of desorption of water vapor from amorphous and crystalline lactose. Thermochim. Acta 2, 143-152.

Bhatt, B. and Rubenstein, M.H., 1983. The use of a flow microcalorimeter to characterise powder surfaces. Drug Dev. Ind.Pharm. 9, 215-222.

Black, D.B. and Lovering, E.G., 1977. Estimation of the degree of crystallinity in digoxin by X-ray and infrared methods. J. Pharm. Pharmacol. 29, 684-687.

Briggner, L.-E., Buckton, G., Bystrom, K. and Darcy, P., 1994. The use of isothermal microcalorimetry in the study of changes in crystallinity induced during the processing of powders. Int. J. Pharm. 105, 125-135.

Buckton, G., 1995. Interfacial phenomena in drug delivery and targeting. Harwood Academic, Amsterdam.

Buckton G. and Beezer, A.E., 1991. The applications of microcalorimetry in the field of physical pharmacy. Int. J. Pharm. 72, 181-191.

Buckton, G. and Darcy, P., 1995. The use of gravimetric studies to assess the degree of crystallinity of predominantly crystalline powders. Int. J. Pharm. 123, 265-271.

Buckton, G. and Darcy, P., 1995a. The influence of additives on the recrystallisation of amorphous spray dried lactose. Int. J. Pharm. 121, 81-87.

Buckton, G. and Darcy, P., 1996. Water mobility in amorphous lactose below and close to the glass transition temperature. Int. J. Pharm. 136, 141-146.

Buckton, G. and Darcy, P., 1999. Assessment of disorder in crystalline powders – a review of analytical techniques and their application. Int. J. Pharm. 179, 141-158.

Buckton, G., Darcy, P. and Mackellar, A.J., 1995. The use of isothermal microcalorimetry in the study of small degrees of amorphous content of powders. Int. J. Pharm. 117, 253-256.

Buckton, G., Choularton, A., Beezer, A.E. and Chatham, S.M., 1988. The effect of the comminution technique on the surface energy of a powder. Int. J. Pharm. 47, 121-128.

Buckton, G., Darcy, P., Greenleaf, D. and Holbrook, P., 1995. The use of isothermal microcalorimetry in the study of changes in the crystallinity of spray dried salbutamol sulphate. Int. J. Pharm. 116, 113-118.

Buckton, G., Yonemochi, E., Hammond, J. and Moffat, A.C., 1998. The use of near infrared spectroscopy to detect changes in the form of amorphous and crystalline lactose. Int. J. Pharm. 168, 231-241.

Buice, R.G., Gold, T.B., Lodder, R.A. and Digenis, G.A., 1995. Determination of moisture in intact gelatin capsules by near-infrared spectroscopy. Pharm. Res. 12, 161-163.

Burt, H.M. and Mitchell, A.G., 1981. Crystal defects and dissolution. Int. J. Pharm. 9, 137-152.

Byrn, S., 1982. Solid state chemistry of drugs. Academic Press, NewYork, pp 7-10.

Byström, K., 1990. Microcalorimetric testing of physical stability of drugs in the solid state. Thermometric Application Note 22004, Thermometric AB, Järfälla, Sweden.

Carstensen, J.T., 1993. Pharmaceutical principles of solid dosage forms. Technomic Publishing Co. INC.

Chidavaenzi, O.C., Buckton, G., Koosha, F. and Pathak, R., 1997. The use of thermal techniques to assess the impact of feed concentration on the amorphous content and polymorphic forms present in spray dried lactose. Int. J. Pharm. 159, 67-74.

Chiou, W.L. and Kyle, L.E. 1979. Differential thermal, solubility and ageing studies on various sources of digoxin and digitoxin powder: Biopharmaceutical implications. J. Pharm. Sci. 68, 1224-1229.

Clegg, J.S., 1986. The Physical Properties and Metabolic Status of *Artemia* Cysts at Low Water Contents: The 'Water Replacement Hypothesis', in Membranes, Metabolism and Dry Organisms. A. Carl Leopold, ed. (Cornell University Press, Ithaca, NY), pp 169-187.

Corrigan, O.I., 1995. Thermal analysis of spray dried products. Thermochim. Acta. 248, 245-258.

Costantino, H.R., Curley, J.G., Wu, S. and Hsu, C.C., 1998. Water sorption behaviour of lyophilised protein-sugar systems and implications for solid-state interactions. Int. J. Pharm. 166, 211-221.

Craig, D.Q.M. and Newton, J.M., 1991. Characterisation of polyethylene glycol solid dispersions using differential scanning calorimetry and solution calorimetry. Int. J. Pharm. 76, 17-24.

Craig, D.Q.M. and Newton, J.M., 1991a. Characterisation of polyethylene glycols using solution calorimetry. Int. J. Pharm. 74, 43-48.

CRC Handbook of Chemistry and Physics 80th Edition, 1999, section 6-3. CRC Press, London.

Darcy, P. and Buckton, G., 1997. The influence of heating/drying on the crystallisation of amorphous lactose after structural collapse. Int. J. Pharm. 158, 157-164.

Darcy, P. and Buckton, P., 1998. Quantitative assessments of powder crystallinity: Estimates of heat and mass transfer to interpret isothermal microcalorimetry data. Thermochim. Acta 316, 29-36.

Demertzis, P.G., Riganakos, K.A. and Kontominas, M.G., 1989. Water sorption isotherms of crystalline raffinose by inverse gas chromatography. Int. J. Food Sci. Tech. 24, 629-636.

Ding, S.P., Fan, J., Green, J.L. Lu, Q., Snachez, E. and Angell, C.A., 1996. Vitrification of trehalose by water loss from its crystalline dihydrate. J. Thermal Anal. 47, 1391-1405.

Dreassi, E., Ceramelli, G., Corti, P., Lonardi, S. and Perruccio, P.L., 1995. Near-infrared reflectance spectroscopy in the determination of the physical state of primary materials in pharmaceutical production. Analyst 120, 1005-1008.

Duncan-Hewitt, W.C. and Grant, D.J.W., 1986. True density and thermal expansivity of pharmaceutical solids: Comparison of methods and assessment of crystallinity. Int. J. Pharm. 28, 75-84.

Ediger, M.D., Angell, C.A. and Nagel, S.R., 1996. Supercooled liquids and glasses. J. Phys. Chem. 100, 13200-13212.

Elamin, A., Ahlneck, C., Alcerborn, G. and Nystrom, C., 1994. Increased metastable solubility of milled griseofulvin depending on the formation of a disordered surface structure. Int. J. Pharm. 111, 159-170.

Ferry, J.D., 1980. Viscoelastic properties of polymers, 3rd edition, New York, John Wiley and Sons.

Fiebich, K., Mutz, M., 1999. Evaluation of calorimetric and gravimetric methods to quantify the amorphous content of desferal. J. Therm. Anal. 57, 75-85.

Flink, J.M., 1975. The retention of volatile components during freeze-drying: a structurally based mechanism. In Freeze drying and Advanced Food Technology. Goldblith, A.S., Rey, L. and Rothmayr, W.W. (eds.), pp 309-329.

Flink, J.M., 1983. Physical properties of foods. Peleg, M. and Bagley, E.B. (eds.), AVI: Westport, pp 473-521.

Florence, A.T. and Salole, E., 1976. Changes in crystallinity and solubility on comminution of digoxin and observations on spironolactone and oestradiol. J. Pharm. Pharmac. 28, 637-642.

Forbes, R.T., Davis, K.G., Hindle, M., Clarke, J.G. and Maas, J., 1998. Water vapour sorption studies on the physical stability of a series of spray-dried protein/sugar powders for inhalation. J. Pharm. Sci. 87, 1316-1321.

Ford, J.L. and Timmins, P., 1989. Pharmaceutical Thermal Analysis: Techniques and Applications. John Wiley & Sons, New York.

Forni, F., Coppi, G., Iannuccelli, V., Vandelli, M.A. and Cameroni, R., 1988. The grinding of the polymorphic forms of chloramphenicol stearic ester in the presence of colloidal silica. Acta Pharm. Suec. 25, 173-180.

Franks, F., 1982. Water – A Comprehensive Treatise, vol 7, Plenum, New York, pp 215-338.

Franks, F. and Grigera, J.R., 1990. Solution properties of low molecular weight polyhydroxy compounds. In Water Science Reviews (ed Franks, F.), Cambridge, Cambridge University Press, Volume 5, The Molecules of Life 187-289.

Franks, F., Hatley, R.H.M. and Mathias, S.F., 1991. Materials science and the production of shelf-stable biologicals. Biopharm. Technol. Bus. 4 (9) 24-34.

Gao, D. and Rytting, J.H., 1997. Use of solution calorimetry to determine the extent of crystallinity of drugs and excipients. Int. J. Pharm. 151, 183-192.

Gimet, R. and Luong, A.T., 1987. Quantitative determination of polymorphic forms in a formulation matrix using the near-infrared reflectance analysis technique. J. Pharm. Biomed. Anal. 5, 205-211.

Gordon, M. and Taylor, J.S., 1952. Ideal co-polymers and the second-order transitions of synthetic rubbers. I. Non-crystalline co-polymers. J. Appl. Chem. 2, 493-500.

Grant, D.J.W. and York,P. 1986. A disruption index for quantifying the solid state disorder induced by additives or impurities. II. Evaluation from heat of solution. Int. J. Pharm. 28, 103-112.

Green, J.L. and Angell, C.A., 1989. Phase relations and vitrification in saccharide-water solutions and the trehalose anomaly. J. Phys. Chem. 93, 2880-2882.

Hailey, P.A., Doherty, P., Tapsell, P., Oliver, T. and Aldridge, P.K., 1996. Automated system for the on-line monitoring of powder blending processes using near-infrared spectroscopy. Part 1. System development and control. J. Pharm. Biomed. Anal. 14, 551-559.

Hanafusa, N., 1985. The Introduction of Hydration Water and Protein with Cryoprotectants, in Fundamentals and Applications of Freeze-Drying to Biological Materials, Drugs and Foodstuffs (International Institute of Refrigeration, Commission C1 Meeting, Tokyo), pp 1-6.

Hancock, B.C. and Zografi, G., 1994. The relationship between the glass transition temperature and the water content of amorphous pharmaceutical solids. Pharm. Res. 11, 471-477.

Hancock, B.C. and Zografi, G., 1997. Characteristics and significance of the amorphous state in pharmaceutics systems. J. Pharm. Sci. 86, 1-12.

Hancock , B.C., Shamblin, S.L. and Zografi, G., 1995. Molecular mobility of amorphous pharmaceutical solids below their glass transition temperatures. Pharm. Res. 12, 799-805.

Hasegawa, J., Hanano, M. and Awazu, S., 1975. Decomposition of acetylsalicyclic acid and its derivatives in solid state. Chem. Pharm. Bull. 23, 86-97.

Haward, R.N., 1973. The nature of polymer glasses, their packing density and mechanical behaviour. In The Physics of Glassy Polymers (ed Haward, R.N.), London, Applied Science, 1-51.

Hersey, J.A. and Krycer, I., 1980. Biopharmaceutical implications of technological change. Int. J. Pharm. Technol. & Prod. Manuf. 1, 18-21.

Hoffman, J.D., 1958. Thermodynamic driving force in nucleation and growth processes. J. Chem. Phys. 29, 1192-1193.

Hollenbeck, R.G., Peck, G.E., Kildsig, D.O., 1978. Application of immersional calorimetry to investigation of solid-liquid interactions: Microcrystalline cellulose-water system. J. Pharm. Sci., 67, 1599-1605.

Hüttenrauch, R., 1983. Modification of starting materials to improve tabletting properties. Pharm. Ind. 45, 435-440.

Hüttenrauch, R. and Keiner, R., 1979. Producing lattice defects by drying processes. Int. J. Pharm. 2, 59-60.

Hüttenrauch, R., Fricke, S. and Sielke, P., 1985. Mechanical activation of pharmaceutical systems. Pharm. Res. 2, 302-306.

Iglesias, H.A. and Chirife, J., 1978. Delayed crystallisation of amorphous sucrose in humidified freeze dried model systems. J. Food Technol. 13, 137-144.

Iglesias, H.A., Schebor, C., Buera, M.P., Chirife, J., 2000. Sorption isotherm and calorimetric behaviour of amorphous/crystalline raffinose-water systems. J. Food Sci. 65, 646-650.

Jakobsen, D.F., Frokjaer, S., Larsen, C., Niemann, H. and Buur, A., 1997. Application of isothermal microcalorimetry in preformulation. I. Hygroscopicity of drug substances. Int. J. Pharm. 156, 67-77.

Jeffrey, G., Huang, D.-B., 1990. The hydrogen-bonding in the crystal structure of raffinose. Carbohyd. Res. 206, 173-182.

Kajiwara, K. and Franks, F., 1998. Crystalline and amorphous phases in the binary system water-raffinose. J. Chem. Soc. Faraday Trans., 93, 1779-1783.

Kajiwara. K., Franks, F., Echlin, P., Greer, A.L., 1999. Structural and dynamic properties of crystalline and amorphous phases in raffinose-water mixtures. Pharm. Res. 16, 1441-1448.

Kamat, M.S., Lodder R.A. and DeLuca, P.P., 1989. Near-infrared spectroscopic determination of residual moisture in lyophilised sucrose through intact glass vials. Pharm. Res. 6, 961-965.

Khankari, R., Chen, L.N., Grant, D.J.W., 1998. Physical characterisation of nedocromil sodium hydrates. J. Pharm. Sci. 87, 1052-1061.

Kirsch, J.D. and Drennen, J.K., 1996. Near-infrared spectroscopic monitoring of the film coating process. Pharm. Res. 13, 234-237.

Konno, T., 1990. Physical and chemical changes of medicinals in mixtures with adsorbents in the solid state. IV. Study on reduced-pressure mixing for practical use of amorphous mixtures of flufenamic acid. Chem. Pharm. Bull. 38 (7), 2003-2007.

Kontny, M.J., Grandolfi, G.P. and Zografi, G., 1987. Water vapour sorption of water-soluble substances: Studies of crystalline solids below their critical relative humidities. Pharm. Res. 4, 104-111.

Kreft, K., Kozamernik, B. and Urleb, U., 1999. Qualitative determination of polyvinylpyrrolidone type by near-infrared spectrometry. Int. J. Pharm. 177, 1-6.

Lane, R.A. and Buckton, G., 2000. The novel combination of dynamic vapour sorption gravimetric analysis ans near infra-red spectroscopy as a hyphenated technique. Int J. Pharm. 207, 49-56.

Lehto, V.P., Laine, E., 1998. Assessment of physical stability of different forms of cefadroxil at high humidities. Int. J. Pharm. 163, 49-62.

Lerk, C.F., 1983. Physico-pharmaceutical properties of lactose. Proceedings of the 22nd International Colloquium on Industrial Pharmacy, Ghent, pp. 59-89.

Lerk, C.F., Adreae, A.C. and de Boer, A.H., 1984. Transitions of lactoses by mechanical and thermal treatment. J.Pharm. Sci. 73, 857-859.

Leung, S.S. and Schultz, D.W., 1996. Kinetics of crystallinity in micronised albuterol sulfate powders. Pharm. Res. (suppl) 13, S-345.

Levine, H. and Slade, L., 1986. A polymer physico-chemical approach to the study of commercial starch hydrolysis products (SHPs). Carbohydrate Polymers 6, 213-244.

Levine, H. and Slade, L., 1989. Response to a letter by Simatos, Blond and Le Meste on the relation between glass transition and stability of a frozen product. Cryo-Letters 10, 347-370.

Lin., J. and Brown, C.W., 1992. Near-IR spectroscopic determination of NaCl in aqueous solution. Appl. Spectrosc. 46, 1809-1815.

Lonardi, S., Viviani, R., Mosconi, L., Bernuzzi, M., Corti, P., Dreassi, E., Murratzu, C. and Corbini, G., 1989. Drug analysis by near-infra-red reflectance spectroscopy. Determination of the active ingredient and water content in antibiotic powders. J. Pharm. Biomed. Anal. 7, 303-308.

Luyet, B., 1960. On various phase transitions occurring in aqueous solutions at low temperatures. Annals of the New York Academy of Sciences, 85, 549-569.

Makower, B. and Dye, W.B., 1956. Equilibrium moisture content and crystallisation of amorphous sucrose and glucose. J. Agric. Food Chem. 4, 72-77.

Masters, K., 1976. Spray drying. An Introduction to Principles, Operational practice and Applications. John Wiley & Sons, New York.

The Merck Index, Twelfth Edition. Merck Research Labs, Division of Merck & Co. Inc., Whitehouse Station, New Jersey. Susan Budavari, ed., pp 1394 – 1395.

Moffat, A.C., Trafford, A.D., Jee, R.D. and Graham, P., 2000. Meeting the International Conference on Harmonisation's guidelines on on validatgion of analytical procedures: Quantification as exemplified by a near-infrared reflectance assay of paracetamol in intact tablets. Analyst 125, 1341-1351.

Mosharraf, M. and Nystrom, C., 1996. The importance of disordered structure in determination of solubility and dissolution rate of sparingly soluble drugs. Pharm. Res. (suppl) 13, S-352.

Nakai, Y., Fukuoka, E., Nakagima, S. and Hasegawa, J., 1977. Crystallininty and physical characteristics of microcrystalline cellulose. Chem. Pharm. Bull. 25, 96-101.

Newton, J.M., 1966. Spray drying and its Applications to Pharmaceuticals. Manuf. Chem. Aerosol News 33-36, (April 1966).

Ng, W.-L., 1975. Thermal decomposition in the solid state. Aust. J. Chem. 28, 1169-1178.

Norris, T., Aldridge, P.K. and Sekulic, S.S., 1997. Near-infrared spectroscopy. Analyst 122, 549-552.

Nyqvist, H. 1983. Saturated salt solutions for maintaining specified relative humidities. Int. J. Pharm. Technol. Prod. Mfr. 4, 47-48.

Oksanen, C.A. and Zografi, G., 1990. The relationship between the glass transition temperature and water vapour absorption by poly(vinylpyrrolidone). Pharm. Res. 7, 654-657.

Olano, A., Corzo, N. and Martinez-Castro, I., 1983. Studies on β-lactose crystallisation. Milchwissenscaft 38, 471-474.

Phipps, M.A. amd Mackin, L.A., 2000. Application of isothermal microcalorimetry in solid state drug development. Phamraceutical Science and Technology Today, 3, 9-17.

Pikal, M.J., Lukes, A.L., Lang, J.E. and Gaines, K., 1978. Quantitative crystallinity determinations for β-lactam antibiotics by solution calorimetry: correlations with stability. J. Pharm. Sci. 67, 767-773.

Pudipeddi, M., Sokoloski, T.D., Duddu, S.P. and Carstensen, J.T., 1996. Quantitative characterisation of adsorption isotherms using isothermal microcalorimetry. J. Pharm. Sci. 85, 381-386.

Roberts, C.J. and Franks, F., 1996. Crystalline and amorphous phases in the binary system water-β,β-trehalose. J. Chem. Soc. Faraday Trans. 92, 1337-1343.

Roos, Y., 1993. Melting and glass transitions of low molecular weight carbohydrates. Carbohydrate Res. 238, 39-48.

Saleki-Gerhardt, A. and Zografi, G., 1994. Non-isothermal and isothermal crystallisation of sucrose from the amorphous state. Pharm. Res. 11, 1166-1173.

Saleki-Gerhardt, A., Ahlneck, C. and Zografi, G., 1994. Assessment of degree of disorder in crystalline solids. Int. J. Pharm. 101, 237-247.

Saleki-Gerhardt, A., Stowell, J.G., Byrn, S.R. and Zografi, G., 1995. Hydration and dehydration of crystalline and amorphous forms of raffinose. J.Pharm. Sci. 84, 318-323.

Salvetti, G., Tognoni, E., Tombari, E. and Johari, G.P., 1996. Excess energy of polymorphic states over the crystal state by heat of solution measurement. Thermochim. Acta. 285, 243-252.

Schmitt, E.A., Law, D. and Zhang, G.G.Z., 1998. Nucleation and crystallisatio kinetics of hydrated amorphous lactose above the glass transition temperature. J. Pharm. Sci. 88, 291-296.

Sebhatu, T., Angberg, M. and Ahlneck, C., 1994. Assessment of the degree of disorder in crystalline solids by isothermal microcalorimetry. Int. J. Pharm. 104, 135-144.

Sebhatu, T., Elamin, A.A. and Ahlneck, C., 1994a. Effect of moisture sorption on tabletting characteristics of spray dried (15% amorphous) lactose. Pharm. Res. 11, 1233-1238.

Sebhatu, T., Ahlneck, A. and Alderborn, G., 1997. The effect of moisture content on the compression and bond-formation properties of amorphous lactose particles. Int. J. Pharm. 146, 101-114.

Seyer, J.J., Lunar, P.E., Kemper, M.S., Majuru, S., 1997. Amorphous content determination in semi-crystalline mixtures using diffuse reflectance near-infrared spectroscopy. Pharm. Res. 14, 445-.

Shalaev, E.Y., 1991. Ph.D Thesis, Institute of Molecular Biology, Koltsovo.

Sheridan, P.L., Buckton, G. and Storey, D.E., 1995. Development of a flow microcalorimetry method for the assessment of surface properties of powders. Pharm. Res. 12, 1025-1030.

Sinsheimer, J.E. and Poswalk, N.M., 1968. Pharmaceutical applications of the near infrared determination of water. J. Pharm. Sci. 57, 2007-2010.

Slade, L. and Levine, H., 1988. Non-equilibrium behaviour of small carbohydrate-water systems. Pure Appl. Chem. 60, 1841-1864.

Skrabanja, A.T.P., de Meere, A.L.J., de Ruiter, R.A., van den Oetalaar, P.J.M., 1994. Lyophilization of biotechnology products. J. Pharm. Sci. Technol. 48, 311-317.

Sokoloski, T.D. and Ostovic, J.R., 1997. Characerisation of the physical and chemical interaction of a freeze-dried peptide with water using isothermal microcalorimetry. J. Pharm. Pharmacol. 49, 32.

Stubberud, L. and Forbes, R.T., 1998. The use of gravimetry for the study of the effect of additives on the moisture-induced recrystallisation of lactose. Int. J. Pharm. 163, 145-156.

Sugisaki M., Suga, H. and Seki, S., 1968. Calorimetric study of the glassy state. IV. Heat capacities of glass water and cubic ice. Bull. Chem. Soc. Jpn. 41, 2591-2599.

Taylor, L.S. and Zografi, G., 1998. The quantitative analysis of crystallinity using FT-Raman spectroscopy. Pharm. Res. 15, 755-761.

Thiel, P.A. and Madey, T.E., 1987. The interaction of water with solid surfaces: fundamental aspects. Surface Sci. Rep. 7, 211-385.

Thompson, K.C., Draper, J.P., Kaufman, M.J., Brenner, G.S., 1994. Characterisation of the crystallinity of drugs: B02669, a case study. Pharm. Res. 11, 1362-1365.

Tong, W.Q., Lach, J.L., Chin, T. and Guillory, J.K., 1991. Structural effects on the binding of amine drugs with diphenyimethyl functionality to cyclodextrine. I. A microcalorimetric study. Pharm. Res. 8, 951-957.

Tzannis, S.T. and Prestrelski, S.J., 1998. Moisture effects of protein-excipient interactions in spray-dried powders. Nature of destabilising effects of sucrose. J. Pharm. Sci. 88, 360-370.

Van Scoik, K.G. and Carstensen, J.T., 1990. Nucleation phenomena in amorphous systems. Int. J. Pharm. 58, 185-196.

Wade, A., 1980. Pharmaceutical Handbook, Pharmaceutical Press, London, pp.592. 19th Edition.

Wadso, I., 1997. Trends in isothermal microcalorimetry. Chem. Soc. Rev. 79-86.

Wang, Y., Veltkamp, D.J. and Kowalski, B.R., 1991. Multivariate instrument standarization. Anal. Chem. 63, 2750-2756.

Ward, G.H. and Schultz, R.K., 1995. Process-induced crystallinity changes in Albuterol Sulfate and its effect on powder physical stability. Pharm. Res. 12, 773-779.

White, G.W. and Cakebread, S.H., 1966. The glassy state in certain sugar-containing food products. J. Fd. Technol. 1, 73-82.

Williams, M.L., Landel, R.F. and Ferry, J.D., 1955. Temperature dependence of relaxation mechanisms in amorphous polymers and other glass-forming liquids. J. Am. Chem. Soc. 77, 3701-3707.

Wunderlich, B., 1981. The basis of thermal analysis. In Thermal Characterization of Polymeric Materials (ed Turi, E.A.), Orlando, Academic Press, 91-234.

York, P. and Grant, D.J.W., 1985. A disruption index for quantifying the solid state disorder induced by additives or impurities. I. Definition and evaluation from heat of fusion. Int. J. Pharm. 25, 57-72.

Yoshioka, M., Hancock, B.C. and Zografi, G., 1994. Crystallisation of indomethacin for the amorphous state below and above its glass transition temperature. J. Pharm. Sci. 83, 1700-1705.

Zografi, G. and Hancock, B.C., 1993. Topics in pharmaceutical sciences Crommelin, D.J.A., Midha, K.K. and Nagai, T., (eds.), Medpharm Scientific Publishers: Stuggart, (1993) pp 405-419.

APPENDIX ONE

X-RAY POWDER DIFFRACTOGRAPHS

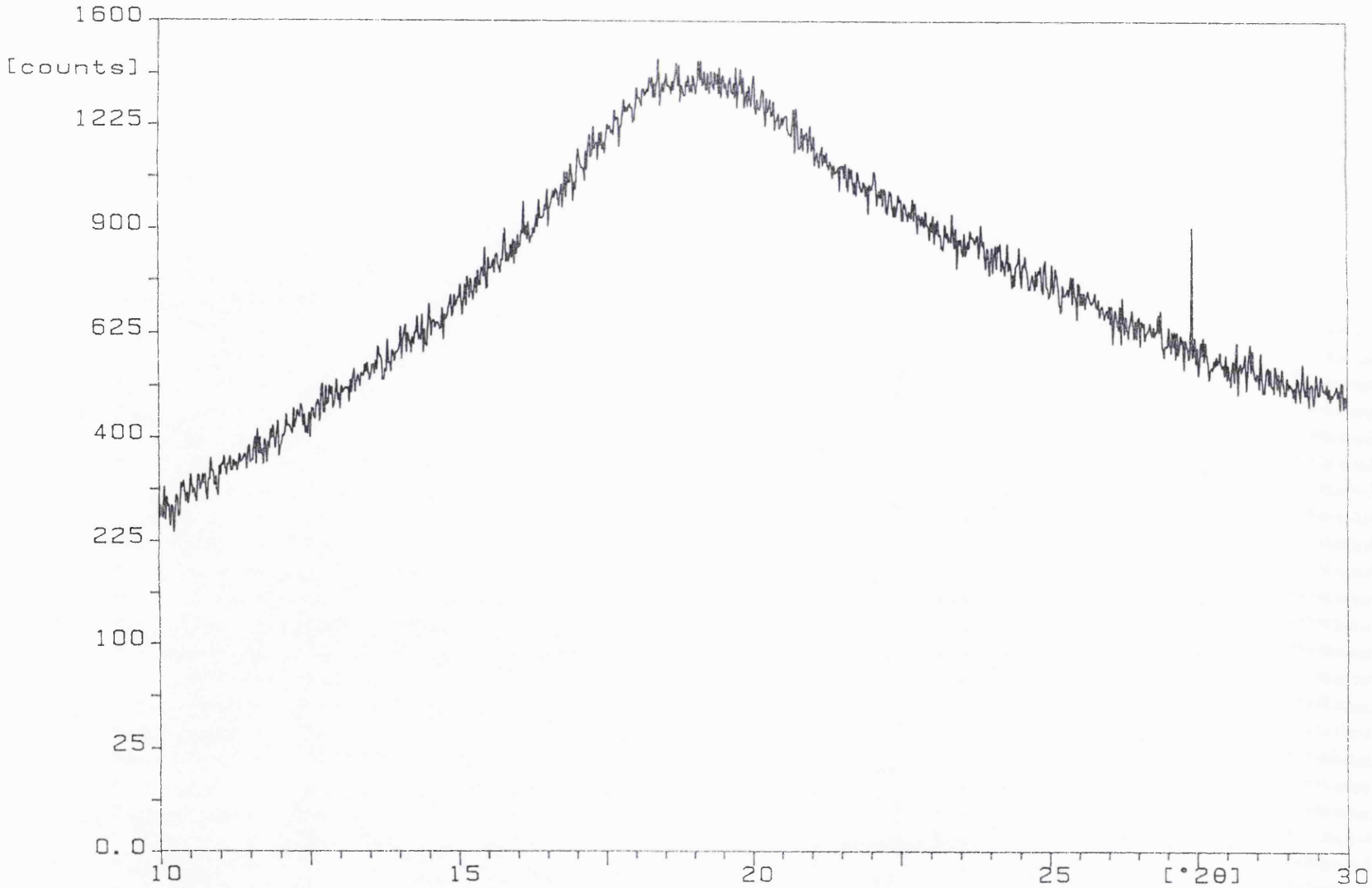

Appendix 1a *X-Ray Powder Diffractograph of 100% amorphous spray-dried lactose.*

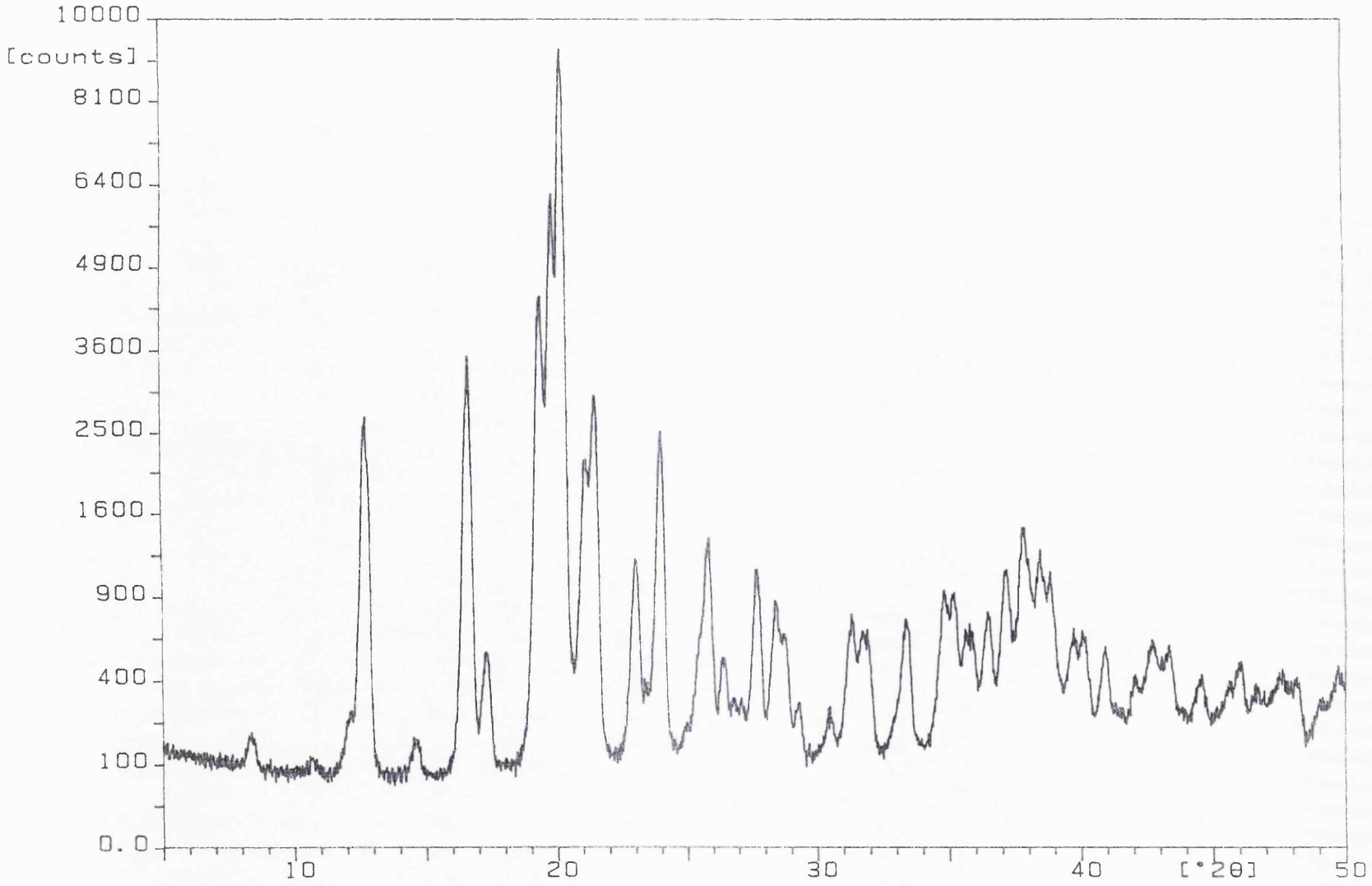

Appendix 1b *X-Ray Powder Diffractograph of 100% crystalline α-lactose monohydrate.*

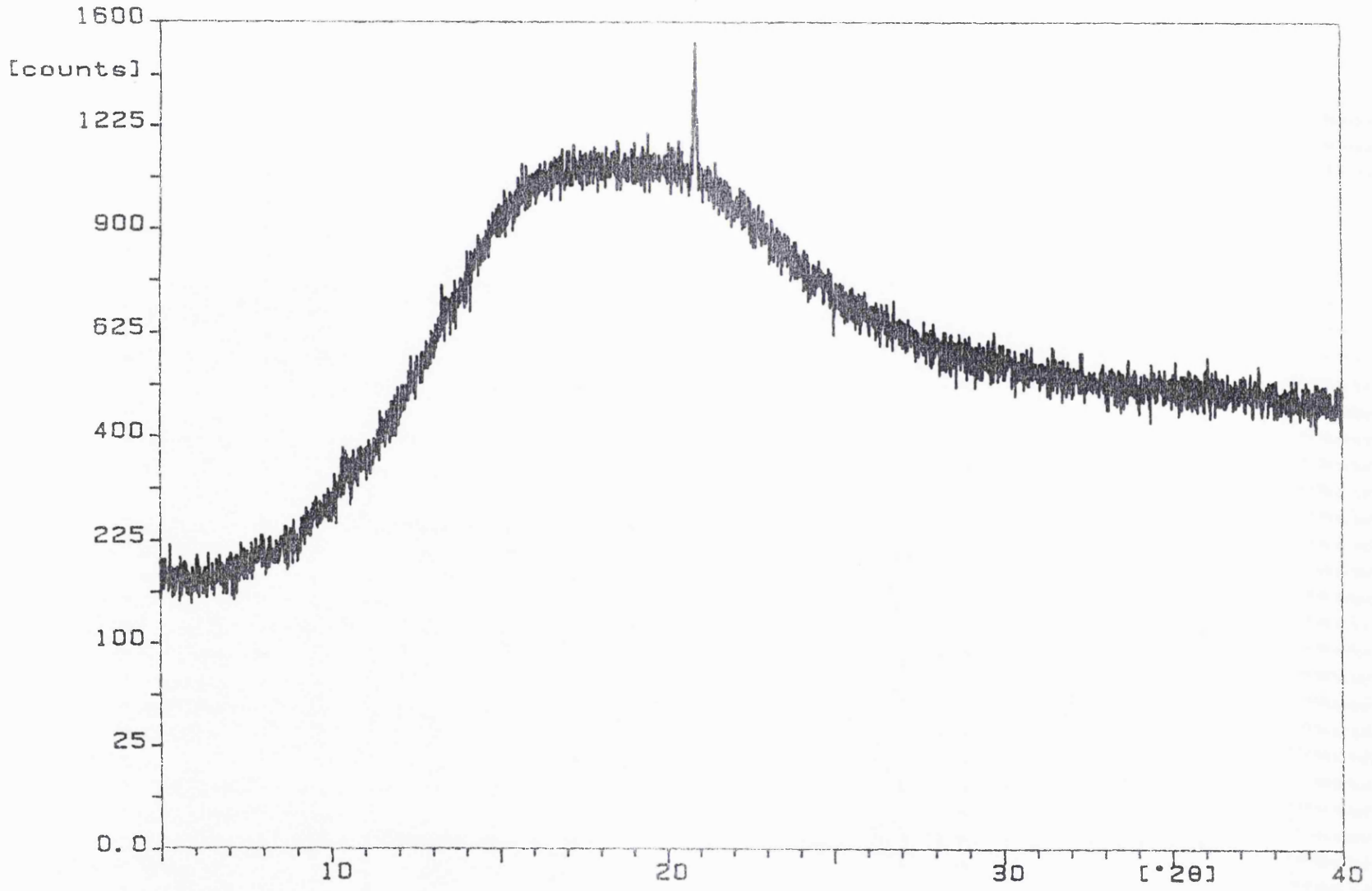

Appendix 1c *X-Ray Powder Diffractograph of 100% amorphous spray-dried raffinose.*

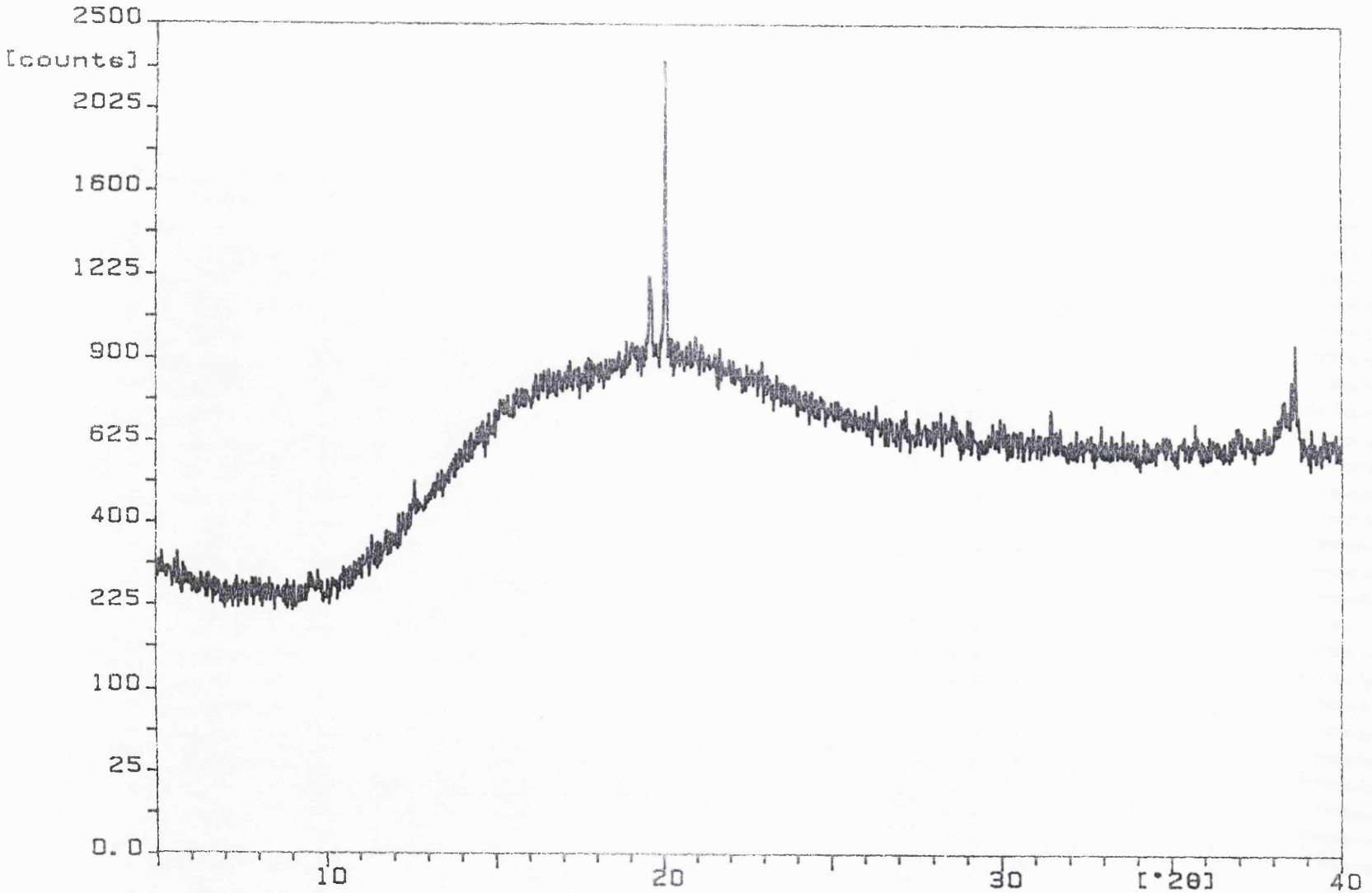

Appendix 1d *X-Ray Powder Diffractograph of 100% amorphous heat-dried raffinose.*

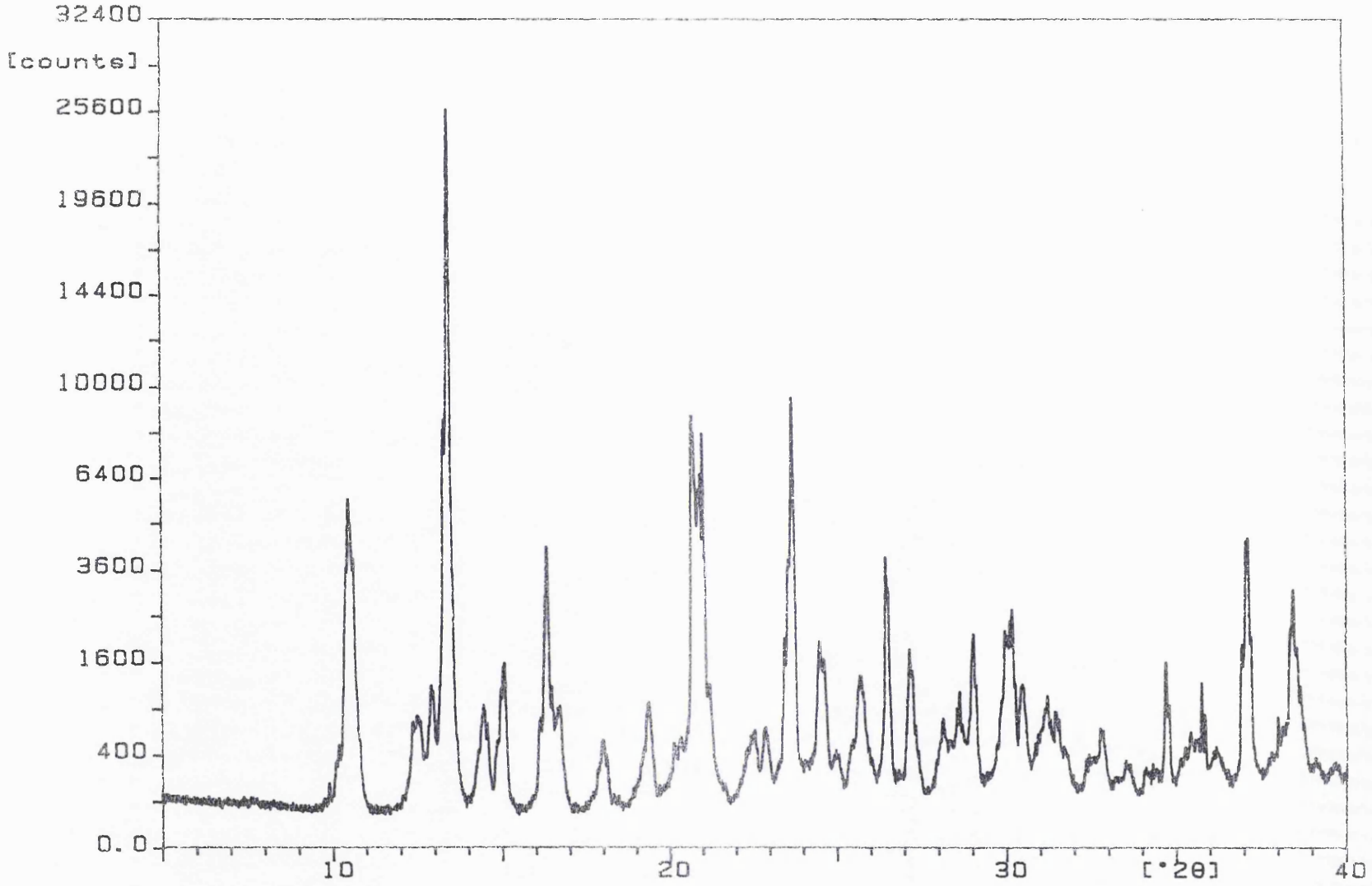

Appendix 1e *X-Ray Powder Diffractograph of 100% crystalline raffinose pentahydrate (as obtained from the supplier).*

APPENDIX TWO

SCANNING ELECTRON MICROGRAPHS

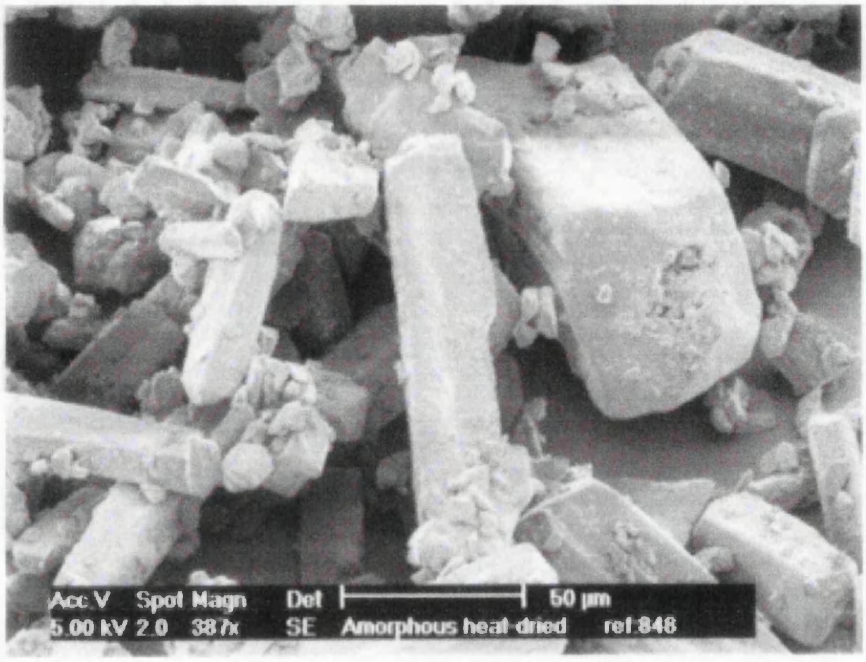

Appendix 2a *Scanning electron micrograph showing the macroscopic needle-shaped crystalline appearance of amorphous heat dried raffinose.*

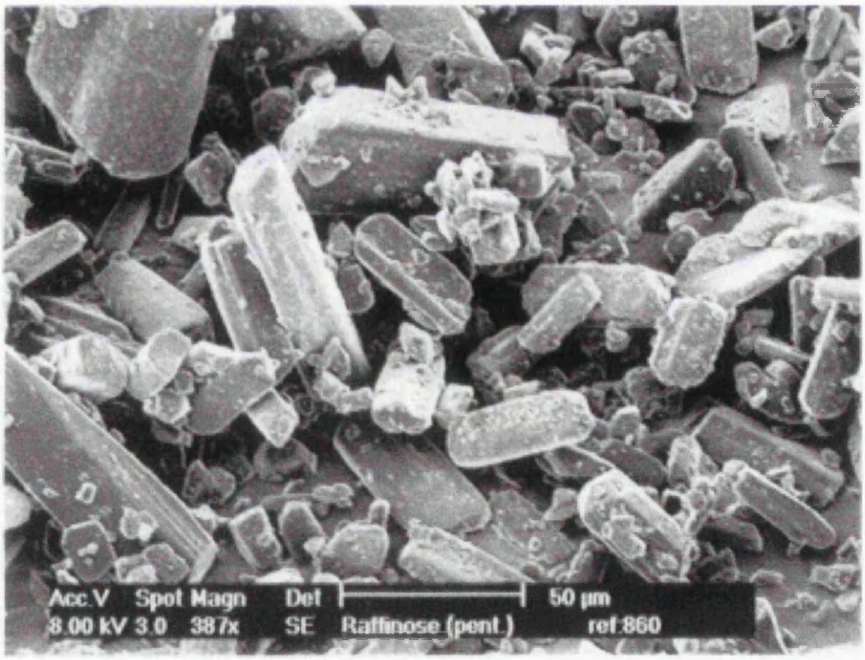

Appendix 2b *Scanning electron micrograph showing needle-shaped crystals of raffinose pentahydrate form.*

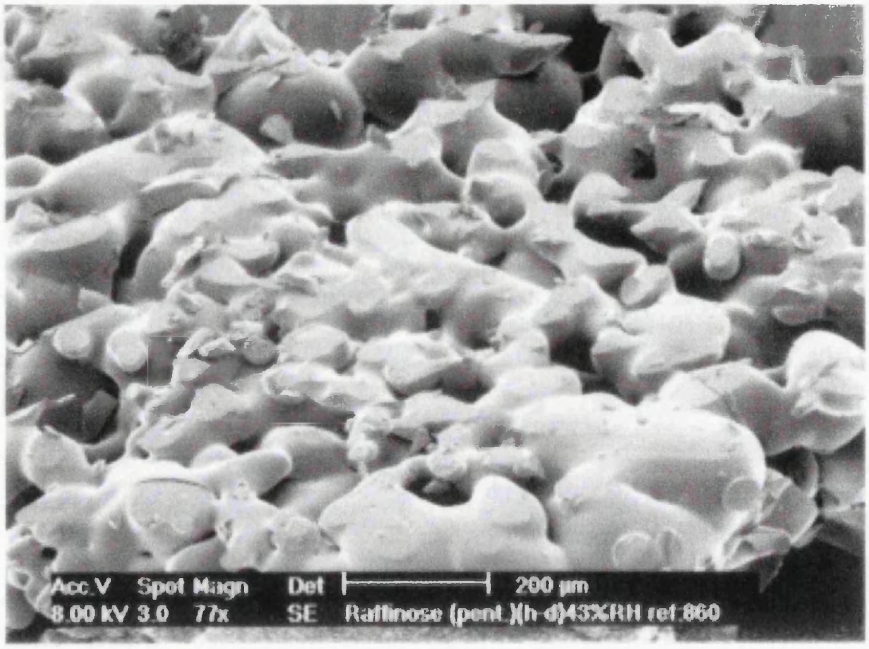

Appendix 2c *Scanning electron micrograph of heat dried raffinose following exposure to 43% RH for 2 months. The collapsed nature of the structure is clearly evident*

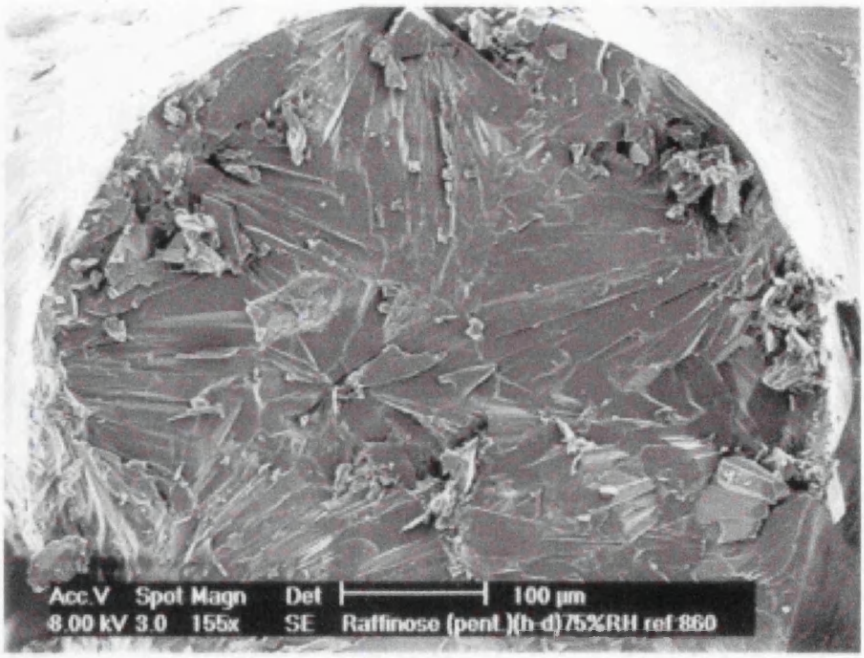

Appendix 2d *Scanning electron micrograph of heat dried raffinose post crystallisation at 75% RH.*

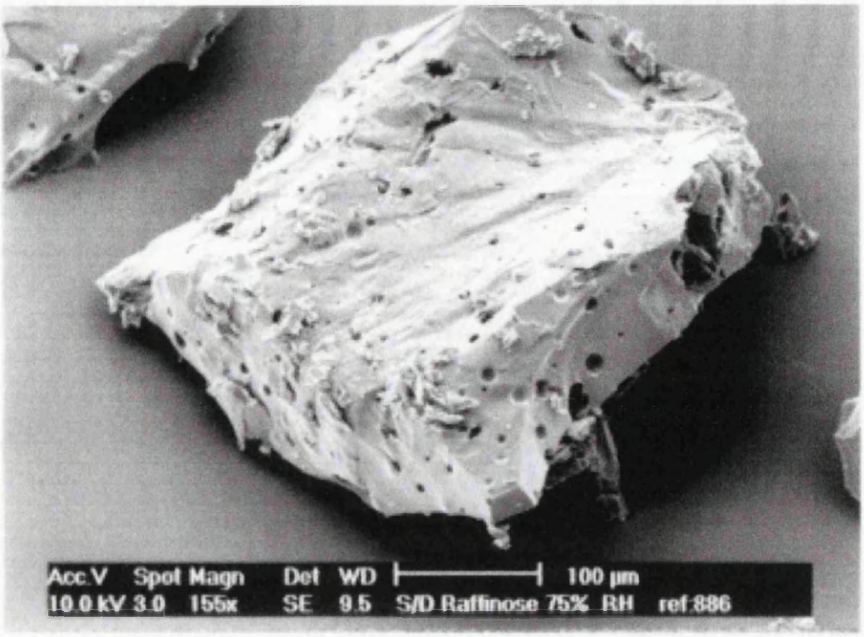

Appendix 2e *Scanning electron micrograph of spray dried raffinose post crystallisation at 75% RH.*

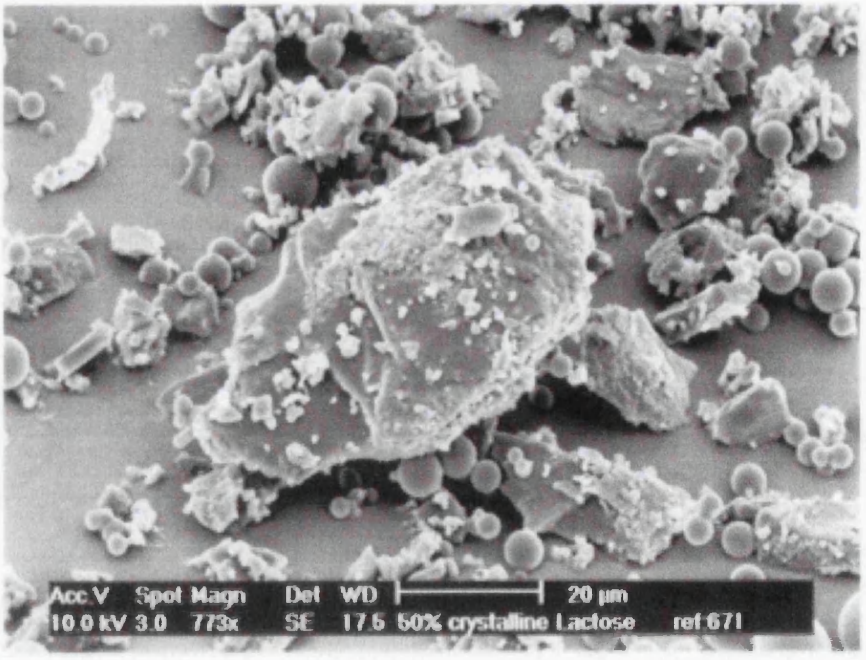

Appendix 2f *Scanning electron micrograph of a 50% amorphous lactose sample, prepared as outlined in Section 2.10. The amorphous spheres can be clearly seen surrounding the larger crystal.*